ENVIRONMENTAL PROGRESS

May, 1982
Vol. 1, No. 2

CONTENTS

Environmental Shorts **M6**

Diffusion Classification of Submicron Aerosols ..... *Dale A. Lundgren and N. Rangaraj* **79**

Catalysts for NO_x Reduction Using Ammonia ..... *S. T. Darian, J. W. Eldridge and J. R. Kittrell* **84**

Adsorption of Automotive Paint Solvents on Activated Carbon ..... *A. Golovoy and J. Braslaw* **89**

The New Physiology of Odor ..... *Robert C. Gesteland* **94**

Regulatory Approaches to Odor Control ..... *Jeanne Philquist* **98**

Characterization of Industrial Odors ..... *Frank H. Jarke and Allan Gaynor* **101**

Temperature Effects on Biological Treatment of Petrochemical Wastewaters ..... *M. P. del Pino and W. E. Zirk* **104**

Soluble-Sulfide Precipitation for Heavy Metals Removal from Wastewaters ..... *James S. Whang, Daniel Young and M. Pressman* **110**

Engineering Aspects of Ozone Generation ..... *James J. Carlins* **113**

Secondary Emissions from Subsurface Aerated Treatment Systems ..... *Raymond A. Freeman* **118**

Electrolytic Removal of Heavy Metals From Wastewaters ..... *B. M. Kim and J. L. Weininger* **121**

Spill of Soluble High-Density Immiscible Chemicals on Water ..... *P. S. Christy and L. J. Thibodeaux* **126**

Hydrocarbon Vapor Incineration Kinetics ..... *C. D. Cooper, F. C. Alley and T. J. Overcamp* **129**

Case-Specific Evaluation of an Atmospheric-Dispersion Model ..... *Keith H. Kennedy, Richard D. Siegel and Mark P. Steinberg* **133**

Modeling of Lead Air Pollution ..... *C. S. Monteith and J. M. Henry* **142**

Mitigation of Acid Rain—Policy Alternatives ..... *Duane A. Knudson and David G. Streets* **146**

Newsletter **M9**

ENVIRONMENTAL®
PROGRESS

May 1982 Vol. 1, No. 2

Environmental Progress is a publication of the American Institute of Chemical Engineers. It will deal with multi-faceted aspects of the pollution problem. It will provide thorough coverage of abatement, control, and containment of effluents and emissions within compliance standards. Papers will cover all aspects including water, air, liquid and solid wastes. Progress and technological advances vital to the environmental engineer will be reported.

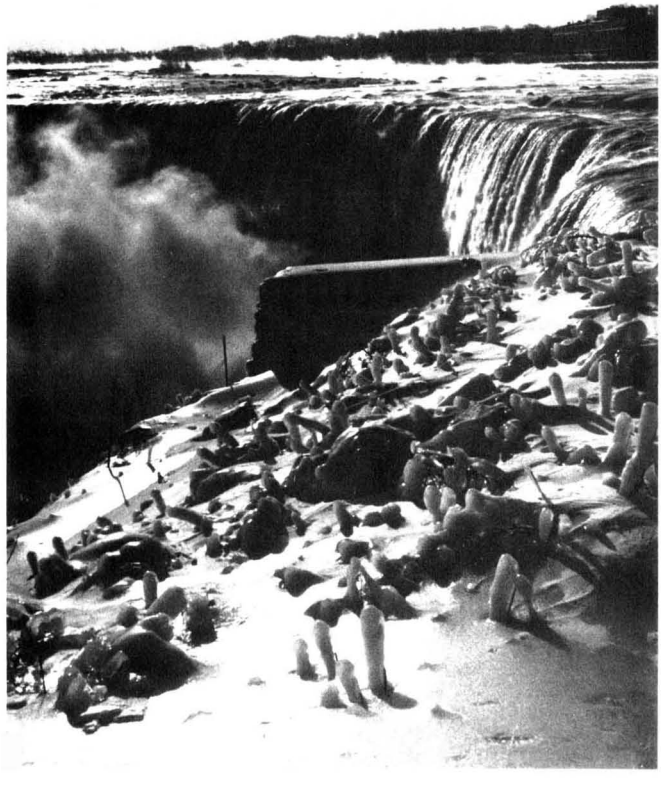

Dawn over Horseshoe Falls.
Photo courtesy Niagara Falls Convention & Visitors Bureau.

Publication Office, 215 Canal Street, Manchester, N.H. Published quarterly by the American Institute of Chemical Engineers, 345 East 47 St., New York, N.Y. 10017. (ISSN 0278-4491). Manuscripts should be submitted to the Manuscript Center, American Institute of Chemical Engineers, 345 East 47 St., New York, N.Y. 10017. Statements and opinions in *Environmental Progress* are those of the contributors, and the American Institute of Chemical Engineers assumes no responsibility for them. Subscription price per year: AIChE members $20; others $40. Single copies $15. U.S. postage is prepaid. Outside the U.S. please add $5 per subscription. Payment must be made in U.S. dollars. Application to mail at second-class postage rates is pending at New York, N.Y. and additional mailing offices.

Postmaster: Please send change of addresses to Environmental Progress, AIChE, 345 East 47 Street, New York, N.Y. 10017.

PLANT/OPERATIONS®
PROGRESS

Plant/Operations Progress is a publication of the American Institute of Chemical Engineers. The papers presented in this quarterly will center on plant safety, loss prevention, and other themes pertinent to efficient plant operation. In addition, material will be included on the problem of unscheduled shutdowns with relation to minimizing loss of productivity.

January, 1982 Vol. 1, No. 1 CONTENTS

Editorial .....

Deflagration Pressure Containment (DPC) for Vessel Safety Design ..... *John Noronha, Joseph T. Merry and William C. Reid*

ONE ORGANISATION'S MEMORY: The Use of a Computerised System to Store and Retrieve Information on Loss Prevention ..... *Ronald W. Fawcett and Trevor A. Kletz*

Intrinsic Safety: Effects on Loss Prevention ..... *William Calder*

Electrical Equipment Used in Hazardous Locations ..... *W. A. Short*

Thermal Stability Evaluation Using Differential Scanning Calorimetry and Accelerating Rate Calorimetry ..... *Michael W. Duch, Kalman Marcali, Michael D. Gordon, Charles J. Hensler and Gerald J. O'Brien*

Mathematical Modeling in Thermal Hazards Evaluation ..... *Michael D. Gordon, Gerald J. O'Brien, Charles J. Hensler and Kalman Marcali*

Fire Tests of Class NFPA IIIA Combustible Liquids Stored in Drums ..... *John E. Rogerson*

Exposure of Steel Drums to an External Spill Fire ..... *M. A. Delichatsios*

NFPA's Impact on the Chemical Industry ..... *Robert P. Benedetti*

Entrance of Dust into Pressurized Enclosures ..... *John E. Rogerson*

Tests of Explosion Venting of Buildings ..... *W. B. Howard and A. H. Karabinis*

Heat Transfer Analysis of Fire Tests on Water-Filled Drums ..... *Frank J. Mikloucich and John A. Noronha*

Safety Analysis for an Allyl Chloride Plant ..... *N. Piccinini, U. Anatra, and G. Malandrino*

This quarterly will serve to keep the practicing engineer apprised of new developments in this crucial area.

Subscription Price per year: **AIChE Members,** $20.00; **Others,** $40.00 U.S. postage is prepaid. Outside the U.S., please add $5.00 per subscription. Payment must be made in U.S. dollars.

ENVIRONMENTAL®
PROGRESS

Environmental Progress is a publication of the American Institute of Chemical Engineers. It will deal with multi-faceted aspects of the pollution problem. It will provide thorough coverage of abatement, control, and containment of effluents and emissions within compliance standards. Papers will cover all aspects including water, air, liquid and solid wastes. Progress and technological advances vital to the environmental engineer will be reported.

February 1982 **Vol. 1, No. 1** CONTENTS

Editorial .....

Environmental Shorts .....

Regulation of Heavy Metals in the Chemical Industry ..... *David I. Brandwein and Gordon T. Brookman*

Residuals Generation and Management in Selected Chemical Industries ..... *Barry S. Langer and Howard D. Feiler*

Relative Effectiveness of Chemical Additives and Wind Screens for Fugitive Dust Control ..... *Dennis C. Drehmel, Bobby E. Daniel and David Cairns*

In-Stack Virtual Impactor ..... *C. J. Woffinden, J. L. Downs, G. R. Markowski and M. J. Fegley*

Selected Conversion of NO_x by Catalytic Reduction with Ammonia ..... *P. M. Hirsch*

Waste Incineration and Heat Recovery ..... *JoAnn E. Ward and Andrew P. Ting*

Prediction of Destruction Efficiencies ..... *C. Dean Wolbach*

Landfarming of Petroleum Wastes— Modeling the Air Emission Problem ..... *L. J. Thibodeaux and S. T. Hwang*

Toxic Emissions from Land Disposal Facilities ..... *Seong T. Hwang*

Limestone Dissolution in Stack Gas Desulfurization ..... *Anthony J. Toprac and Gary T. Rochelle*

Effect of Limestone Type and Grind on SO_2 Scrubber Performance ..... *Chung-Shih Chang, J. Herbert Dempsey, Robert H. Borgwardt, Anthony J. Toprac and Gary T. Rochelle*

Multiple-Pass Water Reuse ..... *D. Bhattacharyya, S. S. Farthing and C. S. Cheng*

Treatment of Solvent-Refined Coal Wastewater ..... *Charles J. Drummmond, Richard P. Noceti and Jack G. Walters*

Newsletter .....

Subscription Price per year: **AIChE Members**, $20.00; **Others**, $40.00
U.S. postage is prepaid. Outside the U.S., please add $5.00 per subscription.
Payment must be made in U.S. dollars.

IMPORTANT: Members of AIChE's Fuels and Petrochemicals Division will automatically receive this quarterly. Subscription to *Energy Progress*[tm] is incorporated in their annual division dues.

Environmental Shorts. . .

The Technical Professional and the Regulatory Process

Stan Margolin, President, Federation of Materials Society, Arthur D. Little, Inc.

Why can't I give input into the regulatory process? How can nontechnical people make regulations on technical matters? To whom do I give input? How do I react to a proposed regulation that has appeared in the *Federal Register?* These are some of the many questions asked by the technical community in their frustrating effort to become involved in the regulatory process.

There are ways to become effectively involved but they require knowing when, how, and where to begin. It takes an understanding of the regulatory process and how regulations are developed, proposed and promulgated.

To begin, Congress has passed a statute and the President has signed into law certain legislation to regulate some type of activity—environment, energy, transportation, consumer product safety and health, etc. A specific agency has been given the executive responsibility to implement the law by the promulgation of regulations, frequently within a specific time frame. Deep in the bowels of an agency or department, a group of people is assigned the task of implementation.

In most cases, developing a regulation requires technical knowledge of the industry, its processes and mode of operation. Often, the regulation being developed will be technology-forcing, so that the variables to be controlled and the method of control need to be analyzed.

Because of requirements set out in the statutes or by the Office of Management and Budget, cost and impact analyses will also be required. These analyses will be assembled along with the proposed regulation. Public review can then be made of the cost/benefit to be derived from the regulation. The agency makes the proposed regulations and the various analyses available from public comment, after which the agency or department reviews the response and makes the proper adjustment before the regulation is promulgated. This is an oversimplification of the development of a regulation!

Where does the technical person have the opportunity to participate? There are two possible approaches, either during the early stages when the effort usually requires extensive technical input, or, during the public reaction phase when the proposed regulation is open for public comment. The preferred approach is during the early stages.

How does one find out what is going on so that input can be made early? This is a major problem facing the technical profession today.

Certain professional and technical societies recognized this problem and have faced it straight on by establishing a Washington presence. In the past decade, the electrical engineers, chemical engineers, mechanical engineers, and ceramic engineers established Washington representation. The chemists are headquartered in D.C.

One of the responsibilities of these offices is to monitor the activities of specific regulatory bodies and determine where technical input can be made early in the rulemaking process. Once an area of activity is known, the appropriate people are contacted and offers of technical assistance are made. Typically assistance is readily accepted as there is always an informational void and proper rule development requires extensive technical information. The Washington representatives react by arranging for the appropriate technical people from their societies to respond to the specific requirements of the regulation.

Quick response is a must! It is also important to ensure that technical input is presented without bias. In many cases, especially where emphasis is placed on corporate bias rather than individual professional bias, the technical information is received with hesitation and some question of credibility. Any evidence of individual bias will cause a discounting of the information provided.

Direct response to the questions being asked should be the rule. Any other response can be dangerous and may raise a question of credibility. Meetings are welcomed, but written documentation is more important, especially if it is well-referenced.

Once the proposed regulation is on the street (in the public), suggestions of meetings with the technical personnel within the regulatory agency will be rejected. During the open-comment period the process involves a written response to the individual assigned to receive public input.

Another way to provide technical input in the regulatory process is to supply information before development of a rule is under consideration. For example, the American Institute of Chemical Engineers assisted the Environmental Protection Agency with discussions of treatment methods for effluent discharges containing organic materials. Even though no one industry was being regulated, the effort dealt with reviews of treatment technologies that could have general applicability.

A third method for providing technical input is for professional societies to hold programs on specific topics and invite participants from the regulatory body, academia and industry to exchange ideas through the presentation of papers, panel discussions and direct interpersonal contact.

The mode of operation one uses is not as important as the quality of information given. If the intent is to provide emotional reactions, nonsubstantive data, presumptions or fears—forget the whole thing. Do not underestimate government professionals, whether on the regulatory side or the legislative side. They are good people, most of them well-trained in their disciplines. Their motivation may be different from most, but they are working under legal statutes and can be attacked by pressure groups for not following the letter of the law. Good technical information will create a link with these people—bad information will create a barrier.

We in the technical community must become more active when regulations rely heavily on technical input. If we don't, then we should expect poorly written rules and regulations that would result in unhealthy socio-economic conditions. The engineers and scientists in industry, government and academia have a responsibility to fulfill. Let us provide the proper technical input into the complex regulatory process that we have established.

NBS Develops Improved Technique for Measuring PCBs in Oils

A hybrid analytical technique developed by scientists at the National Bureau of Standards (NBS) could help industrial chemists solve a longstanding measurement problem—how to determine quickly and accurates the extent of PCB (polychlorinated biphenyl compounds) contamination in lubricating and cooling oil samples.

The NBS technique combines gas chromatography (GC) with high-performance liquid chromatography (HPLC) to achieve detection sensitivities of better than 1 ppm PCB. Major interfering components in an oil sample are first selectively removed with HPLC, and the "clean" sample is then separated into its components using a wall-coated, open-tubular gas chromatographic column.

The Standard Reference Material (SRM) now being prepared and certified by NBS will consist of separate solutions of two commercial PCB mixtures, one each in a transformer oil and motor oil base. The standards will be certified for concentrations of the total PCB content, and informational (uncertified) values will be given for selected individual PCB isomers.

The new SRM, should be useful to the electrical industry, the oil recycling industry, and to environmental monitoring organizations for calibrating analytical PCB monitoring procedures.

LETTERS

Response to Statement of ATLA President

To the editor:

Congratulations on Vol. 1 No. 1! The new journal is off to a good start with a very interesting set of initial articles. This should be the place for some real chemical engineering treatment of environmental problems.

In your "Environmental Shorts . . ." section, you printed some excerpts from Richard F. Gerry, President of the Association of Trial Lawyers of America. I believe a response is required. First, his statement that " . . . 70 to 90% of all modern day cancers are caused by exposure to chemicals . . ." is only correct if one includes cigarette smoke, certain dietary substances, etc.—his implication of only industrial chemicals is false. Secondly, pesticides are based on insect biochemistry and physiology, and effects (if any) on mammals may be quite different (a similar example—antibiotics destroy bacterial cells, but not human cells). He needs to get his facts straight.

Finally, he gets to his real purpose: a "full compensation system" to "victims". How would such matters be decided? I presume he would propose by trials in a court of law. Who would be a major financial beneficiary of all this? Guess who?

Doing a proper job of maintaining a clean environment while actually producing products needed by society is already an expensive effort, and doesn't need these new activities to dissipate the funds that are available.

KENNETH B. BISCHOFF
Department of Chemical Engineering
University of Delaware
Newark, De. 19711

On "Prediction of Destruction Efficiencies"

To the editor:

Dr. Wolbach's paper, "Prediction of Destruction Efficiencies" [*Environmental Progress*, 1, 38-42 (1982)] is, at first reading, a welcome addition to the incineration literature.

But his design equations are wrong (unconservative) by between two and three orders of magnitude depending on furnace temperature. This is so because he assumes that a single value of activation energy E is operative over the entire temperature range of interest.

Such is never the case in incineration. For most reactions, when $T < 1000K$, the reaction rate begins to fall significantly below that predicted from lower temperature kinetics data. This reduction occurs because either energy transport or reactant transport to the target chemical bond becomes the slowest and rate controlling step, whereas at $T < 1000K$ (typically) chemical kinetics is rate controlling. This problem in sequential reactions has been rediscovered about once each decade since the 1930s and was described most recently by Eyring (1).

Above the transition temperature, a further increase in T accomplishes little because diffusional processes have quite low pseudo-activation energies.

What *is* required at incinerator temperatures is lots of turbulence, especially on a micro scale. Wolbach does state that "boiler turbulence will play a significant role." But his equations do not describe its in fact decisive role.

For innocuous chemicals such as PCB's, where 99.99% destruction efficiency is adequate, the design equations presented might be an acceptable approximation: results would be merely disappointing. But for certain esters of phosphonofluoridic acid where 99.999999% efficiency is required, the failure to recognize the decline in activation energy could well be fatal.

I believe that a correction of some kind should be published. Otherwise, your premier issue looks good!

BILLINGS BROWN
3501 S. 3650 E.
Salt Lake City, UT 84109

LITERATURE CITED

(1) Henry Eyring, Starvation Kinetics, Science 1978, 199, 740-3

AIChE ENVIRONMENTAL DIVISION NEWSLETTER

Environmental Division (1970)

It shall (a) further the application of chemical engineering in the environmental field; (b) provide, in cooperation with the national Program Commitee, suitable programs on environmental topics of current interest; (c) provide a communication medium for chemical engineers and other individuals to exchange nonconfidential information concerning all facets of environmental activity; (d) promote publication of papers of interest to chemical engineers in environmental activities; (e) coordinate the Institute's activities with other societies active in the environmental field; (f) act as a source of information for chemical engineers who are not actively engaged in the environmental field to bring to their attention the importance of concern for the environment, the need for its consideration in the design and operation of process plants, and opportunities in research and design of equipment and processes to solve environmental problems; (g) encourage chemical engineering educators to place suitable emphasis on protecting our environment and encourage excellence in courses in environmental engineering.

ENVIRONMENTAL DIVISION

EXECUTIVE COMMITTEE

CHAIRMAN ..... Herman L. Davis
ARCO Chemical Co.
4550 Post Oak Place, Suite 300
Houston, TX 77027-3152 713-960-1222, X260

FIRST VICE CHAIRMAN ..... David L. Becker
NUS Corp.
4 Research Place
Rockville, MD 20850 301-948-7010

SECOND VICE CHAIRMAN ..... Theodore M. Fosberg
Resources Conservation Co.
P.O. Box 3766
Seattle, WA 98124 206-828-2416

SECRETARY ..... Thomas W. Hughes
Monsanto Research Center
Mound Facility
Miamisburg, OH 513-865-4020

TREASURER ..... Louis J. Thibodeaux
University of Arkansas
227 Engineering Building
Fayetteville, AR 72701 501-575-4951

PAST CHAIRMAN ..... Jacoby A. Scher
5519 Yarwell
Houston, TX 77096
(Fluor Engineers & Constructors) 713-662-4062

NEWSLETTER EDITOR ..... Marx Isaacs
1513 Barbee Ave.
Houston, TX 77004 713-523-6049

COUNCIL LIAISON ..... R. H. (Bob) Marshall
9906 Balmforth Lane
Houston, TX 77096 713-723-7678

DIRECTORS

DIRECTOR (1980-1982) ..... Alex Danzberger
Hydrotechnic, Inc.
1250 Broadway
New York, NY 10001 212-695-6800

DIRECTOR (1980-1982) ..... William J. Lacy
U.S. Environmental Protection Agency (RD679)
Washington, D.C. 20460 202-426-2387

DIRECTOR (1981-1983) ..... Stacy L. Daniels
Dow Chemical Co.
1702 Building
Midland, MI 48640 517-636-4991

DIRECTOR (1981-1983) ..... Jack F. Erdman
Union Carbide Corp.
P.O. Box 471
Texas City, TX 77590 713-948-5126

DIRECTOR (1982-1984) ..... D. Bhattacharyya
Department of Chemical Engineering
University of Kentucky
Lexington, KY 40506 606-258-4958

DIRECTOR (1982-1984) ..... Gary L. Leach
2210 South Memorial 713-946-9340
Pasadena, TX 77502
(Merichem Co.) 713-455-1311

(Continued on page M9)

Diffusion Classification of Submicron Aerosols

An "in-stack" diffusion classifier has been designed, constructed, calibrated, and field-tested.

Dale A. Lundgren and Cumbum N. Rangaraj, University of Florida, Gainesville, Fla. 32611

DIFFUSION CLASSIFIER

The recently developed "in-stack" diffusion classifier utilizes a very fine-mesh stainless-steel wire screen for the actual aerosol classification. The same wire-mesh screen was used in the original ambient unit developed and described by Sinclaír and Hoopes [*1*]. The in-stack unit used five stages operated in parallel, each sampling at the same fixed flow rate, to provide five simultaneous size-classified aerosol samples. These samples are collected out on filter media for subsequent weight gain determination and for chemical analysis. Sampling rates are maintained through each stage by using carefully matched critical orifices. The entire unit is housed in a stainless steel cylinder of 25-cm length and 7.5-cm outer diameter.

Screen-type diffusion batteries have also been built and used by Patterson and Calvert [2]. Sinclair, Countess, Liu, and Pui [*3*] have calibrated the screen-type unit at laboratory conditions. Knutson and Sinclair [*4*] have reported on used of the Sinclair Diffusion Battery and Nucleus Counter for sampling ambient aerosols.

The in-stack diffusion classifier consists of five stages; four stages utilize different numbers of identical screen elements for differential particle-size fractionation, while the fifth stage has no screens, so as to provide a total aerosol sample. The physical parameters of each set of screens used in the experiments were measured with a light microscope equipped with a stage micrometer. Each stage is provided with a highly efficient, low reactivity after-filter to collect the particles which penetrate the screens. By varying the number of screens the performance characteristics of each stage can be easily varied to suit individual needs. As the number of screens varies from 1 to 100, the classification varies from about 0.01 to about 0.4 μm diameter.

When an aerosol passes through a set of screens, small particles are deposited on the screens by diffusion and the larger penetrating particles are collected on the after-filter for subsequent weight-change determination and chemical analysis. The efficiency of large particle removal increases with the number of screens, resulting in lower mass penetration and smaller filter weight gains. The raw weights obtained then represent cumulative data.

Each diffusion classifier stage consists of two parts. The screens are placed in the top section and held in place by a retaining ring. The top section has been designed to protect the screens from physical damage and to provide an open area to flow of the same magnitude as the screen open area. The filter is placed in the bottom section and the diffusion classifier is assembled.

EXPERIMENTAL SETUP

The basic experimental setup involved equipment for the generation of reproducible test aerosols of a variety of materials, means for measuring penetrations through a set of screens, flow control and measurement, clean air supply, and an oven capable of providing temperatures of at least 540°C. The overall experimental arrangement is shown in Figure 1.

Building compressed air was purified by passing it through an oil filter and a dryer. This was then split into two streams, each controlled by regulators and followed by absolute filters. One stream was used as the sheath air supply for the TSI Model 3071 Electrostatic Classifier. The other stream was used to provide a metered supply of dilution air and also to operate the Collison atomizer. A syringe pump was used to supply a constant feed of ethanol when a DOP solution was aerosolized in order to maintain the solution level and keep the concentration relatively constant over a long period of time. The output of the atomizer was passed through a single-stage impactor with a cutpoint of 1 μm to remove any large particles and droplets and thus cut down the polydispersity of the aerosols. The output from the Collison atomizer was then mixed with dilution air and passed through a charge neutralizer. The dilution air was supplied in the approximate ratio of 4:1 with respect to the aerosol stream to provide proper conditions for droplet evaporation, while the Kr-85 charge

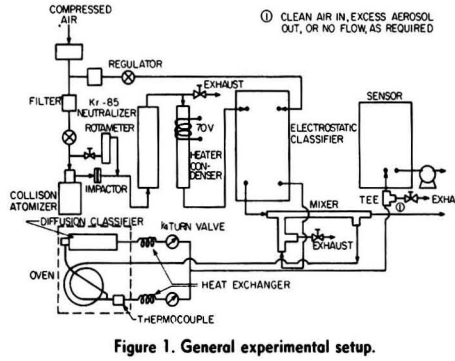

Figure 1. General experimental setup.

ISSN 0278-4491-82-5370-0079-$2.00.

neutralizer was used to return the aerosol to a Boltzmann equilibrium charge distribution from the charged aerosol condition created by the atomization process.

The output from the neutralizer was partially exhausted and the remaining aerosol was passed through a heater-condenser section. This produces a less polydisperse aerosol which is used as input into the TSI Model 3071 Electrostatic Classifier to produce monodisperse aerosols. The monodisperse aerosol is mixed with a controlled flow of dilution air, obtained as excess air from the electrostatic classifier, in a mixer.

The aerosol was sampled through a stainless-steel heat exchanger into the diffusion classifier stage being tested, the assembly being placed inside an oven. The temperature of the heated aerosol stream was measured by a thermocouple-potentiometer arrangement. A bypass system was also constructed so that alternating measurements could be made with and without screens in the aerosol stream to be able to calculate penetrations. This aerosol stream was then cooled in a water-cooled heat exchanger and sampled either by a TSI Model 3068 Aerosol Electrometer or by a TSI Model 3030 Electrical Aerosol Analyzer (EAA) depending on whether the aerosol was charged or uncharged. When the EAA was used, clean air was pumped in or excess aerosol pumped out at a tee just before the EAA aerosol inlet, depending on whether the actual flow rate required in the diffusion classifier was less than or greater than 4 lpm.

EXPERIMENTAL PROCEDURE

The calibration procedure involved generation of monodisperse aerosols with diameters between 0.03 μm and 0.20 μm and studying their penetration through various sets of screens, with flow rate and temperature being the other variables. The flow rates used were 2, 3, 4, and 5 liter/min and the temperatures used were 27°, 149°, 260°, 371°, and 482°C.

Since such a wide range of test conditions were to be used in the experiments, an optimum operating method was developed so as to make data collection more convenient and less time consuming. To decide on the number of screens to be tested the following procedure was followed: The number of screens was chosen so that the penetration of 0.03-μm diameter particle at 3 liter/min flow rate would be approximately 50%. The same method was followed for 0.05-μm, 0.1-μm, and 0.2-μm diameter particles. The number of screens tested was: 0, 5, 10, 20, and 36, respectively.

Once the four sets of screens were decided on, each set was tested one at a time. A chosen set of screens was mounted in the diffusion classifier stage and left in place until a complete series of tests were run. At 27°C and 260°C, the flow rate and particle size were varied, while at the other temperatures the flow rate was fixed at 4 liter/min and the particle size was fixed at the size which had an approximate 50% penetration for the given set of screens at 27°C.

Initially, data were not taken with 0.03-μm particles because of certain problems which will be discussed later in this section. For each setting of a combination of flow rate, particle size, number of screens and temperature, a minimum of 6 penetration measurements were made during a particular experiment and this experiment was, in most cases, repeated on at least 2 other days. In other words, the procedure was performed on at least 3 separate occasions. This was done to check the repeatability of the experiment and to have statistically valid data.

Sodium Chloride Aerosols

Sodium chloride aerosols were used for all high-temperature work. For work at ambient temperatures both DOP and sodium chloride aerosols were used. The chosen solution was atomized in the Collison atomizer at pressures between 10 and 30 psi depending on the experiment. If a DOP solution was used, the syringe pump was used to pump pure ethanol into the Collison atomizer at the same rate as the rate of loss of solution. The heater in the heater-condenser section was arbitrarily set at 70 V. This seemed to heat the aerosol stream enough to bring about solvent vaporization from particle surfaces. The aerosol stream was now passed into the electrostatic classifier. The four air flow paths in the electrostatic classifier were set so that the sheath air and excess air flows were both 20 liter/min, and the polydisperse aerosol and monodisperse aerosol flows were equal and about 3 to 4 liter/min. The monodisperse aerosol and excess air flows were mixed, and a vacuum pump drew the sample aerosol through the diffusion classifier stage and then through the aerosol electrometer where the aerosol concentration was measured.

When experiments were conducted with 0.03-μm particles the EAA was used in place of the aerosol electrometer. The output from the electrostatic classifier was passed through a Kr-85 charge neutralizer, and then through the diffusion classifier stage to the EAA. The rest of the system remained unchanged except for the flow system just ahead of the EAA. This has been described earlier in this section.

This system was run for about 10 minutes before collection of data. Once all the required data were obtained at 27°C, the temperature of the oven was raised to 149°C, the flow in the diffusion classifier stage was adjusted to the actual flow required, and then penetration measurements were made. This process was followed at the other temperature settings except at 260°C where runs similar to those at 27°C were performed. Once such a series of experiments was completed, the diffusion classifier stage was allowed to cool off and then the whole series was repeated with a new set of screens.

LABORATORY EXPERIMENTAL RESULTS

Development of Semi-Emperical Penetration Function

One primary intention of this project was to develop a generalized penetration function which could be used to predict the performance of each stage of the diffusion classifier for any combination of screen number, gas temperature, flow rate, and particle size. This would enable calculation of the diffusion classifiers performance in a high-temperature, industrial gas stream.

Experimentally determined penetrations for various conditions were converted to equivalent single-cylinder efficiencies, η_D. For each of these conditions, the Péclet number, N_{Pe}, was also calculated. To determine the functional relationship, g, between η_D and N_{Pe}, these two variables were plotted as shown in Figure 2. This suggested a linear relationship on the log − log plot. By applying a power-curve fit in a HP − 97 programmable calculator the straight line plotted in Figure 2 was obtained with $r^2 = 0.98$. The equation of this line is

$$\eta_D = 4.3(N_{Pe})^{0.59} \quad (1)$$

and the corresponding penetration function is

$$P = \exp(-4.3n\, S(N_{Pe})^{-0.59}) \quad (2)$$

or, for the nominal 635-mesh screens used in this project,

$$P = \exp(-3.01n\,(N_{Pe})^{-0.59}) \quad (3)$$

where: n = number of screen elements.

Effect of Particle Size on Penetration

Each of the 4 sets of screens mentioned earlier was tested. At 27°C and 260°C, 0.03, 0.05, 0.07, 0.10, 0.15 and

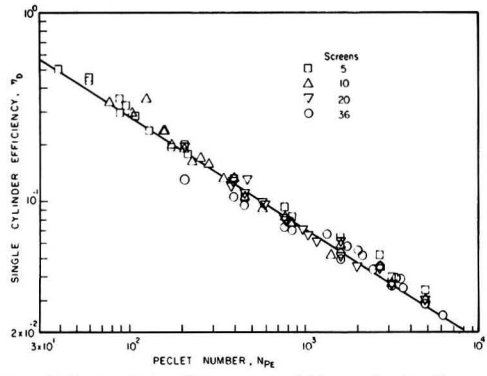

Figure 2. Single-cylinder efficiency versus Péclet number for all experimental data.

0.20-μm diameter monodisperse aerosols were used at a flow rate of 4 liter/min. Penetration increase with particle size for a given set of screens and for a given particle-size penetration was lower at 260°C then at 27°C. The penetration curves become steeper with increasing number of screens. Figure 3 shows this data in a convenient form. The experimental data has been plotted over curves generated from the semi-emperical penetration function. There is very good agreement between the penetration function and experimental data for 5, 10, and 20 screens for both 27°C and 260°C.

Effect of Temperature on Penetration

As before, each of the 4 sets of screens was tested. The approximate d_{p50} of each set of screens at 27°C was used in testing each set of screens at each of the temperatures; i.e., 0.05-μm diameter particles with 10 screens at variable temperature. The test flow rate was 4 liter/min. As would

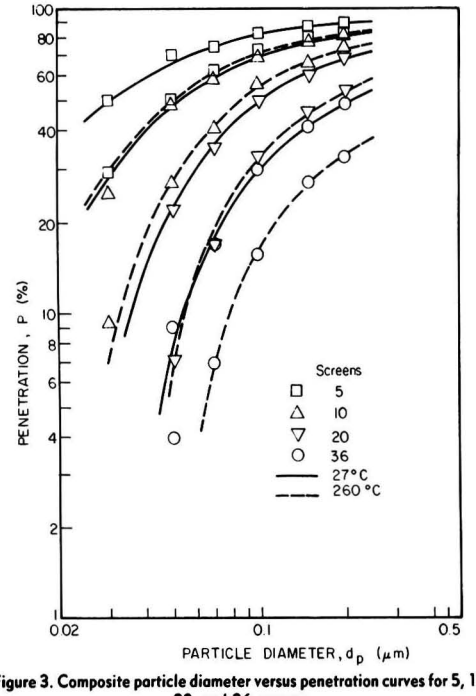

Figure 3. Composite particle diameter versus penetration curves for 5, 10, 20, and 36 screens.

be expected from theoretical considerations, penetration decreases with increasing temperature. The rate of decrease of penetration is almost identical for 5, 10, and 20 screens where, respectively, 0.03, 0.05, and 0.10-μm diameter monodisperse aerosols were used, though the rate is slightly lower for 0.10-μm diameter particles. However, with the 0.20-μm diameter monodisperse aerosols and 36 screens, the rate of decrease is significantly lower. This also agrees with theory as can be seen from the data, going from 27°C to 260°C, for example, the diffusivities, which are inversely proportional to penetration, increase by 85%, 105%, 122%, and 128% for 0.20, 0.10, 0.05, and 0.03-μm diameter particles, respectively. Thus, 0.2-μm particles are less severely affected by temperature and penetration is higher.

Agreement between the experimental data and the semi-emperical curve fit is reasonably good in all cases up to about 370°C. A sudden drop in penetration around 370°C for particle diameters less than 0.2 μm is not simulated well by the model. More work needs to be done at this temperature to study in greater detail the particle and fluid mechanics at such elevated temperatures.

Effect of Flow Rate upon Penetration

As in the case of the temperature-variation experiments, the same sets of screens and particle sizes were used. However, only two temperature conditions, 27°C and 260°C, were used at flow rates of 2, 3, 4, and 5 liter/min. As previously discussed, the difference in the penetration curves at 27°C and 260°C is not as much with 0.2-μm diameter particles as with the smaller particles. Agreement between the experimental data and the semi-emperical penetration function is good for most of the 27°C data. For 260°C data the agreement is only fair and there is an error of approximately 3% between the experimental points and the model. The experimental points are consistently higher or lower than the model. This seems to imply a consistent error in measurement. However, since the penetration function is the result of a power curve "best fit," it is expected that the experimental points will deviate a bit from the curve fit. The composite experimental curves for flow rate as a variable seem to indicate some as yet undetermined inconsistency for the 5-screen data at 260°C.

Effect of Number of Screens on Penetration

Experimental results are in agreement with theory and the data with 5, 10, and 20 screens are quite good. But, for 36 screens, there is some inaccuracy for smaller particle sizes. There seems to be a particular problem in measuring penetrations less than 25% for both the 27°C and 260°C cases for 36 screens at an experimental flow rate of 4 liter/min.

Effect of Aerosol Type on Penetration

It was felt that the calibration of the stages of the diffusion classifier would not be complete without a check for the effect of aerosol type on screen performance. Thus, DOP aerosols were generated and exactly the same experimental procedure was followed as with sodium chloride aerosols. Data was obtained with DOP and sodium chloride aerosols, under similar operating conditions, for the cases of variable particle size and variable flow rate. From this data it appears that DOP penetrations are a little lower than that observed with sodium chloride aerosols. However, DOP aerosol concentrations were not as stable as with sodium chloride aerosols, and this is probably the reason for the observed difference. Thus, with the available data accuracy, aerosol type, as studied, has no significant effect on diffusion-classifier perform-

ance. More work needs to be done with DOP aerosols to further validity the above conclusion.

FIELD TESTING

Laboratory aspects of the use of the diffusion classifier have been discussed in the previous section. In the laboratory calibration only one stage was tested at a time and conditions were well controlled. In the field-testing procedure, the entire diffusion classifier was assembled and tested on several aerosol sources; an oil-fire boiler, several Jet Engineer Test Cells, and a condensation oil source.

Velocity and temperature traverses were first obtained. For field testing, the diffusion classifier was preceded by either a University of Washington Mark III Cascade Impactor, or an Andersen Mark III Cascade Impactor to size fractionate particulate matter larger than about 0.4 μm and prevent overloading of the diffusion-classifier stages. Since only one set of calibrated critical orifices was available at the time of the field test, the sample flow rate was fixed. Thus, to maintain approximately isokinetic conditions, the correct sampling nozzle was chosen. The rest of the sampling system consisted of a probe, hooked-up to a condenser by an umbilical cord, and the sampling box.

Before a sample was drawn from the stack, the diffusion classifier and cascade impactor were left in the stack for about 30 minutes, with the nozzle inlet plugged, to reach temperature equilibrium with the stack gas. Thirty-to sixty-minute samples were then taken. From prior information it was known that the fraction of particles larger than 1 μm was not high and thus no problem with overloading of the impactors was expected.

The impaction plate and the diffusion classifier filter weight gains were measured with a Cahn Model 4700 Automatic Electrobalance. From the weight and flow-rate data the particle-size distribution was determined.

Impaction Surfaces

Two types of impaction surfaces were used: glass-fiber substrates and stainless-steel substrates with Apiezon H coatings. In the diffusion classifier two types of filters were used: glass fiber and Teflon. The collection-surface substrates and filters were heated and desiccated until ready for use.

The primary intention of these tests was to test the operation of the diffusion classifier in hostile environments.

A particle-size classification diameter (D_{p50}) was calculated and used to draw preliminary conclusions from the field data. The 50%-cut points for the cascade impactor were determined from manufacturer's data, and weight fractions in each size range were determined in the usual manner. In the case of the diffusion-classifier data, the following procedure was used. If the flow rate through the cascade impactor was 17.3 liter/min, that through each stage of the diffusion classifier was 3.46 liter/min. In order to make the diffusion classifier and cascade impactor data compatible, the weight gain and gas volume sampled through each of the 5 stages in the diffusion classifier is multiplied by 5, assuming that all stages have identical flow rates. The weight on the filter after a set of 36 screens, for example, represents the weight of all particles greater than 0.27 μm but less than 0.38 μm, which is the cut-point of the last stage of the impactor. To determine the weight of particles greater than 0.14 μm but less than 0.27 μm, subtract the weight on the filter after 36 screens from that on the filter after 20 screens.

DISCUSSION OF FIELD TEST DATA

The first field tests were conducted on an oil-fired boiler with a power-generation capability of 65 megawatts. At the sampling port location, the stack gases were at about 150°C temperature and 13 meter/sec velocity. Samples were obtained at the stack centroid (about 0.5 m from the stack wall). The diffusion classifier was preceded by an in-stack impactor, and was connected to a rigid metal sampling probe. External to the stack was a flexible sampling line leading to a standard U.S. EPA Method 5 condenser and meter box. Sampling times of 30 to 60 minutes were used at an actual sampler inlet flow rate of about 13 liter/min.

The impactor sampling protocol involved using either a University of Washington Mark III impactor with Apiezon H coated stainless-steel collection substrates or an Andersen Mark III impactor with a glass-fiber-filter-covered collection surfaces. In all cases, the collection substrates were stabilized by heat treating at 150°C for one hour and then storing in a desiccator until the time for use. Prior to impactor assembly and use, the collection substrates were tared on a Cahn Electrobalance to the nearest 0.01 mg. Immediately after a test, the collection surfaces were reweighed and then stored in a desiccator for later reweighing and analysis. Sample collection media for the diffusion classifier consisted of 47-mm disks of glass fiber or Teflon filter media. These collection media were conditioned, preweighed, and reweighed, as were the impactor collection surfaces.

After the impactor and diffusion classifier were assembled and the sampling nozzle and sampling proble attached, the entire unit was heated to stack gas temperature by blocking off the nozzle inlet and inserting the entire unit into the gas stream to be sampled. A 30-minute temperature equilibration period was allowed for this warmup. After warmup, the nozzle was uncovered, the unit properly positioned, and the sampling started.

Sampling Rate

Sampling rate through the system was fixed by five identical critical flow orifices in the five parallel diffusion-classifier stages. Flow rate was held constant during the test simply by maintaining a 20-in Hg-vacuum on the meter-box vacuum gauge.

After completion of sampling, the sampling train was removed from the stack, allowed to cool, disassembled, and the collection surfaces and filter media weighed. The inlet nozzle was cleaned to remove deposited material and the quantity of the deposit was later determined. The procedure described above was, in general, used for all tests.

Because stack-gas temperature was near the SO_3 dewpoint temperature, several problems were encountered with condensation of SO_3 and/or collection of H_2SO_4 droplets. In addition, the SO_x and/or NO_x was adsorbed onto (or reacted with) the glass fiber filter media in a mass quantity about equal to the collected particulate matter. This invalidated the weight data obtained using glass fiber filter media in the sampling train. Tests run using Teflon filter media indicated no problem with gas adsorption and gave good results.

Several tests were run on three different jet-engine test cells. In general, the sampling protocol was the same as for the oil-fired boiler tests. Tests run at a second jet-engine test cell were on a clean-burning jet engine. Gas temperatures varied from 90°C to 170°C for various tests. Because of the low aerosol concentration, only one reliable size distribution was obtained. The Figure 4 normalized histogram indicates a bimodal size distribution for this data. A major peak exists between 0.1 and 0.3 μm and a minor peak between 2 and 6-μm diameter. The large peak is probably agglomerated primary combustion aerosol and the smaller peak is probably due to reentrainment of particle agglomerates from the internal baffle surfaces. Over 80% of the aerosol weight was associated with particles in the submicron size range.

Size-distribution data were recently obtained at a third jet-engine test cell while running a very smoky jet engine.

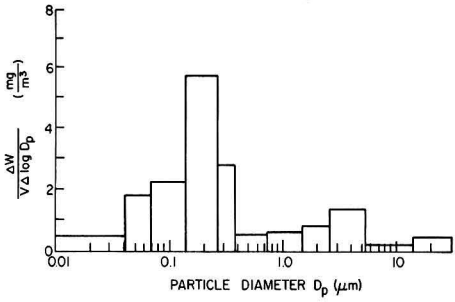

Figure 4. Aerosol distribution for a clean-burning jet engine.

A total of ten measurements were made and the average particle-size distribution is plotted in Figure 5. The average size distribution shows a mode indicating primary aerosol within the 0.005- to 0.05-μm diameter size range and a second aerosol agglomerates mode in the 0.1- to 1-μm size range.

DATA REDUCTION PROCEDURE

The procedure which has been chosen is based on Twomey's nonlinear iterative formula [5]. The basic computer program was obtained from Dr. E. O. Knutson and modified for our use.

The program has been written so that particle-size histograms, geometric mean diameters and standard deviations are calculated and printed out for input mass-percent penetrations. Input data includes flow rate, temperature, and stack pressure. Number of class intervals, width of class interval, and starting value can be set as required.

There are three major sections in this procedure: calculation of penetration characteristics of various numbers of screens from the generalized penetration function; Twomey's nonlinear iterative formula; and calculation of geometric mean diameter, standard deviation and root-mean-square error, and plotting of histograms. Twomey's nonlinear iterative formula is incorporated in an algorithm, which starts with an initial assumption for the size distribution and then refines it by a series of small changes to improve the fit to the observed penetrations. In this case, the initial assumption has been made that the distribution is uniform, which each size having a penetration equal to $1/n$ times the observed penetration in the stage with no screens, which is 100%, where, n is the number of sizes being considered. The refined penetrations are then obtained by applying Twomey's nonlinear iterative formula until the calculated mass-percent penetrations are close to the measured mass-percent penetrations which are input to the program. Normally the number of iterations is restricted to thirty or less. This procedure is explained in greater detail in papers by Knutson and Sinclair [4], and Twomey [5].

The computer program has been used in some preliminary work with field data and has been tested with monodisperse aerosol data and polydisperse aerosol data. Agreement was only fair for the monodisperse aerosol data, and it appears that the program cannot handle data with small standard deviations. In another test, the penetration function for screens, Equation (3), was used to calculate penetrations of a polydisperse aerosol (MMD = 0.1 μm and σ_g = 2) through 5, 10, 20, and 36 screens. These penetrations were then used as input to the program and the resulting outlet distribution characteristics were: MMD = 0.124 μm and σ_g = 2.

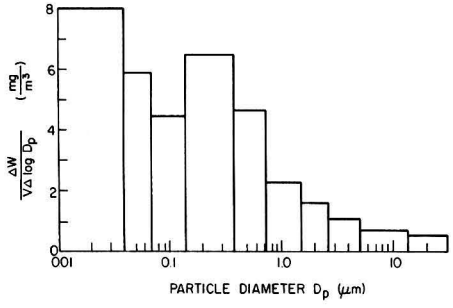

Figure 5. Average aerosol distribution for a smokey jet engine.

ACKNOWLEDGMENTS

This research was jointly funded by the U.S. Air Force and the Environmental Protection Agency (EPA), and was monitored by EPA's Project Officer, Dr. Kenneth T. Knapp.

LITERATURE CITED

1. Sinclair, D., and G. S. Hoopes, "A Novel Form of Diffusion Battery," *J. Amer. Ind. Hyg. Assoc.*, **36**, 39-42 (1975).
2. Patterson, R. G., and S. Calvert, "Submicron Particle Size Measurement with a Screen Diffusion Battery," *EPRI FP-840, Project 723* (1978).
3. Sinclair, D., R. J. Countess, B. Y. H. Liu, and D. Y. H. Pui, "Experimental Verification of Diffusion Battery Theory," *J. Air Pollution Control Assoc.*, **26**(7), 661-663 (1976).
4. Knutson, E. O., and D. Sinclair, "Experience in Sampling Urban Aerosols with the Sinclair Diffusion Battery and Nucleus Counter," in: Proceedings: Advances in Particle Sampling and Measurement, Asheville, North Carolina, 98-120 (1978).
5. Twomey, S., "Comparison of Constrained Linear Inversion and an Iterative Nonlinear Algorithm Applied to the Indirect Estimation of Particle Size Distributions," *J. Computational Physics*, **18**, 188-200 (1975).

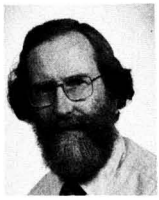

Dale A. Lundgren has been involved in the air pollution engineering field since 1958. Much of his early experiences were in the aerosol filtration area and included the design/development of various aerosol generation and measurement apparatus. He has also recently edited a book titled *Aerosol Measurement*. In 1969, he became Director of Air Pollution Control, Environmental Research Corporation, St. Paul, Minnesota (now a division of Dart Industries). Since the fall of 1972, Dr. Lundgren has been at the University of Florida as a Professor of Air Pollution Control Engineering in the Department of Environmental Engineering Sciences.

Catalysts for NO_x Reduction Using Ammonia

Evaluations of new catalyst compositions and reactor configurations show that the economics of retrofitting can be very favorable.

S. T. Darian, J. W. Eldridge, and J. R. Kittrell, University of Massachusetts, Amherst, Mass. 01003

The emission of nitrogen oxides, NO_x, in both the stack gases from stationary combustion sources and the exhaust gases from mobile combustion sources has become an environmental problem of great concern in the industrialized countries around the world. NO_x poses a significant health hazard as an air pollutant [1]. It also plays a key role in both the photochemical reactions and the secondary particulate formation which promote smog [2]. Still further, it may contribute to the formation of "acid rain," particularly in the eastern United States, southeastern Canada, and western and northern Europe [3].

It is estimated that by 1985 over 70% of the total NO_x emissions in the U.S. will be from stationary sources, primarily utility and industrial boilers [4]. For the level of control of NO_x from these sources anticipated to be required by the Environmental Protection Agency, it is widely believed that selective catalytic reduction using ammonia offers the greatest promise for technical and economic success.

While several reactions are possible between ammonia, the oxides of nitrogen, and excess oxygen, the two of primary interest are usually written as

$$6NO + 4NH_3 \rightarrow 5N_2 + 6H_2O \quad (1)$$

$$5O_2 + 4NH_3 \rightarrow 4NO + 6H_2O \quad (2)$$

It is desired to catalyze the first reaction very selectively, while avoiding or at least minimizing the second.

A catalyst for this application should provide intrinsic activity high enough to permit space velocities of $10^4 - 10^6$ reciprocal hours with conversions of 50-90%, high resistance to deactivation by sulfur compounds, high selectivity to avoid the undesired reaction of ammonia with the excess oxygen present, and cost effectiveness. It is also extremely important for economic reasons that the catalyst system exhibit only a small pressure drop, on the order of 50-100 mm of water.

In the present work, two basically different catalyst compositions were studied. The first was a commercial catalyst, Harshaw V0301, approximately 10% vanadia supported on alumina; the second was a modified molecular-sieve catalyst prepared in our laboratories. The basic design employed for minimizing the pressure drop was that of a parallel-passage reactor, PPR, comprising a set of stainless-steel screens coated on both sides with catalyst particles and mounted in parallel on a steel-rod frame with spaces between them for passage of the gas flowing parallel to the screens.

The variables studied in this research were: the adhesive used to bond the catalyst particles to the screens, the screen mesh size, the catalyst particle size, the catalyst composition, and the reactor temperature.

ISSN 0278-4491-82-5652-0084-$2.00.

Experimental Reactor System

PPR cartridges 38 cm long containing nine parallel catalyst-coated stainless-steel screens (40-mesh) were fabricated in a cylindrical frame sized to fit quite tightly into the 5.08 cm (2 inch, Schedule 40) aluminum pipe, 76 cm long, serving as the non-catalytic reactor shell. An example of such a PPR cartridge is shown in Figure 1. An effort was made to keep a uniform gap width between all screens in all the cartridges. The Reynolds number through the cartridges was below 2000 in all experiments.

A schematic diagram of the overall experimental system is presented in Figure 2. No. 2 fuel oil was burned in a Utica Model 21 furnace to provide flue gas which was then doped with additional nitric oxide from a cylinder to increase the concentration into the range encountered in actual utility boiler flue gas, approximately 500 ppm being chosen for this research. Ammonia gas was then added to provide a concentration of similar magnitude. This gas mixture was drawn through the PPR by a steam ejector, with samples for NO_x, NH_3, and soot analysis being withdrawn by a pump from locations just before and after the reactor. The soot content of the flue gas was <.01 g/scf. The hot gas leaving the reactor had to be cooled (by a water-cooled double-pipe heat exchanger not shown) before entering the rotameter, and a rotameter bypass was necessary

Figure 1. Coated-screen parallel-passage reactor cartridge.

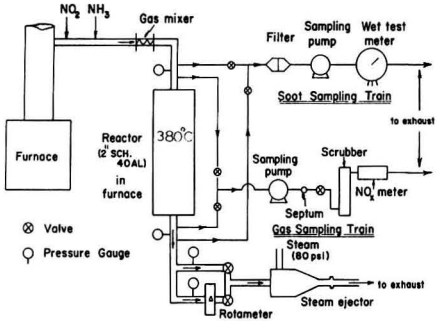

Figure 2. Laboratory deNOx reactor system.

to permit removal of the soot accumulation in the rotameter without shutting down the reactor. The pipe from the furnace stack to the reactor was heated to keep the gas at about 370°C, and the reactor was heated by a Hevi-Duty Electro Co. furnace. Internal thermocouples were located in the entrance of the reactor, in the middle of the cartridge, and at the bottom of the cartridge.

A Thermo-Electron Corp. Model 10AR chemiluminescent analyzer was used to analyze for NO, NO_2, and NH_3. Gas chromatography was used to measure N_2, O_2, and CO_2 in the flue gas. Water vapor content was measured by an EG & G Dew Point Hygrometer. The SO_2 content of the flue gas was low, due to the low sulfur content of the No. 2 fuel oil. However, the catalysts have been shown to be very resistant to high SO_2 concentrations in earlier work in this laboratory.

RESULTS

Comparison of Adhesives

Adhesive, as a binding agent, is critical in this design of a PPR. It should be highly resistant to temperature and also have good durability and low cost for commercial use. It should also provide a catalyst unit of high activity and ease of fabrication.

Five different types of adhesive were tested for their strength, ease of application, and effect on catalyst activity in a parallel coated-screen reactor. The adhesives included: Thurmalox silicone ceramic coating (paint-like), Thermostix 2000 heat-resistant inorganic adhesive (resists temperatures up to 2000°F), Cotronics 944 ceramic adhesive, Cotronics 985 alumina based thixotropic adhesive, and Sauereisen 31 acid-proof cement.

The adhesive was applied to both sides of screens 10 cm in length and 5 cm in width. Then, an even layer of molecular-sieve catalyst, MS I, particles was spread on a flat surface and the screens were placed on top of it. A second layer of catalyst was then spread over the top of the screens. Pressure was applied to the upper layer of catalyst to ensure good binding of catalyst to the screen surfaces. The initial loading of the catalyst adhering to the screens was recorded. The adhesive-catalyst composite was allowed to set at room temperature for two days, except for Thurmalox which was heat treated at 540°C for 8 hours.

Several characteristics of an adhesive are important in providing a useful catalyst-adhesive composite for use in a PPR. The adhesive must be robust to physical deterioration, it must allow a large weight of catalyst to adhere to the support screen, it must coat the screen with a small thickness in order to minimize pressure drop, and it must not produce a chemical or physical effect on the inherent activity of the catalyst. Five different catalyst particle sizes were employed with a variety of adhesives in order to evaluate candidates for use. These were: 12-16, 16-35, 20-35, 35-50, and 50-100 mesh.

To evaluate the robustness of the composites, catalyst losses were measured in three separate tests. First, the composite was exposed to high-velocity air, up to 40 m/sec. Second, each composite was placed in a block and dropped five times from a height of 90 cm. Third, each composite was exposed to a vibrating rough surface (sand) in a standard shaker for four minutes.

For the two smallest particle sizes, later also found to provide superior reactivity and lower pressure drop, the catalyst remaining on the screen after these tests was significantly greater than with the larger particle sizes.

Sauereisen 31 and Thermostix 2000 were the strongest adhesives, Thurmalox and Cotronics 944 were in the middle of the range, and Cotronics 985 was the weakest.

The weight of catalyst attached to a screen is important in that, for a given reactor volume, a higher catalyst density provides a higher conversion. However, the thickness of the adhesive-catalyst-screen composite is also influential for a given reactor volume, in that the gap width remaining between the composites determines the pressure drop of the reactor module. In order to quantify the effect of both variables, a hypothetical reactor design was considered which assessed the amount of catalyst charged to a reactor of fixed volume using a fixed gap width between coated screens.

For computational purposes, a modular reactor design was chosen with a gap which of 1 cm and overall dimensions 50 × 50 × 100 cm. Using the previously measured coated-screen thicknesses and the weights of catalyst adhering to the screens, the number of screens and total catalyst weight in one such reactor module was calculated. The results shown in Table 1 indicate that the best adhesive for such parallel-passage reactors is Thurmalox, from the standpoint of both maximum amount of catalyst and maximum superficial coated-screen area (number of screens) per module. Sauereisen 31 is also useful in this regard. It also happens that Thurmalox is both the easiest to apply and the least wasteful, since it is essentially a premixed paint.

Another key aspect of an adhesive for PPR application is its possible chemical or physical effect on the inherent activity of the catalyst, for any given weight and size of particles contained in the reactor module. Since Sauereisen 31 had been found to be one of the strongest adhesives tested and was also one of the two best on the basis of Table 1, comparative activity tests were performed on a laboratory PPR cartridge using 50-100 mesh MS I bonded with Thurmalox and another cartridge using Sauereisen 31. The Sauereisen 31 cartridge gave conversions substantially lower than the Thurmalox cartridge at 380°C. Its intrinsic reaction velocity constant was 44% less than that of the Thurmalox cartridge. Therefore, Thurmalox was adopted as the cement to be used for the other categories of experiments.

Screen Mesh Size

Another variable in parallel-passage reactors is the screen mesh size supporting the catalyst. It was believed that, with small particles, the screen openings would have

TABLE I. COMPARISON OF CEMENTS IN A PPR MODULE*

	35-50 mesh		50-100 mesh	
	No. screens	kg · MS I	No. screens	kg · MS I
Thurmalox	43	18.0	45	13.5
Sauereisen 31	39	16.8	44	14.0
Thermostix 2000	41	15.6	44	8.4
Cotronics 944	40	16.0	41	9.8
Cotronics 985	39	14.4	40	12.8

an effect on the amount of catalyst on the screens. Four different sizes of screens were used (16 × 16, 20 × 20, 40×40, and 100 × 100 mesh). Thurmalox was used to coat catalyst particles on the screens (100 cm² of screen area). The test was done for both types of catalyst.

It was found that both the weight of catalyst adhering to the screen and the thickness of the coated screen increase substantially as the size of the openings is increased. The openings in the 16-mesh screen, however, were so large that the Thurmalox coating could not be retained. All the laboratory reactor tests were done with cartridges made from 40-mesh screens but, in a larger, commercial reactor module permitting more flexibility in choice of gap width, the thicker 20-mesh coated screens carrying more catalyst might well produce higher NO_x conversion for a given number of screens.

Catalyst Particle Size

Two different catalysts were used to test the effect of particle size on the conversion, Molecular Sieve I and Harshaw V0301. It was realized that larger amounts of catalyst could be bonded to the screens using larger particles. On the other hand, with smaller particles, the available surface area for chemical reaction could increase significantly. Also, smaller particles will provide a smaller pressure drop through the reactor.

1) Tests with Molecular Sieve I. In this experiment, Molecular Sieve I was used to make four cartridges, with different catalyst particle sizes, all bonded with Thurmalox. Each of these was then tested for reactivity at 380°C. The results of this experiment are shown in Figure 3 as percent NO conversion *vs.* space velocity at reaction conditions. Space velocity here is based on the total volume of the catalyst bonded to the screens, calculated as its weight divided by the bulk density of that particle size. Average linear velocities, based on the cross-sectional open area of the passages between the screens in the PPR cartridges, ranged from 2 m/s to 25 m/s. A comparison between different sizes of MS I shows that the activity of the catalyst increases as smaller particle sizes are used. There are also other advantages in using smaller particles. Among them are the decrease in amount of catalyst required for a given conversion, and a significant decrease in pressure drop across the reactor.

Figure 4 shows the measured reactor pressure drop as a function of space velocity. It should be noted that, in those cartridges with the constant number of screens, the smaller the particle the thinner the coated screen; hence, gap width is increased, thereby increasing the cross-section open to gas flow and lowering the linear velocity for a given volumetric flow.

2) Tests with Harshaw V0301. Since the particle-size studies showed significant effects on catalyst activity with MS I, Harshaw V0301 was then used to study the same effects. Four similar experiments were carried out with Harshaw catalyst, using the same reactor configuration as

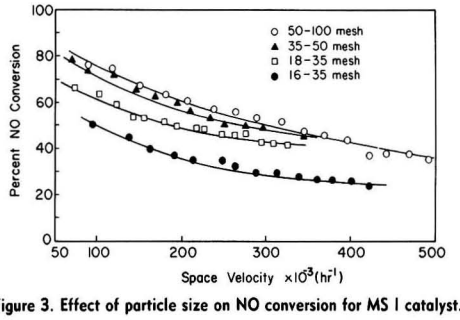

Figure 3. Effect of particle size on NO conversion for MS I catalyst.

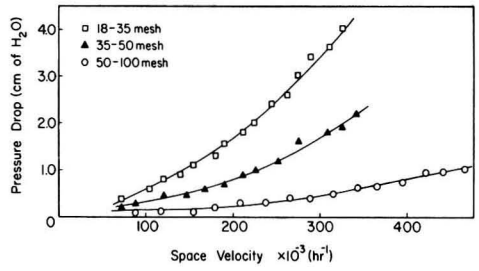

Figure 4. Pressure drop vs space velocity for MS I cartridges.

in the experiments with MS I. However, since in the MS I experiments conversion was still increasing as particle size decreased down to the smallest size used (50-100 mesh), it was decided to use a still smaller size (100-200 mesh) of V0301 to see if an optimum particle size was evident. The comparison between different sizes of Harshaw V0301 catalyst is shown in Figure 5, again in the form of NO conversion *vs.* space velocity. As indicated there, a decrease in particle size again increased the conversion, down to the 50-100 mesh size. The smaller 100-200-mesh particles, however, produced substantially lower conversions. This effect may be due to the particles being so small that most of them become completely wetted by, or submerged in, the adhesive, rendering them catalytically unavailable.

Catalyst Composition Studies

Three catalyst compositions were compared on the same, previously described configuration of PPR cartridges, all with 50-100-mesh catalyst particles bonded to the screens with Thurmalox. They were: Harshaw V0301, MS I, and MS II, a different modification of the same molecular sieve. Figure 6 shows that the conversions ob-

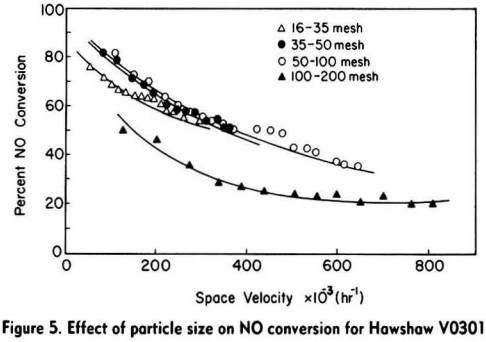

Figure 5. Effect of particle size on NO conversion for Hawshaw V0301.

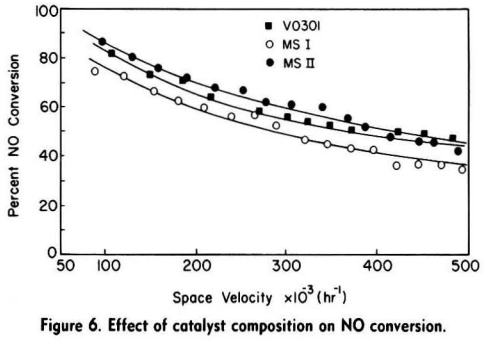

Figure 6. Effect of catalyst composition on NO conversion.

tainable with MS II are about 10% greater than with MS I, and are also somewhat higher than with Harshaw V0301.

Effect of Temperature

Cartridge B, with 18-35-mesh MS I bonded with Thurmalox, was used to study the effect of temperature at four space velocities. The temperature range differed somewhat among these four runs, but spanned approximately 315°-440°C (the maximum attainable with this experimental system). Due to control limitations, the space velocity varied about 10% within each run, so the original data were then scaled to a constant space velocity for each run.

This scaling was done with a model based on first-order, irreversible kinetics for the NO reduction. This model had been shown earlier to correlate experimental data for these operating conditions in the PPR cartridge quite adequately. At each temperature, a reaction rate constant, k_1, was calculated from the experimental data by:

$$k_1 = -(\text{S.V.})\ln(1 - x) \tag{3}$$

where S.V. is the actual space velocity and x is the fractional conversion of NO. This calculated k_1 was then used to scale the NO conversion to the desired constant space velocity for that run.

Figure 7 shows the results of these experiments scaled to constant space velocities. While the conversions here are not high because of the larger particle size, the trend with temperature has been shown to be the same with smaller particles of both MS I and MS II. The key point is that, with these catalysts, the conversion continues to increase with temperature at least up to over 450°C. This is very important in its potential application to NO_x reduction in gas-turbine exhausts, which are normally in that temperature range. Other types of catalyst, including Harshaw V0301, have been shown in this laboratory to produce a sharp decline in NO_x conversion as the temperature is increased in this range. This effect is presumably due to their loss of specificity for the desired reaction as temperature is increased, due to catalysis of the combustion of the ammonia with the excess oxygen present to produce NO_x. Indeed, a net increase in NO_x content from this process is readily attainable at high temperatures with those catalysts.

DESIGN OF FULL-SCALE REACTORS

For design purposes, the experimental data for 50-100-mesh particles of MS I bonded with Thurmalox were modelled using kinetics based on the superficial flat area of the coated screens. The NO_x reduction was taken as irreversible and first order in NO concentration, a basis which had been demonstrated to correlate experimental conversions with this catalyst very well, at least up to about 400°C.

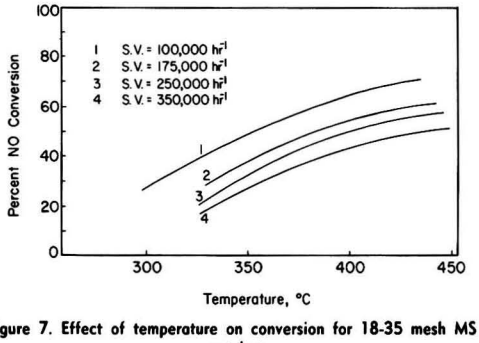

Figure 7. Effect of temperature on conversion for 18-35 mesh MS I catalyst.

The kinetic equation then becomes

$$k_{obs} = -(\text{A.V.})\ln(1 - x) \tag{4}$$

where

k_{obs} = observable reaction rate constant, in m/hr
A.V. = area velocity, in m/hr
x = fractional conversion of NO

The effect of mass-transfer resistances on k_{obs} was included as:

$$k_{obs} = \left(\frac{1}{k_i} + \frac{1}{k_m}\right)^{-1} \tag{5}$$

where

k_i = intrinsic reaction-velocity constant
k_m = mass-transfer coefficient.

Equation (4) was then put into the form:

$$-\ln(1 - x) = \frac{PL}{A_{cs}}\frac{1}{\text{Re}}\frac{1}{\text{Sc}}\left(\frac{1}{\frac{1}{K} + \frac{1}{\text{Nu}}}\right) \tag{6}$$

where

P = perimeter of screens
L = length of screens
A_{cs} = cross-sectional area for gas flow
$K = \dfrac{k_i d_e}{D}$
d_e = equivalent diameter, $d_e = 4R_H$
R_H = hydraulic radius, = cross-sectional area for flow/wetted perimeter
D = diffusivity
Re = Reynolds number, $\dfrac{\rho V_g d_e}{\mu}$
Sc = Schmidt number, $\dfrac{\mu}{\rho D}$
Nu = Nusselt number, $\dfrac{k_m d_e}{D}$
ρ = density
μ = viscosity
V_g = average velocity

Expressing Nu as a function of Re, the equation was transformed to its final form:

$$-\ln(1 - x) = \frac{PL}{A_{cs}}\frac{1}{\text{Re}}\frac{1}{\text{Sc}}\left(\frac{1}{\frac{1}{K} + \frac{1}{a\text{Re}^b}}\right) \tag{7}$$

A nonlinear least-squares computer program was used to fit this model, and the values of the constants found were: $K = 2.14$, $a = 1.4 \times 10^{-4}$, and $b = 1.8$. With these values, the agreement between predicted and observed conversions is reflected in Figure 8. The value found for k_i was 105 m/hr at 380°C.

Preliminary design calculations were then carried out, using this model, for two sizes of power plants, an existing 150-MW boiler for retrofitting with a PPR placed in the ductwork before the air preheater, and a hypothetical 800-MW new power plant. The average empty-duct gas velocities used for these two plants were 12 and 15 m/s, respectively. The PPR height, L, and the pressure drop generated were calculated for several combinations of coated-screen thickness and gap width between screens. Friction factors determined from experimental pressure drop measurements were correlated by:

$$\frac{\Delta P}{L} = \frac{2f\rho V_g^2}{d_e}\frac{1.6}{32.2}\frac{\text{cm H}_2\text{O}}{\text{m}} \tag{8}$$

where f = the friction factor for the PPR.

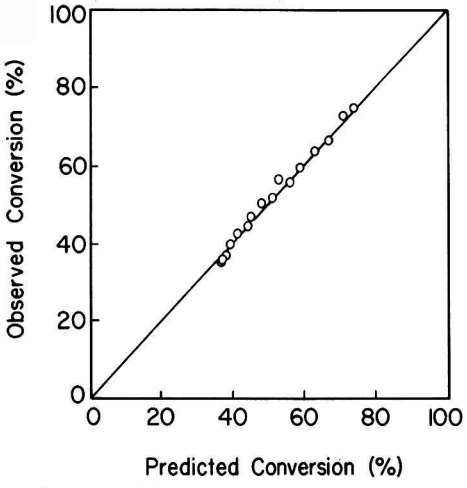

Figure 8. Agreement of observed conversion with that predicted by model.

Pressure drops for the full-scale units were then calculated from this correlation.

Examples of the results are illustrated by the case of a coated-screen thickness of 3.175 mm (⅛") and a gap width of 6.35 mm (¼"). For 50% conversion, the PPR height and pressure drop were predicted at 1.34 m and 2 cm H_2O for the 150-MW plant, and 1.75 m and 3.8 cm H_2O for the 800 MW plant. It should be noted that these differences between the 150- and 800-MW plants are directly attributable to the different empty-duct gas velocities, and not to any inherent effect of plant size *per se*. For 90% conversion, the corresponding figures were 4.5 m and 6.6 cm H_2O for the 150-MW unit, and 5.8 m and 12.6 cm H_2O for the 800-MW unit. If the coated-screen thickness were reduced to 1.6 mm while holding the gap width the same, then more screens would retrofit into the 150-MW plant ductwork, and 90% conversion was projected with PPR height of 3.7 m with a pressure drop of only 4.4 cm H_2O.

Preliminary cost estimates for such PPR units to control NO_x emissions were made for retrofitting the same 150-MW power plant. For 90% NO_x conversion, projected capital investment was $11-12/kW, with operating costs of 0.09¢/kWhr. For 50% conversion, these figures decreased to $3-4/kW and 0.04¢/kWhr, all costs being in 1980 dollars.

CONCLUSIONS

Thurmalox silicone ceramic coating was found to be the preferred adhesive of those tested for bonding catalyst particles to a supporting screen in a coated-screen parallel-passage reactor. The optimum catalyst particle size evaluated was found to be 50-100 mesh, with 35-50 mesh nearly as good. The optimum screen mesh size of those tested was found to be 20 × 20 from the standpoint of maximum catalyst loading attainable, but the coated-screen thickness was substantially greater than with 40 × 40-mesh screens. For a given gap width, this would mean fewer screens in a fixed reactor volume and hence less superficial catalyst area, perhaps resulting in lower conversions.

Of the three catalyst compositions tested, Harshaw V0301 was somewhat more active than the modified molecular sieve, MS I, but the improved modification, MS II, showed greater activity than the Hawshaw catalyst. The NO_x conversion obtained with the modified molecular-sieve catalysts increases as reaction temperature increases, at least up to somewhere over 450°C.

Preliminary design calculations and cost estimates for full-scale PPR units to control NO_x emissions from utility power plants indicate that this approach holds much promise for obtaining high NO_x conversions at high space velocities with low pressure drops, and also with attractively low capital investment and operating costs.

ACKNOWLEDGMENT

Grateful appreciation is expressed for the joint sponsorship of this research by Northeast Utilities Service Co., and New England Power Service Co.

LITERATURE CITED

1. Colucci, A. V., and W. S. Simmons, "Nitrogen Oxides: Current Status of Knowledge," FA-668, Project TR-11900-5 (1978).
2. Goodley, A., "State of California Perspective on NOx Control for Stationary Sources," Proceedings of the Joint Symposium on Stationary Combustion NO_x Control, **5**, 57 (1980).
3. Luken, R. A., "Acid Rain Issues," *ibid.*, **5**, 55 (1980).
4. Ricci, L. J., "EPA Sets Its Sights on Mixing CPI's NO_x Emissions," *Chem. Eng.*, **84** (4), 33 and (8), 84 (1977).

S. T. Darian is a Ph.D. candidate in the Chemical Engineering Department at the University of Massachusetts, doing research in the field of combustion phenomena. He earned his B.S. in Chemical Engineering at the City College of the City University of New York, and his M.S. in Chemical Engineering at the University of Massachusetts on the research reported in this paper.

J. W. Eldridge is a Professor of Chemical Engineering at the University of Massachusetts. He received his B.S. from the University of Maine, M.S. from Syracuse University, and Ph.D. from the University of Minnesota, all in Chemical Engineering. His primary areas of both research and teaching have been applied kinetics and reactor design, and thermodynamics.

J. R. Kittrell is President of KSE, Inc., a consulting engineering firm in Amherst, Mass. He has been employed previously with the University of Massachusetts, Standard Oil of California, and Chevron Research Co. He obtained the Ph.D. degree and M.S. degree in Chemical Engineering from the University of Wisconsin and the B.S. degree in Chemical Engineering from Oklahoma State University. He is the author of about 60 technical papers, an inventor on about 30 patents, and is the coauthor of a book entitled *Towards a National Refining Policy (Australia)*.

Adsorption of Automotive Paint Solvents on Activated Carbon: II. Adsorption Kinetics of Single Vapors

Data for single solvent vapors can be used to make a reasonable estimate of the size of the carbon-adsorption unit required.

A. Golovoy and J. Braslaw, Ford Motor Co., Dearborn, Mich. 48121

In recent years the automotive industry has been investigating and developing various methods for reducing the emissions of volatile organic compounds resulting from spray-painting operations of car and truck bodies. One possible control method is to adsorb the emitted solvent vapors on activated carbon in fixed-bed adsorbers. An extensive review of adsorption technology has been compiled by Juhola [1].

The operation of a fixed-bed adsorber is cyclic, involving adsorption of the solvent vapors up to a predetermined breakthrough concentration or for a fixed period of time followed by desorption and regeneration of the activated carbon, usually with low-pressure steam. Automotive paint formulations contain a multitude of solvents with a wide range of physical properties which influence adsorption and carbon regeneration. In order to apply carbon adsorption technology to automotive painting operations, it is necessary to investigate the adsorption behavior of the organic solvents which are used in paint formulations in the range of concentration found in paint spray booth exhaust air. The ability to predict the breakthrough concentration as a function of time, i.e., the breakthrough curve, of individual solvents and mixtures is important for the determination of the most proper and efficient operation of the adsorbers. In general, when fixed-bed adsorbers are considered for emission control in automotive painting operations, the desired breakthrough concentration, prior to carbon regeneration, is expected to be about 15% that of the inlet solvent laden air.

This paper describes one of a series of studies on the adsorption of automotive paint solvents on activated carbon. In a previous paper, a study on the equilibrium adsorption of paint solvents was presented [2]. The present study is concerned with the kinetics of adsorption of single vapors in a fixed-bed adsorber. Special attention is paid to the initial period of adsorption, that is, when the solvent concentration in the effluent is less than 20% that of the influent.

ADSORPTION KINETICS

The adsorption of gas molecules is kinetically a second-order process, involving interaction between free gas molecules and active sites on the adsorbent surface [3]. During the initial adsorption period, however, when there is an overabundance of active sites, the adsorption can be described by pseudo-first-order kinetics with respect to the concentration of solvent vapor in the gas phase [4].

Wheeler and Robell [5] have shown that, for first-order kinetics with nonselective adsorption, the concentration of the effluent gas stream can be expressed as follows:

$$\frac{C}{C_o} = \left\{1 - \exp\left(\frac{-N_T t}{t_s}\right) + \exp\left[N_T\left(1 - \frac{t}{t_s}\right)\right]\right\}^{-1} \quad (1)$$

where C_o is the inlet gas concentration. In the above expression, N_T is the number of transfer units in the adsorbent bed and is defined by the expression:

$$N_T = \frac{k_A G}{Q\rho_b} \quad (2)$$

where k_A is the pseudo-first-order adsorption rate constant; G is the weight of carbon in the bed; Q is the volumetric flow rate of solvent-laden gas at the temperature and pressure of the bed; and ρ_b is the bulk density of the carbon in the bed. The stoichiometric adsorption time, t_s, is the time required for the flow system to completely saturate the carbon in the bed if all of the solvent in the gas stream has been adsorbed. This stoichiometric adsorption time can be calculated using a simple material balance on the bed, which yields:

$$t_s = \frac{WG}{Q\,C_o} \quad (3)$$

where W is the solvent-adsorption capacity of the carbon at a concentration C_o, in mass of solvent per unit mass of carbon.

For a reasonably long adsorber ($N_T > 4$), Wheeler and Robell [5] show that there is a period of time when $\exp[N_T(1 - t/t_s)]$ is much greater than unity, while $\exp(-N_T\, t/t_s)$ is very small. This is the period of time during which the bed is adsorbing essentially all of the solvent. During this time, Equation [1] can be simplified to yield:

$$\ln\frac{C}{C_o} = \frac{k_A C_o}{\rho_b W}\, t - \frac{k_A G}{Q\rho_b} \quad (4)$$

Equation (4) is governed by two parameters: the pseudo-first-order adsorption rate constant, k_A, and the kinetic saturation capacity, W. Jonas and Rehrmann applied Equation (4), in a slightly modified form, to the study of the adsorption kinetics of several organic vapors in fixed-bed, activated-carbon adsorbers [6, 7, 8]. Their results, which were obtained at an effluent concentration of 1% of the influent, showed that the kinetic saturation capacity, W, has approximately the same value as predicted by the Polanyi-Dubinin correlation [9] for equilibrium adsorp-

ISSN 0278-4491-82-5443-0089-$2.00.

tion capacity under static conditions. In addition, the magnitude of the adsorption-rate constant, k_A, indicates that, for vapors at the concentrations studied, the rate of adsorption is limited by diffusion from the flowing gas to the surface of the activated carbon particles [*8, 10*].

SCOPE OF STUDY

The purpose of the study described in this paper was to determine the range of usefulness of Equations (1) and (4) under conditions similar to those encountered in carbon adsorbers proposed for the control of volatile organic solvent emissions resulting from automobile paint spray operations.

Thus, the concentration of single solvent vapors exiting fixed-bed carbon adsorber were followed to complete breakthrough, e.g., $C/C_o = 1$. Variations in the amount of active charcoal present in the bed allowed a determination of the range of validity of Equations (1) and (4). In addition, the pseudo-first-order adsorption-rate constant, k_A, and the kinetic adsorption capacity of the carbon used were determined experimentally and compared with theoretical values for four paint solvents. These solvents, *n*-butanol, *m*-xylene, cellosolve acetate, and 2-heptanone, are widely used in automobile topcoat and primer formulations and are representative of the alcohols, aromatic hydrocarbons, esters, and ketones commonly used.

EXPERIMENTAL

Materials

The activated carbon used in this study was Columbia JXC 4/6 pelleted activated carbon (Union Carbide, Carbon Products). The physical properties of the activated carbon are listed in Table 1. The surface area was determined in this laboratory by the BET method using carbon dioxide and argon. These gases yielded a surface area of 1201 m^2/g and 1186 m^2/g, respectively. The activated carbon was dried in a vacuum oven at 165°C for 48 hours before use and to determine its bulk density. The technical-grade solvents were used as received. Gas chromatography showed that the solvents were over 99% pure. The relevant physical properties of the solvents used in this study are listed in Table 2.

Equipment

The adsorption system used in this study is a fixed-bed, variable-flow system (560 liter/min maximum), shown schematically in Figure 1. The major components of the system are the activated-carbon bed, air blower, solvent injection unit, and instrumentation. The system is also provided with low-pressure steam and a condenser for desorption, but these were not used in the present study.

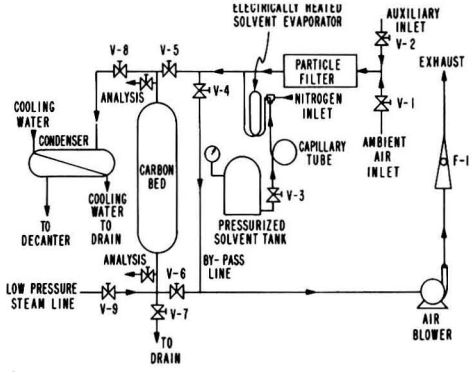

Figure 1. Schematic diagram of carbon adsorption system.

The activated-carbon bed is made of a 36-cm (14-in) long vertical cylinder with an internal diameter of 10.16-cm (4-in). The conduits leading to and from the bed are 3.81-cm (1.5-in) schedule 40 pipe. The carbon bed and conduits are made of type 304 stainless steel. The bed can hold up to 1135 g (2.5 lb) of activated carbon having a bulk density of 0.5 g/cm^3. The flow of solvent-laden air through the bed is in a downward direction. The top of the bed can be easily removed for sampling or replacement of the activated carbon. The entrance and exit of the bed are provided with sampling lines for measuring the composition of the solvent-laden air. In addition, there are several ports along the bed cylinder for monitoring pressure and temperature.

The flow of solvent-laden air through the adsorber is induced by a GAST regenerative, oil-less air blower (GAST Manufacturing Corp., Benton Harbor, Mich.). The blower is equipped with a 1.5 HP motor and is capable of delivering 566 liter/min (20 ft^3/min) against a pressure of a 14.9 kPa (60-in of water). The blower is positioned downstream from the activated-carbon bed, in a suction mode, because it exhausts air at elevated temperatures. This arrangement results in a bed pressure of about 98.2 kPa (737 mm Hg), slightly below atmospheric pressure. The flow rate of the solvent laden air is determined by a Meriam laminar-flow element model 50 MW 20 (Meriam Instruments, Cleveland, Ohio).

The solvent-injection unit consists of a pressurized solvent holding tank, a long capillary tube, and a high-temperature evaporator. The rate of solvent flow through the capillary and into the evaporator is controlled by the pressure in the solvent holding tank. The evaporator is made by coiling into a U-shape a 60-cm long stainless-steel tube of 0.635 cm diameter. The length of the tube is wrap-

TABLE 1. PHYSICAL PROPERTIES OF ACTIVATED CARBON

Surface area (CO_2, Ar; BET method)	1194 m^2/g
Average particle size	0.37 cm
Bulk density	0.461 g/cm^3
Bed void fraction	0.457
Hardness	95
CCl_4 activity, minimum	60%

TABLE 2. PHYSICAL PROPERTIES OF PAINT SOLVENTS

Solvent	Molecular[a] Weight	Liquid[a] Density g/cm^3 @20°C	Vapor[a] Pressure mm Hg @20°C	Dipole[a] Moment Debye	Refractive[a] index ^nD @20°C	Diffusivity[b] in air @25°C and 737 mm Hg cm^2/sec
n-butanol	74	0.810	4.4	1.6	1.3993	0.0888
m-xylene	106	0.864	6.1	0.4	1.4972	0.0709
Cellosolve acetate	132	0.973	1.2	1.8	1.4058	0.0629
2-heptanone	114	0.817	2.6	2.6	1.4088	0.0713[c]

[a] Handbook of Chemistry and Physics, 55th Edition.
[b] Reference [*11*].
[c] Estimated using the method of Fuller, Schettler, and Giddings, reference [*12*].

ped with a heating tape, controlled by a Variac, and is maintained at about 180°C (356°F). A continuous flow of nitrogen (5 liter/min) through the evaporator sweeps all the evaporated solvents and carries them into the main air stream. Because of the evaporator's high heating capacity, the solvents entering it at the low flow rates used in this study evaporate practically immediately. Thus, the concentration of solvents in the influent is easily controlled by the pressure in the solvent holding tank.

Two Beckman model 400 FID analyzers are used for continuous monitoring of the hydrocarbons concentration in the influent and effluent air. The analyzers were calibrated daily using 81 ppm and 818 ppm propane standards.

An in-line relative-humidity meter (General Eastern Instruments Corp., Watertown, Mass., Model 400C) is used to monitor continuously the relative humidity of the influent air to ensure that the moisture content is below levels where water vapor is adsorbed by the bed in significant amounts.

Procedure

Pre-weighed, dry activated carbon was placed in the bed. To avoid exposing the fresh activated carbon to the unsteady-state conditions at the startup of a test, the flow of solvent-laden air was directed initially to the by-pass line (see Figure 1). As soon as steady-state conditions at the desired solvent concentrations were achieved, the flow was directed to the carbon bed and the by-pass line closed. Throughout each test the flow rate and the solvent concentration in the influent and effluent were recorded continuously. Influent temperature and relative humidity, bed temperature and pressure, and effluent temperature were monitored continuously and recorded every hour. The standard operating conditions used in this study are summarized in Table 3.

RESULTS AND DISCUSSION

Applicability of Wheeler and Robell's Equation

Breakthrough data for the four representative solvents studied were obtained at different weights of activated charcoal, ranging from 200 to 600 grams. In the experimental system used, this corresponds to bed heights of 5.3 to 16.0 cm. Experimental data points are shown in Figures 2, 3, 4, and 5 as semilogarithmic plots of C/C_o against time for *n*-butanol, xylene, Cellosolve acetate, and 2-heptanone. For each solvent, the experimental data points were fed to a computer and a non-linear least-squares routine [*13*] was utilized to estimate the best values of the kinetic adsorption capacity and the adsorption-rate constant to be used with Equation (1). The solid curves shown in Figures 2 to 5 were calculated using Equation (1) and the two best-fit kinetic parameters for each solvent. The values of these parameters are listed in Tables 4 and 5, column 1. As can be seen in the figures, reasonable breakthrough time estimates can be obtained from Equation (1) up to a carbon-bed effluent concentration as high as 50 percent of the inlet concentration. This result is reasonable if one considers the net driving force for vapor adsorption. In the case of vapor adsorption on activated carbon, we can write:

$$\frac{dp}{dt} = -k_A(p - p^*) \qquad (8)$$

TABLE 3. STANDARD OPERATING CONDITIONS

Flow rate, liter/min	283 ± 5
Superficial linear velocity, cm/sec	58 ± 1
Influent concentration, ppm	365 ± 10
Bed temperature, °C	25 ± 2
Bed pressure, mm Hg	737 ± 2
Relative humidity, %	40

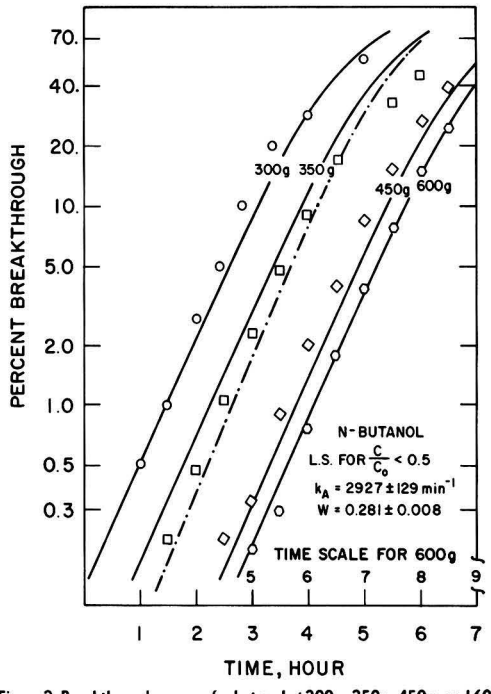

Figure 2. Breakthrough curves of *n*-butanol at 300 g, 350 g, 450 g, and 600 g weight of carbon bed. Points are experimental results. Solid curves are non-linear least-square fit of Equation (1) to experimental data. Broken curve—predicted breakthrough curve at 350 g, based on Equations 1 and 15.

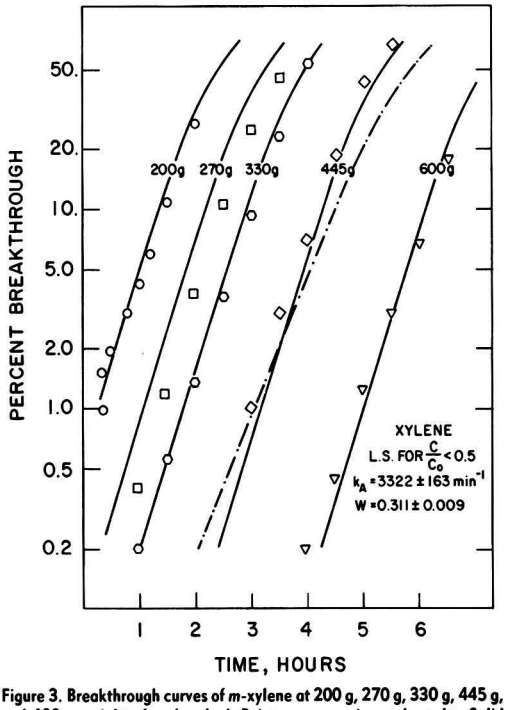

Figure 3. Breakthrough curves of *m*-xylene at 200 g, 270 g, 330 g, 445 g, and 600 g weight of carbon bed. Points are experimental results. Solid curves are non-linear least-square fit of Equation (1) to experimental data. Broken curve is predicted breakthrough curve at 445 g, based on Equations 1 and 15.

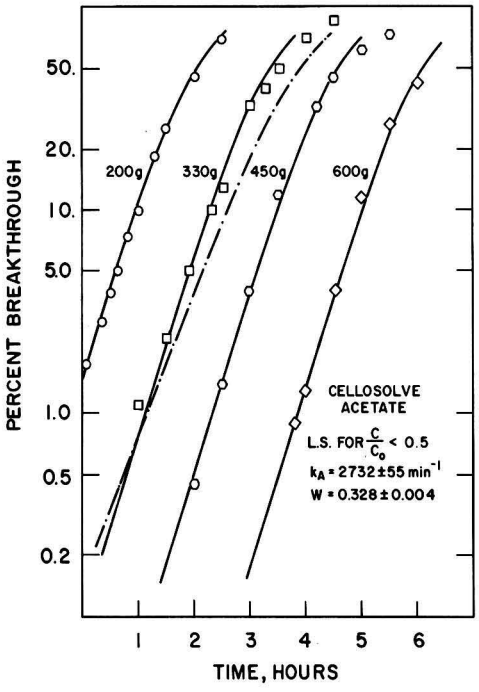

Figure 4. Breakthrough curves of Cellosolve acetate at 200 g, 330 g, 450 g, and 600 g weight of carbon bed. Points are experimental results. Solid curves are non-linear least-square fit of Equation (1) to experimental data. Broken curve is predicted breakthrough at 330 g, based on Equation 1 and 15.

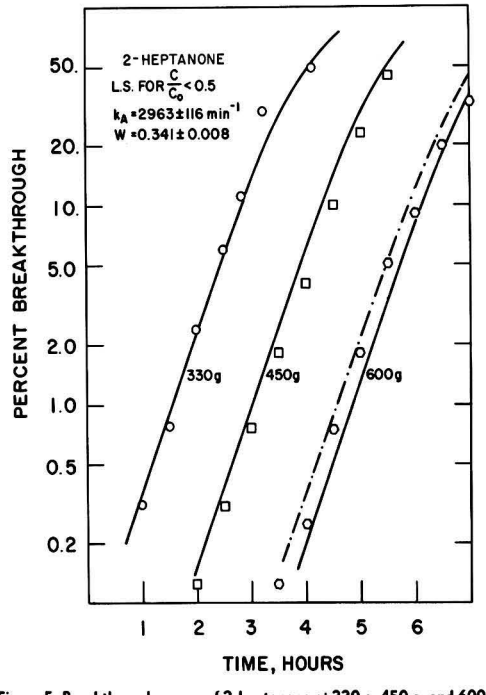

Figure 5. Breakthrough curves of 2-heptanone at 330 g, 450 g, and 600 g weight of carbon bed. Points are experimental results. Solid curves are non-linear least-square fit of Equation (1) to experimental data. Broken curve is predicted breakthrough curve at 600 g, based on Equations 1 and 15.

TABLE 4. ADSORPTION CAPACITY OF ORGANIC SOLVENTS ON COLUMBIA JXC ACTIVATED CARBON

Solvent concentration: 365 ppm
Carbon bed temperature: 25°C
Carbon bed pressure: 737 mm Hg

	Kinetic Capacity gm/gm carbon	Equilibrium* Capacity gm/gm carbon	% Error
n-Butanol	0.281 ± 0.008	0.288	−2.5
m-Xylene	0.311 ± 0.009	0.337	−7.7
Cellosolve Acetate	0.328 ± 0.004	0.380	−13.7
2-Heptanone	0.341 ± 0.008	0.325	+4.9

* Reference [2].

TABLE 5. ADSORPTION RATE CONSTANTS FOR VARIOUS SOLVENTS ON JXC CARBON

	Experimental sec^{-1}	Calculated* sec^{-1}	Error Percent
Butanol	48.8 ± 2.2	54.1	+10.9
m-Xylene	554. ± 2.7	46.6	−13.3
Cellosolve Acetate	45.5 ± 0.92	43.0	−5.6
2-Heptanone	49.4 ± 1.9	46.7	−5.3

* Using Equation (15).
Adsorber operating conditions: V_L = 58 cm/sec
d_P = 0.37 cm
ϵ = 0.457
$\frac{\mu}{\rho}$ air, 25°C = 0.155 cm^2/sec

where p is the partial pressure of adsorbate over the activated carbon, and p^* is the partial pressure of adsorbate in equilibrium with the adsorbate loading of the carbon. Simple calculations using the Polanyi-Dubinin adsorption isotherm [9] and the Dubinin constants for the carbon used [2] show that, for all four solvents considered in the study, the equilibrium partial pressure of solvent p^* above the carbon corresponds to a vapor concentration of less than 3 ppm until the carbon has adsorbed at least 70 percent of its ultimate capacity in equilibrium with the solvent concentration at the inlet of the bed. Thus, for most of the adsorption time, p^* is negligible compared to p, and Equation (8) cannot be distinguished from first-order adsorption with no desorption. Our calculations using Dubinin's correlation to calculate the equilibrium pressures of fourteen different paint solvents indicate that desorption pressures are likely to be negligible for the conditions found in paint spray booths, i.e., 100 to 2000 ppm solvent concentration when compared to adsorber inlet pressures until the carbon has picked up at least fifty percent of its equilibrium capacity of solvent. Equation (1), therefore, is likely to be generally valid for predicting reasonable adsorption breakthrough times.

As discussed in the section on adsorption kinetics, the initial breakthrough of paint solvents can be described by Equation (4). The useful range of this equation can be seen by referring to Figures 2 to 5. Resonably straight lines can be drawn through the experimental data points shown in these figures, up to a C/C_o of about 0.1. This indicates that the adsorption-rate constant of a given solvent does not vary significantly in that range of solvent breakthrough, as suggested by Equation (4). Based on Equation (4), and following the procedure suggested by Jonas and Rehrmann [6], adsorption-rate constants were determined for the four solvents. The respective values of these constants for butanol, xylene, Cellosolve acetate, and 2-heptanone are 49.4, 56.0, 45.8, and 49.3 sec^{-1}. These values are practically the same as those obtained by using Equation (1) (see

Table 5, column 1). Thus, it appears that Equation (4) can be used to describe solvent breakthrough with a reasonable degree of accuracy up to about $C/C_o = 0.1$.

Kinetic Adsorption Capacity

The least-squares values and 2 sigma confidence limits (estimated by linearization for the individual parameters) obtained for the kinetic adsorption capacity of the four solvents studied on JXC carbon are presented in Table 4. The experimental equilibrium adsorption capacity for the same solvents on JXC carbon, obtained in a previous study [2], is also shown in the table. As can be seen in Table 4, the agreement between the experimental values of the equilibrium adsorption capacity and the values calculated assuming first-order kinetics is very good. The maximum difference observed is 13.7 percent for Cellosolve acetate. The good agreement observed indicates that, in the absence of actual breakthrough data, the kinetic equilibrium capacity may be safely approximated using the Dubinin-Polanyi correlation, which was found to predict well the equilibrium adsorption capacity of various paint solvents [2]. Similar results were obtained by Jonas and Rehrmann [6, 8].

Adsorption Rate Constant

When mass transport from the flowing airstream to the surface of the adsorbent particles limits the adsorption rate, it can be shown that the adsorption-rate constant, k_A, is related to the gas mass-transfer coefficient, k_G, by the equation [14]:

$$k_A = \frac{k_G a P V_L}{G_m} \tag{9}$$

where a is the external sorbent particle surface per unit volume of adsorber; P is the total pressure; V_L is the superficial linear gas velocity; and G_M is the molar velocity of the solvent entering the adsorber (in moles per unit time per unit of adsorber cross section).

Most correlations used to relate the gas mass transfer coefficient, k_G, to the other system parameters use the Colburn and Chilton [15] mass-transfer factor j_D defined as:

$$j_D = \frac{k_G P}{G_M} \cdot \left(\frac{\mu}{\rho D_{AB}}\right)^{2/3} \tag{10}$$

where the term in parenthesis is the Schmidt number, Sc, of the flowing gas stream and is the ratio of the kinematic viscosity of the gas (i.e., viscosity, μ, divided by the density, of the flowing gas) to the diffusivity, D_{AB}, of the solvent in the gas stream. Inserting Equation (10) into (9) one obtains the expression

$$k_A = a V_L j_D \left(\frac{\mu}{\rho D_{AB}}\right)^{-2/3} \tag{11}$$

Several correlations are available relating the Colburn and Chilton factor, j_D, to the superficial linear velocity in packed beds of particles [16]. The most recent correlation, derived by Hsieng and Thodos [17], takes the form:

$$j_D = \frac{0.48}{\epsilon(\mathrm{Re})^{0.39}} \tag{12}$$

where ϵ is the void volume fraction in the adsorber, and Re is the Reynolds number of the flowing gas stream, defined as

$$\mathrm{Re} = \frac{d_P V_L \rho}{\mu} \tag{13}$$

where d_P is the average particle diameter in the bed.

The specific surface per unit volume of adsorber, a, is a function of the adsorbent particle size, d_P, and of the volumetric void fraction of the adsorbent bed. For spherical particles and for cylindrical pellets with a length equal to the diameter, it is [16]:

$$a = \frac{6(1-\epsilon)}{dp} \tag{14}$$

Substitution of Equations (12), (13) and (14) into (11) yields the following expression:

$$k_A = 2.88 \frac{(1-\epsilon)}{\epsilon} \frac{V_L}{d_P} \left(\frac{\mu}{d_P V_L \rho}\right)^{0.39} \left(\frac{\rho D_{AB}}{\mu}\right)^{2/3} \tag{15}$$

The least-squares values of the kinetic adsorption-rate constant for the four solvents are compared with the values calculated using Equation (15) in Table 5. As seen in the table, the agreement between experimental and calculated values of the rate constant is excellent. The use of Equation (15) produced estimates of k_A with an average error of 8.8 percent and a maximum error of 13.3 percent. In view of this very close agreement, it appears that mass transfer from the gas stream to the surface of the charcoal particles limits the adsorption rate for conditions encountered in proposed activated-charcoal adsorption systems for control of hydrocarbon emissions from paint spray operations.

Prediction of Breakthrough Curves

In previous paragraphs, we have discussed how the kinetic adsorption capacity and the pseudo-first-order adsorption-rate constant obtained by correlating experimental data with Equation (1) are related to the equilibrium capacity of the carbon for given solvents and the Colburn and Chilton dimensionless mass-transfer factor j_D. The relationship obtained, if suitable for predicting breakthrough curves, can be a simple but powerful tool for designing carbon adsorption systems where actual experimental breakthrough data are not available. In order to determine whether Equation (1), together with Equation (15), may be used to predict reasonable breakthrough times, we have used these equations and experimentally determined equilibrium adsorption capacities of the individual solvents in the carbon used to calculate the dashed curves shown in Figures 2 to 5. As can be seen on these figures, the predicted breakthrough curves are in very good agreement with experimental data. Note that the equilibrium adsorption capacity can also be estimated very well using the Dubinin-Polanyi isotherm and estimates of the solvent-carbon affinity coefficient based on the electronic polarizability of the solvent [2]. Thus, for single solvents it is possible to make reasonable estimates of the required size of a carbon-adsorption air-pollution control system if knowledge of the physical and adsorptive properties of the activated carbon to be used are available. Equations (1) and (15) require only a knowledge of the physical and transport properties of the flowing gas stream and these are usually available in the literature or may be estimated for most solvents currently in use or being considered for automotive paint spray systems.

CONCLUSIONS

The results of a study of the adsorption kinetics of single solvents in a fixed-bed activated-carbon adsorber show that:

1. The adsorption of a solvent vapor on activated carbon follows pseudo-first-order kinetics up to about 50% breakthrough. Up to this value, the Wheeler-Robell equation (1) may be used to describe the breakthrough curve with reasonable accuracy.
2. The rate of adsorption is limited by diffusion from the gas stream to the surface of the carbon particles. The adsorption-rate constant can be estimated with good

accuracy from available correlations of mass-transfer coefficient for diffusion in gases.
3. The agreement between the experimental values of the equilibrium adsorption capacity and the values calculated assuming first-order kinetics is very good. Both can be estimated from the Dubinin-Polanyi correlation.
4. For single solvent vapors it is possible to make reasonable estimates of the size of the carbon-adsorption unit required for a given emission control need, and to predict the breakthrough curves from the transport properties of the solvent and the physical and adsorptive properties of the activated carbon.

ACKNOWLEDGMENT

The authors express their appreciation to E. Beckwith and T. Riley for their helpful suggestions and assistance in the chemical analyses.

NOTATION

a = external sorbent particle surface per unit volume, cm^2/cm^3
C = solvent concentration in effluent gas, g/cm^3
C_o = solvent concentration in influent gas, g/cm^3
d_P = sorbent particle size, cm
D_{AB} = diffusivity of solvent in air, cm^2/sec
G = weight of activated carbon in bed, g
G_m = molar velocity of solvent in influent gas, mole/sec · cm^2
k_A = adsorption rate constant, sec^{-1}
k_G = mass transfer coefficient, g-mole/sec · cm^2 · atm
N_T = number of transfer units in adsorbing bed
p = partial pressure of solvent vapor in air, atm
p^* = equilibrium partial pressure of adsorbed solvent, atm
P = total pressure in bed, atm
Q = volumetric flow rate of air through bed, cm^3/sec
Re = Reynolds number
t = time, sec
t_s = stoichiometric adsorption time, sec
V_L = superficial linear velocity in bed, cm/sec
W = adsorption capacity of carbon, g solvent/g carbon
ϵ = void fraction in bed
ρ = density of air, g/cm^3
ρ_b = bulk density of activated carbon, g/cm^3
μ = viscosity of air, poise

LITERATURE CITED

1. Juhola, A. J., "Package Sorption Device System Study," EPA Publication PB-221138 (1973).
2. Golovoy, A., and J. Braslaw, "Adsorption of Automotive Paint Solvents on Activated Carbon: I. Equilibrium Adsorption of Single Vapors," APCA J., **31**, No. 8 (1981).
3. Heister, N. K., and T. Vermeulen, *Chem. Eng. Progr.*, **48**, 505 (1952).
4. Jonas, L. A., and W. J. Svirbely, *J. Catal.*, **24**, 446 (1972).
5. Wheeler, A., and A. J. Robell, *J. Catal.*, **13**, 299 (1969).
6. Jonas, L. A., and J. A. Rehrmann, *Carbon*, **10**, 657 (1972).
7. Jonas, L. A., and J. A. Rehrmann, *Carbon*, **12**, 95 (1974).
8. Jonas, L. A., and J. A. Rehrmann, *Carbon*, **11**, 59 (1973).
9. Dubinin, M. M., "Chemistry and Physics of Carbon," Vol. 2, pp. 51-120, Marcel Dekker, New York (1966).
10. Emmett, P. H., "Catalysis," Vol. II, p. 150, Reinhold Publishing Co., N.Y. (1955).
11. Lugg, G. A., *Analytical Chemistry*, **40**, No. 7, 1072 (1968).
12. Reid, R. C., and T. K., Sherwood, "The Properties of Gases and Liquids," pp. 531-532, McGraw-Hill Book Co., N.Y. (1966).
13. Stewart, W. E., "LS—Nonlinear Least Squares Fitting and Function Minimization," Chemical Engineering Dept., Univ. of Wisconsin, Madison (1966).
14. Satterfield, C. N., and T. K. Sherwood, "The Role of Diffusion in Catalysis," pp. 35-36, Addison-Wesley Publishing Co., Reading, Mass. (1963).
15. Chilton, T. H., and A. P. Colburn, *Ind. Eng. Chem.*, **26**, 1183 (1935).
16. Hougen, O. A., and K. M. Watson, "Chemical Process Principles, Part Three: Kinetics and Catalysis," pp. 982-995, J. Wiley and Sons Inc., N.Y. (1947).
17. Hsieng, T. H., and G. Thodos, *Int. J. Heat Mass Transfer*, **20**, 331 (1977).

The New Physiology of Odor

New discoveries show that olfactory receptor physiology differs greatly from that of other senses and can explain many experimental phenomena.

Robert C. Gesteland, Northwestern University, and TASC Group, Inc., Evanston, Ill. 60201

Odors can affect animals via three pathways, the olfactory receptor organ, the vomero-nasal organ (which is vestigial in man but probably important in mating behavior in some species), and the bare nerve endings in the mouth and nose which are from that nerve which provides general sensory information from the head. Most odor sensations arise in the olfactory receptors, nerve cells located in the nasal cavity which are excited by a large number of chemical substances, often at exceedingly low concentrations. Odor perception adapts rapidly. The intensity of the sensation declines with continued exposure to the odor source. The time course for adaptation and recovery when the odor source is removed is measured in minutes or hours. There may also be a longer lasting process which suppresses odor sensations. Anecdotal evidence exists for a condition sometimes called occupational anosmia, in which individuals are insensitive to odors characteristic of their own workplace but not to odors of different compositions and similarly low concentrations in other chemical environments. The effects appear to last for weeks. Little is known about long-term odor sensitivity changes, whether occurring spontaneously or induced by processes external to the body. Recent discoveries lead me to speculate that both conventional adaptation and long-term sensitivity changes are related to growth processes in the olfactory sensory neurons, a situation quite different from that which occurs in the other sensory organs.

ISSN 0278-4491-82-5845-0094-$2.00.

OLFACTORY EXCITATION

The sequence of events which leads to excitation of the olfactory receptor includes inspiration of odor vapor-laden air into the nasal cavity, solution of the vapor into the watery mucus which separates the sensory epithelium from air, diffusion to the surface of the fine ciliary processes which project from the receptor nerve cell, and interaction with the ciliary macromolecules of the membrane to effect a change in ionic permeability properties of the membrane. There are of the order of 10^8 neurons in the patch of tissue in the nose which constitutes the olfactory receptor organ. Each cell responds to many different chemical substances, but different cells are responsive to different subsets of the group of chemicals which smell. A persistent and unsolved problem has been to characterize these subsets and from this to derive a description of the way in which complex mixtures are resolved into different perceptions.

The sensations mediated by the bare nerve endings of the sensory nerve which are found throughout the mucous membranes of the nasal and oral cavity are called the common chemical sense. These are thought to be rather non-specific and evoked by higher concentrations of substances than those which stimulate the olfactory organ. The nerve endings are not in such close contact with the inspired air, since they are separated from it by a layer of epithelial and connective tissue cells as well as the overlying mucus. The role commonly attributed to this odor-sensing system is that of signalling high and potentially damaging chemical substance concentrations.

Two generalizations characterize the current state of our knowledge about the physiological effects of odors and the processes which mediate odor perception. First, we know appallingly little about any aspect of the chemistry and physiology of olfaction. Second, recent discoveries provide some clues to the wrong turns of the past and we now have exciting new hypotheses and fresh experimental avenues to test them [*1*].

WHAT CAN WE SMELL?

What is the present state of odor physiology? Most evident is that we can provide no precise answer to the question "What can man smell?" There is no complete list of odorous chemical compounds, nor accepted values of the mean concentrations for detection for most of them for the average human. Thus, we have no precise way of assessing whether your particular nose is a typical one or whether you have enhanced or reduced function. It is of course possible to determine if a person is grossly deficient but this is hardly an accomplishment of pride. It is roughly equivalent to limiting vision characterization to determination of whether or not an individual can see light or color at all. Current methods of assessing olfactory acuity are so dependent upon the experimental context and show so much variability from one individual to the next that a standard for human sensitivity to odor cannot be written.

There have been many attempts to group odorous substances into categories, where all substances in a particular group are similar in some way. There is general lack of agreement between any two of the proposed schemes and, as a result, no accepted theory which can relate perceptual attributes to physical structure or chemical reactivity of odorous substances. Significant success has been achieved when working within narrowly limited molecular classes. The synthetic fragrance industry works extensively studying the effects of substitution of reactive groups and isomeric rearrangements to achieve modified odor properties [2]. However, since there is no accepted set of relationships between odor chemistry and the physiology of membrane receptor sites, the successes of the fragrance synthesizers are not yet guides to determination of the mechanism. Some progress has been made in the search for individuals with deficient sensitivity to certain groups of compounds [3]. If such deficits can be inherited, a key to the basis for molecular discrimination would exist.

Odor-profile descriptions, in which individuals are asked to select those adjectives from a long list which characterize the odor of a particular compound, have also proved to be technologically useful [*4*]. However, correlations among performances of different individuals are low, which suggests that sociological processes involving learning about odors are not easily eliminated. As a result it has not been possible to find which aspects of the profiles obtained are measures of physiological processes and which are acquired by social interactions.

Psychophysical studies on odor similarities using multidimensional scaling methods show that a single parameter, pleasantness, is more important than all other aspects of sensory experience [5]. One hopes that clues to the chemical processes involved in olfactory sensation will appear in a more useful form than this.

ADAPTATION PHENOMENA

Careful investigation of adaptation phenomena are similarly confounding. Continuous exposure to a particular odor at a fixed concentration causes a progressive reduction in sensitivity to that odor. When the odor ceases, sensitivity recovers. Exposure to one odor also reduces sensitivity to a variety of other odors but this reduction in sensitivity is always less than the decrease in sensitivity to the adapting odor. Other sensory-organ systems show similar phenomena and analysis of such experiments has been of fundamental importance in determining the underlying processes involved. For example, the adsorption spectra of the pigments mediating color vision were accurately predicted from adaptation data long before it was possible to make spectrophotometric measurements on single receptor neuron pigments. However, olfactory cross-adaptation experiments show that the phenomenon is generally not reciprocal. Exposure to odor B reduces sensitivity to odor A by a different function than exposure to A reduces sensitivity to B. This non-reciprocity is not characteristic of the other senses.

Early goals of determining the nature of receptor sites were based upon the notion that those substances showing cross adaptation act on the same receptor sites. Absence of cross effects would indicate that different receptors are involved. The discovery of the complexity of cross adaptation dimmed hopes for simple determination of receptor mechanisms.

NEUROPHYSIOLOGY

When psychophysical methods result in ambiguity and complexity, sensory science looks to neurophysiology, cell biology, and biochemistry for dissection of the process into its components. Of these, only neurophysiological data existed in significant amounts until recently. However, explorations of the nose with microelectrodes to learn about the messages in the sensory neurons did not fulfill the hope of untangling the puzzle. Instead it increased the chaos [6]. A measure of the response of the population of receptor neurons is the voltage change at the surface of the receptor epithelium. The magnitude of the voltage change evoked by an odor increases with the log of the odor concentration [7]. It results because the effect of the stimulus on the receptor membrane is to increase membrane permeability and the resulting ionic current flow produces a voltage across the resistance of the tissue. The magnitude of the effect changes in an orderly way for compounds in a homologous series. However, there is little correlation between the magnitude of the responses of two radically different substances and their perceived intensities. Adaptation is small. Repeated presentations of a stimulus evoke

identical responses. This suggests that adaptation is occurring higher in the brain.

It is also possible to use small electrodes to measure the responses in single receptor neurons. Early results from such experiments showed that each cell responded to a wide variety of substances and that substances in the group affecting one cell were usually not identical to those in the group affecting another cell. Unlike the voltage-change measure, however, many receptor cells became insensitive to a stimulus if it was repeated a few times [*8*]. Attempts to find categories of cell types failed. There is little indication that there is any small number of different cell types, and therefore little hope that electrophysiological studies on olfactory receptors will lead to an orderly model describing the ways in which the nose sorts out complex mixtures or to a basis for organization of odor perceptions into an orderly space. Again there was considerable dismay. The agreements between neural response and perception in both audition and vision presaged a similar success in olfaction. There is hope that experiments on higher levels within the olfactory brain will produce the longed-for order but studies at this level are few.

This brief summary of the recent state of the science is a worst-case view. It leaves out a large body of solid experimental work upon which real progress has been based. My point is simply that there was little hope of reconciling the disparate bodies of information in the recent past.

It seems likely to me that we are now at the dawn of the decade when we will come to understand the olfactory sense. Surprising experimental discoveries show that we erred in assuming that the biology of the sense of smell would parallel that of other sensory systems. A consensus opinion is emerging in support of olfactory research. The abilities of man to sense odors and the changes which result from aging, disease, occupational exposure to chemicals, and the environment have become interesting. Now that the questions are being asked, marked improvements in technology are appearing.

Realization that we might have been asking the wrong questions began with the discovery that the olfactory system is not static. A general characteristic of the mammalian nervous system is that the neurons of which it is constituted are irreplaceable. They develop early in life, establish connections, and perform their appropriate functions until they die. When a neuron dies, an element of the sense organ or brain is lost. The receptor neurons of the nose are the exception [*9*, *10*]. These cells are continually formed throughout life. Precursor cells migrate into the nasal epithelium, differentiate and acquire the characteristics of a nerve cell, and grow thin projections from opposite poles of the cell body. One of these extends toward the surface of the nasal epithelium. The other grows the long distance to the brain and establishes the connections with the neurons there. After a message-transmitting life of two to four weeks, the receptor neuron and its processes die and are resorbed. A new precursor cell moves in to fill the void. It is estimated that the entire life cycle is five to eight weeks in length. At any given time, a part of the population of cells in the olfactory organ is in an immature state and not in contact with the brain, another part is mature and contributing to the sensations of smell, and another part is worn out and shrinking.

NEW PROTEIN

A protein unique to the olfactory receptor neuron has been found and the time course of its appearance provides information about the events of the cell's life cycle [*11*]. In the rat fetus, olfactory receptor neurons are first seen 12 days after conception. The marker protein first appears in some of these neurons 6 days later and the rat is born 3 days after that. The first neuron processes grow to reach the brain and establish connections capable of transmitting messages at the same time as the protein appears. The protein marks those neurons which are mature and connected. The marker is seen in patches, as if several thousand nerve cells started developing at the same time. If the nasal epithelium in an adult animal is removed, it regenerates over a period of weeks. The sequence of events seen during regeneration is like that which occurs during embryonic development. We suppose that the embryo can serve as a model of the events continually occurring throughout life as the olfactory receptors are replaced.

A major change in physiological properties co-occurs with the appearance of marker protein and with connections to the brain. Responses of single neurons to odors in embryos can be measured. When we do this we find no neural activity before day 12. During the next 6 days the cells are most unusual. Each cell responds to every odorous substance we try. These young cells, though not connected to the brain, are responsive but cannot distinguish between different smells. After the marker protein appears, the cells abruptly change in sensitivity. They become highly sensitive to some compounds and insensitive to others [*12*]. Thus, only those cells which are selective and therefore useful for distinguishing one compound or mixture from another are able to contribute to the perceptual process.

Now some of the confusion of the earlier physiological experiments vanishes. The bewildering variety of response properties of single cells takes place at least partially because the electrode thoroughly intermixes the data from non-selective cells with that from selective cells. Electrodes measuring the summed ionic currents of the cell population showed little correlation between the magnitude of the response and the perceived intensity of different stimulus substances. We have found that most of the ionic currents come from that group of immature, unconnected cells which respond non-selectively [*13*]. The contribution of the selective, connected cells which constitute perceived odor signals is undetectable by the experimental method. Similarly, much of the evidence for localization of response to different compounds can be accounted for by the patchy regeneration process. There are always regions of low responsiveness where the neurons have not differentiated, other regions of generalized irritability, and still others which are selective. The experiments to determine whether or not cells receptive to a particular compound group are located near to each other now can be designed.

CILIARY PROCESSES

Another observation which may have important implications has to do with growth of the portion of the cell where the odor molecules act. The fine ciliary processes extending up into the mucus are necessary for odor reception. When they are experimentally removed, responses of the cells to odors cease. As they regrow, the response increases proportionally during the early stages of growth. The response reaches its asymptotic value when the cilia are about 25% of their mature length. What is more surprising is the rapid rate of growth of these processes (20 μm per day in the frog). Growth occurs at the base, where the cilium grows out of the cell [*14*]. One reasonable hypothesis is that the ciliary membrane receptor sites are irreversibly denatured by interaction with the stimulus and that new sites are incorporated in newly synthesized cilium membrane. Old, denatured sites are removed by their movement to the distal regions as the new membrane is generated at the base. This would account for the observation that only the proximal parts of the cilia contribute to the response. The growth rate is fast enough to account for adaptation processes. Non-reciprocal cross-adaptation may simply reflect a differential rate of synthesis of receptor-site macromolecules.

METABOLIC CHANGES

There is evidence that long and continued exposure to odors causes changes in structure and metabolism of areas of the olfactory brain to which groups of receptors project [*15, 16*]. There are also observations that many commonly-encountered organic vapors physically disorganize the structure of the olfactory receptor neurons. The time courses of these effects are measured in weeks, not hours. Here we are probably seeing expression of the normal process of cell replacement. In a mammal, new neurons functionally connected to the brain should be available about 3 weeks after the pathologically active odorous source is removed. If occupational anosmia is real, it will be interesting to measure the period of time required for the restoration of normal function.

GROWTH PROCESSES

Thus there are two growth processes available which must be considered in interpreting experimental data. The rapid one, cilia extension, can replace a receptor membrane in an otherwise healthy cell. The slow one replaces the whole cell. The nose may well be one of the best assay tissues for potential chemical toxicity. It is one of the first tissues contacted by vaporous substances. Effects can be detected by microscopic observation of living, unstained tissue. There are built-in systems which repair the damage.

Emerging advances in technology promise significant improvements in experimental methods. Techniques have been developed for growing functional olfactory receptor organs and parts of the olfactory brain in culture chambers using precursor tissues from early embryos [*17*]. Dissociated cells from the receptor organ and from the brain can now be grown in cell culture and the processes which occur as they connect to each other can be directly observed [*18*]. The mature receptor organ can be dissociated into separate, living cells and the membrane surface biochemistry and biophysics can be studied [*19*]. Two new olfactometric methods have been described which, taken together, may allow olfactory acuity testing that is as dependable and simple as tests for auditory and visual acuity. A scratch-and-sniff microencapsulation method will allow rapid screening for sensitivity to a large number of compounds [*20*]. A monolayer desorption olfactometer delivers a wide range of accurately known vapor concentration without the complex equipment required for accurate vapor-phase dilution and liquid dilution methods [*21*].

We know very little about the physiological effects of odors. Recent discoveries are likely to change this situation in the near future.

This work was supported in part by NSF Grant No. BNS 78-17479 and NIH Grant No. NS-14663.

LITERATURE CITED

1. Mair, R. G. and R. C. Gesteland, "Processes in Olfactory Reception," "Cosmetic Science," Vol. 2 (M. M. Breuer, ed.), pp. 83-123, Academic Press, N.Y. (1980).
2. Beets, M. G. J., "Structure Activity Relationships in Human Chemoreception," Applied Science, London (1978).
3. Amoore, J. E., *Nature*, **214**, 1095-1098 (1967).
4. Dravnieks, A., *et al.*, *Chem. Senses Flavour*, **3**, 191-225 (1978).
5. Woskow, H. M., in "Theories of Odour and Odour Measurement," (N. Tanyolac, ed.), Roberts College, Istanbul, pp. 147-189 (1968).
6. Lettvin, J. Y. and Gesteland, R. C. *Cold Spring Harb. Symp. Quan. Biology*, **30**, 217-225 (1965).
7. Ottoson, D., in "Handbook of Sensory Physiology" (L. Beidler, ed.), Vol. IV, Part I, pp. 95-131 (1971).
8. Gesteland, R. C., in "Structure-Activity Relationships in Chemoreception" (G. Benz, ed.), pp. 161-168, Information Retrieval, London (1976).
9. Graziadei, P. P. C., *Tissue and Cell*, **5**, 113-131 (1973).
10. Moulton, D. G., *Ann. N. Y. Acad. Sci.*, **237**, 52-61 (1974).
11. Farbman, A. I. and F. L. Margolis, *Dev. Biol.*, **74**, 205-215 (1980).
12. Gesteland, R. C., *et al.*, *Olfaction and Taste*, **7**, 143-148 (1980).
13. Adamek, *et al.*, *Soc. Neurosci. Abstr.*, **6**, 243 (1980).
14 Mair, R. G., *et al.* (in press) (1981).
15. Pinching, A. J. and K. B. Doving, *Brain Res.*, **82**, 195-204 (1974).
16. Greer, C. A., *et al.*, *Soc. Neurosci. Abstr.*, **6**, 306 (1980).
17. Farbman, A. I. and R. C. Gesteland, *Olfaction and Taste*, **5**, 107-110 (1975).
18. Farbman, A. I., personal communication (1981).
19. Kleene, S. J. and R. C. Gesteland, *Brain Res.*, **229**, 536-540 1981.
20. Doty, R. L., personal communication (1981).
21. Gesteland, R. C., *et al.*, *Olfaction and Taste*, **7**, 463-464 (1981).

Robert Gesteland is Professor in the Department of Neurobiology and Physiology at Northwestern University in Evanston, Ill., and is President of the Taste and Smell Consulting Group, Inc. He is the holder of B. S. and S. M. degrees in Electrical Engineering from the University of Wisconsin and M.I.T., respectively and a Ph.D. in Neurophysiology from M.I.T. His research is on the biophysical and cellular processes involved in the sense of smell and on measurement of olfactory responses within the nervous system.

Regulatory Approaches to Odor Control

Is it possible to enact workable regulations covering odor emissions? Here's how it has been done in Texas.

Jeanne Philquist, Texas Air Control Board, Austin, Texas 78723

APPROACHES TO ODOR CONTROL

Regulatory control of odor has traditionally been the responsibility of state and local governments. While regulatory approaches vary, methods typically have included one or more of the following: control under general nuisance regulations, control by establishing specific compound limits, and/or control by establishing odor intensity standards and ambient measurement techniques. Each method has advantages and disadvantages.

Public nuisance regulations enable official investigation and public prosecution of cases that otherwise would be left to prosecution in the private sector. Additionally, testimony of complaining witnesses can serve as convincing evidence that a community annoyance in fact exists. Arguments, however, have been advanced that nuisance law should be supplemented by more scientific and more comprehensive regulatory approaches to odor control.

Some control agencies have been successful in establishing specific emission limitations for odorous compounds. Difficulties in enforcement, however, have been cited for compounds with low odor thresholds and certain industries have claimed that such limitations are discriminatory. It also can sometimes be difficult to correlate specific emission limits with the prohibition of community annoyance.

The third regulatory approach depends on sensory evaluation of odors in the ambient air. A violation, for example, may be documented if the odor is still detectable after a given number of dilutions with equal volumes of clean air. Another approach to quantified measurement is to reference or match the odor intensity of an air sample to a known compound at a given standard. These approaches have clear advantages over general nuisance regulations; they also have been criticized as arbitrary, unfair, or unreasonably expensive. Problems cited are with establishing a link between standards or dilution factors selected and community annoyance, with obtaining ambient air samples, and with assuring the objectivity of observers or odor panels.

A number of state and local agencies have begun experimenting with these and other defined methods for measuring odor. Model odor control ordinances have been proposed which rely on weighting factors such as odor intensity, duration, frequency, offensiveness, time of day, and so forth, which are combined in a formula to yield an "odor perception index" for establishing the magnitude of the annoyance. Another approach that has been proposed would rely essentially on public-attitude surveys in affected communities and with control groups to establish both the existence of a community odor problem and the success of efforts to cure it. Both methods have been cited as meritorious in attempting objective determination of community annoyance, although the former lends itself to criticism for being arbitrary, and the latter for being time consuming and unwieldy as a mechanism for regulatory control [*1*].

STUDIES REQUIRED BY FEDERAL CLEAN AIR ACT AMENDMENTS

Congress, in passing 1977 Federal Clean Air Act Amendments, asked EPA to investigate federal control of odors. Section 403(b) of the 1977 Federal Clean Air Act Amendments required EPA to conduct a study and prepare a report to Congress on the effects on public health and welfare of odors or odorous emissions, the sources of such emissions, the technology or other measures available for control of such emissions, the costs of such technology or measures, and the costs and benefits of alternative measures or strategies to abate such emissions. Congress required the report to include an evaluation of whether air-quality criteria or national ambient air-quality standards for odors should be established under the Federal Clean Air Act, and to determine other strategies or authorities under the Clean Air Act that are available or appropriate for abating such emissions. In response, two reports were prepared, one by the National Academy of Sciences (NAS) under contract to EPA, and one by EPA based on findings of the NAS. Both were presented to Congress on February 19, 1980.

NAS REPORT: ODORS FROM STATIONARY AND MOBILE SOURCES

This report was prepared in 1979 to assist EPA in determining the effects of odors and odorous emissions on public health and welfare and in analyzing strategies or authorities available or appropriate under the Federal Clean Air Act for abating such emissions. The report provides considerations on whether and under what circumstances odorant sources should be controlled in order to reduce the effects of perceived odors. NAS found no clear-cut answer to the question posed by Section 403(b) of the Federal Clean Air Act as to whether national ambient air-quality standards should be established for odorous substances. NAS did, however, find the subject of odor control to be ". . .riddled with uncertainties of methodology, of measurement, of perception and of social preference" [2].

Three approaches to federal odor regulation under the Clean Air Act are posed and evaluated in the report: establishment of national ambient air-quality standards, establishment of performance standards for new and existing sources, and odor control through economic incentives. The report queries, "To what extent is federal intervention justified at all in a field where nuisance law and local and

ISSN 0278-4491-82-5641-0098-$2.00.

state ordinances have been the traditional modes of regulation?" Conclusions included that it would be burdensome to control odors through the State Implementation Plan process and that uniform national standards may leave too little room for variable community preferences. Justifications for federal odor standards cited in the report are the resolution of jurisdictional disputes, the uniform control of industrial growth, and the protection of public health. NAS found uncertainties associated with odor control to protect public health and recommended further research in this area.

The NAS summarized its assessment as follows:

□The legal treatment of odor problems has come a long way from judicial applications of time-honored nuisance doctrine to laws increasingly based on quantitative measurement. There is no getting around the fact, however, that odors are perceptions whose intensity, impact, and significance are difficult to assess. If we are to get beyond the subjectivities and vagaries of classical nuisance law, it will be necessary to determine acceptability of odors through quantitative measures or qualitative comparisons that can be repeated, without loss of validity or reliability, at different times and in different places. These capabilities are essential to establishing a sound technical basis on which to set ambient or emission standards for odors under federal, state, or local law [3].

Following are recommendations contained in the NAS report.

First, the adverse effects of odors on human beings are variable, and knowledge about the effects is very incomplete. Thus it would be difficult to devise widely accepted standards. Second, although odor perception can be assessed and some odorous substances can be measured by modern instrumental methods, the two sets of results are difficult to relate to each other. Furthermore, the methods are costly and time-consuming.

If, in spite of these problems, federal ambient air-quality or emission standards for odors were to be established, NAS's recommended approach would incorporate the following features:

- The standard should be related to a measurement of odor perception and expressed in terms of the perceived magnitude, or intensity, of the odor. Intensity should be assessed by comparing it with that of a specified concentration of a standard reference odorant.
- Duration and frequency of exposure to odor are important determinants of human response, and should be taken into account in the establishment of standards.
- Offensiveness or inoffensiveness of a given odor is also an important determinant of human response. Consideration should be given to specifying exemptions or relaxations of standards when an odor is known to be inoffensive.
- Exemptions also should be considered for industries in areas far from population centers or in cases where odor abatement is excessively expensive.
- Finally, special types of odor standards for agricultural and mobile sources should be defined [4].

In recognition of the difficulties that would confront the establishment of federal ambient air-quality or emission standards for odors, NAS concluded that various kinds of studies are needed. Specifically, NAS found that more basic research and scientific information is needed on the effect of odors on humans, and animals where relevant, and on the mechanism whereby the presence of an odorous airborne contaminant is translated to neural signals that result in odor perception. NAS also concluded that studies were needed on individual sensitivity to odors, to identify differentially sensitive subgroups of the population, and on odorant dispersion modes to improve currently available mathematical dispersion models. Attention should also be given to duration and magnitude of human exposures resulting from the release of odorous matters to the atmosphere, and on differences between point, area, and mobile sources, according to the report [5].

U.S. EPA REPORT TO CONGRESS

EPA's report provides a survey of current state and local odor regulations, evaluates the effectiveness of regulations that would be candidates for promulgation under the Federal Clean Air Act, and evaluates advantages and disadvantages of alternate Clean Air Act regulatory strategies. The report concludes that federal regulatory involvement in odor control does not appear to be warranted for the following reasons:

- Odors are not caused by a single pollutant, but rather are a subjective perception which may result from differing combinations of numerous odorants. It is therefore difficult to associate any specific health or welfare effect to a given odor concentration.
- Measurement techniques are considered generally inadequate for regulatory purposes.
- Methods to correlate ambient odor levels to a defined community annoyance level are not always reliable.
- Community tolerances or odor annoyance levels vary widely [6].

EPA also found problems with requiring Best Available Control Technology (BACT) as an odor control mechanism for new or existing sources under Section 111 of the Clean Air Act. First, this approach would require best controls nationwide, whereas a source type may be a problem only in certain areas or situations. Second, it provides no guarantee that a community odor annoyance level will not be exceeded, especially where fugitive odor sources are located in close proximity to one another. Third, assessing and/or regulating all odor sources would require an inordinate expenditure of federal, state, and local agency resources that are already fully extended to meet other Clean Air Act requirements. The report concludes that local and state odor control procedures appear to be generally adequate and are probably more cost effective than a uniform national regulatory program under the Federal Clean Air Act [7].

ODOR REGULATION AND ENFORCEMENT IN TEXAS

The following comments on odor control in the State of Texas, and the Texas Air Control Board's research efforts into odor control and regulation are provided within the context of federal investigation of the subject.

TEXAS CLEAN AIR ACT

Under the Texas Clean Air Act, odors are considered air contaminants. The Act mandates that:

. . . no person may cause, suffer, allow or permit the emission of any air contaminant or the performance of any activity which causes or contributes to, or which will cause or contribute to a condition of air pollution [8].

The Act further provides that the Texas Air Control Board consider the character and degree of injury to, or interference with, health and physical property of the people; social and economic value of the source; location priority; and the technical practicability and economic reasonableness of reducing or eliminating emissions from the source in establishing regulatory control programs [9]. The Texas Air Control Board (TACB) has designed its current odor control program to strike a balance between the rights of persons to live free from offensive odors and the rights of establishments to conduct activities which, by their nature, emit a certain amount of odor.

Odor control is accomplished through the Texas Air Control Board's new source review process and under a general rule prohibiting the creation of nuisance conditions.

TACB ODOR RELATED REGULATIONS

Issuance of permits for new construction or modification is the Board's control mechanism for new sources and its most effective control measure. Legal authority for the Board's regulation on permitting new sources was provided in 1971 amendments to the Texas Clean Air Act. The regulation requires any person who plans to construct any new facility or to engage in the modification of any existing facility which may emit air contaminants to obtain a construction permit from the TACB prior to beginning work on the facility. If a permit to construct is issued, an operating permit must be applied for within 60 days after the facility has begun operating. Under this regulation, proposed facilities or modifications are required to be in compliance with all rules and regulations of the Board and with the intent of the Texas Clean Air Act, meet all applicable federal new-source performance standards and, at a minimum, utilize Best Available Control Technology (BACT) [*10*].

Through provisions of this regulation, the Board has been able to assure that odor-producing processes are adequately controlled. During new-source review, agency engineers work closely with representatives of the proposed facility to arrive at cost-effective, viable means to prevent or control potential odors. The Board has rarely experienced problems with facilities constructed and operated pursuant to one of its permits.

Odorous emissions from existing sources are controlled under TACB General Rule 101.4 governing nuisance conditions. This rule prohibits the discharge of air contaminants in such concentration or duration as are or may tend to be injurious to or to adversely affect human health or welfare, animal life, vegetation, or property, or as to interfere with their normal use and enjoyment [*11*].

TACB ODOR ENFORCEMENT

Currently, TACB staff assume that an odor nuisance does not exist unless complaints are received. Each year the Board receives three to four thousand complaints, more than half of which are odor related. TACB's long-standing policy is that all complaints are investigated. When the complaint is verified and the field inspector determines that odorous emissions are causing nuisance conditions, a notice of violation is issued and the owner or operator of the source is asked to submit a detailed plan to abate the odors within a reasonable time. After the plan is submitted and approved, TACB staff monitor progress of and compliance with the plan and, at its completion, perform an inspection and determine the final compliance status. If no valid additional complaints are received, the matter is considered resolved.

If at any time during this process it is determined that the owner or operator of the subject facility is either unable or unwilling to bring operations into compliance with Board rules and regulations, or the provisions of the Texas Clean Air Act, several enforcement options are available. In most cases, management representatives of the facility are invited to participate in an administrative enforcement conference with TACB staff and to propose measures to achieve compliance.

Formal enforcement may include direct referral to the Texas Attorney General for initiation of civil action in State District Court. Civil penalties of fifty to one thousand dollars per day of operation in violation of TACB rules may be assessed. Injunctive relief also is available and is generally obtained.

Another formal enforcement option is the issuance of a Texas Air Control Board Order, which involves a public hearing. The hearing affords an opportunity for all complainants to testify. It also provides a useful forum both to establish the severity of the odor problem and for representatives of the odor source to present the company's position before a state agency with expertise in determining both the existence of an odor problem and the control technology necessary to abate the emission source.

An advantage of the public hearing process and Board Order is that requirements of the order are essentially odor regulations with specific conditions. Violations of the Board Order are then subject to court action. If litigation becomes necessary, the court can rule on violations of the specific and quantitative standards and conditions of the order as well as the more general provisions of TACB's nuisance regulation and the Texas Clean Air Act [*12*].

ODOR RESEARCH

During the past several years, TACB has performed several reviews of the technical and policy aspects of odor regulation. In 1977, an Odor Regulation Advisory Committee was appointed. Comprised of staff and representatives of agricultural industry, the committee studied alternative approaches to controlling odor. More recently, a staff project was undertaken to review pertinent literature, consider limitations inherent in the nuisance method of odor regulation, and recommend changes in the Board's regulatory approach to odor control.

Both the advisory committee and the staff concluded that the nuisance approach system of controlling odor was as effective as any currently available, but that it could in many instances be aided by quantification of the concentrations of odorous material in the ambient air. Specific recommendations were made to study and, if appropriate, develop a quantitative odor-evaluation system using a butanol referencing method.

In March of this year the Board entered into an interagency agreement with Texas A & M University to perform a field test evaluation of a butanol referencing method. Grant funds provided by the EPA were used to design and construct a testing device suitable for field use, conduct field trials at various odor producing sources, and provide a detailed manual on procedures for conducting odor intensity evaluations. This project is scheduled for completion during July 1982. Prior to the development of any recommendation to incorporate the butanol referencing method into Board Regulations, staff will evaluate project results to assure that the method produces repeatable results, that it may be employed with a reasonable allocation of staff resources, and that measurements taken actually account for both the objectionability and intensity of the odor being measured.

GENERAL OBSERVATIONS ON ODOR REGULATION

The following comments are offered for consideration as prerequisites to a strong program of regulatory odor control.

First, a regulatory agency should have established procedures for handling complaints, including written records of all findings. As noted earlier, TACB staff investigate and report on all complaints received. Additionally, the Board's Compliance Division and Regional Offices maintain up-to-date files and chronology logs documenting the resolution of all violations of TACB rules or regulations discovered during investigation. Detailed guidelines governing compliance and enforcement matters have been developed and with few exceptions, are strictly followed.

Second, every effort should be directed toward eliminating subjective judgments in odor enforcement activities. Formal enforcement actions resulting in issuance of a Board Order and thereby establishing source specific emission limits and measurement techniques assists TACB in establishing objective bases for compliance determinations. Also, the TACB/Texas A & M contract for field testing evaluation of the butanol referencing method hopefully will give the Board capability to minimize the

need for subjective judgments by those investigating complaints.

Third, regulatory limits should not be applied before it is clearly established that an odor nuisance does exist. Some agencies accomplish this by requiring that a certain minimum number of complaints be received from different households, within a specified period of time, prior to performing an investigation. In Texas, this particular approach would not enhance the Board's regulatory efforts since many complaints are received on sources located in rural areas. Determinations of nuisance conditions or that a source has the potential to create a condition of air pollution are made on a case-by-case basis [*13*].

Fourth, various control technologies and methods are available to odor producing sources. These may be described as follows:

- Process modification,
- Dilution of the odorants in the atmosphere,
- Absorption of the odorants at ambient temperatures by dissolving them in a suitable liquid,
- Adsorption of odorants in a highly porous solid,
- Oxidation of the odorants with air, and
- Modification of the perception of the odor [*14*].

With possibly one exception, the Board strongly believes it is within the purview of the affected source, not the regulatory agency, to prescribe the technology selected. The possible exception is for the last technology cited. Caution should be exercised in consideration, and less so acceptance, of a proposal by an odor emitting source to abate odors by emitting additional compounds into the atmosphere.

Finally, cost of control techniques should be considered in imposing regulations on a source. It is important that significant investments in control equipment result in definite reductions in community annoyance, and not simply reductions in a level of odorous emissions [*15*].

LITERATURE CITED

1. National Academy of Sciences, Committee on Odors from Stationary and Mobile Sources, "Odors from Stationary and Mobile Sources," Washington, D.C. (1979), pp. 412-414.
2. *Ibid.*, p. 405.
3. *Ibid.*, p. 423.
4. *Ibid.*, pp. 8-9.
5. *Ibid.*
6. D. Kent Berry, "U.S. EPA Report to Congress on Odors: Summary," Paper No. 80-57.1 presented at the 73rd Annual Meeting of the Air Pollution Control Association, Montreal, Quebec; June, 1980, pp. 9-10.
7. *Ibid.*
8. Texas Clean Air Act, Article 4477-5, §401(a), V.T.C.S.
9. *Ibid.* §3.13.
10. Texas Air Control Board Regulations, 31 TAC Chapter 116, Revised March 20, 1980, Rule 116.3, pp. 1-10.
11. *Ibid.*, 31 TAC Chapter 101, p. 16.
12. Waid, Kenneth R., "Enforcement of Nuisance Regulations for Odor Control—Texas Experience," Paper No. 77-38.5 prepared for presentation at the 70th Annual Meeting of the Air Pollution Control Association, May 5, 1977.
13. Wiersema, JoAnn, James H. Price, and Roger R. Wallis, "Odor Project Report (Austin)," Texas Air Control Board (March, 1980), pp. 3-7.
14. National Academy of Sciences, pp. 6-7.
15. Wiersema *et al.*, p. 4.

Jeanne Ann Philquist has worked for the Texas Air Control Board in various capacities since 1978. Her current position is group leader with the Compliance Division of the Control and Prevention Program. Responsibilities include overseeing compliance and enforcement activities in six of the state's twelve air quality control regions. She also performs special research projects for the agency. A 1970 Phi Beta Kappa graduate of the University of Texas, she has been previously employed with the Texas Governor's Office as a public information officer and plans coordinator and with the Hawaii Board of Education. In college she was named 1970 Outstanding Student.

Characterization of Industrial Odors

An essentially subjective problem is attacked by the method of gas-chromatographic "sniffing." A state-of-the-art review.

Frank H. Jarke and Allan Gaynor, IIT Research Institute, Chicago, Ill. 60616

The most frequently received complaint by regulatory agencies concerns industrial odor emissions. While these odorous emissions are generally not life-threatening, they do represent the only pollutant that is humanly detectable. Therefore, in order to maintain a respectable community relationship, companies may spend millions of dollars trying to isolate and control an odor-emission problem.

The first step in the solution of any problem involves an assessment of the magnitude and nature of the problem, but how does one characterize an odor?

Odor is a little understood phenomenon that is the sensation produced by the action of certain chemicals on receptors in the nose. As a result of the lack of understanding of the processes that occur when a chemical vapor is perceived as odorous, objective measurement by analytical instrumentation alone of the magnitude and character of an odor is not possible. Therefore, the characterization of odors requires human input in the form of panels of people. While it would seem that the use of human panels does not allow for objective measurements, an understanding of the properties of odors does allow the development of measurement methodologies that do allow judgments to be made and conclusions to be drawn toward the solution of an odor problem.

There are four sensory attributes of odors; threshold, intensity, character, and quality. Threshold is the minimum amount of an odorous vapor that can be detected. It can be expressed in any convenient units, but is typically reported in parts per million or parts per billion.

Compilations of odor thresholds exist and are readily available [*1*]. The threshold of a substance is a "concensus value" in that a panel of typically eight or nine people using various olfactometers agree on the value. It is not like a boiling point and there are a number of variables that can affect the results.

ISSN 0278-4491-82-5920-0101-$2.00.

Intensity describes "how strong" an odor is. It is directly related to the concentration of the odorous substance through an empirical equation worked out by Stevens known as the Psychophysical Equation. This equation:

$$S = k\,C^n$$

describes the perception of all human sensations; taste, touch, sight, sound, and smell. The equation stated simply: "The perceived intensity is proportional to the concentration of a stimulus raised to a power." Techniques for making intensity measurements will be discussed in the next section.

Quality is the term applied to what a odor "smells-like." Odor, unlike the other senses, does not possess a language. There are names for colors, names for sounds, but no names for odors. The lack of precise words for each odor (each human can possess a familiarity with over 50,000 odors), however, does not prevent the establishment of a vocabulary for describing odors. Words such as "skunk-like", "pungent", "rose-like" and "smells like a wet dog" can all be used to describe the quality of an odor.

Hedonic Tone is used to describe whether an odor smells good or bad; is liked or disliked. Generally, all pollutant odors are undesirable because they interfere with a person's right to be free of nuisances. If you have ever passed a bakery or perfumery, the odor is generally very pleasant; however, living in that type of environment can be very annoying.

All odors are caused by chemicals and, as such, these chemicals lend themselves to the whole range of analytical measurement techniques available in the chemical laboratory today. In the next section the various sensory and analytical methodologies and their application will be discussed.

METHODS FOR EVALUATING SENSORY ASPECTS OF ODORS

Threshold

There are two basic methods for making odor-threshold measurements-STATIC and DYNAMIC. The static method is represented by the "syringe method" or ASTM standard D-1379-81. This method was one of the first methods developed for making odor-threshold determinations and a great deal of information in the literature has resulted from the use of this method. Many agencies currently specify this test method. The syringe method is a difficult test to use and requires a great deal of patience as well as rather expensive and fragile equipment.

An improvement over the static method is the dynamic method known as dynamic dilution olfactometry, [2]. The static method involves the batch dilution of an odor using glass syringes. The dynamic method involves the dilution of an odorous substance by flowing air streams. A number of methods are available commercially, and each has its own characteristics. There are at least six variables from one commercial version to the other, and the lack of standard operating technique can present problems in inter-laboratory comparisons of data; however, the use of the same techniques within one laboratory allows one to make comparisons and draw conclusions concerning an odor.

The six variables are: 1) the method of dilution, 2) olfactometer/nose interface, 3) schedule of presentation, 4) selection of panelists, 5) number of panelists and 6) data treatment. It is not within the scope of this paper to deal with each of these in depth, and the reader is referred to the recent paper by Dravnieks and Jarke [3].

The commercially available dynamic olfactometers differ in the six variables mentioned above. This produces results that can vary over as much as two orders of magnitude. Therefore, a need clearly exists for standardization in the method of operating this equipment.

Intensity

The use of intensity measurements may be a better way of attacking odor pollution problems. The odor from a factory or plant is usually perceived at many times its threshold value. Also, the knowledge of how many dilutions are required to lower an ambient odor to its threshold is not very useful in a problem solving or regulatory sense.

Three methods exist for making intensity measurements. The first is category scaling. This is familiar to most of us as a five-point scale. Category scales are excellent for community wide surveys as they require very little instruction on their use; however, they are prone to compression at the extremes and give very little resolution.

An alternative to category scales which is gaining in popularity is magnitude estimation. Magnitude estimation is a form of open-ended personalized category scaling, but differs in that responses are generally related by their ratios.

In magnitude estimation the panelist is allowed to assign numbers freely to stimuli based on the magnitude of the stimulus they sense. For example, the first stimulus is given and the panelist is asked to respond with a number at least equal to 10. The panelist is then given the remaining stimuli and asked to rank them relative to the first stimulus, remembering the magnitude of the first response. These responses are then normalized over the entire panel, which puts each panelist's response on the same scale.

A comparison of the data in Figure 1 clearly shows the value of magnitude estimation compared to category scaling. A response of 4 for one stimulus and of 2 for another on a category scale does not mean that one stimulus was twice as strong as the other, but may be 15 times stronger.

While category scaling may be used effectively to draw conclusions, magnitude estimation can be used more effectively in making analytical determinations of the effect of changing process parameters or in measuring the degree of success of an abatement program.

A third alternative for intensity measurements is the use of reference scales [4]. The ASTM has adopted this procedure in a method published as E-544. It requires the use of a set of standard odors whose concentrations are accurately known. Usually a binary scale is used, that is, each successively higher odor is twice the concentration of the previous one. This, then, is a log scale and can be related to the test stimulus through the Steven's equation to the concentration of the unknown stimulus. We have used the referencing method at IITRI for a number of years in many odor-pollution investigations. At IITRI we have developed the dynamic scale shown in Figure 2. The details of the use of such an apparatus is given in ASTM E-544 and the details will not be given here.

Quality

Odor quality and hedonic tone are less well developed and are analytical methods; however, some progress is being made in standardizing these procedures.

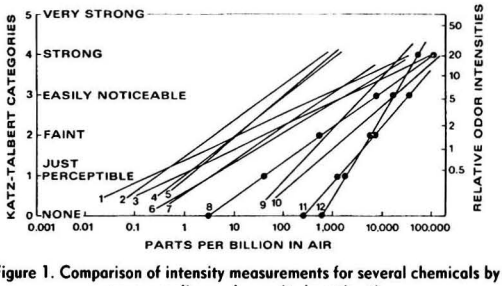

Figure 1. Comparison of intensity measurements for several chemicals by category scaling and magnitude estimation.

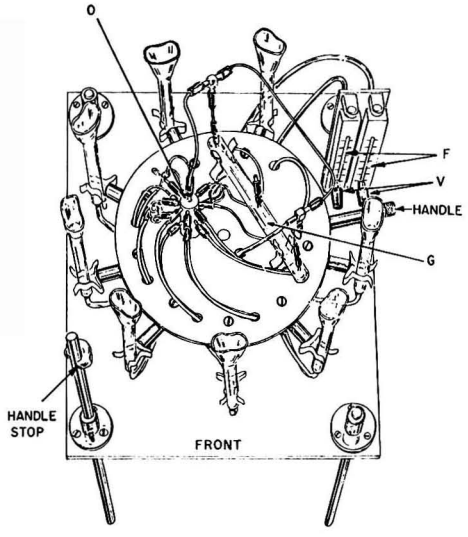

Figure 2. IITRI Dynamic dilution binary-scale olfactometer for suprathreshold intensity measurements.

Quality describes what an odor smells like. Early attempts at measuring odor quality relied on the panelist's use of free-descriptors. This becomes extremely cumbersome to interpret, when one realizes that panelists may have several words to describe the same odor.

Dravnieks [5] has been experimenting with an odor-quality evaluation list in which each panelist is limited to 146 descriptors. Each descriptor used is rated using a category scale in order to provide weighting. Preliminary results indicate that use of this procedure may result in an extremely high degree of correlation between the descriptors used by a group of panelists and duplicate measurements made in a blind fashion over wide periods of time. Data such as this could be invaluable in shedding light on the mechanism that produces the sensation of odor in humans.

Hedonic Tone

Hedonic tone is not very useful in conducting odor-abatement programs. As mentioned earlier, even pleasant odors such as perfume odors can be unpleasant in the context of an odor-nuisance problem. It is known, however, that in general odors become more unpleasant as the intensity increases. Attempts to develop a non-numeric-based measurement method have been slowed due to the lack of usefulness of such measurements.

Analytical methods

The methods described in the previous section all deal with subjective odor measurements made by panels of people. The information that is obtained relates to the actual sensation perceived by these panelists, and can be very effectively used in an odor-abatement program. However, the effective design of odor-removal equipment also requires a knowledge of the chemical nature of the vapors causing the odor.

The human nose is extremely sensitive to very low concentrations of odorous chemicals, as low as parts per trillion in some cases. This is much lower (6 orders of magnitude) than the most sensitive analytical equipment, and has effectively precluded the use of analytical equipment in the solution of odorous problems until recently.

The development of preconcentration techniques [6] has greatly facilitated the collection of adequate sample volumes for subsequent investigation by gas chromatography or combined gas chromatography-mass spectrometry. Using these procedures, the concentration and identity of all the chemical compounds in an effluent stream can be measured down to parts per trillion. The use of capillary-column chromatography has improved the resolution and sensitivity to the point that extremely complicated mixtures of hundreds of compounds can be handled. In many industrial odor problems, many chemical compounds are being exhausted, but usually only a few very minor components are responsible for the odor. In many cases, an emission-control device can remove 90-95% of the chemical compounds from an exhaust stream, but the odor problem still remains. This is because the emission-control device was not designed to control the odorous compound, but only to remove total organics. Thus, simply identifying all of the components of an exhaust stream may not help in indicating which chemical is actually causing the odor problem. Therefore, a means for identifying only the odorous components of an exhaust stream is needed.

This technique is known as organoleptic sensing or more commonly "GC-sniffing". GC-sniffing involves a rather simple concept. The effluent from a gas-chromatography column is split into two streams. One stream is directed to the flame ionization detector of the GC, while the second stream is presented to one or more panelists for sniffing. As a compound exits the gas-chromatography column, as indicated by the presence of a detected peak on the chart paper, the panelist(s) sniff the other stream and then annotate the gas chromatogram as to the presence or absence of odor, quality of the odor, and intensity. Once the odorous peaks have been located by GC-sniffing, it is an easy matter to identify these peaks by GC-mass spectrometry.

CONCLUSIONS

In this paper a review of the current state-of-the-art in odor investigation has been presented. It is clear that any attempt at solving an odor problem is a complex undertaking requiring the efforts of not only analytical chemists, but also statisticians, panelists, and in some cases psychologists, as well as engineers.

LITERATURE CITED

1. "Compilation of Odor and Taste Threshold Values Data" ASTM Publication DS-48A. Frank Fazzallari, Editor.
2. Dravnieks, A., W. H. Prokop, and W. R. Boehne, "Measurement of Ambient Odors Using Dynamic Forced-Choice Triangle Olfactometer." J. Air Pollution Control Association, *28* (1124) 1978.
3. Dravnieks, A. and Frank H. Jarke, "Odor Threshold Measurement by Dynamic Olfactometry: Significant Operational Variables." J. Air Pollution Control Association, *30*, 1284 (1980).
4. Turk, Amos, Edward D. Switala, and Samuel H. Thomas, "Suprathreshold Odor Measurements by Dynamic Olfactometry—Principles and Practice." J. Air Pollution Control Association, *30*, 1289 (1980).
5. Dravnieks, A., F. C. Bock, J. J. Powers, M. Tibbetts, and M. Ford, "Comparison of Odors Directly and Through Profiling." Chemical Senses and Flavors, *3*, 191 (1978).
6. Jarke, Frank H., A. Dravnieks, and Sydney M. Gordon, "Organic Contaminants in Indoor Air and Their Relation to Outdoor Contaminants", ASHRAE Transaction, No. 2620, (1980).

Temperature Effects on Biological Treatment of Petrochemical Wastewaters

Empirical models make it possible to determine the most significant variables and operating parameters affected by temperature.

M. P. del Pino and W. E. Zirk, Union Carbide Corp., South Charleston, West Va. 25303

PREVIOUS STUDIES

Lin *et al.* [1] evaluated 26 years of data compiled from 13 activated-sludge wastewater treatment plants located in Canada and Northern USA. The authors determined a temperature correction coefficient θ of 1.125, significantly different from unity at the five percent level of significance. This means that a temperature drop of 10°C would require an increase in the mean hydraulic retention time of 80% considering that all other conditions remain constant. Eckenfelder *et al.* [2] reported θ values between 1.055 and 1.10 for activated-sludge plants treating organic-chemical wastewaters. Ludzack *et al.* [3], studied the effects of temperature in continuous activated-sludge bench units and concluded that acclimation to different wastewater feeds required about five times as long at 5°C as at 30°C. In the same studies they also found that BOD_5 and COD removals were about 10 percent higher at 30°C than at 5°C. Keefer [4] analyzed the operating data collected for a period of 20 years of the activated-sludge units at the Back River which serves most of Baltimore (Maryland) and found that at a sewage flow of 18-22 mgd the BOD_5 removals increased from 84.5% at 12°C to 91.5% at 26°C. Hunter *et al.* [5] conducted activated-sludge semi-batch studies using artificial sewage and found that the BOD_5 removals increased rapidly from 79.1% at 4°C to 92.3% at 20°C.

B. A. Sayigh [6] conducted activated-sludge laboratory studies with continuous stirred-tank reactors and concluded that the effects of temperature using domestic sewage, organic-chemicals wastewaters and petrochemical wastewaters are specific for a given type of wastewater. The author also found that the higher the sludge age, the less the susceptibility of the process to variations in temperature. Berthouex *et al.* [7] developed linear and time series models relating effluent BOD_5 to influent BOD_5, MLSS, temperature, and hydraulic retention time based on three years of data compiled at the Madison Sewage Treatment Plant (Wisconsin). They found no significant effect of temperature on performance when gradual changes in temperature (4-24°C) occurred. Lacroix *et al.* [8] developed empirical models to represent the municipal wastewater-treatment plants of Fort Wayne, Indianapolis, Marion, Richmond, and Valparaiso (Indiana). From these models it appeared that low-temperature operation slightly affected the performance of the sewage treatment plant based on effluent suspended solids and BOD_5 values.

ISSN 0278-5889-82-5877-0104-$2.00.

The literature reviewed shows conflicting results of the effects of temperature on wastewater treatment plant (WWTP) performance. However, in most cases the adverse effects of temperature depended on the type of substrate to remove, acclimation period to temperature changes and the hydraulic retention time of the treatment system.

DISCUSSION

In this study we discuss and present the interrelationship among the following variables for Union Carbide Corporation plants, A, B and C biosystems:

1. Hydraulic retention time (HRT).
2. Mixed-liquor volatile suspended solids (MLVSS).
3. Temperature (temp)
4. Effluent total suspended solids (TSS)
5. Total and soluble chemical oxygen demand (COD).
6. Total and soluble biochemical oxygen demand (BOD).

The selected statistical design for this study is a 2-level factorial in three variables by a 3-level in one variable: $2^3 \times 3^1$. Therefore the number of experiments to run is 24.

The independent variables are:

1. Hydraulic retention time (2-levels).
2. Biomass concentration as mixed-liquor volatile suspended solids (2-levels).
3. Temperature (2-levels)
4. Influent substrate concentration as COD or BOD_5 (3-levels).

The dependent variables are:

1. Effluent substrate concentration as COD or BOD_5.
2. Effluent total suspended solids.

All the experiments were run with eight 10-liter reactors with internal clarifiers (see Figure 1) during three phases at these levels:

Reactor No.	Temperature	MLVSS	HRT
1	−	−	+
2	−	−	−
3	−	+	+
4	−	+	−
1A	+	−	+
2A	+	−	−
3A	+	+	+
4A	+	+	−

+ upper level − lower level

Figure 2 shows a 2^3 factorial design.

Eight activated sludge continuous stirred-tank reactors (CSTR) were operated simultaneously during three phases

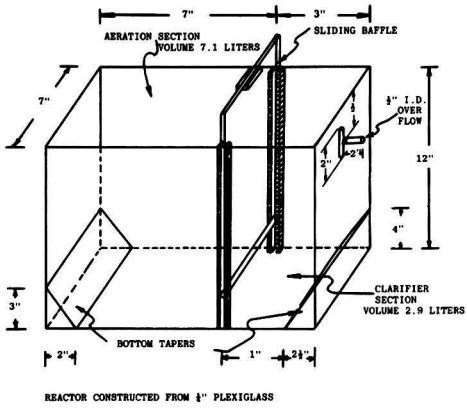

Figure 1. Reactor design.

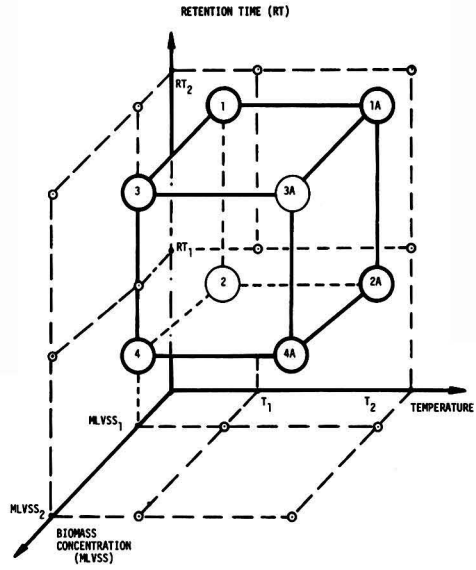

Figure 2. 2^3 factorial

with three different plant waste-water samples (influents to the WWTP's). The reactors were mildly aerated and mixed to minimize evaporation and simulate actual field operation. Parameters such as pH (influent, effluent, and mixed-liquor), influent flow, dissolved oxygen (DO), oxygen uptake rate (OUR), temperature, and air flow were monitored daily.

Ammonia nitrogen (as NH_4Cl), orthophosphate (as KH_2PO_4 or K_2HPO_4) and iron (as $FeCl_3$) were added to the CSTR's influent wastewater to maintain at least these COD—N—P—Fe ratios: 100 mg influent COD:2.5 mg NH_3—N:0.5 mg PO_4—P:0.2 mg Fe. The addition of iron possibly is not needed in most of the plants; however, it was added in this study to minimize any adverse effects.

The ranges of the independent variables studied for the three waste-water treatment plants are:

Plant	Influent COD(mg/liter)	Influent BOD^5(mg/liter)	Hydraulic Retention Time	MLVSS mg/liter	Temperature °C
A	1500-2050	360-590	40-60 hrs.	2000-4000	10-25
B	5350-7510	2940-5000	3-6 days	1500-3000	10-25
C	1830-3090	770-1830	20-40 hrs.	2000-4000	12-25

The above ranges encompass the experimental region studied. The models developed are representative of this experimental region and it is unadvisable to extrapolate beyond this region.

The wastewater characteristics of the samples used in this study are shown on Tables 1, 2 and 3.

Empirical Models

Two types of empirical models were developed from these studies. The first type was formed by regressing (Effluent BOD_{5TOTAL} — Effluent $BOD_{5SOLUBLE}$) and (Effluent COD_{TOTAL} — Effluent $COD_{SOLUBLE}$) on Effluent TSS. The second type was the log-linear model. Here we regressed the natural logs of each of the three dependent variables (Effluent $BOD_{5SOLUBLE}$, $COD_{SOLUBLE}$ and TSS) on the natural logs of three of the independent variables (MLVSS, retention time, and influent substrate concentration as COD or BOD_5) and temperature, the fourth independent variable.

The empirical models developed for Plants A, B and C biosystems are:

Plant A

(1a) Effluent $BOD_{5TOTAL} = 2.06 + 0.21$ Eff TSS + Eff BOD_{5SOL} $\quad R^2 = 69.1\%$
[7.02]

(2a) Effluent $COD_{TOTAL} = 33.4 + 0.72$ Eff TSS + Eff COD_{SOL} $\quad R^2 = 60.9\%$
[5.87]

(3a) Effluent $BOD_{5SOL} = 304.7\,(MLVSS)^{-0.37}_{[4.59]} * e^{-0.05\,Temp}_{[12.72]}$ $\quad R^2 = 89.3\%$

(4a) Effluent $COD_{SOL} = 181.0(Inf\ COD_{SOL})^{0.126}_{[1.87]} * e^{-0.012\,Temp}_{[4.34]}$ $\quad R^2 = 51.6\%$

(5a) Effluent $TSS = 0.08(MLVSS)^{0.78}_{[2.5]}$ $\quad R^2 = 22.1\%$

Statistical t values for each of the coefficients are represented by brackets.

The R^2 values represent the approximate percentage of total variation within the data being explained by the equations; the last model (Effluent TSS) explains approximately 22.1% of the total variation which shows a weak correlation. The first two models illustrate the relationship among the effluent total and soluble substrate concentration, as COD or BOD_5, and the TSS. The last three models shows that retention time does not affect the effluent BOD_5, COD, or TSS within the ranges studied. The influent substrate concentration seems to affect the effluent

TABLE 1. WASTEWATER CHARACTERISTICS OF THE SAMPLES USED IN THIS STUDY

Plant-A			
Phase No.	I	II	III
Date Sampled	2/22/79	3/15/79	3/30/79
pH	9.1	8.0	7.7
Total COD, mg/liter	1500	2017	2054
Soluble COD, mg/liter	1220	1774	1690
Total BOD_5, mg/liter	365	562	592
Soluble BOD_5, mg/liter	351	342	408
SOC*, mg/liter	350	440	450
Ammonia-N, mg/liter	7	12	12
TKN**, mg/liter	33	78	33
Ortho Phosphate-P, mg/liter	0.6	1.2	0.6
TSS, mg/liter	125	70	350
VSS, mg/liter	79	36	195
Total Dissolved Solids, mg/liter	2170	4680	5320
COD/BOD_5 ratio	4.1	3.6	3.5
Characteristics After 2-hour Air Stripping:			
pH	9.1	8.3	8.4
Soluble COD, mg/liter	1034	1579	1527
Soluble BOD_5, mg/liter	234	645**	420***
SOC, mg/liter	300	430	410
% Removals by Stripping:			
Soluble COD	15.2	11.0	9.6
Soluble BOD_5	33.3	<0***	<0***
SOC	14.3	2.2	8.9

* SOC: soluble organic carbon.
** Total Kjeldahl nitrogen which includes some organic nitrogen plus ammonia nitrogen.
*** BOD_5 increased after stripping possibly due to stripping of toxic or inhibitory compounds.

TABLE 2. WASTEWATER CHARACTERISTICS OF THE SAMPLES USED IN THIS STUDY

Plant-B			
Phase No.	I	II	III
Date Sampled	4/19/79	4/30/79	5/14/79
pH	5.8	5.7	5.6
Total COD, mg/liter	5348	6707	7512
Soluble COD, mg/liter	4957	6536	6879
Total BOD_5, mg/liter	2940	3405	5000
Soluble BOD_5, mg/liter	2820	3345	4800
SOC,* mg/liter	1650	1850	2100
Ammonia-N, mg/liter	168	94	21
TKN**, mg/liter	221	201	50
Ortho Phosphate, mg/liter PO_4	34	22	32
TSS, mg/liter	84	272	232
Total Dissolved Solids, mg/liter	2144	3900	5366
COD/BOD_5 ratio	1.82	1.97	1.50
Characteristics After 2-Hours Air Stripping:			
pH	4.5	6.1	5.8
Soluble COD, mg/liter	4652	6066	6625
Soluble BOD_5, mg/liter	2800	2880	4600
SOC, mg/liter	1600	2050	2200
% Removals by Stripping:			
Soluble COD	6.2	7.2	3.7
Soluble BOD_5	0.7	13.9	4.2
SOC	3.1	—	—

* Soluble organic carbon.
** Total Kjeldahl nitrogen.

COD soluble (4a); however, this effect is somewhat weak as the low t value indicates ($t = 1.87$). In general, temperature and to a lesser extent the MLVSS concentration seem to be the dominant operating parameters for the Plant A WWTP biosystem within the ranges studied. Figures 3, 4, and 5 present selected contour maps of models 3a, 4a and 5a.

The relationships among effluent total and soluble substrate concentrations and effluent TSS are illustrated in the first two models. The third and fourth models show that the effluent soluble BOD_5 and COD strongly depend on the F/M (Influent BOD_5 or COD*HRT^{-1}*$MLVSS^{-1}$) and temperature. The last model shows that the level of effluent TSS is affected by the MLVSS concentration, the influent substrate concentration (BOD_5) and the temperature. Figures 6, 7 and 8 present selected contour maps of models 3b, 4b and 5b.

Plant B

(1b) $\text{Effluent } BOD_{5TOTAL} = -15.75 + 0.596\ \text{Eff TSS} + \underset{[12.55]}{\text{Eff } BOD_{5SOL}}$ $R^2 = 87.7\%$

(2b) $\text{Effluent } COD_{TOTAL} = 17.2 + 1.42\ \text{Eff TSS} + \underset{[9.52]}{\text{Eff } COD_{SOL}}$ $R^2 = 80.5\%$

(3b) $\text{Effluent } BOD_{5SOL} = 1242(MLVSS)^{-1.0}_{[4.01]}*(HRT)^{-1.04}_{[4.68]}*(\text{Inf } BOD_{5SOL})^{0.93}_{[3.72]}*e^{-0.105\,\text{Temp}}_{[11.10]}$ $R^2 = 89.6\%$

(4b) $\text{Effluent } COD_{SOL} = 0.63(MLVSS)^{-0.24}_{[2.43]}*(HRT)^{-0.19}_{[2.23]}*(\text{Inf } COD_{SOL})^{1.1}_{[4.75]}*e^{-0.017\,\text{Temp}}_{[4.69]}$ $R^2 = 73.9\%$

(5b) $\text{Effluent TSS} = 7.2(MLVSS)^{-1.08}_{[2.74]}*(\text{Inf } BOD_{5TOTAL})^{1.53}_{[3.67]}*e^{-0.075\,\text{Temp}}_{[5.00]}$ $R^2 = 68.9\%$

Plant C

(1c) $\text{Effluent } BOD_{5TOTAL} = 7.0 + 0.29\ \text{Eff TSS} + \underset{[2.03]}{\text{Eff } BOD_{5SOL}}$ $R^2 = 15.7\%$

(2c) $\text{Effluent } COD_{TOTAL} = 12.6 + 0.43\ \text{Eff TSS} + \underset{[1.41]}{\text{Eff } COD_{SOL}}$ $R^2 = 8.3\%$

(3c) $\text{Effluent } BOD_{5SOL} = 4.77(MLVSS)^{-0.54}_{[1.66]}*(HRT)^{-0.77}_{[3.04]}*(\text{Inf } BOD_{5SOL})^{0.85}_{[2.78]}*e^{-0.051\,\text{Temp}}_{[3.52]}$ $R^2 = 60.5\%$

(4c) $\text{Effluent } COD_{SOL} = 8.04(MLVSS)^{-0.16}_{[2.48]}*(HRT)^{-0.24}_{[4.64]}*(\text{Inf } COD_{SOL})^{0.81}_{[8.58]}*e^{-0.02\,\text{Temp}}_{[6.85]}$ $R^2 = 88.2\%$

(5c) $\text{Effluent TSS} = 41.93\ e^{-0.041\,\text{Temp}}_{[3.00]}$ $R^2 = 29.1\%$

TABLE 3. WASTEWATER CHARACTERISTICS OF THE SAMPLES USED IN THIS STUDY

	Plant-C		
Phase No.	I	II	III
Date Sampled	7-10-79	7-26-79	8-16-79
pH	6.7	10.7	9.7
Total COD, mg/liter	2348	1830	3094
Soluble COD, mg/liter	2213	1790	2859
Total BOD_5, mg/liter	1050	767	1830
Soluble BOD_5, mg/liter	1042	600	1770
SOC*, mg/liter	440	445	795
Ammonia-N, mg/liter	58	36	40
TKN**, mg/liter	90	66	47
Ortho Phosphate, mg/liter PO_4	0.64	2.0	0.28
TSS, mg/liter	168	58	34
Total, Dissolved Solids, mg/liter	2116	1882	2288
COD/BOD_5 Ratio	2.24	2.39	1.69
Characteristic After 2-Hour Air Stripping			
pH	7.73	8.6	8.15
Soluble COD, mg/liter	1835	1507	2244
Soluble BOD_5, mg/liter	705	457	1230
SOC*, mg/liter	430	445	565
% Removals by Stripping			
Soluble COD	17.1	15.8	21.5
Soluble BOD_5	32.3	23.8	30.5
SOC*	2.3	—0—	28.9

* Soluble Organic Carbon
** Total Kjeldahl Nitrogen

The relationships among effluent total and soluble substrate concentrations and effluent TSS are very weak as shown in the first two models with low R^2 and t values. The

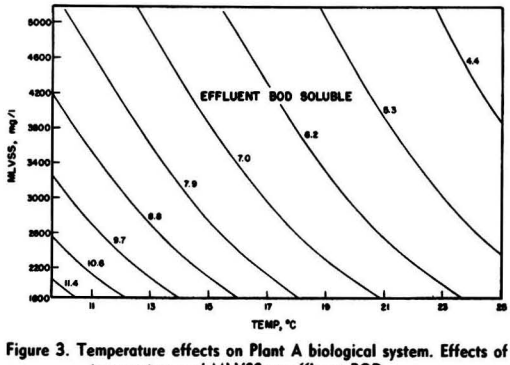

Figure 3. Temperature effects on Plant A biological system. Effects of temperature and MLVSS on effluent $BOD_{soluble}$.

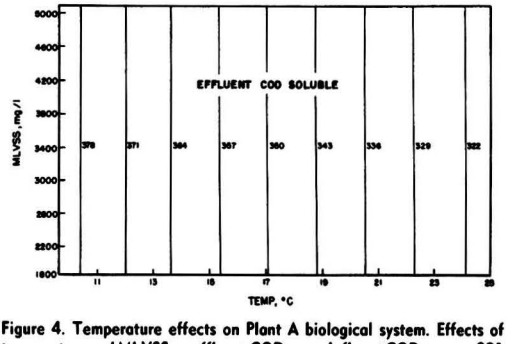

Figure 4. Temperature effects on Plant A biological system. Effects of temperature and MLVSS on effluent $COD_{soluble}$. Influent $COD_{soluble}$ = 891 mg/liter.

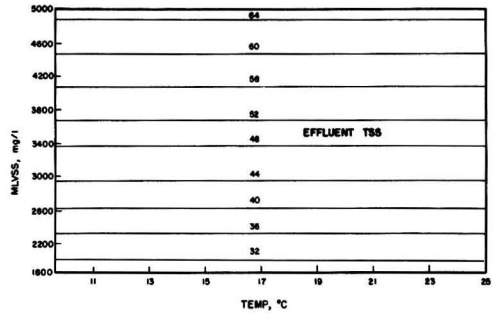

Figure 5. Temperature effects on Plant A biological system. Effects of temperature and MLVSS on effluent TSS.

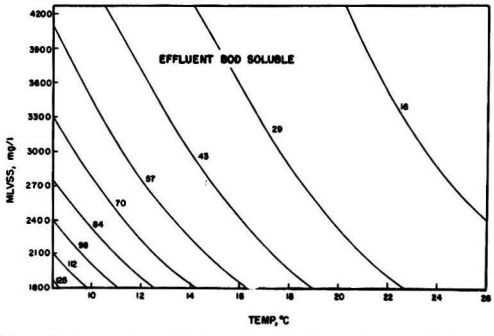

Figure 6. Temperature effects on Plant B biological system. Effects of temperature and MLVSS on effluent $BOD_{soluble}$. RT = 3 days, influent $BOD_{soluble}$ = 2609 mg/liter.

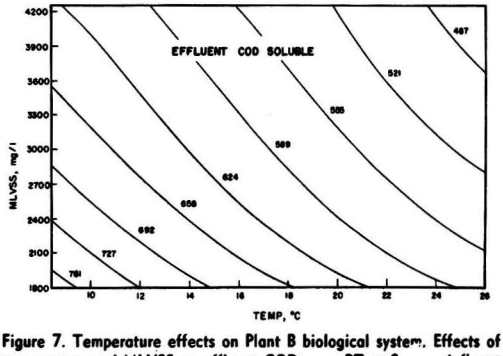

Figure 7. Temperature effects on Plant B biological system. Effects of temperature and MLVSS on effluent $COD_{soluble}$. RT = 3 ., influent $COD_{soluble}$ = 5012 mg/liter.

third and fourth models illustrate that the effluent soluble BOD_5 and COD are affected by the F/M (Influent BOD_5 or COD * HRT^{-1} * $MLVSS^{-1}$) and temperature. The last model illustrates that the only parameter that affected the effluent TSS was the temperature; however, the model only explained 29.1% (R^2) of the total variation within the data. Figures 9, 10, and 11 present selected contour maps of models 3c, 4c and 5c. A 3-dimensional representative of effluent BOD_5 soluble for each of the plants illustrating the effects of MLVSS and temperature is presented in Figures 12, 13, and 14.

In these laboratory studies, the effect of temperature on sludge compactness and settleability as measured by the sludge-volume index (SVI) and the initial settling velocity (ISV) tests was not conclusive in those biological reactors

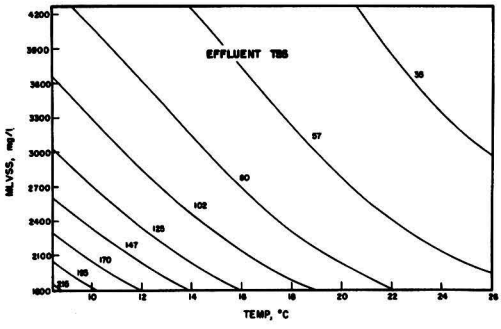

Figure 8. Temperature effects on Plant B biological system. Effects of temperature and MLVSS on effluent TSS. Influent BOD_{total} = 2801 mg/liter.

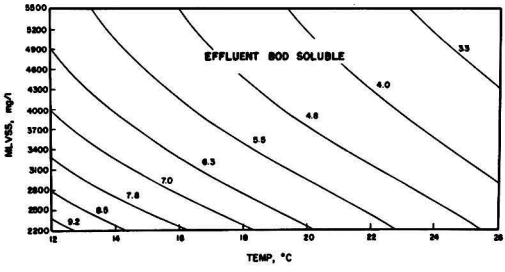

Figure 9. Temperature effects on Plant C biological system. Effects of temperature and MLVSS on effluent $BOD_{soluble}$. RT = 20 hours, influent $BOD_{soluble}$ = 641 mg/liter.

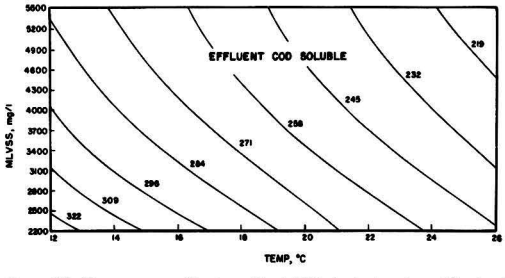

Figure 10. Temperature effects on Plant C biological system. Effects of temperature and MLVSS on effluent $COD_{soluble}$. RT = 20 hours, influent $COD_{soluble}$ = 1527 mg/liter.

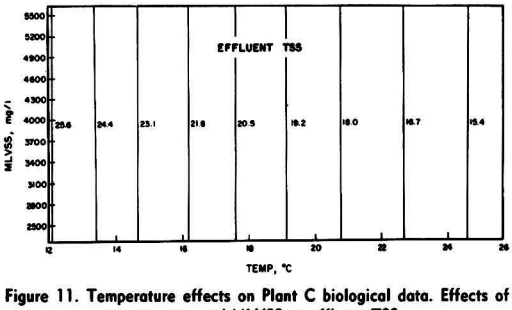

Figure 11. Temperature effects on Plant C biological data. Effects of temperature and MLVSS on effluent TSS.

operated with Plant A wastewaters. However, the sludge compactness and settleability were generally better at low temperature in those biological reactors operated with

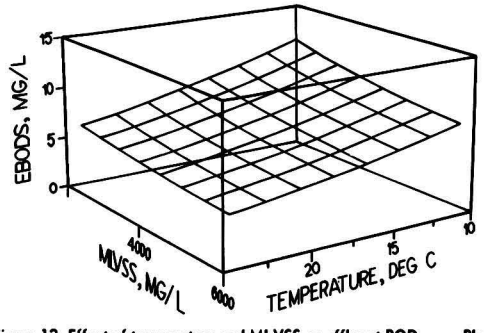

Figure 12. Effect of temperature and MLVSS on effluent $BOD_{soluble}$. Plant A study.

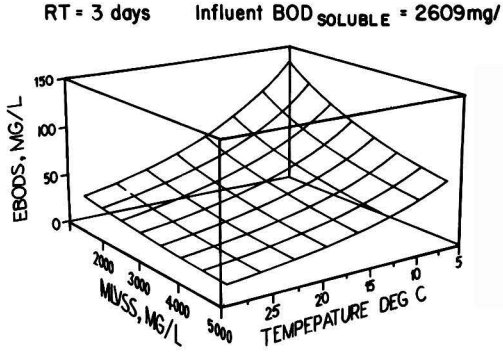

Figure 13. Effect of temperature and MLVSS or effluent $BOD_{soluble}$. Plant B study. RT = 3 days, influent $BOD_{soluble}$ = 2609 mg/liter.

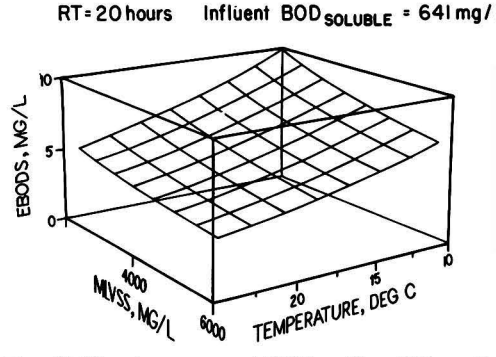

Figure 14. Effect of temperature and MLVSS on effluent $BOD_{soluble}$. Plant C study. RT = 20 hours, influent $BOD_{soluble}$ = 641 mg/liter.

Plants B and C waste-waters. No empirical model could be developed to significantly correlate the independent variables with either the SVI or the ISV.

Biological Reaction Kinetics—Temperature Coefficient θ

The data compiled during these three studies were analyzed assuming first-order kinetics and Grau's Model which uses a multiple zero-order concept. The mathematical expressions for these two models in completely mixed activated-sludge processes are:

$$\text{First order} \ldots . \frac{So - Se}{Xv \cdot t} = k\,Se$$

$$\text{Grau's Model} \ldots \frac{So(So - Se)}{Xv \cdot t} = K\,Se$$

where,

So = total concentration of substrate (COD, BOD_5 . . .) on the influent stream (mg/liter)

Se = soluble concentration of substrate on the effluent stream (mg/liter)

Xv = MLVSS concentration kept under aeration (mg/liter)

t = hydraulic retention time (days)

k, K = removal-rate coefficients

It is assumed that all the non-soluble COD or BOD_5 in the influent is dissolved in the reactor and consumed by the biomass as substrate. However, as most of the non-soluble COD or BOD_5 in the effluent is biomass, it is not considered to be substrate. For this reasons, So is expressed as the total concentration of the influent substrate and Se as the soluble concentration of the effluent substrate.

The calculated reaction-rate coefficients and the temperature correction coefficients θ, based on the modified Arrhenius expression $K_{T1} = k_{T2}\theta^{(T1-T2)}$ for the three plant wastewaters studied (measuring the substrate as BOD_5) are:

Plant	Temperature Range (°C)	F/M Range ($KgBOD_5$/day/Kg MLVSS)	Reaction Rate Coefficients $k^{(1)}$	Reaction Rate Coefficients $K^{(2)}$	θ Values First Order	θ Values Grau's Model
A	9.9 24.6	0.051-0.14	0.00787 0.0159	4.34 8.51	1.049	1.047
B	9.8 25.2	0.12-0.77	0.00537 0.0228	25.5 100.4	1.098	1.093
C	12.2 24.7	0.092-0.54	0.0249 0.0611	25.3 62.6	1.074	1.075

(1) First order reaction-rate coefficient (l/mg/day)
(2) Grau's Model reaction-rate coefficient (day^{-1})

All these calculated temperature correction coefficients are much higher than the usual accepted values of 1.01-1.03 for municipal wastewaters.

The adverse effects of low-temperature operation (10-12°C) are more pronounced in those wastewaters from Plants B and C. Of the three independent variables studied in addition to temperature (HRT, MLVSS, and influent substrate concentration), the adverse effects of short retention time (HRT) operation on effluent substrate concentration are clearly shown in the Plant B models and to a somewhat lesser extent in the Plant C models. The effect of retention time is not significant in the Plant A models, which indicates that the plant might be able to reduce the retention time even further. The effect of MLVSS on the effluent substrate concentrations is more pronounced in the Plants A and B models than in those developed for Plant C. Finally, the influent substrate concentration effect is strongest in models developed from the Plant B study and to a somewhat lesser degree in those developed from the Plant C study; however, the effect is practically nil for the models developed from the Plant A study. Table 4 summarizes these effects for each of the plants.

TABLE 4. EFFECTS OF INDEPENDENT VARIABLES ON VARIOUS RESPONSES FOR EACH PLANT

Response	RT	MLVSS	Influent Substrate Concentration	Temp
Plant-A Independent Variables				
Effluent $BOD_{SOLUBLE}$	NE	S	NE	VS
Effluent $COD_{SOLUBLE}$	NE	NE	W	S
Effluent TSS	NE	M	NE	NE
Plant-B Independent Variables				
Effluent $BOD_{SOLUBLE}$	S	S	M-S	VS
Effluent $COD_{SOLUBLE}$	M	M	S	S
Effluent TSS	NE	M	M-S	S
Plant-C Independent Variables				
Effluent $BOD_{SOLUBLE}$	M	W	M	M-S
Effluent $COD_{SOLUBLE}$	S	M	VS	S
Effluent TSS	NE	NE	NE	M

Legend: VW = Very Weak Effect, W = Weak Effect, M = Moderate Effect, S = Strong Effect, VS = Very Strong Effect, NE = No Effect

CONCLUSIONS

- The empirical models developed and presented herein are of two types. The first type shows a linear relationship between effluent total BOD_5 or COD and effluent soluble BOD_5 or COD and TSS. The second type are of this form:

Effluent Substrate conc. (as BOD_5, COD, or TSS) = $HRT^{\alpha} * MLVSS^{\beta} * e^{\gamma Temp.} *$ Influent Substrate conc.$^{\delta}$

- More drastic effects of temperature on the biological treatment of petrochemical wastewaters as compared to that on municipal wastewater have been illustrated.
- The mathematical models and contour maps developed have been used to determine optimum operating conditions within the ranges studied to comply with present and future effluent standards. Extrapolation beyond the regions of experimentation studied is not recommended.
- The effect of temperature on sludge compactness and settleability as measured by the sludge volume index (SVI) and the initial settling velocity (ISV) were inconclusive and no empirical model could be developed.
- Statistically designed experiments were utilized to develop the mathematical models and contour maps presented herein. This allows for obtaining more information from fewer experiments.

LITERATURE CITED

1. Lin, K. C. and G. W. Heinke, "Plant Data Analysis of Temperature Significance in the Activated Sludge Process", *JWPCF*, **49**, No. 2 (February, 1977).
2. Eckenfelder, W. W., J. A. Roth and E. D. McMullen, "Factors Affecting the Effluent Quality from Activated Sludge Plants

Treating Organic Chemicals Wastewater," Proceedings of the 30th Industrial Waste Conference, Purdue University (1975).
3. Ludzack, F. J., R. B. Schaffer, and M. B. Ettinger, "Temperature and Feed as Variables in Activated Sludge Performance", *JWPCF*, **33**, No. 2 (February, 1961).
4. Keefer, C. E., "Temperature and Efficiency of the Activated Sludge Process", *JWPCF*, **34**, No. 11 (November, 1962).
5. Hunter, J. V., "Temperature and Retention Time Relationships in the Activated Sludge Process", Proceedings of the 21st Industrial Waste Conference, Purdue University (1966).
6. Sayigh, B. A., "Temperature Effects on the Activated Sludge Process", Ph.D. thesis presented in May, 1977, University of Texas at Austin.
7. Berthouex, P. M., W. G. Hunter, L. Pallesen, and C. Y. Shih, "The Use of Stochastic Models in the Interpretation of Historical Data from Sewage Treatment Plants", *Water Research*, **10**, 689-698 (1976).
8. Lacroix, P. G. and Don E. Bloodgood, "Computer Simulation of Activated Sludge Plant Operation", *JWPCF*, **44**, No. 9, (September, 1972).

M. P. del Pino is a project scientist in the Union Carbide Corporation Technical Center in South Charleston, WV. He earned his chemical engineering degree in 1962 at Las Palmas University, Spain. Since 1974 he has been working in Research and Development in the environmental area at Union Carbide Corporation.

Wayne E. Zirk is an advanced statistician at the Union Carbide Technical Center in South Charleston, WV. He earned his BS and MS degrees in statistics and BA degree in mathematics at West Virginia University. Since 1979 he has been employed as a statistical consultant in the R&D's Applied Math and Statistics group.

Soluble-Sulfide Precipitation for Heavy Metals Removal from Wastewaters

Engineering details of a treatment plant scheduled to be operational in September, 1981.

James S. Whang, AEPCO, Inc., Rockville, Md. 20850; Daniel Young, JRB Associates, McLean, Va. and M. Pressman, Army Mobility Equipment Research & Development Command, Fort Belvoir, Va.

As part of the Nation's effort to protect the environment from pollution, the U.S. EPA has begun to control industrial dischargers of wastewater to publically owned treatment works (POTW's). Through the National Industrial Wastewater Pretreatment Regulations and Program under the Clean Water Act of 1977, EPA established a list of 34 categorical industries, for which national industrial wastewater pretreatment standards were to be promulgated. Among the 34 categorical industries, the electroplating industry is the first one, for which national pretreatment standards have been promulgated [*1*].

In order to comply with applicable wastewater-pretreatment standards, electroplaters which discharge to POTW's must pretreat wastewater. There are several treatment technologies available for treating electroplating wastewater, each with its own advantages and disadvantages. This technical paper examines the design aspects of a pilot treatment plant which uses the soluble-sulfide precipitation process to remove heavy metals from an electroplating wastewater.

NATURE OF PROJECT

Tobyhanna Army Depot in Tobyhanna, Pa., owns and operates an electroplating facility. Wastewater from the plating shop has been discharged in combination with other wastewaters from the Army Depot to a trickling-filter plant. Characteristically high concentrations of metals in the wastewater have frequently caused upset of the trickling filter, and have contaminated the plant's sludge. This has brought about a need for special sludge-disposal arrangements. Under funding by the Army Mobility Equipment Research & Development Command (MERADCOM), industrial wastewater was characterized and a treatability study was performed in order to develop and evaluate alternative treatment methods [2]. These study efforts concluded that the soluble-sulfide precipitation process would be most cost-effective and acceptable, based on the following reasons [2, 3].

- Low solubility of metal sulfides improves metal-removal efficiency over the conventional hydroxide process (see Table 1).
- Metal-sulfide precipitates are very fine. However, this problem can be effectively overcome by adding an anionic flocculant to facilitate liquid-solids separation.
- Metal-sulfide sludge exhibits better thickening properties and dewaterability than metal-hydroxide sludge from the hydroxide precipitation process.
- Metal-sulfide sludge is three times less subject to leaching (at pH = 5.0 ± 0.2 for 24 hours under either oxidizing or non-oxidizing conditions) as compared to hydroxide sludge (see Table 2), and therefore final disposal is easier and safer.

The Tobyhanna plating facility basically generates three wastewater streams. It is necessary to segregate these wastewater streams in order to effectively utilize the soluble-sulfide process. These three wastewaters are: 1) cyanide-bearing rinse water, 2) chromium-bearing rinse water, and 3) other alkaline and acid rinse waters. Substances present in each of the three wastewaters are as follows:

- Cyanide-bearing wastewater: cadmium, copper, and cyanide.

ISSN 0278-4491-82-5877-0110-$2.00. *The American Institute of Chemical Engineers, 1982.

TABLE 1. COMPARISON OF HYDROXIDE AND SULFIDE PRECIPITATION PROCESSES

Parameter	Wastewater Sample (mg/liter)	Hydroxide Precipitation at pH = 9		Sulfide Precipitation at pH = 8	
		Filtrate (mg/liter)	% Removal	Filtrate (mg/liter)	% Removal
Pb	4.4	3.4	23	<1.0	>77
Total Cr	33.0	18.0	45	2.6	92
Zn	2.1	1.3	38	<0.5	>76
Cd	4.8	0.7	85	0.5	90
Cu	17.0	11.0	35	2.5	85
Ni	14.0	11.0	21	3.1	78
Total Metals	75.3	45.4	—	<10.2	—

TABLE 2. COMPARISON OF LEACHATABILITY OF HYDROXIDE AND SULFIDE SLUDGES

Parameter	Metal Hydroxide Sludge			Metal Sulfide Sludge Under Oxidizing Environment			Metal Sulfide Sludge Under Non-Oxidizing Environment		
	Sludge Cake Composition (mg/kg Dry)	Leachate Comp. (mg leached/ kg sludge)	% of Metal Leached from Sludge Cake	Sludge Cake Composition (mg/kg Dry)	Leachate Comp. (mg leached/ kg sludge)	% of Metal Leached from Sludge Cake	Sludge Cake Composition (mg/kg Dry)	Leachate Comp. (mg leached/ kg sludge)	% of Metal Leached from Sludge Cake
Pb	21,000	91	0.43	25,000	<27	<0.11	25,000	<27	<0.11
Cr	15,000	390	0.26	17,000	<27	<0.06	17,000	<27	<0.016
Zn	10,000	39	0.39	12,000	25	0.21	12,000	<13	<0.11
Cd	23,000	72	0.31	23,000	310	1.30	23,000	220	0.96
Cu	73,000	440	0.60	79,000	<27	<0.34	79,000	<27	<0.34
Ni	57,000	280	0.49	52,000	2,100	4.0	52,000	500	0.96

- Chromium-bearing wastewater: sodium, chromate, and additives.
- Other alkaline and acid wastewaters: sodium, nickel, aluminum, tin, iron, lead, zinc, chloride, sulfate, nitrate, phosphate, and other additives.

In addition to these three streams of continuous-flow wastewaters, the plating facility dumps spent solutions of various compositions periodically. The frequency of dumping ranges from once every month to once a year. These spent solutions have to be bled into the proposed pretreatment system at a slow, controlled, rate.

SOLUBLE SULFIDE TREATMENT PROCESS AND DESIGN CRITERIA

In order to effectively use the soluble-sulfide precipitation process to remove metals, three prerequisite treatment steps are needed.

1) Cyanide in the cyanide-bearing wastewater must be oxidized by chlorination to carbon dioxide and nitrogen, as shown by the following equations. This is necessary to prevent complexing of cyanide with metal ions in the subsequent treatment processes.

$$2NaCN + 2NaOCl \rightarrow 2NaCNO + 2NaCl \quad \text{(First Stage)} \qquad (1)$$

$$2NaCNO + 3NaOCl + H_2O \rightarrow 2CO_2\uparrow + N_2\uparrow + 2NaOH + 3NaCl \quad \text{(Second Stage)} \qquad (2)$$

2) Chromium (6-valent) in the chromium-bearing wastewater must be reduced by sodium metabisulfite to chromium (3-valent) as shown by the following equations to facilitate subsequent chromium precipitation by sulfide:

$$Na_2S_2O_5 + H_2O \rightarrow 2NaHSO_3 \qquad (3)$$

$$2H_2CrO_4 + 3NaHSO_3 + 3H_2SO_4 \rightarrow Cr_2(SO_4)_3 + 3NaHSO_4 + 5H_2O \qquad (4)$$

3) Neutralization of combined flows of all three wastewater streams.

The neutralized wastewater is then treated with sodium bisulfide to form metal-sulfide precipitates. The reactions for 2-valent metals and 3-valent metals are shown, respectively, as follows:

$$M^{+2} + HS^- + OH^- \rightarrow \underline{MS} + H_2O \qquad (5)$$

$$2M^{+3} + 3HS^- + 3OH^- \rightarrow \underline{M_2S_3} + 3H_2O \qquad (6)$$

Based on the results of the treatability study [2], the design criteria [4] were developed and are summarized in Table 3.

TABLE 3. DESIGN CRITERIA

Treatment Unit Process	Design Criteria*
Cyanide Oxidation by Chlorination	
First Stage	pH > 10.5; 350mv < ORP < 400mv; and t < 5 min
Second Stage	pH > 8.0; 580mv < ORP < 620mv; and t = 0.5-1 hr
Chromium Reduction by Sodium Metabisulfite	pH < 3.0; 250mv < ORP < 300mv; and t = 60 min
Soluble Sulfide Precipitation of Metal Ions	pH = 8.0; excess free sulfide ion > 1.0mg/l; and t = few seconds.

* ORP = Oxidation Reduction Potential in Millivolts.
t = React Time.

DESIGN INPUT CONDITIONS AND EFFLUENT QUALITY REQUIREMENTS

The plating facility operates on one 8-hour shift a day, 5 days a week. The design conditions for the treatment system and effluent quality requirements are summarized in Table 4.

TREATMENT FACILITY DESIGN

Based on the design criteria derived from the treatability study, a continuous flow-through treatment system was designed. The treatment process flow diagram [*4*] is presented in Figure 1. The liquid process stream consists of two separate flow-equalization sumps for chromium and cyanide wastewaters, respectively; a 4-compartment cyanide-oxidation unit which uses chlorination; a 2-compartment chromium-reduction unit which uses sodium metabisulfite; an equalization basin to combine all three wastewater streams; a neutralization unit; a 2-compartment sulfide-addition tank with pH adjustment; a flash mix tank; a flocculation tank; a laminar clarifier; a polishing filter; and a clear well equipped with a hydrogen-peroxide feed system to oxidize excess residual sulfide. Polishing filter backwash water is diverted back to the equalization basin for further treatment.

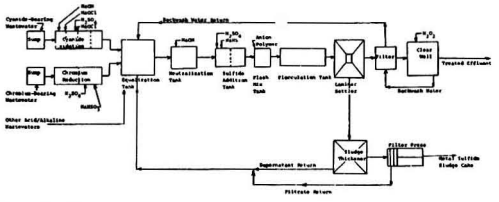

Figure 1. Treatment process flow diagram (soluble-sulfide precipitation process).

The sludge-processing stream consists of a gravity sludge thickener and a frame-type filter press. Both the thickener supernatant and the filter-press filtrate are returned to the equalization basin for further treatment.

Major process design specifications of the system are presented in Table 5. The anticipated chemical consumption rates are summarized in Table 6. The entire treatment system was designed to fit into a space 15 feet wide, 65 feet long, and 13 feet high.

TABLE 4. DESIGN CONDITIONS AND EFFLUENT QUALITY REQUIREMENTS

Wastewater Source	Daily Flow @ 8Hrs/Day
Chromium-Bearing Wastewater	7,600 l/day*
Cyanide-Bearing Wastewater	15,000 l/day
Acid/Alkaline Wastewater	45,400 l/day
TOTAL =	68,100 l/day

Characteristics of Wastewater Composite and Effluent Quality

Pollutant	Influent (mg/l)	Effluent Standard (mg/l)
Cu	17.0	1.8
Ni	5.2	1.8
Cr	42.0	2.5
Zn	2.6	1.8
Pb	4.4	0.3
Cd	5.9	0.5
Sn	5.0	1.0
Al	10.0	0.5
Fe	10.0	—
Total Metal	102.1	5.0
Cyanide	100.0	0.23

* l/day = liters/day

SAFETY FEATURES OF DESIGN

There were a number of design features which were included on the basis of personnel safety considerations. These safety features included:

- A continuous ventilation system for the cyanide tank, the chromium tank, and the sulfide tank to exhaust toxic gas such as chlorine, hydrogen cyanide, and hydrogen sulfide which could occur due to abnormal operating conditions.
- Process-control devices which are equipped with alarms to warn personnel of conditions conducive to hazards such as low pH in the cyanide tank, high or low pH in the neutralization tank, and low pH in the sulfide tank. There are also water-level controllers and alarms.
- Oxygen masks, all-purpose fire extinguishers, eye washers, emergency showers, automatic sprinkler system, and emergency exit markings.

CONCLUSIONS

Based on a comprehensive wastewater characterization program and a treatability study, the soluble-sulfide precipitation process was selected for heavy metals removal from electroplating wastewater at the Tobyhanna Army

TABLE 5. PROCESS DESIGN SPECIFICATIONS

Unit Process	Liquid Volume	Detention Time	Other Pertinent Conditions
Cyanide Oxidation			
Stage I	470 l*	14 min @ 34 lpm**	pH > 11.0; 350mv < ORP < 400mv
Stage II	1,910 l	60 min @ 32 lpm	7.8 < pH < 8.2; 580mv < ORP < 620mv
Chromium Reduction	1,590 l	100 min @ 16 lmp	pH < 2.5; 250mv < ROP < 300mv
Neutralization	1,700 l	12 min @142 lpm	7.8 < pH < 8.2
Sulfide Addition	1,700 l	12 min @142 lpm	7.8 < pH < 8.2; free S = ion > 1 mg/l
Flash Mix	190 l	80 sec @142 lpm	Anion Flocculant Conc. = 10 to 15 mg/l
Flocculation	980 l	6.9 min @142 lpm	
Laminar Settling	9,080 l	64 min @142 lpm	Surface Loading = 25.7 lpm/m²
			Tube Surface Loading Rate = 4.6 lpm/m²
Polishing Filter	N.A.	N.A.	Surface Area = 2.2 m²
			Loading Rate = 84.7 lpm/m²
Sludge Thickener	8,330 l	4 days @ 35 lpm Sludge Flow	Continuous Decant
Filter Press	N.A.	N.A.	0.056 cu. meter Capacity/Cycle

* l = liters.
** lpm = liters per minute.

TABLE 6. CHEMICAL CONSUMPTION RATES

Unit Process	Chemical & Consumption Rate	
Cyanide Oxidation	NaOCl	380 l/wk* @15% Sol.
	NaOH	95 l/wk @10% Sol.
	H_2SO_4	190 l/wk @10% Sol.
Chromium Reduction	$NaHSO_3$	210 l/wk @ 3% Sol.
	H_2SO_4	75 l/wk @25% Sol.
Neutralization	NaOH	230 l/wk @40% Sol.
Sulfide Addition	NaHS	380 l/wk @20% Sol.
pH Adjustment for Sulfide Process Flocculation	H_2SO_4	260 l/wk @25% Sol.
	Anionic Polymer	190 l/wk @ 4% Sol.
Oxidation of Residual Sulfide in Effluent	H_2O_2	Minimum

* l/wk = liters per week

Depot. This process is advantageous in terms of metals-removal efficiency, solids and liquid separation, sludge-thickening capability and dewaterability, and sludge stability for disposal by landfill. The treatment plant discussed in this paper is scheduled to be operational by September, 1981. Operating data will be presented when they become available.

LITERATURE CITED

1. U.S. Environmental Protection Agency, "Effluent Guidelines and Standards: Electroplating Point Source Category—Pretreatment Standards for Existing Sources," *Federal Register*, **46**, No. 18, 9462-9473 (Wednesday, January 28, 1981).
2. Walden Division of Abcor, Inc., "Engineering Analysis and Feasibility Study for Treatment of Plating Shop Rinsewaters," Prepared for the Army Mobility Equipment Research and Development Command (MERADCOM), Fort Belvoir, Va. (October, 1978).
3. Knocke, W. R., N. M. Ghosh, and J. T. Novak, "Vacuum Filtration of Metal Hydroxide Sludges," *Journal of the Environmental Engineering Division*, **106**, No. EE2, *Proceedings of the American Society of Civil Engineers*, 363-376 (April, 1980).
4. AEPCO, Inc., and JRB Associates, "Design of Soluble Sulfide Precipitation Facility for Electroplating Wastewaters," Tobyhanna Army Depot, prepared for the Army Mobility Equipment Research and Development Command (MERADCOM), Fort Belvoir, Va. (November, 1980).

Engineering Aspects of Ozone Generation

A large number of parameters must be taken into account in the proper design of practical, economically attractive ozone generators and systems.

James J. Carlins, Union Carbide Corp., Tonawanda, N.Y. 14150

ELECTRICAL CHARACTERISTICS OF A CORONA DISCHARGE

Ozone generation is accomplished commercially by the passage of a dry, oxygen-bearing gas through a corona discharge. The rate of ozone production depends upon many factors, including the feed gas, contaminants in the feed gas, the ozone concentration achieved, the power density in the corona, the coolant temperature and flow, and the effectiveness of the cooling system. These parameters must be carefully scrutinized to design practical, economically attractive ozone generators and systems.

A corona is characterized by a low-current electrical discharge across a gas-filled gap with a voltage gradient on the order of the sparking (electrical breakdown) potential of the gap. During breakdown, the gas becomes partially ionized and a characteristic diffused bluish glow results. A typical corona cell consisting of two metallic electrodes separated by a gas-filled gap and a dielectric material is depicted in Figure 1. An oxygen-bearing gas flows through

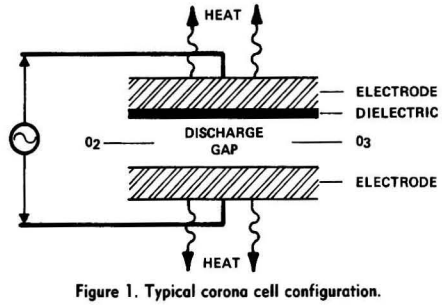

Figure 1. Typical corona cell configuration.

ISSN 0278-4491-82-5451-0113-$2.00.

the discharge gap while high voltage is applied to the electrodes. The electric energy input to the corona is dissipated primarily as heat with smaller portions going to light, sound, and chemical reactions.

Electrically, a corona cell presents a capacitive load to the power supply due to both the gas-filled gap and the dielectric materials present. The capacitance formulas for the two basic corona cell geometrics are:

Concentric Tube:

$$C = \frac{2\pi\epsilon\epsilon_0 L}{\ln(b/a)} \quad (1A)$$

Parallel Flat Plate:

$$C = \frac{\epsilon\epsilon_0 A}{t} \quad (1B)$$

Where,

b = outer radius, m
a = inner radius, m
L = length of dielectric material, m
t = dielectric thickness, m
ϵ_0 = permittivity of free space, farad/m
ϵ = relative dielectric constant
A = surface area of dielectric material, m²
C = capacitance, farad

Typically, the dielectric material chosen has a high dielectric strength (volts/mm) and a high relative dielectric constant, such as glass or ceramic.

Corona occurs when the voltage applied to the gas-filled gap exceeds the sparking potential of the gap, V_s. Cobine [1] reports the sparking potentials for air and oxygen to be:

$$V_s = 29.64\ pt_g + 1350 \text{ (air)} \quad (2A)$$

$$V_s = 26.55\ pt_g + 1480 \text{ (oxygen)} \quad (2B)$$

where p is the absolute gas pressure, in kilopascals, and t_g is the gap length (thickness), in millimeters. Considering the corona cell as a capacitive voltage divider, a relationship between the corona start potential, V_{cs} and V_s can be obtained as

$$V_{cs} = V_s(C_d + C_g)/C_d \quad (3)$$

where C_d and C_g are the dielectric and gap capacitances respectively. V_{cs} is defined as the minimum voltage that must be applied across the corona cell to obtain V_s across the gap. Because the gas in the gap becomes conductive with an impressed voltage of V_{cs}, the voltage drop across the gap itself remains essentially constant at V_s with further increases in the applied voltage. Utilizing this, Rosenthal *et al.* [2], have successfully modeled a conducting corona discharge gap as a zener diode, which characteristically maintains a constant voltage drop during conduction. This allows the characteristic shape of the dielectric potential during conduction to be mathematically approximated as:

$$V_d = V_0 \sin(\omega t) - V_s \quad (4)$$

By calculating the charge stored on the dielectric and the displacement current through the dielectric material, the instantaneous corona power draw can be expressed as

$$P_i = wC_dV_sV_0 \cos(\omega t) \quad (5)$$

Power Equation

An expression for the average power can then be obtained by integrating the instantaneous power over the duration of the corona and accounting for the number of corona discharges per second (2f). The result is:

$$P = 4C_dV_sf\left[V_0 - \frac{C_d + C_g}{C_d} V_s\right] \quad (6)$$

An understanding of the power equation, Equation 6, reveals the theoretical basis for the various practical designs commercially available. That is, for a given geometry, gap thickness, and gas pressure, the power draw of the corona can be increased: by operating at higher frequencies; by employing thinner dielectrics with higher dielectric constants; and by operating at higher peak driving voltages.

Dielectric thickness

From a practical standpoint, however, minimum dielectric thicknesses are usually dictated by structural considerations, material quality (freedom from imperfections), and dielectric strength. In addition, high peak voltages tend to enhance dielectric failures due to correspondingly high voltage stresses. Finally, for a given dielectric cooling system, extremely high power densities (watts/m²) also increase dielectric failures due to dielectric heating. This factor imposes practical limits on power density and stringent requirements for an effective cooling system for highest dielectric reliability. Therefore, a practical compromise between high power draw, cooling efficiency, dielectric reliability, and maintenance must be obtained. Utilizing this rationale, the thrust of the state-of-the-art developments currently in progress throughout the industry follows trends toward: higher quality and thinner dielectrics; thinner corona gaps; higher operating frequencies; lower driving voltages; higher corona power levels per unit electrode area; and improved cooling of both the dielectric material and the corona discharge.

Rosenthal, *et al.* [2] have developed a valuable tool for investigating the electrical operation of a corona cell. By creating an oscilloscope plot of corona cell voltage, $V(t)$, *versus* charge, $Q(t)$, characteristic information concerning cell capacitances and critical voltages can be obtained. The resultant idealized parallelogram is depicted in Figure 2. The two slopes of the parallelogram represent reciprocal capacitances for the conducting, C_d, and nonconducting, C_T, portions of the corona cycle. With these values, the gap capacitance, C_g, can then be calculated using the relationship $C_g = C_dC_T/(C_d - C_T)$. The straight lines indicate constant dynamic capacitances. The peak driving voltage, V_0, and sparking potential, V_s, are also readily obtainable as indicated. The energy dissipated per cycle can be determined by computing the area enclosed by the parallelogram.

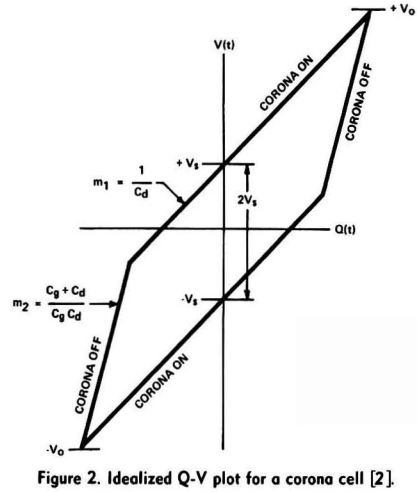

Figure 2. Idealized Q-V plot for a corona cell [2].

OZONE YIELD

The range of representative values of the corona specific energy for commercial ozone generators is illustrated in Figure 3. Notice that the energy efficiency decreases rapidly at higher ozone concentrations. This is a direct result of the back reaction for decomposition of ozone to oxygen. The back reaction is favored not only by higher ozone concentrations, but also by higher temperatures due to the thermal instability of ozone. The strong inverse relationship between the half-life of ozone and temperature is illustrated in Table 1. Therefore, efficient heat removal from the corona strongly influences the net specific energy.

There are several approaches to varying ozone production. By maintaining a constant corona power and varying the feed-gas flow rate, the relative yield will vary with a characteristic represented by Figure 4. For very low flows, the ozone concentration is very high. Therefore, small quantities of ozone are produced because the specific energy is very high. Alternatively, by maintaining a constant gas flow rate and varying the corona power level, relative ozone yields as shown in Figure 5 are common. Note that the yield increases more slowly at higher power levels. Depending on the efficiency of the corona cooling system, it is possible to increase the corona power and therefore heat generation to the point that the curve asymptotes and no further ozone yield is achieved. In fact, the curve can eventually fold over so that any additional increase in corona power will decrease ozone yield.

In Figure 6, representative energy values are shown for the production of ozone, with dry air as the feed gas. Again, a range of values is given to represent the major types of commercial generators available at this time. As is suggested by Figure 6, it is generally not economically attractive to generate high ozone concentrations (>2.0 wt.% O_3) with air feed. Because the oxygen concentration in the air is about 21% that in pure oxygen, one might expect the specific energy for ozone production from air to be about five times greater than that for production from oxygen. In fact, only about twice as much energy is required for the concentrations of practical interest. Therefore, it seems that nitrogen is not an inert diluent but must somehow contribute to ozone formation. Popovich *et al.* [5] suggest that activated nitrogen atoms collide with and dissociate oxygen molecules in the corona, which increases the atomic oxygen concentration and enhances ozone production.

TABLE 1. UNCATALYZED THERMAL DECOMPOSITION OF OZONE IN $O_3 + O_2$ MIXTURES [4]

Temp. °C	K	Half-Life for Indicated Initial Concentrations[a]			
		Wt. %→	5	2	1.0	0.5
		Vol. %→	3.333	1.333	0.667	0.333
120	22.4		11.2[b]	28[b]	56[b]	112[b]
150	1.40		41.8	104.5	209	418
200	0.030		0.9	2.2	4.5	9.0
250	0.00133		0.04	0.10	0.20	0.40

[a] $t_{1/2} = \frac{K \cdot 100}{(\text{vol \% } O_3)}$, in seconds.

[b] In minutes.

Ozone Generation

Ozone generation is an extremely inefficient process. The theoretical heat of formation of ozone is reported to be 0.835 kwh/kg [6]. If one assumes that the actual corona cell

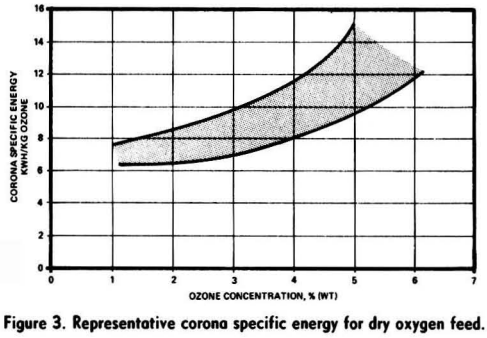

Figure 3. Representative corona specific energy for dry oxygen feed.

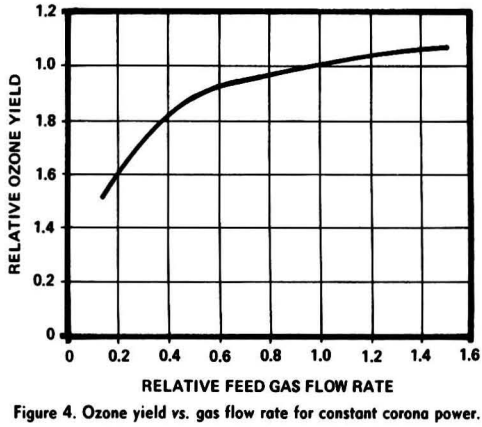

Figure 4. Ozone yield vs. gas flow rate for constant corona power.

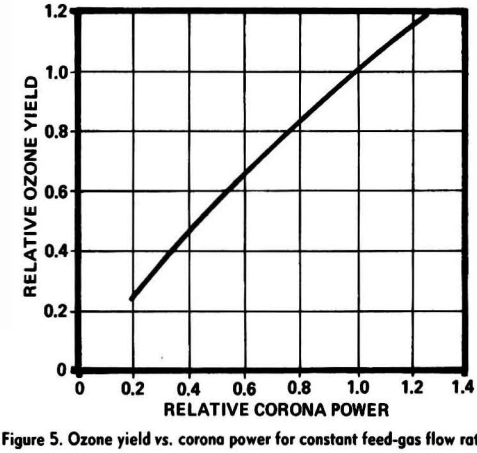

Figure 5. Ozone yield vs. corona power for constant feed-gas flow rate.

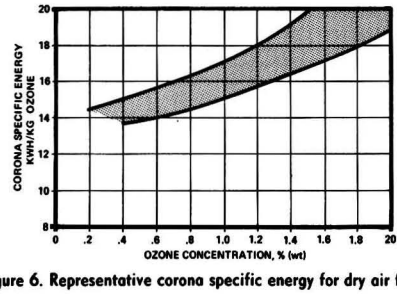

Figure 6. Representative corona specific energy for dry air feed.

specific energy required to produce ozone at 2% (wt) from oxygen is 7 kwh/kg, then it is evident that 88% of the electrical energy supplied to the corona is wasted and ultimately must be rejected from the generator. Likewise, for 15.5 kwh/kg using air feed gas, 95% of the corona energy must be rejected. With these high inefficiencies present, an effective cooling system for heat rejection is essential. Due to this influence on heat removal, the ozone yield from essentially all generators is sensitive to changes in the temperature of the coolant used. For air-cooled generators, the coolant is usually ambient air. For water-cooled or water/oil-cooled units, the excess heat is ultimately rejected to water. The relative influence of cooling-water temperature on the ozone yield for a typical water-cooled generator is depicted in Figure 7 [7].

Corona gap uniformity can also affect ozone production. Recall that the power draw is proportional to $V_s(V_0 - V_{cs})$, Equation 6, and that V_s and V_{cs} are both functions of gap thickness. If the gap thickness is relatively non-uniform, narrower portions will tend to draw more power per unit area and therefore establish a hotter corona with less efficient ozone production (kwh/kg). Further, if the narrowing of the gap is severe enough to cause a gas-flow restriction in that region, then the localized ozone concentration and the specific energy can increase even further. Therefore, the establishment of a uniform gap is necessary to achieve the maximum ozone generation efficiency.

Effect of Diluents

Diluents in the feed gas have a strong and generally detrimental influence on the ozone yield in a corona. The most common detrimental diluent is water vapor. Trace amounts of water can substantially reduce the ozone output from an ozone generator. The relative yield as a function of the feed-gas dew point is presented in Figure 8 [8]. Typically, the feed gas is dried to an atmospheric dew point of at least −40°C and usually to below −60°C. Typically, the increase in ozone yield more than compensates for the additional cost of drying the feed gas to such low dew points. In addition, the presence of water vapor can create nitric acid (HNO_3) within the corona cell, which can deteriorate downstream piping and equipment.

In a closed oxygen loop recycle system, the contactor off-gas must be dried before recycling back to the ozone generator. If the recycle compressor, dryer, and piping components are not ozone-compatible, then an in-line

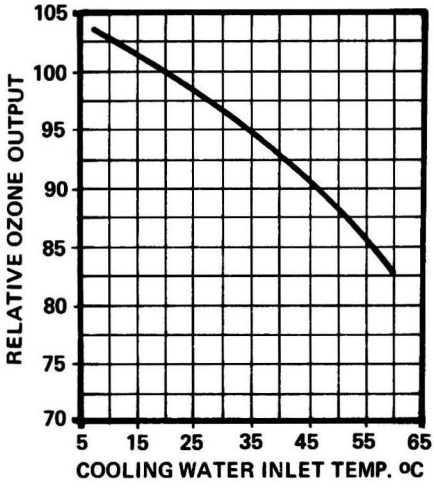

Figure 7. Typical effect of cooling-water temperature on ozone production [7].

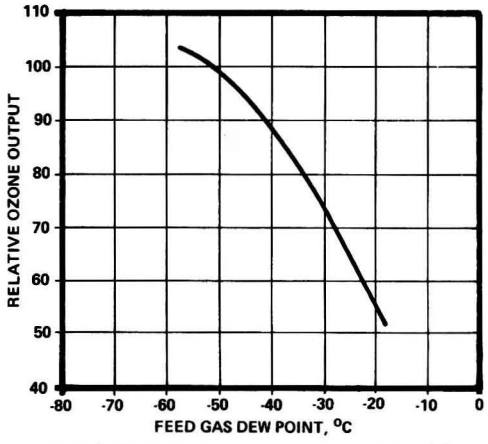

Figure 8. Effect of water vapor on ozone production [8].

ozone-destruction system must also be used after the contactor. To keep the diluent gas (nitrogen, carbon dioxide, argon, etc.) concentrations from increasing in the recycle loop, some of the recycled gas is vented to the atmosphere. The vent flow is adjusted to control the diluent concentrations at a desired value. The oxygen lost during this venting process must then be replenished from a separate supply to maintain the oxygen inventory.

To optimize the design of an oxygen-rich recycle system, the influence that nitrogen, argon and carbon dioxide have on ozone production must be determined. Cromwell and Manley [9] and Rosen [10] present data indicating that the ozone yield actually increases between 2% and 7% as the first 5% to 8% (vol.) of nitrogen is added to pure oxygen. The Cromwell and Manley data is presented in Figure 9. The factor E is the ratio of the ozone yield with the listed diluent divided by the yield with pure oxygen, assuming all other generator operating parameters remain constant.

SYSTEM DESIGN CONSIDERATIONS

An ozone generator-feed gas must be essentially free of hydrocarbons, corrosive vapors, and any other substance that can react in the oxygen/ozone/corona environment to cause safety hazards or damage to the equipment. Of the three factors required for an explosion (fuel, oxidant, and an ignition source), two are already present in the corona environment. Fuel-like materials must be kept out of the feed-gas stream. If hydrocarbons are potentially present, hydrocarbon analyzers should be installed to disconnect the corona power if hydrocarbon concentrations approach

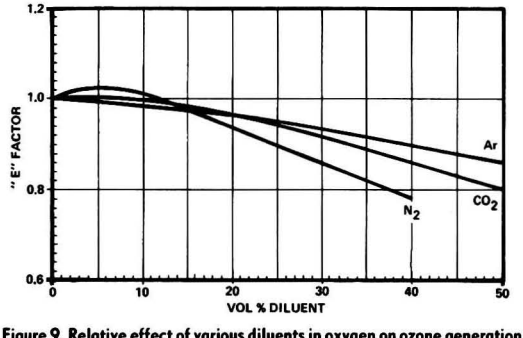

Figure 9. Relative effect of various diluents in oxygen on ozone generation efficiency [9].

25% of the lower explosive limit (LEL). In addition, fluorocarbons such as Teflon or refrigerants can be broken down to form fluorine which can attack the dielectric material, potentially accelerating dielectric failure. Also, cooling fluids circulated around the outside of the corona cell may leak past seals and enter the corona space, resulting in the formation of a varnish-like coating on the dielectric surfaces. When this happens, the dielectrics must be cleaned as the coating reduces the efficiency of ozone production. Finally, the feed gas should be filtered to about 5μ particle size to prevent small desiccant or other particles from entering the corona. Desiccant fines have been reported to cause a brown stain on dielectric surfaces [*11*].

The feed-gas pressure should not be allowed to vary uncontrollably. As gas pressure influences the corona power draw and the voltage applied across the dielectrics, wide pressure variations can cause unreliable generator operation. Excessive corona power may cause fuses or breakers to open and excessive applied voltages can cause premature dielectric failure.

An ozone system must be designed to prevent bulk water from entering the generator. This situation can occur due to malfunctioning float valves for water-ring feed-gas compressors or condensation traps on feed-gas dryers. Bulk water in the corona cell leads to concentration of the corona, high current density, and localized dielectric heating, causing premature dielectric failure. Even if a detection system interrupts the corona power before the water enters the corona cells, any debris in the water will be deposited on the cell surfaces. This debris must be removed prior to continued operation. Malfunctions or operating errors may also force liquid from the ozone contactor back into the generator. Therefore, the system design and operating procedures must also prohibit flammables, corrosives, or moisture migration back from the ozone contactor to the generator.

For water-cooled generators, the quality of the cooling water is important to minimize fouling of the heat-transfer surfaces. Fouling will lead to reduced heat-transfer efficiency and therefore, higher ozone generation and higher maintenance costs. Likewise for air-cooling generators, the cooling air must be free of blown moisture, debris, visible dust, and aerosols of corrosive, oily, or conducting materials.

COMMERCIAL OZONE GENERATORS

A variety of types of commercial-scale ozone generators are presently available. The basic differences between these units are: corona cell geometry; power supply type; heat rejection techniques; and operating conditions. As stated previously, typical corona cell geometries consist of parallel flat plate and concentric tube configurations. Both are viable alternatives and represent the basic building block for a design.

Three basic heat-rejection media are presently popular: forced air convection, water cooling, and oil cooling with subsequent heat rejection to water through a heat exchanger. The obvious advantage of forced air convection is the lack of a continuous water requirement which can lead to a lower net operating cost. On the other hand, water and/or oil cooling can offer a lower heat-rejection reservoir temperature, which can lead to improved efficiency if properly designed. In the end, economic trade-offs between water usage and corona-cell efficiency lead to an optimum design. In addition to the heat-rejection media, the method of heat rejection is also important. For example, a corona cell with cooling on both sides of the gas-filled gap will run cooler. In essence, the cooler a corona cell operates, the more efficient it becomes, due to the temperature dependence of the equilibrium reaction between ozone and oxygen.

A review of the power Equation (6) reveals that, for any given corona cell with a constant feed gas pressure, C_d, C_g, and V_s are constant. Therefore, power consumption is directly proportional to frequency, f, and peak voltage, V_0. This presents two convenient methods for controlling ozone production: voltage and frequency variation. With this knowledge, three types of power conditioning circuits have become commercially popular for supplying energy to the corona cell. These are shown in block diagram form in Figure 10. The simplest power conditioning circuit utilizes a fixed low frequency (50-60 Hz) and a variable-voltage transformer preceding the high voltage, step-up transformer (Figure 10A). The second circuit adds one additional complexity (Figure 10B), a frequency conversion usually accomplished with a motor/generator set. This fixed medium-frequency (400-600 Hz) circuit once again utilizes a variable-voltage transformer for power variation. The final conditioning circuit utilizes a fixed corona voltage and a variable frequency to control power consumption (Figure 10C). Typically, this is accomplished through rectification of the incoming power with subsequent chopping of the dc bus voltage, utilizing a solid state (thyristor) inverter bridge.

Each of the above circuits offers advantages and disadvantages. A fixed low-frequency generator requires a high peak voltage (14-32 K volt) to achieve an adequate power density within the corona cell. However, a high peak voltage creates a high dielectric stress, which tends to decrease the lifetime of the dielectric material. On the other hand, the simplicity of the power-supply design is a distant advantage with low maintenance costs. High-frequency operation (2000-2500 Hz) allows for a high power density at a low peak voltage (8-10 Kvolt peak) increasing the lifetime of the dielectric material. This higher power density is primarily important for ozone generation from high-purity oxygen feed gases in high concentration ozone production (>3 wt.% O_3). The fixed medium-frequency generators offer a compromise between power supply complexity and high operating peak voltages.

In the final analysis, an ozone generator must be designed with the best features for a given marketplace. An economic evaluation including equipment cost, operating costs (corona efficiency and cooling costs), maintenance costs (power supply and corona cell reliability), and replacement-part costs must be closely considered to choose the proper design for a given application.

LITERATURE CITED

1. Cobine, J. D., "Gaseous Conductors," Dover Publications, Inc., New York, p. 163.

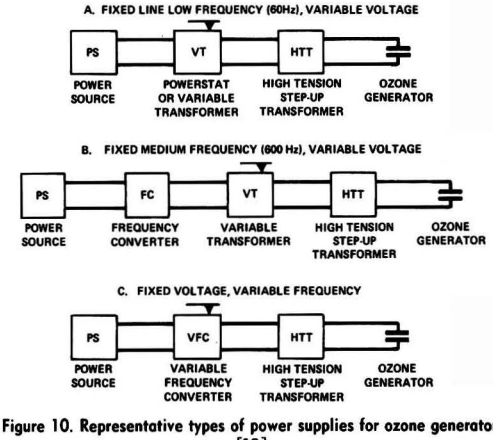

Figure 10. Representative types of power supplies for ozone generators [*12*].

2. Rosenthal, L. A. and D. A. Davis, "Electrical Characteristics of a Corona Discharge for Surface Treatment", IEEE/IAS, Vol. 1A-11, No. 3 (May/June, 1975).
3. Reynolds, S. I., "Test Methods for Measuring Energy in a Gas Discharge", Symposium on Corona, Special Technical Publication No. 198, American Society for Testing Materials.
4. Kirk-Othmer, "Encyclopedia of Chemical Technology," Second Edition John Wiley & Sons, Inc., Vol. 14 (1967), pp. 410-416.
5. Popovich, M. P., Yu. N. Zhitnev, and Yu. V. Filippov, "Spectroscopic Investigation of Mixtures of Nitrogen with Oxygen and with Ozone in the Silent Electric Discharge", *Russian Journal of Physical Chemistry*, **45**, (2) (1971).
6. Diaper, E. W. J., "Practical Aspects of Water and Wastewater Treatment, with Ozone", "Ozone in Water and Wastewater Treatment," F. L. Evans, III, editor. Ann Arbor Publishers, Inc., Ann Arbor, Mich. (1972) p. 145.
7. Liao, P. B., R. K. Allen, and V. C. Oblas, "Ozone Disinfection for Olympia Wastewater Treatment Plant", International Ozone Institute Technical Symposium, Los Angeles, California, May, 1979.
8. Cochrane Environmental Systems Division, Crane Company, Bulletin 30.23, King of Prussia, Pa. (1975).
9. Cromwell, W. E. and T. C. Manley, "Effect of Gaseous Diluents on Energy Yield of Ozone Generation from Oxygen", *Ozone Chemistry and Technology Advances in Chemistry Series No. 21*, (Washington, D.C. American Chemical Society, 1959), p. 304.
10. Rosen, H. M., "Ozone Generation and Its Relationship to the Economic Application of Ozone in Wastewater Treatment", "Ozone in Water and Wastewater Treatment," F. L. Evans III, editor, (Ann Arbor Publishers, Inc., Ann Arbor, Mich., 1972), pp. 106-108.
11. Bean, E. L., "Ozone Production and Costs", *Ozone Chemistry and Technology, Advances in Chemistry Series No. 21*, (American Chemical Society, Washington, D.C. 1959) p. 430.
12. Laroque, R. L., Private Communication to R. G. Clark (July, 1979).

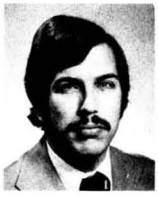

James J. Carlins was born in Pittsburgh, Pa. He received a B.S. degree in Engineering Science from the Pennsylvania State University in 1975. Since then, he has been employed by the Union Carbide Corporation Environmental Systems Engineering Department and has been involved in the design of ozone generation equipment since 1976. He is also a graduate candidate in Mechanical Engineering at the State University of New York at Buffalo.

Secondary Emissions from Subsurface Aerated Treatment Systems

A mathematical attack on the air-stripping of pollutants from subsurface layers in wastewater-treatment basins.

Raymond A. Freeman, Monsanto Co., St. Louis, Mo. 63166

MATERIAL BALANCES

The material-balance model for an activated sludge treatment system is shown in Figure 1. The material balances for the organic, microorganisms, and oxygen may be written as:

$$C_iF_i + F_rC_r = C_oF_o + r_aV + N_a \quad (1)$$

$$B_iF_i + F_rB_r = B_oF_o - r_bV \quad (2)$$

$$O_iF_i + F_rO_r = O_oF_o + r_{oxy}V - N_{oxy} \quad (3)$$

The first term in the above equations represents the quantity of material contained in the feed to the system. The second term represents the material recycled from the clarifier. The first term on the right-hand-side of the equation represents the material contained in the basin effluent. The second term represents the material formed or degraded by biological oxidation in the basin. The third terms on the right in Equations (1) and (3) are the stripping rate for the organic and the rate of oxygen transfer, respectively. The overall material balances around the entire system are likewise:

$$C_iF_i = N_a + C_eF_e + C_wF_w \quad (4)$$

$$B_iF_i = B_eF_e + B_wF_w \quad (5)$$

$$N_{oxy} + O_iF_i = O_eF_e + O_wF_w \quad (6)$$

These equations completely describe the behavior of the aeration basin. There are two main parameters in the above equations. The mass transfer between the air stream and the basin contents must be found. Likewise, the rate of biological oxidation of the organic must be determined.

MASS TRANSFER

Several investigators [2, 3] have found that the bubble diameter far away from a subsurface aerator is constant and independent of sparger design. The bubble size was found

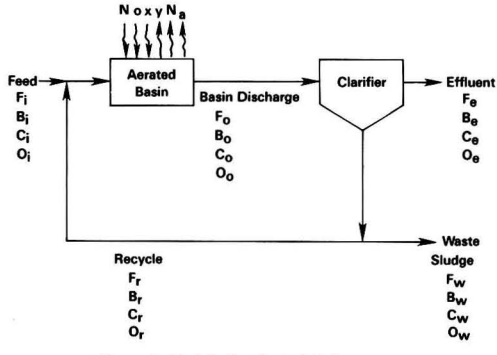

Figure 1. Model of activated-sludge system.

ISSN 0278-4491-82-5977-0118-$2.00. ®The American Institute of Chemical Engineers, 1982.

to be mainly dependent on the power input to the liquid. By assuming that the bubble diameter is constant over the entire depth of the liquid, an analytical solution for the mass transfer between bubbles and liquid is possible. The mass transfer to the bubble may be written as:

$$A_B K_x (X_1 - X^*) dT = \frac{V_B \text{den}_g}{Mw_{\text{air}}} dy \tag{7}$$

Subject to boundary conditions:

$$\text{B.C.1 } @T = 0,\ y = y_1$$
$$\text{B.C.2 } @T = t_h,\ y = y_2$$

To solve Equation (7) assume that:

1. The basin is well mixed and the liquid concentration is uniform in the basin.
2. The gas is completely mixed inside a bubble and the concentrations are uniform.
3. The mass-transfer coefficient between the bubble and the liquid in the basin does not vary with depth.
4. The molar density within a bubble does not change during the mass transfer. The average molar density of the bubble remains constant as the bubble rises through the liquid in the basin.

Solving for the concentrations of organic and oxygen within the bubble as it breaks the basin surface yields:

$$y_2 = mX + (y_1 - mX)\exp\left[\frac{-6K_x t_h Mw_{\text{air}}}{D_B \text{den}_g m}\right] \tag{8}$$

The bubble diameter may be estimated by use of Calderbank's [4] correlation:

$$D_B = 4.15 \frac{St^a}{(P/V)^b \text{den}_l^{\,c}} g_{hf} + 0.09\ cm \tag{9}$$

With:

$$a = 0.6$$
$$b = 0.4$$
$$c = 0.2$$

Assuming 100-percent efficiency of energy transfer between the gas and liquid, Towell [5] proposed:

$$(P/V) = V_g \text{den}_l g \tag{10}$$

By simple extension, the power dissipation of a water-air mixing jet may be estimated as:

$$(P/V) = V_g \text{den}_l g + V_l \text{den}_l g \tag{11}$$

Towell found that the rise velocity of air bubbles fits the following empirical correlation:

$$V_s = 27.43 \text{ cm/sec} + 2V_g \tag{12}$$

The gas-holdup fraction may be estimated as:

$$g_{hf} = \frac{V_g}{V_s} \tag{13}$$

The interfacial area can be estimated as:

$$a_r = 1.44 \frac{(P/V)^b \text{den}_l^{\,c}}{S_f^a} \left[\frac{V_g}{V_t}\right]^{1/2} \tag{14}$$

Many investigators have found that the rate of mass transfer to a rising bubble is controlled by the liquid film that surrounds the bubble.
For two films the overall mass-transfer coefficient is given as:

$$\frac{1}{K_x} = \frac{1}{mk_g} + \frac{1}{k_l} \tag{15}$$

if k_g is very large:

$$K_x = k_l \tag{16}$$

The liquid-film coefficient may be estimated using Calderbank's relation as:

$$K_l (\text{Sc})^{1/2} = 0.42\left[\frac{(\text{den}_l - \text{den}_g)\text{vis}_l g}{(\text{den}_l)^2}\right]^{1/3} (3600) \frac{\text{den}_l}{Mw_{\text{water}}} \tag{17}$$

The distribution coefficient, m, between the gas and liquid may be computed as:

$$m_i = \frac{P_{i\,i}}{P_T} \tag{18}$$

The activity coefficient may be estimated using the Van Laar equation. For a binary mixture the equations become:

$$\ln_1 = A_{12}\left[\frac{A_{21}X_2}{A_{12}X_1 + A_{21}X_2}\right]^2 \tag{19}$$

$$\ln_1 = A_{12}\left[\frac{A_{21}X_2}{A_{12}X_1 + A_{21}X_2}\right]^2 \tag{20}$$

The above system of equations completely describes the mass transfer from a sterile treatment system. In an actual treatment system, the microorganisms will be eating up the organic at some rate. This competitive mechanism must be taken into account to properly model the behavior of the treatment system.

BIOLOGICAL OXIDATION KINETICS

Previously Freeman [1, 6] used the Gerber [7] model to describe the biological oxidation process in a treatment basin. Any consistent kinetic expression may be used to describe the biological reaction. However, the kinetic model chosen must provide the following relationships:

1. The yield of microorganisms per gram of organic degraded must be included.
2. The consumption of oxygen per gram of organic degraded must be included.
3. The reaction expression should ideally relate microorganism, organic, and oxygen concentrations to the rate of reaction.

The overall biological reaction may be expressed as:

$$t\,O_2 + sA \longrightarrow B + H_2O + CO_2 + \text{products} \tag{21}$$

If the rate of biological oxidation is given as:

r_a = rate of biological oxidation of organic, gram/hour

the rates of oxygen usage and microorganism production are related as:

$$r_{oxy} = \frac{s}{t} r_a \frac{Mw_{oxy}}{Mw_a} \tag{22}$$

$$r_b = s\, r_a \frac{Mw_b}{Mw_a} \tag{23}$$

The above set of equations describes the operation of an activated-sludge plant. A mathematical model of the clarifier has not been included. However, by setting the concentration of microorganisms in the effluent and recycle streams, all other system parameters may be calculated. The model is complex and requires the solution of three simultaneous non-linear equations in three unknowns.

MODEL VERIFICATION

Freeman [6] reported the experimental results obtained when acrylonitrile was treated in a subsurface activated-sludge apparatus. Included in the study were data for air

stripping of acrylonitrile from a sterile biologically inactive system. By solving for the amount of air stripping and liquid concentrations using Equations (1) thru (20), a direct comparison with experimental data is possible. Table 1 gives the results of this comparison.

An examination of the experimental data indicates that some air stripping was occurring in the clarifier. The model presented in this paper does not include a model for air stripping from the clarifier. The mass transfer from the clarifier surface could be modeled using the equations previously presented for surface aeration [*1*]. However, the model presented here seems to predict the mass transfer to the atmosphere adequately. In actual practice, biological degradation will be occurring. The liquid-phase concentrations will be much lower than measured for the sterile case. Consequently, the mass transfer from the clarifier will be greatly reduced, and the model error will therefore decrease.

TABLE 1. COMPARISON OF MODEL PREDICTIONS WITH EXPERIMENTAL DATA

Variable	Predicted	Measured
Basin Effluent Concentration	365 mg/liter	367 mg/liter
"AN" Concentration in Air	1377 mg/liter	1200 mg/liter
"AN" Stripped to Air	0.108 gr/hr	0.0938 gr/hr

NOTATION

A_{12} = Van Laar constant
A_{21} = Van Laar constant
A_B = Surface area of an air bubble, cm²
a_r = interfacial area per unit volume of basin, cm⁻¹
B = Concentration of microorganisms, g/cm³
C = Concentration of organic, g/cm³
D_B = Diameter of an air bubble, cm
den_l = density of liquid in basin, g/cm³
den_g = average density of air as it passes through the basin, g/cm³
F = Flow rate, cm³/hr
g = acceleration due to gravity, 980.62 cm/sec²
g_{hf} = gas-holdup fraction
K_r = Overall mass-transfer coefficient between air and water, gmole/hr-cm²
k_g = Gas-film mass-transfer coefficient, gmole/hr·cm²
k_l = Liquid-film mass-transfer coefficient, gmole/hr·cm²
Mw_i = Molecular weight of component i, gm/gmole
m = distribution coefficient between gas and liquid = y/x
N_a = Loss of organic to the atmosphere, g/hr
N_{oxy} = Oxygen transfer to the basin, g/hr
P/V = Power per unit volume of basin, g-cm²sec³·cm³
r_a = Rate of organic disappearance, g/hr·cm³
r_b = Rate of microorganism growth, g/hr·cm³
r_{oxy} = Rate of oxygen consumption in the basin, g/hr·cm³
Sc = Liquid-phase Schmidt number
St = Surface tension, g/sec²
s = Stoichiometric coefficient in Equation (21)
T = time, hr
t = Stoichiometric coefficient in Equation (21)
t_h = Rise time for a bubble in the basin, hr
V = Volume of aeration basin, cm³
V_B = Volume of an air bubble, cm³
V_g = Superficial velocity of gas in the basin, cm/sec
V_l = Velocity of liquid injection into the basin, cm/sec
V_s = Velocity of rise of a large number of bubbles, cm/sec
V_t = Terminal velocity of a single rising bubble, cm/sec
vis_l = Viscosity of liquid, g/cm·sec
X = Mole fraction of organic in liquid
X^* = Mole fraction in liquid that would exist if the liquid were in equilibrium with the gas in the bubble
y = Mole fraction in gas
y_1 = Mole fraction in bubble at bottom of basin
y_2 = Mole fraction in bubble as it breaks the basin surface
i = Activity coefficient of substance i

LITERATURE CITED

1. Freeman, R. A., "Stripping of Hazardous Chemicals From Surface Aerated Waste Treatment Systems," *Proceedings on Control of Specific (Toxic) Pollutants,* Florida Section, Air Pollution Control Association (APCA), p. 464 (February, 1979).
2. Akita, K. and F. Yoshida, "Bubble Size; Interfacial Area and Liquid Phase Mass Transfer Coefficients in Bubble Columns," *Ind. Eng. Chem., Process Design Develop.,* **13,** 84 (1974).
3. Kawagoe, M. K. Hakoo and T. Otake, "Liquid Phase Mass Transfer Coefficients and Bubble Size in Gas Sparged Contactors," *J. Chem. Eng. Japan,* **8,** 254 (1975).
4. Calderbank, P. H., "Mass Transfer," Chapter 6 of *Mixing,* edited by V. W. Uhl and J. B. Gray, Academic Press, New York (1967).
5. Towell, G. C., Strand, C. P. and Ackerman, G. H., "Mixing and Mass Transfer in Large Diameter Bubble Columns," *AIChE-I, Chem. Eng. Symposium Series,* No. 10; London: *Inst. Chem. Eng.,* 10-97 (1965).
6. Freeman, R. A., J. M. Schroy, J. R. Klieve, and Archer, "Experimental Studies on the Rate of Air Stripping of Hazardous Chemicals From Waste Treatment Systems," 73rd Annual APCA Meeting, Montreal, Canada, June 22-27 (1980). Reprint Number 80-16.7.
7. Gerber, V. Ya., V. M. Sharafutdinov, and Gerceridov, "Kinetics of Biochemical Oxidation of Refinery Wastewaters," *Chem. Technol. Fuels Oils (USSR),* **12,** 826 (1976).

Raymond A. Freeman is an Engineering Specialist in the Engineering Technology Group of Monsanto Corporate Engineering. He serves as a general process consultant to the corporation in the areas of risk assessment and process design. He holds B.S., M.S. and Ph.D. degrees in Chemical Engineering from the University of Missouri—Rolla. He joined Monsanto as a process engineer in 1974. He is a registered professional engineer in Mo., a member of the American Institute of Chemical Engineers and the American Association for the Advancement of Science.

Electrolytic Removal of Heavy Metals from Wastewaters

Elimination of end-of-the-line treatment is the key to important savings of capital and operating costs.

B. M. Kim and J. L. Weininger, General Electric Co., Schenectady, N.Y. 12301

Within the next few years new and stringent environmental regulations will come into effect for the electroplating and metal-finishing industries. These regulations, promulgated on the local and national level, particularly by the Environmental Protection Agency, are placing stringent effluent levels on heavy metal discharges for plants involved in such operations. The conventional treatment of such wastewater impurities takes place at the end-of-line and involves treatment of large volumes of wastewater by chemical precipitation. This operation entails large capital costs and produces vast volumes of metal-containing sludges. Consequently, several other technologies are being investigated to reduce or eliminate the end-of-line treatment by removing metallic impurities at the source. Examples of such treatments are ion exchange, reverse osmosis, electrodialysis, or electrolytic cleanup of wastewater [*1*]. This report focuses on the electrolytic removal of metallic wastes from plating processes. Electrolytic deposition of the impurities has the advantages that the metals are recovered at relatively low capital and operating costs, that no chemicals are required for the process, and that no sludges are formed.

The major challenge to the development of this process is the requirement of large mass transfer in electrode reactions with dilute solutions. This has been accomplished by using an electrolytic reactor in which the active electrode material for cathodic deposition is made of carbon fibers. These provide a large surface area, thereby achieving the appropriate current densities for the required large removal rates.

ELECTROLYTIC REACTOR FOR WASTEWATER CLEANUP

The following types of electrodes have been developed for use in electrolytic reactors: planar, rotating cylinders, packed or fluidized beds, and foamed, slurry, and vibrating electrodes. Mass-transfer rates are enhanced both by stirring the solution (forced convection) and by increasing the effective surface area of the electrodes. In an early review of electrolytic reactors, Houghton and Kuhn [2] compared attainable current densities of different types of reactors, normalizing them with respect to the plane-parallel electrode arrangement (Table 1).

In packed-bed electrodes, porous carbon or graphite, graphite pellets [3], metal beads and screens [*4*], or metallized glass spheres [5] have been used. The electrode of our choice was a bed of electrically conducting carbon fibers with a fiber diameter of 8 μm. Depending on the compression of the fiber mat, large surface areas of 100-300 cm^2/cm^3 of electrode volume can be achieved, even when the porosity of the fiber mat is higher than 95%. This large void volume made it possible to contain large metal deposits without undue increase in the low resistance to the liquid flow.

TABLE 1. POSSIBLE REACTOR DESIGN

Electrodes	Current Densities (mA/cm^2)
Parallel Plates	0.5-3
Parallel Mesh	1
Rotating Disk	3-10
Rotating Cylinder	7-40
Packed Bed	6-120
Fluidized Bed	6-120
Slurry Electrode	—
Vibrating Electrode	—

A schematic of the reactor is shown in Figure 1. The current collector, carbon pad, separator, and another carbon pad and current collector are arranged in sequence as in a filter press. Stainless-steel and titanium screens served as current collectors for cathode and anode, respectively. Separators were made of non-woven porous plastic sheets.

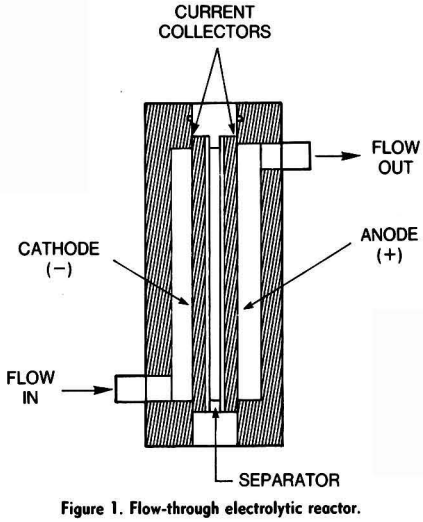

Figure 1. Flow-through electrolytic reactor.

ISSN 0278-4491-82-6241-0121-$2.00.

In all cases the carbon fibers were the effective and active part of the cathode. At relatively low applied voltages they could also be used as anodes, but at higher voltages they were subject to oxidation, so that, under more stringent operating conditions, a commercial, dimensionally stable anode metal oxide was used.

Different electrode housings were designed for easy assembly and disassembly of the reactor and accessibility to the loaded cathode. Generally, for removal of metals, the electrolytic reactor was operated in a recirculating mode. In such an application, short flow paths at high flow rate are permissible, whereas a long flow path at slow flow rate is required for complete removal of metals in a reactor with a single pass throughput.

The main application of our reactor was the removal of metallic impurities from the dragout tank of an electroplating line. Following the electroplating tank, the dragout tank is the first rinse tank in line. Consequently, the metal concentration is highest in this tank among all the rinse tanks, as shown in Figure 2. Low metal concentrations in the exit stream can be achieved by continuously removing metals from the tank, thereby operating at the source of pollution.

The metal deposited in the reactor can be disposed of or it can be recycled to the plating bath, either as pure metal for the anode in the plating bath or in concentrated solution by addition to the electrolyte.

The following rate equation is applicable to a batch operation of the electrolytic reactor, as well as to the recirculating mode. With mass-transfer control between the solution and the electrode surface, the rate of removal is given by

$$\log_e \frac{C_t}{C_o} = -\frac{kAt}{V} \qquad (1)$$

where

A = electrode surface area
C_t = metal concentration at time t
C_o = metal concentration at time o
k = mass-transfer coefficient
V = volume of reservoir

Then, the removal rate at time t, kAC_t, is determined by the slope of the plot of $\log_e C_t/C$ *vs.* time (t).

The limiting current density (i_{lim}) in this case is

$$i_{lim} = nFk\dot{C}_t \qquad (2)$$

where

F = Faraday's constant
n = number of electrons

EXPERIMENT

Two different sizes of electrolytic reactors containing the same type of carbon-fiber cathodes and anodes were used. The smaller reactor A had 7.6-cm (3-in) diameter electrodes, 0.95 cm (3/8-in) thick. It was used for rate studies in a recirculating flow system. The larger reactor B had electrodes 15.2 cm (6-in) in diameter and 1.3 cm (1/2-in) thick. It was used for simulation tests of dragout-tank cleanup operation as well as on-site cleanup tests.

In Figure 3 the schematic shows the flow system and electric circuitry. A filter was necessary to remove particulates in an on-site test. The pressure transducer was used to record pressure buildup due to metal deposition in the reactor. A D.C. power supply capable of operating at constant current and constant voltage was employed. Potentials of anode and cathode against an Hg/HgO reference electrode, interelectrode potential, and current supplied to the reactor were monitored. Concentrations of metals in the solution were measured by analyzing samples with an atomic absorption spectrophotometer.

Experiment on rate studies using reactor A involved measuring the concentrations of metals in the reservoir as the solution recirculated through the electrolytic reactor. The volume of the reservoir was 500 ml and the flow rate varied from 40 to 180 ml/min. The effect of flow rate, applied potential, and impurity concentration on the removal rate was studied at constant applied potential or constant current. Constant-current operation at some maximum value followed by constant potential was found a suitable procedure. At constant current there was a tendency for the applied potential to increase slowly. When a maximum desirable potential was reached, the second phase began by switching from constant current to constant potential.

Metal Cleanup from Dragout Tank

Laboratory simulation and on-site metal-cleanup experiments were performed with emphasis on removal of zinc and silver. The simulation experiments were performed by continuously adding simulated Zn or Ag plating solution to a reservoir while recirculating the mixed rinse solution through the electrolytic reactor. The composition of the Zn plating solution was 9.35 g/liter ZnO and 90 g/liter NaOH; that of the Ag plating solution was 7.8 g/liter AgCN and 7.8 g/liter KCN. The dragout rates were 1.25 g/hr for the Zn line and 1.5 g/hr for the Ag line.

On-site tests were carried out in a manufacturing plant involved in various electroplating and metal-finishing operations. Heavily used Zn and Ag plating lines were chosen for electrolytic cleanup. By removing these metals at the source (dragout tanks), the end-of-line treatment was expected to be significantly simplified. This would result in significant savings in capital investment for the end-of-line treatment plant.

RESULTS AND DISCUSSION

Removal of Zinc

Reactor A was used for rate measurements in a recirculating flow mode. In this system the reservoir volume

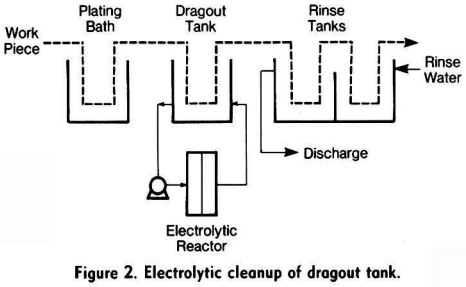

Figure 2. Electrolytic cleanup of dragout tank.

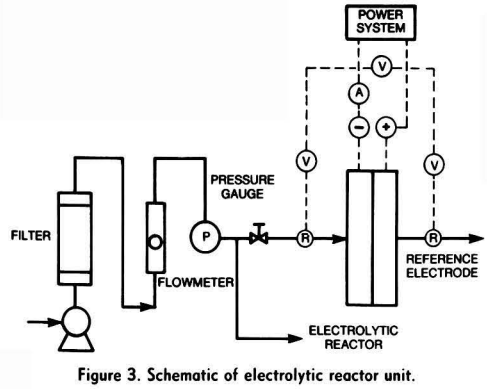

Figure 3. Schematic of electrolytic reactor unit.

was 500 ml. The reactor's cathode contained carbon felt as the active material, which averaged about 2.5 g. For the given geometry this was equivalent to 97% porosity and 92 cm^2/cm^3 of actual surface area per unit volume of the porous electrode. For the following experiments the initial concentration of zinc in 1 N NaOH was 700 mg/liter.

a) Effect of flow rate on zinc removal: The removal of zinc by the reactor at two different flow rates is illustrated in Figure 4. The experiments took place at a constant cell voltage of 6 volts with a range of voltage changes from open-circuit to steady-state for the cathode (*vs.* Hg/HgO reference electrode) of −0.13 V to −0.456 V, and for the cell from 0.16 to 6.0 V. As expected, higher flow rates gave higher removal rates. Thus, at 143 ml/min, 0.29 g/hr of Zn was removed, and at 168 ml/min, the removal rate was 0.70 g/hr. Other details of the experimental conditions are shown in Table 2. Current densities for the two cases were 160 and 50 ma/cm^2 of projected surface area. This corresponded to current efficiencies (for removal from 700 to 100 mg/liter) of 22 and 17% for the low and high flow, respectively.

b) Effect of constant voltage: The results of three different constant-voltage experiments are plotted in Figure 5. Voltages of 4.5, 5.0, and 6.0 V were constant with a flow rate of 136 ml/min. The current efficiencies (from 700 to 100 mg/liter) were 45, 42, and 22% for the 4.5, 5.0, and 6.0 V tests. This corresponded to removal rates at 100 mg/liter of 0.10, 0.19, and 0.28 g/hr for the three cases, with increasing removal rate at higher voltage. Obviously, the higher overvoltage resulted in a larger current, but it also entailed greater gas evolution from the system. The gas evolution, in turn, produced better mixing, giving higher removal rates but lower current efficiencies.

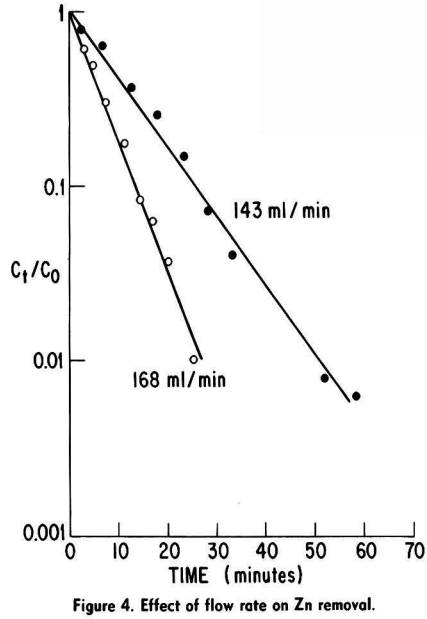

Figure 4. Effect of flow rate on Zn removal.

Removal of Silver

The results of a typical silver experiment are shown in Table 2. In this case the reservoir contained 500 ml of AgCN + 1 M KCN solution (5,500 mg/liter Ag, 3,800 mg/liter CN^-).

Reactor A was operated in a recirculating mode at a flow rate of 100 ml/min and a 2-ampere constant current (44 ma/cm^2). This gave an average cell voltage of 3.5 V with cathode potentials (measured *vs.* Hg/HgO) of +0.49 V at open-circuit and in a range of −1.11 to 0.172 V during constant-current operation. The removal rate at 100 mg/liter was 0.47 g/hr and the current efficiency 82% (with respect to 100 mg/liter). After one hour of operation, the initial Ag concentration had decreased from 5,500 to 153.5 mg/liter in the reservoir; the effluent from the reactor was 7.1 mg/liter at that time.

Figure 6 is a scanning electron micrograph of the cathode surface partially covered with silver. The cathode has a random distribution of carbon fibers ranging from 8 to 20 μ in diameter and a large void volume between fibers. Ag, deposited under the given experimental condition, consists of crystallites as large as 10 μ. Bridging takes place between deposits of adjacent fibers.

Removal of Copper

Copper was removed from an actual wastewater solution derived from an electroless plating operation. The proprietary commercial solution—Cuposit CP 74 (Shipley Co.) contained 11% NaOH, 0.25% Cu, and 6% formaldehyde. An unspecified amount of chelating agent (and/or possible unknown components of the solution) prevented removal of Cu by more conventional means.

In this case the reservoir volume was 218 ml, a flow rate of 42 ml/min was used, and the reactor was operated under a combined galvanostatic/potentiostatic control, i.e., initially, the operation was at a constant current of 3.3 A, but within minutes the voltage increased to a maximum of 12 V, at which time the control switched over to a constant-voltage mode. Consequently, in this second phase the current decreased from 3.3 to 0.31 A. The total amount of electricity used in this experiment was 2,258 coulombs, equivalent to 0.742 g Cu. Since 0.661 g Cu were actually deposited, this amounted to a current efficiency of 89%. The cost of electricity for this deposition at 5¢/kwh was $0.68/kg. Cu, lower than the value of the recovered copper.

Zinc Removal from Dragout Tank

With the larger reactor B, the actual operating conditions of a full-sized electroplating line were simulated in order to establish the long-term use of a reactor (with an effective cathode diameter of 15 cm) in terms of operating condi-

TABLE 2. SUMMARY OF RECIRCULATING FLOW EXPERIMENTS

Exp. No.	Metal	Initial Conc. (mg/l)	Wt. of C (g)	Flow (ml/min)	Mode	Avg. A or V	Removal*1 Rate (g/hr)	Current*2 Eff. (%)
1	Zn	693	2.69	143	6V	2.2A	0.28	22
2	Zn	706	2.56	168	6V	7.4A	0.70	17
3	Zn	690	2.43	136	4.5V	0.41A	0.10	45
4	Zn	737	2.43	136	5V	0.71A	0.19	42
5	Ag	5500	—	100	2A	3.5V	0.47	82
6	Cu	3000	1.2	42	—	—	0.15	89

Note: 1. Removal rate at 100 mg/l
2. Current efficiency from initial concentration to 100 mg/l.

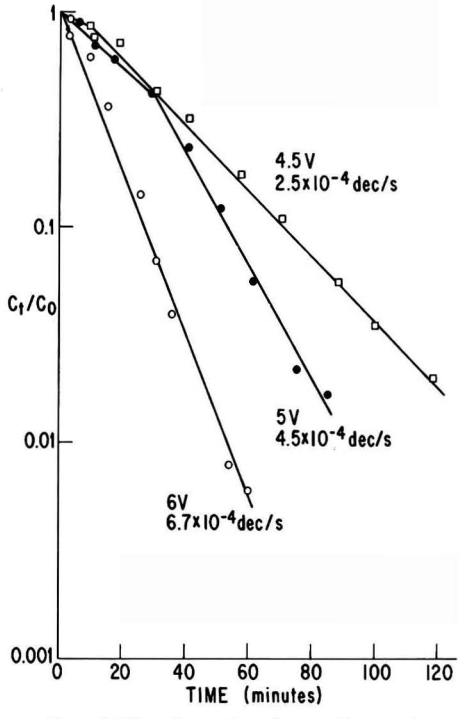

Figure 5. Effect of operating voltage on Zn removal.

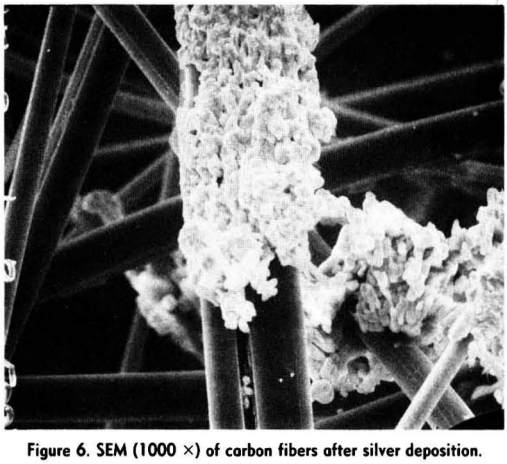

Figure 6. SEM (1000 ×) of carbon fibers after silver deposition.

tions, lifetime, and failure modes. The reactor had a metal-oxide anode and a carbon-felt electrode, 1.3 cm (1/2-in) thick, weighing about 20 g.

In order to simulate the full-scale industrial application the electrolytic reactor was placed in a recirculating system in which the electrolyte was pumped with a submersible pump at the rate of 1 liter/min from a reservoir (dragout tank) through the reactor (Figure 7). In the test, the dragout tank was simulated by a reservoir of 52 liter capacity, i.e., 1/10 the actual size of the dragout tank in the electroplating line, but the impurity addition was equal to that encountered in the plant—about 1.25 g/hr.

Overall, the flow rate of 1 liter/min and the current of 5A were held constant. Depending on cell performance, the voltage varied between 4 and 7 V. The tank concentration

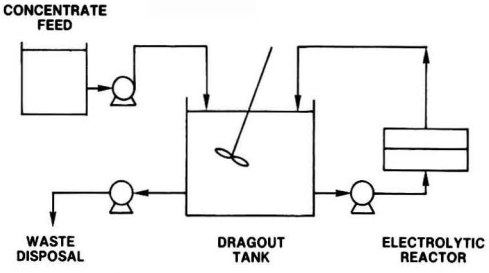

Figure 7. Simulation of metal removal from dragout tank.

could be maintained at approximately 200 mg/liter. The difference between inlet and outlet concentrations of the reactor ranged from 50 to 80 mg/liter. During the course of the test, the internal pressure of the cell increased less than 101 kPa (3 psi), as the void volume of the cathode filled up to the extent of 15%.

The actual recovered weight of zinc was 214 g; that calculated from the difference in concentration between reactor inlet and outlet and the flow rate was 235 g. The amount of electricity used was 779 AH, corresponding to an average current efficiency of 23% over the total test period of 6.5 days and a daily rate of 34.6 g Zn deposited per day.

Toward the end of the test period, the Zn concentration in the dragout tank could not be maintained below 200 mg/liter, and symptoms of dendrite formation started to appear. These were a decrease in cell voltage (to less than 4), a decrease in gas evolution (41 to 4 ml/min), and a decrease in electrolytic cell resistance (0.24 to 0.15 ohm). On disassembly of the cell, short circuits or dendrites were actually diagnosed as the cause of cell failure. These dendrites were globular and their growth was substantially retarded by the separator layers.

Removal of Silver from Dragout Tank

A similar simulation test was performed for silver cleanup at a rate of 1.5 g/hr. A typical operating condition for 0.4 A was a cathode potential of −1.38 V (*vs.* Hg/HgO electrode) and an anode potential of + 0.63 V (*vs* Hg/HgO).

During 17 days of operation the Ag concentration was maintained below 70 mg/liter, and the concentration difference between inlet and outlet was 20 to 50 mg/liter Ag at a flow rate of 1 liter/min. Total charge passed was 229.5 AH equivalent to 924 g. The actual deposit recovered was 921 g, giving a 99% current efficiency. This corresponded to occupation of 51% of the cathode void volume. The cathode had changed in appearance from a carbon felt to a solid though porous disk of silver. Failure after 17 days of operation at a rate higher than in the commercial plating line occurred because of dendrite formation along the rims of the electrodes.

Field Test of Electrolytic Reactor

The simulation tests described above were corroborated in field tests on silver and silver electroplating lines in a manufacturing plant.

For this purpose a portable electrolytic cleanup system was constructed. It consisted of an assembly of two reactors, one for operation, the other for standby, which were connected to a panel provided with pressure gage, flowmeter, ammeter, and voltmeter. The flow and electric circuits, shown in Figure 3, largely duplicated the previous laboratory conditions. For example, a submersible pump was located in the dragout tank. The only differences with respect to the simulation tests were the larger size of the dragout tank (112 liter), the intermittent introduction of

metallic pollutant into the tank, and the need for removal of sludge and scum from the actual plating line to prevent particulates from entering the reactor. This was accomplished by a filter unit.

In actual operation of the silver electroplating line at the dragout rate of 1.5 g/hr, the electrolytic reactor was operated for 70 days, maintaining the Ag dragout concentration less than 25 mg/liter.

Economics

Although accurate economic analysis cannot be performed at the present stage of development, an approximate comparison of conventional and electrolytic methods will be made for a typical plant as an example.

A hypothetical plant, which has two Zn electroplating lines, three Ag lines, and a Cr line is considered here. If heavy metals are removed at the source by electrolytic reactors, the end-of-line treatment will be significantly simplified. For example, let us consider that the current effluent at the plant has an average Zn concentration of 10 mg/liter. When the Zn concentration in the dragout tank is reduced by the electrolytic process to 1/10 of the plating concentration in the tank, the average Zn effluent concentration becomes 1 mg/liter. In the dragout tank of alkaline Zn plating, the maximum allowable Zn concentration would be 200 mg/liter, based on a Zn batch concentration of 2,000 mg/liter.

This results in the following reduction of capital cost for the cleanup system (Figure 8). For conventional end-of-line processes, cyanide oxidation, chrome reduction and neutralization, and precipitation of other heavy metals would be required. The capital cost for such a system to handle 570 liter/min is estimated to be $730,000, and the operating cost for 379 liter/min is estimated to be $34,000/year, excluding analysis cost for monitoring. Approximately $20,000 of this would be related to heavy-metal removal by hydroxide precipitation and other sludge-treatment and disposal cost.

If the heavy metals are removed at the source by the electrolytic process, only chrome reduction, cyanide oxidation, and pH control would be required at the end-of-line. The cost of such system is estimated to be $180,000. The difference of $550,000 would be the margin for cost reduction by electrolytic source treatment.

In the plant, the subject of this example, electrolytic reactors for 2 Zn lines and 3 Ag lines will be required for continuous operation. The capital cost for reactors has not been established, but it would be much less than the margin of $550,000 previously determined.

The electricity cost for operating the reactors is very small. The current efficiency of 15% at 200 mg/liter would be used as a conservative value. At the removal rate of 20 g/hr, the electricity cost would be $166/year. The cost for Zn removal would be $2.28/kg Zn based on 5¢/kwh. There are, of course, other operating costs with respect to accessory equipment as well as cathode replacement, labor, and maintenance. Considering these costs, the operating cost of the electrolytic process would still be lower than the conventional chemical precipitation process. In conclusion, the electrolytic process for at-source treatment shows an economic incentive over the conventional treatment process.

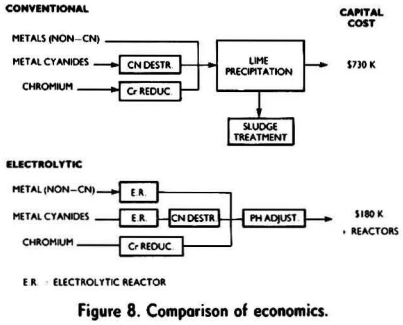

Figure 8. Comparison of economics.

CONCLUSIONS

An electrolytic reactor with a cathode made of carbon fibers and an anode made of carbon fibers or metal oxide effectively removes toxic metals from wastewater. The carbon-fiber pad provides a large surface area and large void volume, allowing a high removal rate with minimum flow resistance. Electrolytic reactors designed for high flow rate with short flow path are effective for metal cleanup in a recirculating flow mode. One specific application of such reactors is the cleanup of a dragout tank in an electroplating line. By continuously removing the metals at the same rate as they are introduced by dragout from the plating bath, it is possible to eliminate the end-of-the-line treatment. This source treatment by an electrolytic process greatly simplifies the wastewater-treatment process and results in savings of capital and operating costs.

LITERATURE CITED

1. Skovronek, H. S. and M. K. Stinson, "Advanced Treatment Approaches for Metal Finishing Wastewaters (Part I)", *Plat. Sur. Fin.*, **64**(10), 30-38 (1977).
2. Houghton, R. W. and A. T. Kuhn, "Mass-Transport Problems and Some Design Concepts of Electrochemical Reactors", *J. Appl. Electrochem.*, **4**, 173-190 (1974).
3. Bennion, D. N. "Electrochemical Removal of Copper Ions from Very Dilute Solutions", *J. Appl. Electrochem.*, **2**, 113-122 (1972).
4. Keating, K. B. and J. M. Williams, "The Recovery of Soluble Copper from an Industrial Chemical Waste", *Resource Recov. and Consv.*, **2**, 39-55 (1976).
5. Ng, P. K., "Trielectrode Electrochemical Reactor with an Improved Porous Electrode for Silver Recovery", *J. Electrochem. Society*, **128**(4), 792 (1981).

B. M. Kim is responsible for R&D in wastewater treatment, coal gas cleanup and membrane processes at GE R&D Center. His research interest has been in separation processes, pollution control and bioengineering. He has more than 30 publications in these areas.

J. L. Weininger has been associated with the GE R&D Center since 1953. He holds twenty-four patents and is the author of 40 publications. His research involved electrochemical science and he has participated in symposia dealing with theoretical and applied aspects of electrochemical technology.

Spill of Soluble High-Density Immiscible Chemicals on Water

Just what happens when a hazardous chemical is accidentally spilled into water? Here's a graphic picture, based on actual experience.

P. S. Christy, Texas Eastman Co., Longview, Tx. 75602, and
L. J. Thibodeaux, University of Arkansas, Fayetteville, Ark.

INTRODUCTION

Accompanying the continued growth of the chemical industry is the ever increasing likelihood of chemical contamination of the nation's rivers and streams. This contamination may result from inadvertent releases from production facilities, transportation accidents involving barges or other water carriers, or runoff from spills involving land carriers. These spills may be classified into three main categories: soluble compounds that mix rapidly with the water, immiscible (insoluble or slightly soluble) compounds that float on water, and immiscible compounds that sink to the bottom of the watercourse. This third category comprises 47% of some 250 chemicals listed in a report for the EPA by Pilie *et al.* [*1*] as hazardous materials having a high probability of being involved in spills into or near watercourses. Surprisingly, spills of this nature have in the past received minimal study.

The task of investigating the spill of heavy ($\rho > 1$), immiscible chemicals in the interest of developing an analytical model of a predictive nature was therefore undertaken in June, 1977, at the Chemical Hazards Research Laboratory on the University of Arkansas campus. The work was conducted under a grant from the Department of Transportation. The computer model resulting from this work will provide information on the location and size of the initial on-bottom contaminated area, the projected lifetime of the chemical, and the resulting cup-mixing concentration profile at the spill site. This information should assist authorities in the assessment of individual spill incidents with regard to ecosystem exposure, alternate water sources for industry and the public, and plans for recovery and cleanup.

DISCUSSION OF MODEL

The spill of a heavy, immiscible chemical from a point source into a river or stream is a complex process. Information on the nature of the spill as well as the physical characteristics of both the chemical spilled and the watercourse itself are important in determining the fate of the chemical. Efforts were made to limit program inputs to information that would be readily available to the user. Where this was not possible, a guide for the estimation of values was provided to the user.

The study of a chemical-spill incident can be divided into two distinct phases: the actual release and destination of the chemical, and the chemical dissolution process. In studying the first phase, extensive laboratory observations were made by Lewis [2] of spills into both quiescent and flowing systems. Briefly, the chemicals were found to quickly form a jet of chemical, extending from and roughly the same diameter as the rupture or outlet of the spill container. This quickly disintegrates (due to the high interfacial shear encountered by the jet), ultimately resulting in the formation of a stable swarm of drops of varying size. As the drops fall, differences in their settling velocities result in both horizontal and vertical classification. The chemical spreads out over a portion of the stream bottom, with the smaller drops striking bottom further downstream than the larger drops (see Figure 1). Equations were developed and tested by Lewis for the determination of the minimum and maximum drop diameters. By calculating the settling velocity of these drops, and knowing the river depth and average velocity, the distance each drop travels before striking bottom may be determined. In this manner, the length and location of the on-bottom chemical can be estimated.

In order to determine the width of the contaminated area, a correlation developed by Mourot [3] using variables associated with droplet and jet formation was employed. This correlation was originally developed for determining the area of contamination resulting from a spill in quiescent water. However, spreading due to stream turbulence in the direction of the stream width was felt to be negligible, allowing the use of this correlation as an estimate of the width of the contaminated area in a flowing system.

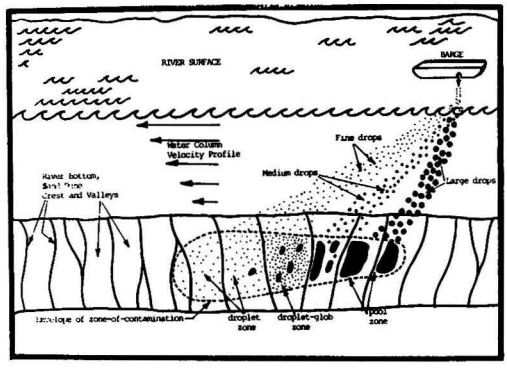

Figure 1. Hypothetical spill into river.

ISSN 0278-4491-82-5794-0126-$2.00.

Dissolution commences immediately upon contact of the chemical with the water. However, the duration of a spill is typically short when compared to the on-bottom lifetime of an immiscible or slightly miscible chemical. Therefore, only the on-bottom dissolution was considered in this model.

The following differential equation describes the dissolution of chemical A:

$$\frac{dM_A}{dt} = -K_r A_{mt}(X_{A0} - X_{Ab}) \quad (1)$$

where M_A = mass of chemical A
K_r = water-side mass-transfer coefficient, mol/length^2 · t
A_{mt} = interfacial mass transfer area, length^2
X_{A0} = mole fraction in equilibrium with water at the interface
X_{Ab} = cup-mixing mole fraction in the stream

At this point, the problem of developing a reasonable dissolution model was broken up into two parts: determination of the interfacial mass-transfer area of the on-bottom chemical, and evaluation of the mass-transfer coefficient, K_r.

MASS TRANSFER AREA

As dissolution occurs, the mass-transfer area of a chemical decreases in porportion to the mass remaining. Hence, in order to integrate Equation (1), the relationship between the interfacial area and the mass remaining at any time must be known. The geometric make-up of the stream bottom therefore becomes an important parameter, as it determines the shape of the on-bottom chemical and, ultimately, its dissolution rate.

In general, a stream bed is made up of regular bedforms, the commonest of which is the sand dune. These are wave-like structures, having a gentle, gradually varying upward slope and an abrupt downstream surface. The length and height of the dunes are dependent on the depth and velocity of the river and the character of the bottom sediment. When the drop swarm resulting from a typical chemical spill strikes bottom, coalescence in the areas of high drop accumulation occurs. A significant portion of the chemical will roll into the sand wave troughs and form pools of liquid that are triangular in cross section. Chemical coalescing on the flatter regions of the stream bed will form flat, pancake-like globs. The remainder of the chemical will remain in the form of drops, scattered primarily around the spill periphery. The formation of and dissolution from the three primary shapes, drops, globs, and waves, were the basis for the dissolution calculations used in this model.

The geometry of each shape was used to derive the following relationships between surface area and mass:

Waves
$$A_{mt} = \left[\frac{2M_w \lambda L^{1/2}}{\rho_c \Delta}\right] \quad (2)$$

Globs
$$A_{mt} = \frac{M_g}{\rho_c h_g} \quad (3)$$

Drops
$$A_{mt} = \left[\frac{36 M_d^2 \pi^{1/3}}{\rho_c^2}\right] \quad (4)$$

where M_w = mass in wave
Δ = height of wave, L
λ = length of wave, L
L = width of wave, L
ρ_c = density of chemical, M/length^3
A_{mt} = interfacial area, L^2
M_g = mass in globs
h_g = height of glob, L
M_d = mass of drops

Wave-dimension information was necessary in order to use Equation (2) for determining the mass-transfer area of the chemical in wave form. A subsequent literature survey yielded an equation found to be reliable in predicting the bedform dimensions under specified hydraulic conditions. In the glob shape equation, the height of the glob is dependent on interfacial tension forces and remains constant for a given chemical as dissolution proceeds. An equation for this parameter was also tested for reliability and incorporated into the model. These equations were substituted into Equation (1) and integrated to yield the following equations for determining the mass remaining at time t:

Waves
$$M_{Af}^{\frac{1}{2}} = M_{A0}^{\frac{1}{2}}\left[1 - \frac{K_r X_{A0} t}{\rho_c \Delta_r}\right] \quad (5)$$

where Δ_r = initial height of chemical in the wave, L

Globs
$$M_{Af} = M_{A0} \exp\left[-\frac{K_r X_{A0} t}{\rho_c h_g}\right] \quad (6)$$

Drops
$$M_{Af}^{1/3} = M_{A0}^{1/3}\left[1 - \frac{2K_r X_{A0} t}{\rho_c d}\right] \quad (7)$$

where d = initial drop diameter

The total mass of chemical remaining at any time is the sum of the contributions from all three shapes.

Due to the inherent differences in their interfacial area to mass ratio, dissolution will occur much more rapidly from the drops than from the wave forms. The globs will take on more intermediate values. The distribution of the initial mass into these three shapes is therefore crucial to the accurate prediction of the resulting stream concentration. Efforts to develop a predictive model for evaluating the mass distribution for different spills were largely unsuccessful. The distributions ultimately used in the model rely on empirical methods and judgements made after studying and observing numerous spills. The nature of the chemical release was recognized as important in determining this distribution. For this reason, logic was incorporated into the program to supply approximate distributions resulting from three basic spill scenarios:

1) Contamination from land-source runoff. No stable droplet cloud is formed, and the predominant shape is that of waves.
2) A small quantity of chemical spilled into a relatively large stream, resulting in little coalescence. Drop shape predominates, with relatively little contribution from waves and globs.
3) The previously described scenario, that of a spill from a point source into a relatively large stream. All three shapes are present to an appreciable extent.

MASS TRANSFER COEFFICIENT

Thibodeaux [4] reviewed the literature and, using relationships derived for systems that exhibited similar behavior, developed models for determining the overall mass-transfer coefficient from a stream bed with naturally occurring bedforms. Dissolution was viewed as resulting from both natural and forced-convection contributions. To account for the natural convection contribution, a dimensionless relationship was derived using transport analogies in an equation developed for natural-convection heat transfer from a downward facing plate. The following equation:

$$Nu_q = 9.22(Gr \times Sc)^{1/6} \quad (8)$$

resulted from a linear regression program utilizing the results of two dozen experiments to determine the coefficient and exponent. The dimensionless numbers were defined in the following manner:

$$Nu = \frac{K_n L_c}{c\mathcal{D}} \tag{9}$$

where K_n = natural convection mass-transfer coefficient, mol/length$^2 \cdot t$
L_c = pool length
c = molar density of water, mol/length^3
$\mathcal{D}$ = molecular diffusivity of the chemical in water, L^2/t

$$Gr = \frac{L_c^3 g \zeta \Delta X}{\nu^2} \tag{10}$$

where g = gravitational constant, L/t^2
$\zeta = \frac{1}{\rho}\left(\frac{\partial \rho}{\partial x}\right) T$, coefficient of volume expansion
ΔX = difference in mole fraction solubility of the chemical in water and the mole fraction in the bulk fluid
ν = kinematic viscosity, L^2/t

$$S_c = \frac{\nu}{\mathcal{D}} \tag{11}$$

Chang [5] tested the dependence of experimental forced-convection mass-transfer coefficients from both flat and undulated beds on several stream parameters, and found that K_f correlated best with V_*, the stream-bottom friction velocity. Thibodeaux [4] used this information to select and modify a two-sublayer model for the calculation of K_f. The modifications were made necessary by the presence of sand waves and their effect on the laminar sublayer thickness. The following equation resulted from the use of Chang's regression analysis in the evaluation of the constants:

$$Nu_f = \frac{6.352\ Re^*\ Sc^{1/3}}{1 + 9.6(\Delta - \Delta_c)^{\frac{1}{2}}} \tag{12}$$

where Nu_f = Nusselt number for forced convection
Re^* = Reynolds number, $V_* L/\nu$
Δ = wave height, L
Δ_c = height of chemical in the wave, L

K_c, the overall mass-transfer coefficient, is simply calculated as the sum of the natural (K_n) and forced (K_f) convection mass-transfer coefficients.

MODEL VERIFICATION

The veracity of the computer model was tested by attempting to simulate the results of both laboratory tests and documented spill incidents. The mass distributed into the three primary geometric shapes was in each case adjusted until the best fit of each data set was obtained. These results were used as a guide in the selection of the representative values chosen for the mass distributions incorporated into the model for the different spill scenarios.

Figure 2 contains data from Daigre's [6] documentation of a major chloroform spill in the Mississippi River in 1973. This information was the most extensive spill documentation available at the time of this research, and provided a unique opportunity to test the capabilities of the model on an actual spill. The spill occurred on August 19, when a barge carrying three tanks of chloroform was damaged near Baton Rouge, Louisiana, during makeup of a river tow. The barge collapsed in the middle and sank, releasing the contents of two 70,000-gallon tanks, or approximately 7.7×10^5 kg. The Louisiana Division of the Dow Chemical Company, located 16.3 miles downstream, began sampling and analyzing their intake water later the same day. Thibodeaux [4] used an evaporation rate constant of 2.16×10^{-3} cm/s for chloroform to correct the Dow Chemical Company data back to the spill site. It is this data which is presented in Figure 2. The close simulation of the documented data throughout the duration of the spill incident attests to the extreme flexibility of the model, due primarily to the consideration given to the formation of different chemical shapes on the stream bottom.

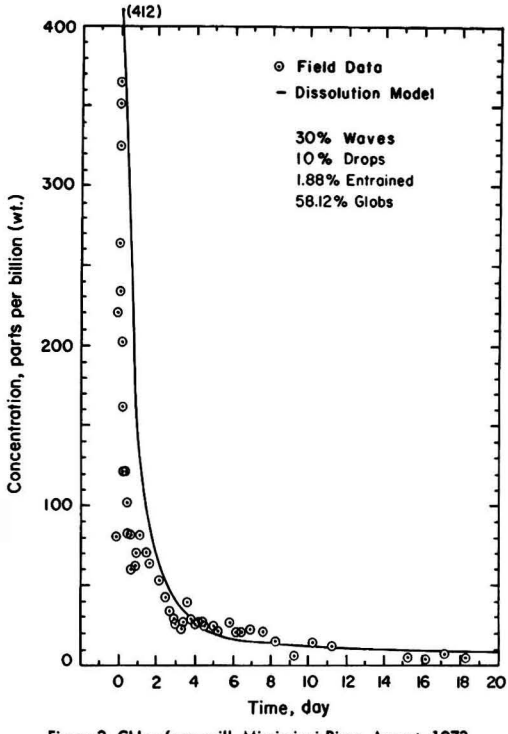

Figure 2. Chloroform spill, Mississippi River, August, 1973.

CONCLUSIONS

The information provided by this model includes the location and size of the on-bottom chemical mass, the dissolution lifetime of the chemical, and the cup-mixing concentration profile at the spill site. This model represents the only verified scheme for assessing the impact of the spills of high density ($\rho > 1$), immiscible chemicals into rivers. As such, it should be of assistance to officials in cautioning downstream water users, evaluating cleanup options, and assessing the impact of the spill on the stream biota.

P. S. Christy currently works for the Research and Development Division of Texas Eastman Company in Longview, Tx. A native of Dardanelle, Arkansas, she received both her B.S. and M.S. degrees in Chemical Engineering from the University of Arkansas. Her thesis research work, conducted under a grant to Dr. L. J. Thibodeaux from the Department of Transportation, is the subject of this research.

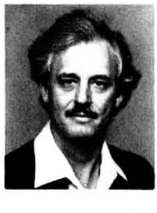

Louis Thibodeaux is Professor of Chemical Engineering at the University of Arkansas, Fayetteville, Arkansas. His teaching and research interests are in the area of mass transfer and diffusion. Recent emphasis of his work has been transport phenomena associated with chemicals in the natural environment. He has done consulting work for several chemical companies and is a member of the AIChE, ACS and AAS.

A copy of the final report (see literature citation [7]) may be obtained from the National Technical Information Service, U. S. Department of Commerce, Washington, D. C. 20004. Copies of the computer program may be obtained from the authors upon request.

LITERATURE CITED

1. Pilie, R. J., R. E. Baier, R. C. Ziegler, R. P. Leonard, J. C. Michalovic, S. L. Pek, and D. H. Bock, "Methods to Treat, Control and Monitor Spilled Hazardous Materials," EPA, Cincinnati, Ohio (1975).
2. Lewis, D. J., M.S. Thesis, Chemical Engineering Department, University of Arkansas (1977).
3. Mourot, M. W., M.S. Thesis, Department of Chemical Engineering, University of Arkansas (1977).
4. Thibodeaux, L. J., L. K. Chang, and D. J. Lewis, "Dissolution Rates of Organic Contaminants Located at the Sediment Interface of Rivers, Streams, and Tidal Zones," "Contaminants and Sediments," Vol. 1, Ann Arbor Science, Inc., Ann Arbor, Mich. (1980).
5. Chang, L., M.S. Thesis, Chemical Engineering Department, University of Arkansas (1978).
6. Daigre, G. W., Dow Chemical Company, in private communication with Dr. L. J. Thibodeaux, University of Arkansas (1976).
7. Thibodeaux, L. J. and P. S. Christy, "Spill of Soluble, High Density Immiscible Chemicals on Water," Final Report for U. S. Department of Transportation, Contract No. DOI-OS-70040, Report No. CG-UOA-80-011, Washington, D. C. (August, 1980).

Hydrocarbon Vapor Incineration Kinetics

The authors propose a first-order model for predicting the kinetics in afterburners—a key factor in emission control.

C. D. Cooper,* F. C. Alley, and T. J. Overcamp, Clemson University, Clemson, S.C. 29631

BACKGROUND

Certain industrial operations produce waste streams of air with low concentrations of volatile organic compounds (VOC). One means of controlling these emissions is to heat the contaminated air stream to a temperature high enough to oxidize the organics to carbon dioxide (CO_2) and water (H_2O). Sufficient residence time at high temperature must be allotted to ensure completion of the reactions; turbulence and flow patterns in the reaction chamber are also important factors. Physical size of the afterburner and fuel gas consumption are the two key design variables. Because both depend strongly on combustion rates, knowledge of reaction kinetics is required to optimize the design and operation of an afterburner.

Mills *et al.* [1] published some of the first guidelines for design of an afterburner. An empirical design procedure was enumerated by Danielson [2]. Hemsath and Susey [3] published some of the first kinetic data for certain compounds specifically for afterburner applications. In their article, they also presented a good review of various designs of afterburners. In a study related to fire suppressants. Seshadri and Williams [4] reported kinetics for the combustion of vapors of several heavy hydrocarbons (HC). Barnes *et al.* [5] reviewed the literature on hydrocarbon combustion with emphasis on afterburner systems applications. Recently, Lee *et al.* [6] reported kinetic data for a number of organic compounds from which they proposed a general correlation for predicting the temperature required for destruction of organic vapors in an afterburner. Their predicted temperature depends on nine variables including auto-ignition temperature, molecular weight, molecular structure, and residence time (in a plug flow reactor). Cooper [7] obtained data for two HC and carbon monoxide (CO) in a pilot-scale afterburner. However, in the few studies reported in the literature, the kinetic constants for some compounds are often vastly different for different investigators (see Table 1). Such similar compounds as methane, ethane, and propane have been reported in one study to have widely dissimilar kinetics [6].

THEORY

Although the actual mechanism of HC combustion is undoubtedly quite complex, several authors have had success in modelling these complex reactions with global kinetics, i.e.:

$$\text{rate} = -\frac{d[\text{HC}]}{dt} = k_1\,[\text{HC}][\text{O}_2] \qquad (1)$$

where: k_1 = second-order rate constant, liter/mole · s
[ ] = concentration, moles/liter

or, in the presence of excess oxygen

$$-\frac{d[\text{HC}]}{dt} = k_2[\text{HC}] \qquad (2)$$

where: k_2 = psuedo-first-order rate constant, s^{-1}, which includes oxygen concentration

Thus, for a typical afterburner with mole fractions of oxygen of about 0.15 and HC of about 0.001, Equation (2) is often used to model the kinetics. In this model, the rate constant is usually presumed to be of Arrhenius form, i.e.:

$$k_2 = A\,e^{-E/RT}$$

where: A = pre-exponential factor, s^{-1}
E = activation energy, kcal/mole (1 kcal = 4186 J)
R = gas constant, kcal/mole · K
T = temperature, K

Although this pseudo—first-order model is often used to describe HC combustion reactions (especially in afterburner applications), it is by no means universal. Dryer and Glassman [8], Glassman *et al.* [9], and Williams *et al.* [10] report results in which the kinetics are best represented by models which are not first-order in HC. Some kinetic data that have been reported in the literature are

* Current address: University of Central Florida, Orlando, Fla. 32816.

ISSN 0278-4491-82-5566-0129-$2.00.

summarized in Table 1. Only models which are first order in the HC are reported in this table.

Although the Arrhenius model is an empirical expression, there are several theoretical kinetic models which are similar in form. Classical collision theory gives a rate constant of the form

$$k \alpha T^{1/2} e^{-E/RT} \tag{4}$$

while transition-state theory gives a rate constant of the form

$$k \alpha T e^{-E/RT} \tag{5}$$

Other theories result in higher order temperature dependence.

Let us assume that a collision between an oxygen molecule and an HC molecule must occur for the combustion process to begin. The bimolecular reaction rate (in molecules/cc · s) is given in general by Gardiner [*11*] as:

$$\text{rate} = \left(\frac{8\pi k_B T}{\mu}\right)^{1/2} \sigma_R^2 (e^{-E'/RT}) N_A N_B \tag{6}$$

where:

μ = an inverse average molecular mass, g/molecule, i.e.,
$\mu = m_A m_B/(m_A + m_B)$
k_B = Boltzmann constant
E' = theoretical activation energy
σ_R = hard sphere reactive cross section, cm
N_A, N_B = molecular concentration of species A and B, molecule/cc

In equation (6) the reactive cross section is related to the collision cross section σ_{AB}^2 (from the kinetic theory of gases) through a steric factor, S.

Equation (6) can be written in terms of molar concentrations recognizing that the Boltzmann constant can be related to the ideal gas law constant through Avogadro's number. We can thus rewrite equation (6) as:

$$-r_A = Z' S T^{1/2} e^{-E'/RT} [\text{A}][\text{B}] \tag{7}$$

where $Z' = 2.753(10)^{25} \sigma_{AB}^2 \mu^{-1/2}$, liter/(mole · s · $K^{1/2}$)

$-r_A$ = disappearance rate of A, $\frac{\text{moles}}{\text{liter} \cdot \text{s}}$.

If we denote [B] as the oxygen concentration, it can be written as

$$[\text{O}_2] = f_{o_2} \frac{P}{R'T} \tag{8}$$

where: f_{o_2} = mole fraction oxygen
P = absolute pressure, atm,
R' = gas constant, $0.08205 \frac{\text{liter} \cdot \text{atm}}{\text{mole} \cdot \text{K}}$.

Because of the excess oxygen in afterburners, f_{o_2} is approximately constant throughout the reaction. For these conditions, the second-order expression of Equation (7) can be converted to a first-order expression, i.e.

$$-r_{\text{HC}} = Z' S f_{o_2} \frac{P}{R'T} T^{1/2} e^{-E'/RT} [\text{HC}] \tag{9}$$

Note that, if we arbitrarily "modify" the collision-theory approach by changing the exponent on temperature from 1/2 to 1.0 (the exponent expected from the transition-state theory), the two temperature terms in Equation (9) cancel out and we are left with an equation of Arrhenius form

$$-r_{\text{HC}} = A' e^{-E'RT} [\text{HC}] \tag{10}$$

with A' being a semi-empirical pre-exponential factor given by

$$A' \equiv Z' S f_{o_2} \frac{P}{R'} . \tag{11}$$

TABLE 1. SELECTED REPORTED KINETIC CONSTANTS FOR HYDROCARBON INCINERATION

Hydrocarbon	Rate Expression*	Values of Constants: A, s^{-1} (or as noted)	Values of Constants: E, cal/gmole	Temperature Range	Source**
Methane	$k[X]$	$1.68\,(10)^{11}$	52,100	1200-1500°F	Lee *et al.* [6]
Natural Gas	$k[X]$	$1.65\,(10)^{12}$	49,300	1300-1600°F	Hemsath and Susey [3]
Ethylene	$k[X]$	$1.37\,(10)^{12}$	50,800	1200-1500°F	Lee *et al.* [6]
Ethane	$k[X]$	$5.65\,(10)^{14}$	63,600	1200-1500°F	Lee *et al.* [6]
Ethane	$k[X]$	$7.01\,(10)^{9}$	39,200	950-1060°K	Cooper [7]
Propylene	$k[X]$	$4.63\,(10)^{8}$	34,200	1200-1500°F	Lee *et al.* [6]
Propane	$k[X]$	$5.25\,(10)^{19}$	85,200	1200-1500°F	Lee *et al.* [6]
Butene	$k[X]$	$3.74\,(10)^{14}$	58,200	1200-1500°F	Lee *et al.* [6]
Hexane	$k[X]$	$6.02\,(10)^{8}$	34,200	940-1020°K	Cooper [7]
Hexane	$k[X]$	$4.5\,(10)^{12}$	52,500	1300-1600°F	Hemsath and Susey [3]
Cyclohexane	$k[X]$	$5.13\,(10)^{12}$	47,600	1300-1600°F	Hemsath and Susey [3]
Benzene	$k[X]$	$7.43\,(10)^{21}$	95,900	1275-1500°F	Lee *et al.* [6]
Benzene	$k[X][\text{O}_2]$	$6.0\,(10)^{14}$	36,000	1300-1700°K	Seshadri and Williams [4]
Heptane	$k[X][\text{O}_2]$	$2.2\,(10)^{15}$ $\text{cm}^3/\text{gmole} \cdot \text{s}$	38,000	1300-1700°K	Seshadri and Williams [4]
Toluene	$k[X]$	$6.56\,(10)^{13}$	58,500	1300-1600°F	Hemsath and Susey [3]
Toluene	$k[X]$	$2.28\,(10)^{13}$	56,500	1275-1500°F	Lee *et al.* [6]
Iso-octane	$k[X][\text{O}_2]$	$4.5\,(10)^{14}$ $\text{cm}^3/\text{gmole} \cdot \text{s}$	35,000	1300-1700°K	Seshadri and Williams [4]
Decane	$k[X][\text{O}_2]$	$1.6\,(10)^{15}$ $\text{cm}^3/\text{gmole} \cdot \text{s}$	37,000	1300-1700°K	Seshadri and Williams [4]
Hexadecane	$k[X][\text{O}_2]$	$8.2\,(10)^{14}$ $\text{cm}^3/\text{gmole} \cdot \text{s}$	35,000	1300-1700°K	Seshadri and Williams [4]
Kerosene (C_{10} H_{20} approx)	$k[X][\text{O}_2]$	$5.4\,(10)^{14}$ $\text{cm}^3/\text{gmole} \cdot \text{s}$	35,000	1300-1700°K	Seshadri and Williams [4]

* $k = Ae^{-E/RT}$, units as noted; $[X]$ = concentration of hydrocarbon
** Numbers in ( ) refer to enumeration in the Literature Cited Section of this work.

Because the temperature terms in Equation (9) cancel out when the exponent is changed from 1/2 to 1.0, A' is not a direct function of temperature (Z' does vary slightly with T, however). Thus, the final representation of the rate constant is

$$k' = A' e^{-E'/RT}. \quad (12)$$

PROCEDURE

The possibility of finding a general correlation for predicting vapor-incineration kinetics is, of course, quite appealing. It was with this objective in mind that the data in Table 1 were collected. It is noted that there may be some intrinsic differences between the sources reported in Table 1. For instance, Hemsath and Susey [3] reported total hydrocarbons destruction rates, while Lee *et al.* [6] reported destruction rates of specific compounds. Lee *et al.* [6] used an externally heated narrow-bore quartz tube, while Cooper [7] used an LPG-fired, pilot-scale afterburner. Recognizing the limitations in combining the data in Table 1, they were analyzed as described below.

A computer program was written which read in the reported rate expressions and constants from Table 1. From these data, a value of the pseudo-first-order rate constant (with oxygen concentration built into A') was calculated as explained below for each compound at each of six equally spaced temperatures from 940 to 1140 K. An average reported oxygen mole fraction of 0.20 was used for the data of Hemsath and Susey [3]. A reported oxygen mole fraction of 0.15 was used for the data of Cooper [7]. An oxygen mole fraction of 0.20 was assumed for the other studies. These calculated rate constants were then used in the development of a general correlation for HC-vapor incineration kinetics.

The theoretical collision rate, Z', was calculated by a procedure due to Hirschfelder *et al.* [12] as summarized by Gardiner [11]. This calculation involved using the Lennard-Jones collision integral to calculate an effective collision diameter between a given hydrocarbon molecule and an oxygen molecule assuming hard-sphere behavior. For the lower molecular weight compounds the Lennard-Jones force constants were available in standard tables. For those compounds for which the force constants were tabulated, it was observed that at a given temperature there was a good correlation between the calculated collision rate Z' and molecular weight and molecular type as shown in Figure 1. For the heavier HC, the relationships in Figure 1 were simply extrapolated. It should be noted that the calculated values of Z' increased slightly with decreasing temperature. For various HC, the values of Z' at 940 K are six to eleven percent higher than those at 1140 K.

Evaluating the steric-factor function from a theoretical basis is extremely difficult. To make this technique useable we required a simple representation for S. Choosing methane as the reference molecule, it was found that reasonably consistent results were obtained if the steric factor was represented by

$$S = 16/\mathrm{MW}, \quad (13)$$

where:

MW = molecular weight.

The following procedure was used to calculate a "theoretical" activation energy for each compound. Using a collision rate Z' from Figure 1, and a steric factor calculated as explained above, a value of A' was calculated at each temperature using Equation (11). At each temperature, a value of k from equation (3) was calculated using the data in Table 1. Equating k to the k' from Equation (12) at each of the six temperatures, values of E' were obtained as follows:

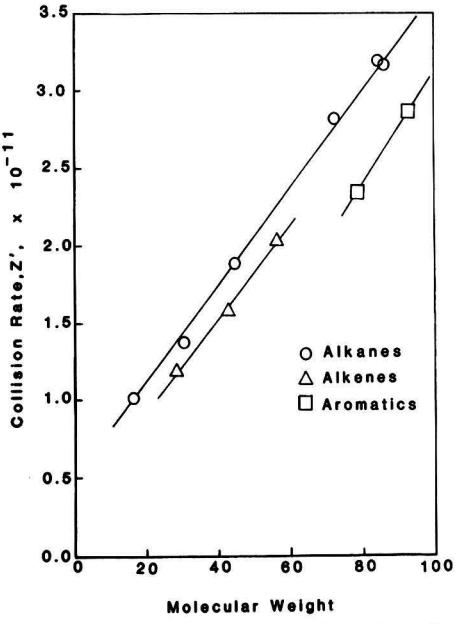

Figure 1. Calculated collision rate as a function of molecular weight and molecular type (at T = 1140 K).

$$E' = RT \ln\left(\frac{A'}{k}\right) \quad (14)$$

The six values of E' thus obtained were averaged and a standard deviation obtained for E' over the 200 degree K temperature range.

RESULTS

The results of the above calculations are presented in Table 2. The small standard deviations of E' indicate that, over the range 940-1140 K, the reaction rates for many of the compounds can be modeled adequately using the proposed model. In addition, Kanury [13] states that most hydrocarbon combustion reactions have activation energies on the order of 40 kcal/mole, so the results obtained by this method appear to be reasonable.

The calculated activation energies are portrayed as a function of molecular weight in Figure 2. For the steric-factor function chosen, the calculated activation energy is a slowly decreasing function of molecular weight. However, the correlation with molecular weight is due in part to the form of the steric-factor function assumed. Excluding two points, all of the calculated activation energies lie within 1.5 kcal/mole of the correlation line. Based on these limited data and subject to the approximations involved in this technique, a general correlation for activation energy as a function of molecular weight was proposed as follows:

$$E' = -0.00966\,(\mathrm{MW}) + 46.08 \quad (15)$$

where

E' = predicted activation energy (kcal/mole) for use in Equation (12).

APPLICATION

These results can be applied (with appropriate caution) to the estimation of the incineration kinetics of a given compound in an afterburner for temperatures in the range of 940 to 1140 K. From the molecular weight and Figure 2, find E'. Calculate S from Equation (13) and find Z' from

TABLE 2. CALCULATION OF "THEORETICAL" ACTIVATION ENERGIES FROM REPORTED DATA AND THEORETICAL PRE-EXPONENTIAL FACTORS

Compound	Data Source*	Experimental** A	Experimental** E	"Theoretical" A'_{avg} $s^{-1} \times 10^{11}$	"Theoretical" E'_{avg} kcal/gmole	Std. Dev. kcal/gmole
Methane	1	$1.68\ (10)^{11}$	52.1	2.55	52.96	0.03
Methane	2	$2.13\ (10)^{11}$	44.8	2.55	45.17	0.06
Ethylene	1	$1.37\ (10)^{12}$	50.8	1.70	46.50	0.36
Ethane	1	$5.65\ (10)^{14}$	63.6	1.83	47.00	1.25
Ethane	4	$6.98\ (10)^{9}$	39.2	1.37	45.36	0.39
Propylene	1	$4.63\ (10)^{8}$	34.2	1.52	46.18	0.80
Propane	1	$5.25\ (10)^{19}$	85.2	1.72	44.83	2.96
Butene	1	$3.74\ (10)^{14}$	58.2	1.47	41.99	1.23
Benzene	1	$7.43\ (10)^{21}$	95.9	1.22	44.59	3.77
Benzene	3	$6.00\ (10)^{14}$	36.0	1.22	45.23	0.74
Cyclohexane	2	$8.33\ (10)^{11}$	48.3	1.54	44.81	0.32
Hexane	2	$4.81\ (10)^{12}$	52.5	1.50	45.33	0.60
Hexane	4	$6.02\ (10)^{8}$	34.2	1.12	45.00	0.70
Toluene	1	$2.28\ (10)^{13}$	56.5	1.26	45.76	0.86
Toluene	2	$1.82\ (10)^{13}$	56.0	1.26	45.73	0.82
Heptane	3	$2.20\ (10)^{15}$	38.0	1.50	44.96	0.58
Iso-octane	3	$4.50\ (10)^{14}$	35.0	1.48	45.22	0.82
Decane	3	$1.60\ (10)^{15}$	37.0	1.46	44.57	0.64
Kerosene	3	$5.40\ (10)^{14}$	35.0	1.46	44.82	0.80
Hexadecane	3	$8.20\ (10)^{14}$	35.0	1.43	43.91	0.76

* Data Sources: 1. Lee *et al.* (1979)
2. Hemsath and Susey (1974)
3. Seshadri and Williams (1975)
4. Cooper (1980)

** Refer to Table 1 for entire rate expression and proper units.

Figure 1. For an expected mole fraction of oxygen, calculate A' from Equation (11). Finally, calculate k' from Equation (12) for any given temperature. From this estimate of the rate constant, efficiency of HC destruction can be projected, making appropriate approximations regarding heat loss (or gain) and plug flow (or deviation from it).

Very recently, these correlations were used to design an industrial-scale afterburner for a compound with unknown kinetics. So far, there has been very good agreement between predictions and actual operating performance [*14*].

CONCLUSIONS

In the absence of experimental data for a specific compound in a specific afterburner system, the above correlations for A' and E' can be used to estimate the kinetics of hydrocarbon combustion for use in designing an afterburner. However, care should be exercised, and the design should be tested for sensitivity to these parameters. These results are really only valid for the range of temperatures used in this study. Conversely, a different range of temperatures would result in slightly different numerical results. Of course, if destruction of carbon monoxide controls the design (as is often the case), higher temperatures may be required and the HC kinetics become less critical. In this particular procedure, we have ignored the CO question, concentrating on predicting HC kinetics. For final designs, experimental data should be used when available, but these correlations are reasonable for screening studies and preliminary designs.

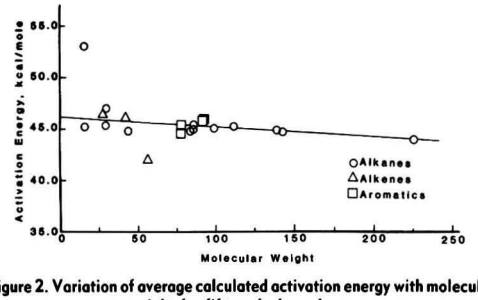

Figure 2. Variation of average calculated activation energy with molecular weight for fifteen hydrocarbons.

C. David Cooper is currently Associate Professor in the Civil Engineering and Environmental Sciences Department at the University of Central Florida, with teaching interest in air pollution control. He has degrees in chemical engineering from Clemson University and Rice University. Prior to joining the academic world, he worked six years with Exxon at their Baytown refinery. He is presently registered as a Professional Engineer in the states of Florida and Texas.

Forrest C. Alley is a professor of Chemical Engineering at Clemson University. He received BS and MS degrees in chemical engineering from Auburn University and a PhD in Environmental Engineering from the University of N.C.

Thomas J. Overcamp received a B.S. in 1968 from Michigan State University and an S.M. in 1970 and Ph.D. in mechanical engineering in 1973 from the Massachusetts Institute of Technology. He was a research associate at the Graduate Program in Meteorology at the University of Maryland from 1972 to 1975. In 1975 he joined the faculty at Clemson University where he is Associate Professor of Environmental Systems Engineering. His current research is in air pollution meteorology and air pollution control.

LITERATURE CITED

1. Mills, J. L., W. F. Hammond, and R. C. Adrian, "Design of Afterburners for Varnish Cookers," *J. Air Poll. Control Assoc.*, **10**, No. 2, 161 (1960).
2. Danielson, J. A. (ed), *Air Pollution Engineering Manual*, 2nd ed. Research Triangle Park: U.S. Environmental Protection Agency (1973).
3. Hemsath, K. H. and P. E. Susey, "Fume Incineration-Kinetics and Its Applications," *AIChE Symp. Ser.*, **70**, 137, 439 (1974).
4. Seshadri, K. and F. A. Williams, "Effect of CF_3Br on Counterflow Combustion of Liquid Fuel with Diluted Oxygen," in: Halogenated Fire Suppressants, ACS Symp. Ser., **16**, American Chemical Society, Washington, D.C. (1975).
5. Barnes, R. H., A. A. Putnam, and R. E. Barrett, "Chemical Aspects of Afterburner Systems," Topical Report to U.S. Environmental Protection Agency, Contract No. 68-02-2629. Columbus, Ohio: Battelle Laboratories (1978).
6. Lee, K. C., J. L. Hansen, and D. C. Macauley, "Predictive Model of the Time-Temperature Requirements for Thermal Destruction of Dilute Organic Vapors," 72nd Annual Meeting of the Air Pollution Control Association, Paper No. 79-10.1, Cincinnati, Ohio (June 24-29, 1979).
7. Cooper, C. D., "Prediction of Time-Temperature Design Parameters for a Hydrocarbon Vapor Incinerator," Ph.D. Dissertation presented to Clemson University, Clemson, S.C. (August, 1980).
8. Dryer, F. L. and I. Glassman, "High Temperature Oxidation of CO and CH_4," Fourteenth Symposium (International) on Combustion, 987 (1973).
9. Glassman, I., F. K. Dryer, and R. Cohen, "Combustion of Hydrocarbons in an Adiabatic Flow Reactor: Some Considerations and Overall Correlations of Reaction Rate," paper presented in San Antonio, Texas (April 21-22, 1971,), cited in Ref. 1.
10. Williams, G. C., H. C. Hottel, and A. C. Morgan, "The Combustion of Methane in a Jet-Mixed Reactor," Twelfth Symposium (International) on Combustion, 913 (1969).
11. Gardiner, Jr., W. C., "Rates and Mechanisms of Chemical Reactions," W. A. Benjamin, Inc., New York (1969).
12. Hirschfelder, J. O., C. F. Curtiss, and R. B. Bird, "Molecular Theory of Gases and Liquids," John Wiley and Sons, New York (1974).
13. Kanury, A. Murty, "Introduction to Combustion Phenomena," Gordon and Breach Science Publishers, New York (1975).
14. Blackwood, T. R., Monsanto Company, Inc., Personal Communication (1981).

Case-Specific Evaluation of an Atmospheric-Dispersion Model

An analysis of the problem of predicting urban air quality, based on actual data for the Milwaukee, Wisconsin area.

Keith H. Kennedy and Richard D. Siegel, Stone & Webster Corp., Boston, Mass. 02107
Mark P. Steinberg, Wisconsin Electric Power Co., Milwaukee, Wis.

The following discussion presents the results of a case-specific evaluation of the performance of the RAMF version of the Environmental Protection Agency's (EPA) RAM [*1*] atmospheric-dispersion model. RAM is a steady-state Gaussian model developed by EPA to estimate air-quality concentrations of relatively nonreactive pollutants emitted from point and area sources over averaging times from an hour to a day. A complete description of RAM, including its basis, applicability, and data requirements has been prepared by Turner and Novak [2].

An evaluation of the suitability of the urban version of RAM for air-quality simulation was performed in late 1978 and early 1979, as part of a feasibility study for compliance with the Prevention of Significant Deterioration (PSD) and Emission Offset (EO) requirements for a proposed cogeneration facility in downtown Milwaukee, Wisconsin. According to both of EPA's recently proposed urban/rural classification systems [3], Milwaukee County is an urban area.

The foregoing analysis was judged necessary in light of the controversy surrounding the model's efficacy, and the fact that EPA's planned comprehensive validation effort of the urban version of the model for the St. Louis area is not complete due to a lack of funds. Preliminary validation results indicated the sensitivity of the model to the method of aggregation of area sources [4, 5]. In general, the model did not perform well on a one-to-one temporal comparison of measured and predicted concentrations at each receptor. However, RAM did perform fairly well when comparing frequency distributions [5].

The objective of this paper is to present an abbreviated discussion of the results of the foregoing analysis, thus adding to the data base required for ultimate validation of this model. One of the major concerns of this analysis was to evaluate the relative accuracy of predictions compared to measurements based on maximum *versus* average emission-rate assumptions.

Although the RAM formulation includes many options and versions, RAM was only evaluated in a mode which is frequently used in modeling studies for regional State Implementation Plan (SIP) control strategy evaluations and new source reviews. This mode is RAMF, which can calculate 24-hour concentrations (from hour-by-hour simulation) and provide frequency distributions for a full year of meteorological data. This version is most compatible for comparison of concentrations with ambient air-quality standards since highest second-highest concentrations are the basis for short-term standards and RAMF identifies these values.

PREVIOUS STUDIES

RAM is one of the models recommended in the EPA's "Guideline on Air Quality Models" [3, 6] and is currently favored by the Agency's regional offices and most State agencies as the technique for use in evaluating short-term

ISSN 0278-4491-82-5437-0133-$2.00.

concentration impacts from multiple sources in urban environments. RAM was originally approved by EPA for use in urban and rural settings [6]. However, current EPA practice is to use MPTER [3] in rural situations. The urban version of RAM is, however, a highly controversial model in that its use has been the subject of litigation in the SIP process in Ohio. Arguments were advanced in that case that the model is relatively unproven and unvalidated, and tends to overpredict-ground level concentrations under certain meteorological conditions [7, 8]. These arguments were dismissed because the petitioners failed to convince the Court that the model grossly overpredicted concentrations, and because of the Clean Air Act's requirement that EPA protect the public health with an adequate margin of safety. Analyses have indicated that the rural version of RAM tends to be a better predictor of measured concentrations in the vicinity of the Ohio power plants, possibly because population densities and surface roughness indices indicated the area to be more rural than urban in character [9, 10].

Results obtained by Morgenstern *et al.* [11] in the Indianapolis, Indiana area also indicated that the urban version of RAM overpredicted concentrations and produced larger mean errors, standard deviations, and mean-square errors at the upper percentiles of the frequency distributions under several source emission-rate scenarios than did the rural version of RAM. According to EPA's population density procedure [3], Indianapolis is an urban area for dispersion modeling purposes (approximately 800 people/km^2) [12]. Roginski and Kummler [13] and Kummler *et al.* [14] have demonstrated that the urban version of RAM overpredicts concentrations in (Wayne County—Detroit, Michigan; Hodanbosi and Peters [15] report similar findings for the Cleveland area, although a more favorable comparison was found for highest and second highest values.

Guldberg and Kern [12] have also supported the argument that RAM (urban) tends to produce overly conservative results in their work in the Indianapolis and Michigan City (Indiana) areas.

Another effort involving an evaluation of RAM in urban and rural settings compared model performance with observed tracer dispersion [16]. This study has added to the uncertainty with regard to RAM efficacy by showing, in general, that it was unable to predict highest or average concentrations within a factor of two.

A thorough review of most of these studies is presented in a recent paper by Ellis and Liu [17] which concluded:

1. The performance of the urban version for several of the studies may be due to the areas not being sufficiently urban to justify use of the urban mode.
2. The lack of Good Engineering Practice (GEP) stacks for many sources in these cities may account for the high measured concentrations which cannot be explicitly predicted by RAM but are accounted for by the larger McElroy-Pooler diffusion coefficients.

The article concludes with a recommendation for additional validation efforts, including analysis for different size cities.

DATA PREPARATION

The RAM model evaluation in Milwaukee was conducted for short-term sulfur-dioxide (SO_2) concentrations using 1976 air quality, meteorology, and emission inventory data.

Emissions Data

The data base for the emission inventory compiled for RAMF was that of the seven-county Southeastern Wisconsin Air Quality Control Region (AQCR). The areal coverage provided by this inventory approximates 7,000 sq. km. The base inventory was compiled by the Wisconsin Department of Natural Resources (WDNR) with assistance from the Southeastern Wisconsin Regional Planning Commission, as part of the air quality attainment and maintenance plan development for the AQCR.

The WDNR area source grid system was aggregated to 73 area sources for input to RAMF, with resolution determined by emission-density analysis. Grid square side lengths varied from 1.6 km (1 mile) in downtown Milwaukee, to 20.9 km (13 mile) in outlying regions approximately 50 km from the downtown area. All line sources from 5 separate source categories and 141 point sources which emitted between 10 and 25 tons/year of SO_2 were added to the combined file of 19 separate area source categories. The effective area source heights were assigned to one of three categories based on an emission-weighted average of the component area, line, and small-point source effective heights.

The modified WDNR point-source inventory consisted of all sources which emitted at least 25 tons/year of SO_2 within 50 km of the downtown Milwaukee area. There were 49 such sources. Fifteen of the 25 most significant point sources in the inventory, as determined by the emission inventory preprocessor RAMQ, were located within about 10 km of downtown Milwaukee, as shown in Figure 1. An extensive investigation of the validity of the point-source inventory was performed by 1) systematic comparison with the 1975 National Emissions Data System inventory for the region, 2) engineering analysis of all plant parameters, and 3) utilization of actual 1976 annual average operation and maximum design data for the Wisconsin Electric Power Company (WE) facilities included in the inventory (12 of the 49 sources).

Two versions of the point-source inventory, one based on peak (maximum) SO_2 emission rates, and the other based on annual average SO_2 emission rates, were compiled for input to RAMF. The purpose of the dual inventory was to test the hypothesis that maximum measured concentrations at each Milwaukee County SO_2 monitoring site in 1976 would be bracketed by maximum RAM-predicted concentrations from these two data bases. Since stack exit parameters were only available for maximum-load conditions for most of the point sources in the inventory, it was expected that utilization of these parameters with annual average emission rates for the entire point-source inventory would cause underprediction of maximum short-term concentrations. It was also expected that peak emission rates for the entire inventory would lead to overprediction of maximum short-term concentrations. This expectation arose from a survey of average

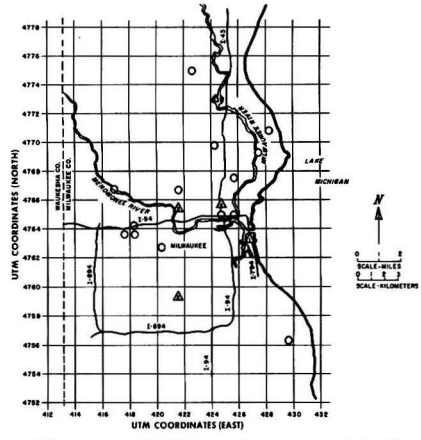

Figure 1. Milwaukee ambient SO_2 monitoring site and significant point source locations. Legend: ○ significant point source; △ receptor and SO_2 ambient monitoring station (with number).

daily loads at the WE sources on the days with maximum measured or predicted 24-hour concentrations at each site. This survey indicated that source loads on these days were often under 50 percent and were frequently close to the capacity factor used in the annual average emission-rate modeling case.

In order to enhance the accuracy of predictions, hourly variability of emission rates is the preferred input to model calculations. However, as is the case for most regional air-quality studies, this data was not available. To partially compensate for this limitation and to evaluate its effect on predictions, a limited analysis was performed to determine the influence on model performance of daily variation of emission rates for some of the most significant point sources in the inventory.

Meteorological Data

The 1976 meteorological data were obtained from the National Climatic Center (NCC) and consisted of hourly surface data from General Mitchell Field in Milwaukee and upper air data from Austin Straubel Field in Green Bay.

Post-1964 NCC surface data is coded only every third hour. Therefore, the remaining hours were digitized from raw (WBAN) data and were merged with the existing coded data. The data was then sent to NCC for quality assurance checks.

The upper air data obtained from NCC were used prior to the discovery of an error in their mixing-height algorithm. A qualitative analysis of potential impact on study results was performed by applying criteria developed by EPA from their generic assessment of the impact of the error. This analysis indicated that very few, if any, of the high modeled concentrations would be influenced by this error.

Ambient Monitoring Data

All SO_2 ambient air-quality data collected in the Southern Wisconsin-AQCR in 1976 were obtained from WDNR. However, due to the temperature instability problems associated with bubbler methods and their withdrawal as reference techniques and the desire to obtain 3-hour average comparisons with model predictions, all bubbler data was disregarded. Only continuous flame-photometric SO_2 data were utilized in the model evaluation. Five such monitoring sites existed in Milwaukee County in 1976, but one of these sites collected data for less than 15 percent of the hours during the year and was thus eliminated from the analysis. Figure 1 depicts the location of the remaining four sites relative to the 15 most significant proximate point sources described previously.

Preliminary modeling analyses of the Milwaukee region indicated that the locations of the monitoring sites generally correspond to receptors of high predicted pollutant concentrations. Site 3 is the only exception, representing a location of average predicted air-quality levels for the Milwaukee region.

Federal Reference methods were utilized at the four sites. Meloy Laboratories flame-photometric detector sulfur analyzer model number SA-160 instruments were used at Sites 1 and 2 and model number SA-185 instruments were used at Sites 3 and 4. Hourly data recovered at the monitoring sites ranged from 69 percent at Site 1 to 83 percent at Site 3.

RAM Modeling

The RAMF computer model was executed to generate SO_2 concentration predictions at the selected monitoring sites for comparison with the measured data. The pollutant half-life option for RAM was not utilized because of the relative stability of SO_2 and the proximity of most major point sources to most receptors (see Figure 1).

After the 1976 emissions data were formulated for model input by the RAM emission preprocessor, RAMQ, and hourly meteorological data for 1976 were formulated for model input by the RAM meteorological preprocessor, RAMMET, hourly computations for a full year were performed using the RAMF version of RAM. Although RAMF computes cumulative frequency distributions for previously computed 24-hour averages, it was not used for averaging or frequency distributions in this study. Instead, all hourly concentrations at each receptor were output to a magnetic tape. The blocked, non-running-time period averages (3-hour and 24-hour) and the cumulative frequency distributions were generated by small computer programs external to RAM for greater computational efficiency. However, the same techniques employed in RAMF were used for both data manipulations. A small subset of these results was compared with a RAMF-manipulated data set and the results were found identical. Two sets of the two predicted concentration files (both the peak and annual average point-source emission-rate model runs) were prepared. One set was screened to eliminate estimates for those hours during which no corresponding valid monitoring data were available and one set was unmodified. The hourly ambient monitoring data were also input to the external programs for time period averaging and cumulative frequency distribution development.

BACKGROUND ASSESSMENT

EPA's proposed revision to the "Guideline on Air Quality Models" [3] states that "background air quality relevant to a given source includes those pollutant concentrations due to natural sources and unidentified man-made sources." Contributions to maximum SO_2 concentrations from natural sources in urban areas can generally be regarded as negligible. Since a comprehensive inventory of emissions was used in this study, the only potential background which required assessment was that due to transport from distances beyond the geographical extent of the sources in the emission inventory to the SO_2 monitors. This distance is greater than 50 kilometers for the four downtown Milwaukee monitors. The only major urban area close enough to have a potential impact on background SO_2 concentrations in Milwaukee is Chicago, located about 150 kilometers to the south.

To assess the potential impact of transported SO_2 from Chicago on maximum concentrations at each site, an evaluation of wind direction and persistence was performed on the three days of highest measured concentrations at monitoring sites 1 and 2 (see Figure 1). Each of these sites is located south of most major point sources in the modeling inventory and, as such, a maximum concentration, measured with a persistent southerly wind, could have been influenced by transported SO_2 from the Chicago area. None of the days analyzed had persistent winds from any southerly sector. It appears that the SO_2 background would have a small impact on maximum concentrations. Since this contribution was judged small, no background SO_2 concentrations were added to model predictions at the four monitoring sites.

RESULTS

Cumulative Frequency Distribution Comparisons

The concentration files at each site were summarized for comparison using Cumulative Frequency Distributions (CFD) of measured and predicted (reflecting both annual average and peak point-source emission rates) values. The predicted concentration files which were screened to eliminate missing or invalid monitoring data hours were utilized in this initial comparison. Comparative plots of the CFDs at the four monitoring sites are presented in Figures 2 and 3 for 3-hour and 24-hour SO_2 averages, respectively.

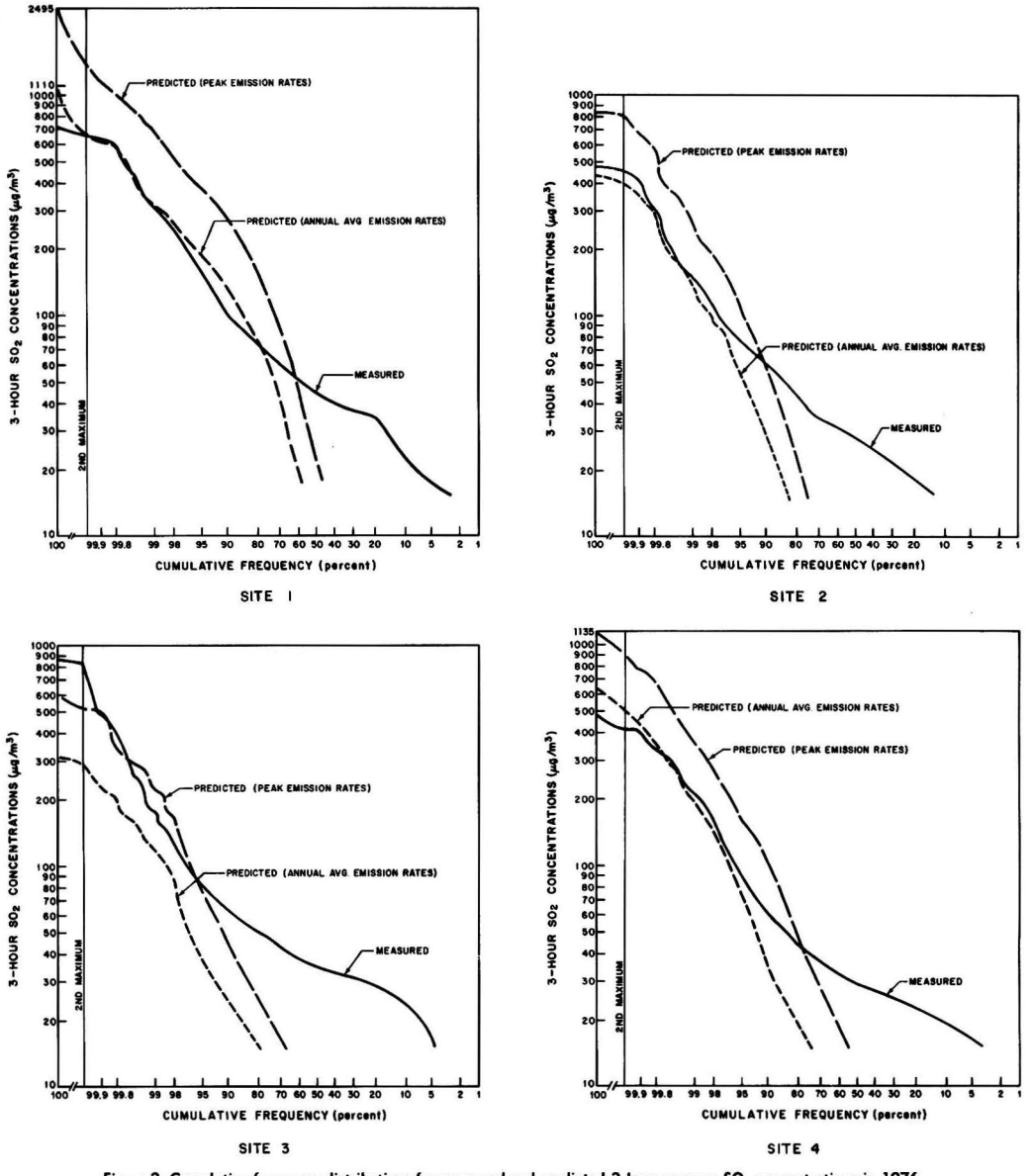

Figure 2. Cumulative frequency distributions for measured and predicted 3-hour average SO_2 concentrations in 1976.

Figure 2 shows that RAMF-predicted 3-hour SO_2 concentrations using annual average emission rates compared well to measured concentrations at the upper percentiles (above 95 percent) of the CFDs at three of the four sites. As hypothesized, RAMF overpredicted maximum 3-hour SO_2 concentrations at these three sites when peak point-source emission rates were used. The overprediction at these sites was generally by a factor of two. At the remaining site, RAMF underpredicted significantly using annual average emission rates, but predicted relatively well with peak emission rates except for the extreme values (highest and second highest).

Figure 3 illustrates similar concentration distributions for 24-hour averages, with the major difference being slightly lower predicted values relative to measured values than for the 3-hour averages. The upper percentiles of the 24-hour average CFDs are in better agreement with the hypothesis that the two sets of predicted concentrations would bracket the measured values.

Ratios of predicted to measured concentrations for 3- and 24-hour maximum and second maximum SO_2 concentrations are shown in Table 1. Based on these comparative data, the 24-hr annual average emission rate file was examined in more detail for further analyses.

Evaluation of the Effect of Eliminating Predicted Concentration Hours Corresponding to Missing Monitoring Data

A variation to the original methodology of CFD comparisons was undertaken using the entire file of predicted concentrations in 1976 rather than just those averaging periods for which valid monitoring data were collected. The rationale for eliminating those hours was that since the study consisted of concentration comparisons, it might

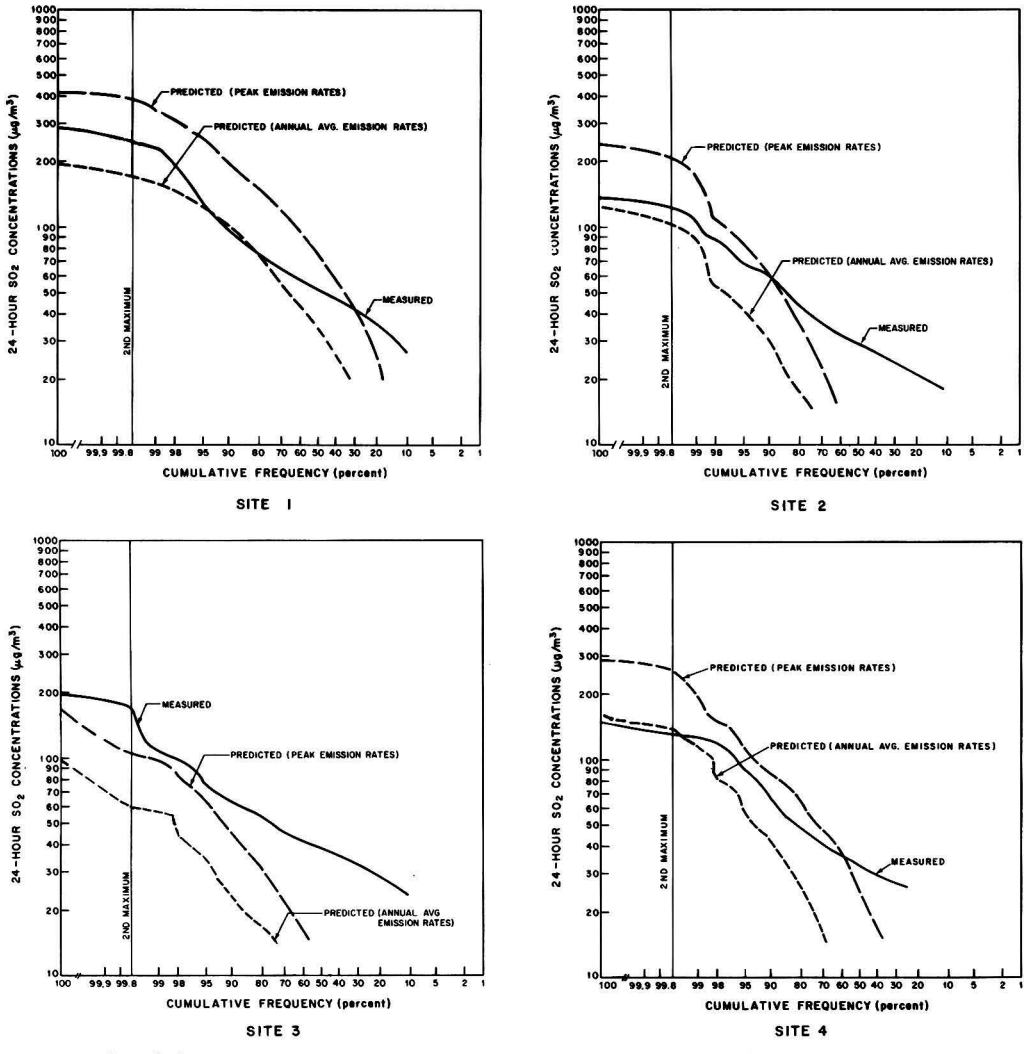

Figure 3. Cumulative frequency distributions for measured and predicted 24-hour average SO_2 concentrations in 1976.

not be valid to include a day with potential "worst-case" meteorology in the predictions if there were no corresponding measured data. However, comparison of CFDs for short-term averaging periods is, in a sense, an admission that modeling techniques are not yet precise enough for a one-to-one short-term comparison. An argument could, therefore, be made that as much data as is available for predicted concentrations should be utilized.

To assess the impact on the evaluation of model performance of eliminating predictions for invalid or missing monitoring data hours, 24-hour measured and predicted concentrations (with annual average point-source emission rates) throughout 1976 were tabulated. Those days with high predicted concentrations which were eliminated from the initial CFD comparisons were then identified. It was determined that no significant change would occur in the upper percentiles of the CFDs at Sites 1 and 4 if a full year of predicted concentrations were utilized. The changes in the predicted CFDs at Sites 2 and 3 are shown in Figure 4. The adjusted CFD at Site 2 is only changed slightly from the initially predicted CFD. At Site 3, the curve changed significantly because the second maximum predicted concentration occurred on a day with no monitoring data. After this change, the slope of the predicted CFD looks very similar to the measured CFD and the predicted second maximum becomes approximately a factor of two below the measured second maximum. This had previously been the only maximum or second maximum predicted 24-hour average concentration (utilizing annual average point-source emission rates) which was not within approximately a factor of two of the corresponding maximum or second maximum measured concentration (see Table 1). In summary, the effect on predicted CFDs of eliminating predictions for hours with missing monitoring data was significant for only one of the four sites.

Evaluation of the Effect of Daily Emission Variations on Predictions

One of the primary functions of the emission preprocessor, RAMQ, is to determine the most significant point and area sources based on probable ambient air-quality impact. In addition to the hourly concentrations output on tape, 24-hour average SO_2 concentrations throughout 1976

TABLE 1. RATIOS OF PREDICTED TO MEASURED CONCENTRATIONS FOR 3- AND 24-HOUR MAXIMUM AND SECOND MAXIMUM SO_2 CONCENTRATIONS

Site	Averaging Time	Annual Average Point Source Emission Rates: Maximum Predicted Concentration ($\mu g/m^3$) / Maximum Measured Concentration ($\mu g/m^3$)	Annual Average Point Source Emission Rates: 2nd Max. Predicted Concentration ($\mu g/m^3$) / 2nd Max. Measured Concentration ($\mu g/m^3$)	Peak Point Source Emission Rates: Maximum Predicted Concentration ($\mu g/m^3$) / Maximum Measured Concentration ($\mu g/m^3$)	Peak Point Source Emission Rates: 2nd Max. Predicted Concentration ($\mu g/m^3$) / 2nd Max. Measured Concentration ($\mu g/m^3$)
1	3 Hr.	$\frac{1,050}{705} = 1.49$	$\frac{660}{660} = 1.00$	$\frac{2,495}{705} = 3.54$	$\frac{1,485}{660} = 2.25$
	24 Hr.	$\frac{196}{284} = 0.69$	$\frac{167}{243} = 0.69$	$\frac{429}{284} = 1.51$	$\frac{375}{243} = 1.54$
2	3 Hr.	$\frac{420}{470} = 0.89$	$\frac{405}{455} = 0.89$	$\frac{820}{470} = 1.74$	$\frac{810}{455} = 1.78$
	24 Hr.	$\frac{121}{138} = 0.88$	$\frac{105}{123} = 0.85$	$\frac{233}{138} = 1.70$	$\frac{203}{123} = 1.65$
3	3 Hr.	$\frac{310}{860} = 0.36$	$\frac{285}{820} = 0.35$	$\frac{600}{860} = 0.70$	$\frac{520}{820} = 0.63$
	24 Hr.	$\frac{97}{196} = 0.49$	$\frac{59}{168} = 0.35$	$\frac{181}{196} = 0.92$	$\frac{102}{168} = 0.61$
4	3 Hr.	$\frac{620}{475} = 1.31$	$\frac{510}{415} = 1.23$	$\frac{1,135}{475} = 2.39$	$\frac{910}{415} = 2.19$
	24 Hr.	$\frac{153}{148} = 1.03$	$\frac{138}{130} = 1.06$	$\frac{287}{148} = 1.94$	$\frac{254}{130} = 1.95$

were output directly from RAMF to determine contributions from the twenty-five most significant point sources and the ten most significant area sources, as determined by RAMQ.

Daily capacity factors (loads) for 1976 were obtained for five of the major point sources (as determined in RAMQ and the RAM daily source contribution files) for both the three highest measured and predicted days at Sites 1-4. Source contributions on the maximum days were factored (Daily Capacity Factor/Annual Average Capacity Factor) to obtain more accurate estimates of predicted concentrations on these days. These adjusted predictions were not utilized in the primary CFD analyses since not all daily concentrations in 1976 could be modified accordingly. In addition, concurrent stack parameters could not be obtained at these specific modified loads. Only the source emission rates were modified. The purpose of this exercise was only to qualitatively evaluate the magnitude of the limitation posed by the lack of hourly or daily emissions data.

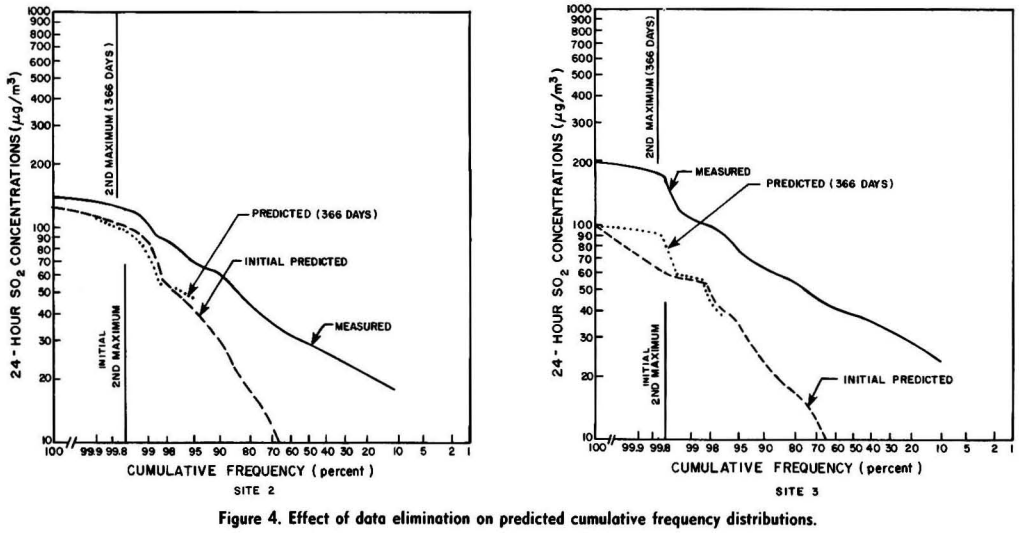

Figure 4. Effect of data elimination on predicted cumulative frequency distributions.

The three maximum predicted 24-hour concentrations at Sites 1-4, adjusted for daily emissions, are shown in Figure 5. These assume valid predictions for 366 days and no change in the other 363 concentrations. The figure shows that maximum concentration estimates decreased at Sites 2, 3, and 4 and increased slightly at Site 1. The only significant change, however, was at Site 2, where the maximum concentration estimate decreased about 20 percent.

Evaluation of Conditions Responsible for Maximum Concentrations

For each site, comparative measured and predicted 24-hour SO_2 pollution roses were prepared to evaluate overall model performance by relating the meteorological conditions responsible for measured maximum concentrations to the predicted maximum concentrations. This was accomplished by analyzing and comparing the effect of wind direction on concentrations. The results provided an indication of the RAM model's specific predictive capability relative to the various dominant point sources influencing each monitoring site as well as insight into potential emission inventory deficiencies.

In addition, for each of the three maximum measured and predicted days at each site, an analysis of hourly meteorological and daily emission source conditions responsible for the maximum concentrations was undertaken. The scope of this particular analysis was limited in that individual emission-source contributions to total concentrations were only known on a daily basis, whereas total concentrations and meteorological data were available on an hourly basis.

This analysis is particularly important since days of maximum measured and predicted concentrations rarely coincided. The analysis was, therefore, performed primarily to determine if meteorological conditions creating measured and predicted maximums at each site were similar.

The example pollution roses shown in Figure 6 were constructed by segregating measured and predicted concentrations into quantitative brackets for specified wind-direction intervals. This analysis was performed only for

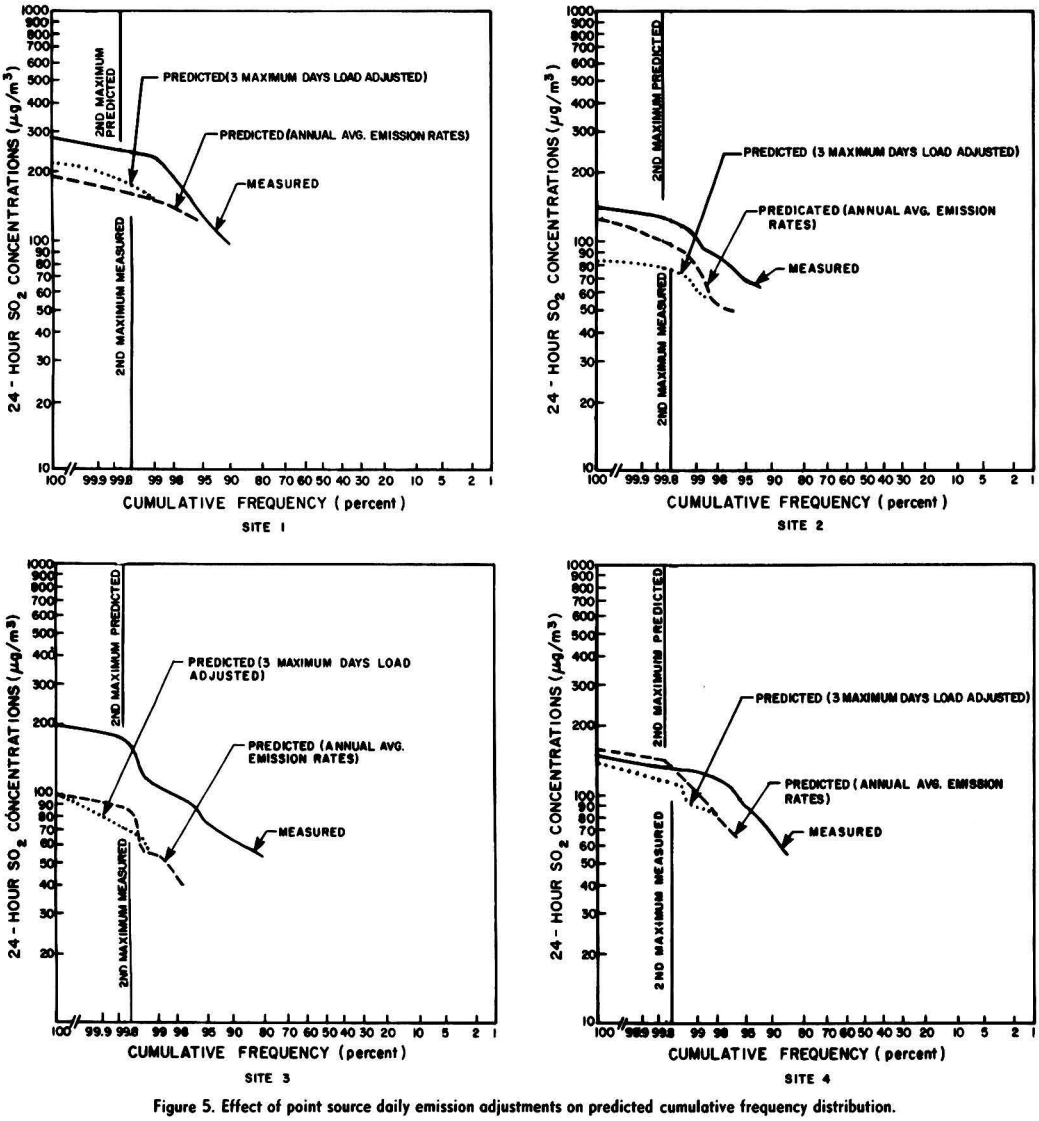

Figure 5. Effect of point source daily emission adjustments on predicted cumulative frequency distribution.

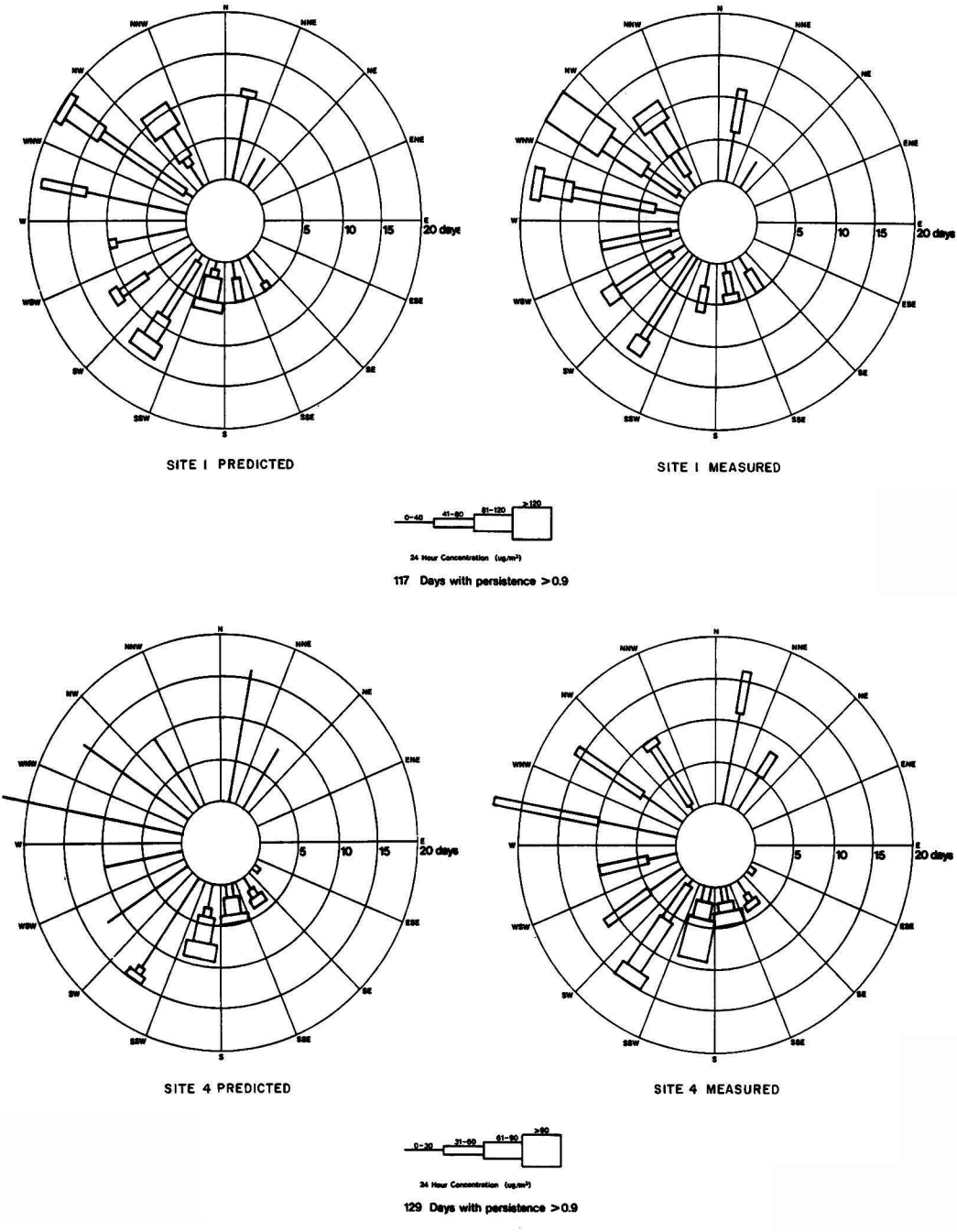

Figure 6. Comparison of 24-hour average SO_2 pollution roses.

those days having valid monitoring data and high wind persistence.

The pollution roses at all sites shown strong westerly tendencies for highly persistent wind conditions. Therefore, in general, those monitoring sites located east of major point sources (Sites 1 and 4) tended to have higher measured and predicted 24-hour average concentrations than those sites located generally to the west or south (Sites 2 and 3). This trend was also demonstrated in the CFDs.

The tendency of persistent westerly flows also precluded the specialized meteorological phenomenon of lake-induced fumigation from being a dominant factor in the highest measured 24-hour concentrations. This was expected since the phenomenon generally only persists for portions of a given 24-hr period. Analysis of hourly meteorological conditions on days with high measured concentrations showed that lake-induced fumigation did not significantly contribute to 24-hour concentrations at

any sites. If the phenomenon had been an important consideration, adjustments would have been necessary in performing this comparison since RAM can not account for it. The effect of lake-induced fumigation on 3-hour concentrations, however, could still be significant but has not been analyzed.

A comparison of the two Site 1 roses in Figure 6 shows a good correlation of concentrations in all directions. The respective length of the rose in each direction, which represents the number of days with high wind persistence, will always be identical for the roses at each site. Comparisons are made of the width of the rose in each direction (representing 24-hour SO_2 concentrations). Strong influences from two major point sources (located to the northwest and south-southwest) on maximum concentrations can be seen on both roses. However, predicted maxima appear to be somewhat more strongly influenced by the south-southwesterly source than shown by the measured data. Measured maxima appear more strongly influenced by the northwesterly source than predicted. The analysis of the three highest measured and predicted maximum concentration days at Site 1 generally showed strong influences from the two major point sources during meteorological conditions consisting of neutral stabilities, highly persistent winds, and generally medium to high wind speeds.

At Site 2, little similarity was found between the meteorological conditions creating maximum measured and predicted concentrations. All three highest measured concentrations were during periods of highly persistent winds from the direction of a major point source, medium to high wind speeds, and neutral stabilities with deep mixing layers. The second and fourth highest predicted day were created by conditions similar to these but with somewhat lower wind speeds. However, the first and third highest predicted concentrations resulted from conditions typical of a stable atmosphere (low wind speeds) with limited mixing depths. The first meteorological scenarios (neutral stabilities, high wind speeds) were underpredicted at this site and the second (stable atmosphere, limited mixing layer) were overpredicted. The highest predicted concentrations at this site are suspect, however, due to acknowledged poor model predictive capability at the low wind speed conditions associated with the maxima.

As with Site 2, Site 3 showed relatively significant underpredictions in all directions with the most severe discrepancies in the westerly directions. Due to the lack of major point sources west of Site 3, the RAM modeling did not predict the occasional medium to high concentrations which were measured on days with predominant westerly winds. This may indicate potentially significant background concentrations under certain meteorological conditions at this site which were unaccounted for in this analysis.

An excellent correlation between the predicted and measured roses does exist at Site 4. As seen in Figure 6, both roses depict high concentrations during the occurrence of winds from southerly sectors, indicating probable significant influences from three major point sources in these sectors.

All maximum concentrations at Site 4 (both measured and predicted) occur with relatively persistent winds at moderate (predicted) to high (measured) wind speeds, primarily from the direction of a major point source due south. Neutral stabilities and relatively deep mixing layers also predominate on all of the maximum days.

CONCLUSIONS

The primary conclusion of this evaluation is that the urban version of RAM was able to predict short-term concentrations relatively accurately in this study. These results alone cannot substantiate a conclusion as to the overall efficacy of the model in urban areas. However, these study results should add to the extensive data base required to make such a determination. Continued effort in model validation for a variety of urban areas is strongly recommended. Detailed hour-by-hour comparisons should be performed to identify deficiencies in the basic model formulations. It is believed that the relatively good agreement between measured and predicted values in this case is due, at least in part, to the detailed attention given to the input parameters. Applying the hypothesis of Ellis and Liu, [17] the good agreement may also be partially due to high measured concentrations from a number of stacks shorter than GEP found in Milwaukee.

Specific conclusions reach in this analysis of the RAM model are as follows:

- Background concentrations of SO_2 do not, in general, significantly contribute to maximum short-term concentrations at the monitoring sites analyzed. However, transported SO_2 may have some influence on average short-term (and long-term) concentrations at sites located west and south of the major point sources (Sites 2 and 3) due to the predominant westerly winds in the region.
- Characterization of daily or hourly emission variations was not critical since most of the dominant point sources in the Milwaukee region have relatively minor emission variations (generally within 20 percent of the annual average). When a detailed emission characterization is not available, caution should be taken in the selection of an appropriate emission rate to utilize on an annual basis for the point-source inventory. In this case, and probably in many other studies, the utilization of peak emission rates for the entire inventory to predict maximum short-term concentrations is overly conservative. Annual average emission rates yielded more accurate estimates of the actual conditions which created maximum 3-hour and 24-hour SO_2 concentrations.
- Eliminating predicted concentration hours corresponding to invalid or missing ambient monitoring data (generally about 25 percent of the 24-hour predictions) produced little effect on maximum predicted concentrations (CFDs) at the four sites.
- Meteorological characteristics on the days of 24-hour maximum predicted concentrations compared well with those characteristics on the days of maximum measured concentrations. This correlation was best at Sites 1 and 4, which, along with Site 2, showed best comparison of measured and predicted maximum concentrations. The good comparison at Sites 1 and 4 is significant because both sites are located relatively close to dominant point sources.

LITERATURE CITED

1. U.S. Environmental Protection Agency, "User's Network for Applied Modeling of Air Pollution (UNAMAP), (Version 3)," Computer Program on Magnetic Tape, NTIS PB 277 193, National Technical Information Service, Springfield, Virginia.
2. Turner, D. B. and J. H. Novak, "User's Guide for RAM," Volumes I and II, EPA-600/8-78-016 a and b, U.S. Environmental Protection Agency, Environmental Sciences Research Laboratory, Research Triangle Park, N.C. (1978).
3. U.S. Environmental Protection Agency, Office of Air Quality Planning and Standards, "Guideline on Air Quality Models—Proposed Revisions," Research Triangle Park, N.C. (1980).
4. Ruff, R. E., H. S. Javitz, and J. S. Irwin, "Development and Application of a Statistical Methodology to Evaluate the Real-time Air Quality Model (RAM)," Second Joint Conference on Applications of Air Pollution Meteorology, Conference Papers, pp. 663-669, American Meteorological Society, Boston, Mass. (1980).

5. Ruff, R. E., "Evaluation of the RAM Model Using the RAPS Data Base," Final Report Part 2: Results, SRI International (1980).
6. U.S. Environmental Protection Agency, Office of Air Quality Planning and Standards, "Guideline on Air Quality Models," EPA-450/2-78-027, Research Triangle Park, N.C. (1978).
7. "Description and Evaluation of the U.S. EPA Urban RAM Model Used in the Development of SO_2 Emission Standards for the State of Ohio," Enviroplane, Inc., Rutherford, N.J. (1977).
8. "Validation Study of Two Versions of the USEPA Urban RAM Model, the USEPA Rural RAM Model and Two other Prediction Models for the Eastlake Power Plant and Surrounding Background Sources of SO_2, Emissions Based on Use of up to Twenty-one Months of Monitoring Data," Prepared for Cleveland Electric Illuminating Company by Enviroplan, Inc. (Ref. No. 7842) by Enviroplan, Inc., Rutherford, N.J. (December, 1978).
9. Kramer, B. M., and D. G. Fox, "Air Quality Modeling: Judicial, Legislative, and Administrative Reactions," Second Joint Conference on Applications of Air Pollution Meteorology, Conference Papers, pp. 683-686, American Meteorological Society, Boston, Mass. (1980).
10. *Federal Register*, Vol. 44, No. 235, 69928.
11. Morgenstern, P., M. J. Geraghty, and R. A. McKnight, "A Comparison Study of the RAM (Urban) and RAMR (Rural) Models for Short-term SO_2 Concentrations in Metropolitan Indianapolis," Presented at the 72nd Annual Meeting of the Air Pollution Control Association, Cincinnati, Ohio, Paper No. 79-2.2, June, 1979.
12. Gulberg, P. H., and C. W. Kern, "A Comparative Validation of the RAM and PTMTP Models for Short-Term SO_2 Concentrations in Two Urban Areas," *Journal of the Air Pollution Control Association*, **28** (9), 907-910 (1978).
13. Roginski, G., and R. Kummler, "Analysis of the RAM and Modified SAI Models Comparative Validation Study in Detroit," 89th National Meeting of the American Institute of Chemical Engineers, Portland, Oregon, August, 1980.
14. Kummler, R. H., B. Cho, G. Roginski, R. Sinha, and A. Greenberg, "A Comparative Validation of the RAM and Modified SAI Models for Short-Term SO_2 Concentrations in Detroit," *Journal of the Air Pollution Control Association*, **31**(3), 253-255 (1981).
15. Hodanbosi, R. F., and L. K. Peters, "Evaluation of RAM Model for Cleveland, Ohio," *Journal of the Air Pollution Control Association*, **31**(3), 253-255 (1981).
16. Londergan, R. J., D. R. Murray, N. E. Bowne, and H. Borenstein, "A Comparison of Predictions from Standard Short-term Air Quality Models with Observed Tracer Dispersion," Second Joint Conference on Applications of Air Pollution Meteorology, Conference Papers pp. 642-649, American Meteorological Society, Boston, Mass. 1980.
17. Ellis, H. M., and P. C. Liu, "Review of the Performance of the RAM Model in Predicting Highest Measured Concentrations," *Journal of the Air Pollution Control Association*, **31**(2), 148-152 (1981).

Keith H. Kennedy functions as a Lead Engineer in the Environmental Engineering Division of Stone and Webster Engineering Corporation. He is primarily responsible for the direction of air quality studies associated with a variety of power, process, and industrial projects. He also coordinates all air quality activities associated with coal-derived synthetic fuel projects. He received a B.S. degree in Civil and Environmental Engineering from Cornell University and a M.S. degree in Civil Engineering (Environmental Studies) from Northeastern University. He is a member of the Tau Beta Pi Association and the Air Pollution Control Association.

Richard D. Siegel is a consultant in the Environmental Engineering Division of Stone & Webster specializing in air quality related issues. His responsibilities include project management of selected environmental studies, analyses, and permit applications and business development activities for the Division. He is also responsible for advising members of the Environmental Division, Stone & Webster projects, and clients on the implications of evolving regulations and laws in the air quality area. He received his B.A. and M.A. in Chemical Engineering from Tufts University in Medford, Massachusetts, and his Ph.D. from Lehigh University, also in Chemical Engineering. He is a member of several technical societies and is particularly active in the American Institute of Chemical Engineers (AIChE). He is a previous chairman of AIChE's Environmental Division and is currently chairman of its Air Technical Section. He has chaired and co-chaired nearly two-dozen technical symposia in air pollution control and is the author of over 90 journal articles, books, reports, interviews, and presentations.

Mark P. Steinberg is superintendent of the Air Quality Division in Wisconsin Electric Power Company's Environmental Department. His responsibilities include the air quality permitting of generation expansion facilities, overseeing compliance of existing facilities with regulatory requirements and tracking air quality legislative and regulatory developments. He has been employed with Wisconsin Electric since 1972. He holds B.A.'s and M.A. degree in meteorology from Rutgers University (1969) and the University of Wisconsin (1971). respectively.

Modeling of Lead Air Pollution

How effective has the use of unleaded gasoline been in reducing air pollution by lead? A case-history study from Baton Rouge, Louisiana.

C. S. Monteith, Gulf South Research Institute, New Orleans, La. 70186
J. M. Henry, University of Tennessee, Chattanooga, Tenn.

The rise in atmospheric lead concentrations since the Industrial Revolution has been established by analysis of snow and ice samples from northern Greenland [*1*]. The increased concentrations are of concern because lead adsorbed to particles may be inhaled and absorbed through the lungs into systemic circulation, adversely affecting the central nervous system, peripheral nerves, kidneys, and the hemopoietic system [2]. Of foremost concern are the subtle behavioral changes experienced by children chronically exposed to low concentrations of lead.

The Environmental Protection Agency (EPA), responsible for setting the ambient air quality standard for lead to protect human health and public welfare, set this standard

ISSN 0278-4491-82-5838-0142-$2.00.

in 1978 at 1.5 $\mu g/m^3$ averaged over a calendar quarter [3]. States were required to develop State Implementation Plans to demonstrate that the standards would be attained and maintained. Atmospheric dispersion modeling is required to demonstrate that the standard will not be violated in the vicinity of a significant point source, and a modified rollback model or an atmospheric dispersion model must demonstrate ultimate attainment of the standard in the vicinity of any air-quality monitor which has recorded lead concentrations in excess of the standard.

Major sources of atmospheric lead are vehicular and industrial emissions. Vehicular lead emissions are being controlled by the use of unleaded gasoline and the mandated increase in fuel economy. Significant industrial sources, according to the EPA, include primary and secondary lead smelters, primary copper smelters, lead gasoline additive (tetraethyl lead) plants, lead-acid storage battery manufacturing plants producing over 2,000 batteries per day, and any other source emitting 22,700 kg (25 tons) or more of lead per year.

This study was performed to determine whether vehicular emissions should be included with industrial emissions when demonstrating attainment of the ambient air quality standard for lead. The impact on ambient lead concentrations of the phaseout of leaded gasoline and improved automobile fuel economy was examined by modeling vehicular emissions for 1972 and 1978.

BACKGROUND

The Louisiana Air Control Commission (LACC) prepared a lead implementation plan for the State of Louisiana [4]. The lead-emission inventory lists two significant point sources of lead in the Baton Rouge area, a tetraethyl lead plant and a secondary lead smelter. Dispersion modeling of the emissions from these two sources, excluding automotive lead emissions, was performed by the State using CRSTER. The results indicated that emissions from the point sources alone would not cause the standard to be violated.

The LACC maintained a high-volume air sampler at one site in Baton Rouge for the period covering the first quarter of 1976 through the first quarter of 1979. The quarterly arithmetic average lead concentration at the Baton Rouge site exceeded 1.5 μ/m^3 for 3 of the 13 quarters, as shown in Figure 1. Modified rollback modeling performed by the LACC showed that a 19 percent reduction of total emissions would be required to attain the standard in the Baton Rouge area. The LACC estimated that a reduction in total lead emissions of at least 33 percent will occur by 1983 as a result of the phaseout of lead additives in gasoline.

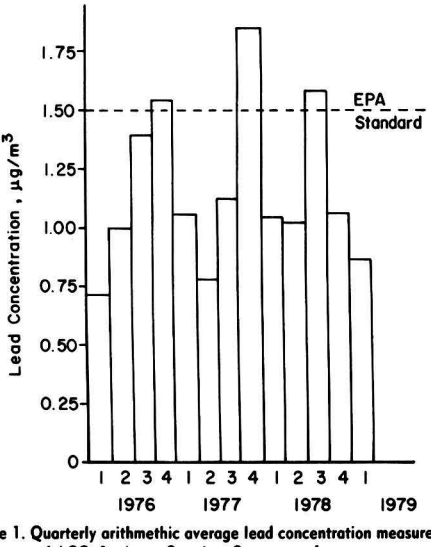

Figure 1. Quarterly arithmethic average lead concentration measured by LACC. 1-winter, 2-spring, 3-summer, 4-autumn.

DISPERSION MODELING

In this study, the quarterly average ambient lead concentrations in Baton Rouge resulting from automotive and industrial emissions in 1972 and 1978 were predicted using the Climatological Dispersion Model (CDM) published by EPA [5]. CDM, a Gaussian model, has been used for calculating ambient concentrations of sulfur dioxide in urban areas from point and area sources [6, 7]. The assumption is made that the sources are continuously emitting a pollutant at a constant rate, and that the meteorological conditions over a short period of time, such as an hour, can be regarded as steady-state [8].

Meteorological information was obtained from the National Weather Service STAR program. Note that the seasonal quarters for which the meteorological data are compiled are one month ahead of the calendar quarterly averaging times on which the lead standard is based. For example, the meteorological winter quarter consists of December, January, and February, while the first calendar quarter consists of January, February, and March.

MODELING AUTOMOTIVE EMISSIONS

An area-source emission inventory was established by dividing the Baton Rouge area into a grid of 156 squares, each having a width of 860 m, and each assigned to one of three districts according to vehicular traffic usage: central business district, central city, and suburbs. Contiguous grid squares falling within a single category were combined to form a larger square whenever possible.

Estimates of the number of vehicle-kilometers traveled within a twenty-four hour period in 1972 and a projection of the kilometers traveled in 1990 in the three districts were obtained from the Louisiana Department of Transportation and Development. An estimate of the number of vehicle-kilometers traveled in 1978 was calculated from the 1972 and 1990 data by linear interpolation. The number of vehicle-kilometers traveled in each area, tabulated by road type, are listed in Table 1. An emission rate was calculated for each type of roadway using 1972 and 1978 conditions and the recommended EPA procedure [9]. The average speeds were assumed to be 32 km/hr for local traffic, 56 km/hr for arterial traffic, and 97 km/hr (in 1972) or 88 km/hr (in 1978) for freeway traffic.

The following equation was used to estimate the rates of emission of lead from vehicles [9]:

$$e_{n,s} = \frac{a_s Pb_n v}{f_{n,s}} \qquad (1)$$

where

$e_{n,s}$ = emission rate for calendar year n and speed s (g/day)
a_s = percentage of lead burned that is exhausted
Pb_n = probable pooled average lead content of gasoline in year n (g/liter)
v = vehicle-kilometers traveled (vehicle-km/day)
$f_{n,s}$ = average fleet fuel economy for calendar year n and speed s (vehicle-km/liter)

The percentage of lead burned which is exhausted to the atmosphere was determined from the relationship established by EPA based on a number of studies [9]. This percentage increases with increased vehicle cruise speed. Values are listed in Table 2.

The EPA estimates of 0.74 g/liter (2.8 g/gal) and 0.21 g/liter (0.8 g/gal) as the probable pooled average lead con-

TABLE 1. VEHICLE-KILOMETERS TRAVELED AND EMISSION RATES FOR EACH AREA OF BATON ROUGE IN 1972 AND 1978.

Area of city	Traffic type	1000 vehicle-km traveled per day		Emission rate (kg/day)		Emission rate (kg/day/m²)	
		1972	1978	1972	1978	1972	1978
central business district	local	3	3	0.102	0.024		
	arterial	32	35	1.35	0.321		
	freeway	0	0	0	0		
	total			1.45	0.345	0.242	0.058
central city	local	864	1030	24.9	6.22		
	arterial	1,950	2,210	82.6	19.7		
	freeway	642	871	35.8	8.82		
	total			143	34.8	2.20	0.535
suburbs	local	713	980	20.5	5.92		
	arterial	1,810	2,300	76.8	20.4		
	freeway	323	639	18.0	6.5		
	total			115	32.9	1.36	0.387

tent of gasoline in 1972 and 1978, respectively, were used in calculating the emission rates. The average fleet fuel economies for 1972 and 1978 were calculated for each speed using the following equation [9]:

$$f_{n,s} = \frac{\sum_{i=1967}^{1974} C_{s,i} E_{c,i} m_i}{E_{1974}} E_n C_t \qquad (2)$$

where

$C_{s,i}$ = speed-dependent fuel economy correction factor for model year i

$E_{c,i}$ = city/highway combined fuel economy for model year i (km/liter)

m_i = fraction of annual travel by model year i vehicles (nondimensional)

E_{1974} = base year (1974) fuel economy (km/liter)

E_n = average fleet economy for projection year, 1972 or 1978 (km/liter)

C_t = traffic flow correction factor; C_t = 1.2297 for free-flow traffic; C_t = 0.866 for stop-and-go traffic

The results of dispersion modeling of only the vehicular emissions using CDM are expressed as the quarterly arithmetic average lead concentrations at ground-level receptors. The highest values are shown in Table 3. The maximum concentrations for all four calendar quarters were located in the central city area of Baton Rouge. The near-maximum isopleths for 1972 are shown in Figure 2.

The significant decrease in ambient lead levels resulting from vehicular exhaust between 1972 and 1978 is due to the decrease in the average pooled lead concentration of gasoline from 0.74 g/liter in 1972 to 0.21 g/liter in 1978 and the increased average fuel economy (Table 2).

MODELING AUTOMOTIVE AND INDUSTRIAL EMISSIONS

The industrial emission rates, obtained from the most recent Emission Inventory Questionnaires on file with the LACC, were 3.3 g/sec for the tetraethyl lead plant and 0.36 g/sec for the secondary lead smelter. The location of the tetraethyl lead plant is shown in Figure 3; the secondary lead smelter is located off the map to the northwest. For all quarters, the maximum lead concentrations due to both vehicular and industrial emissions were located in the northwestern suburbs of the city, near the tetraethyl lead plant. Emissions from the secondary lead smelter were found to have no observable effect on the ambient lead concentration in Baton Rouge.

The results of the modeling are shown on isopleth maps for the autumn quarters of 1972 and 1978, the quarters having the highest lead concentrations (Figures 3 and 4). The contributions of vehicular and industrial emissions are listed in Table 4 for the 4 quarters of 1972 and 1978. In 1972, automobile emissions were the source of approximately 35 percent of the total ambient concentration. By 1978, the contribution from automobiles had dropped to 10 percent. As distance from the tetraethyl lead plant increases, the relative contribution of vehicular emissions increases significantly.

The results of dispersion modeling for 1978 emissions were compared with the average quarterly lead concen-

TABLE 2. PERCENTAGE OF LEAD BURNED THAT IS EXHAUSTED AND AVERAGE FLEET FUEL ECONOMY FOR THE THREE REGIONS OF THE CITY IN 1972 AND 1978.

Year	Traffic type	Speed (km/hr)	Percent of lead burned that is exhausted, a_s	Average fleet fuel economy $f_{n,s}$ (vehicle-km/liter)
1972	local	32	15.0	3.67
1972	arterial	56	27.5	4.59
1972	freeway	97	53.5	6.76
1978	local	32	15.0	5.31
1978	arterial	56	27.5	6.63
1978	freeway	88	47.7	10.1

1 km/liter = 2.35 mi/gal

TABLE 3. THE MAXIMUM AMBIENT LEAD CONCENTRATIONS RESULTING FROM AUTOMOTIVE EMISSIONS IN 1972 AND 1978.

Calendar quarter	Maximum lead concentration (μg/m²)	
	1972	1978
winter	1.08	0.22
spring	1.06	0.22
summer	1.23	0.25
autumn	1.33	0.27

TABLE 4. CALCULATED MAXIMUM LEAD CONCENTRATIONS ($\mu g/m^3$) FOR EACH QUARTER OF 1972 AND 1978 RESULTING FROM THE SUMMATION OF AUTOMOTIVE AND INDUSTRIAL EMISSIONS.

	1972			1978		
Quarter	Automotive	Industrial	Total	Automotive	Industrial	Total
winter	0.7	1.6	2.3	0.1	1.6	1.7
spring	0.7	1.2	1.9	0.1	1.2	1.3
summer	0.8	1.4	2.2	0.2	1.4	1.6
autumn	0.9	1.8	2.7	0.2	1.8	2.0

trations measured from January 1976 through February 1979 by the LACC at a location in the northwestern suburbs of Baton Rouge (Figure 1). As shown in Table 5, there is good agreement between the measured and predicted concentrations for all quarters except autumn.

CONCLUSIONS

The results of modeling automotive and industrial lead emissions show that while automobiles in the Baton Rouge area were a significant source of lead in 1972, the phaseout of leaded gasoline and the increase in fuel economy have resulted in a lower contribution (0.20 $\mu g/m^3$) by automobiles to the ambient lead concentration in 1978.

The areas having the greatest potential for exceeding the ambient air quality standard can be identified using CDM. This information can be used to determine the optimal location for an ambient air monitor to demonstrate compliance with the ambient air quality standard. This is particularly clear by reference to Figure 4, in comparison with the results in Tables 4 and 5. The CDM predicts that a differently placed monitoring station would measure a significantly higher concentration.

TABLE 5. COMPARISON OF LEAD CONCENTRATION ($\mu g/m^3$) PREDICTED BY CDM AND MEASURED AT THE LACC MONITOR.

Quarter	LACC monitor (1976-1979)	CDM (1978)	Error factor
winter	0.9	0.6	1.5
spring	0.9	0.7	1.3
summer	1.4	1.4	1
autumn	1.5	0.6	2.5

ACKNOWLEDGEMENT

This work was done at Tulane University with the facilities of the Tulane Computer Center.

LITERATURE CITED

1. Hall, S. K., "Lead Pollution and Poisoning," *Environ. Sci. Tech.*, **6**, 30 (1972).
2. Hammond, P. B., and R. P. Beliles, in *Toxicology: The Basic Science of Poisons* (J. Doull, C. D. Klaassen, and M. O. Amdur, ed.), p. 409, Macmillan Publishing Co., Inc., New York (1980).

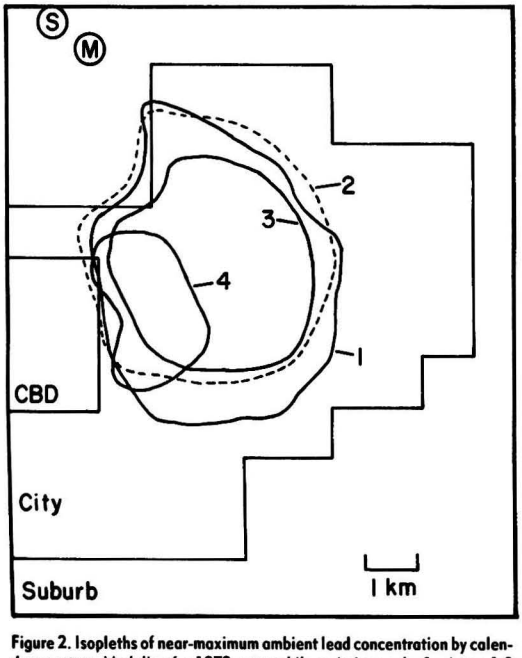

Figure 2. Isopleths of near-maximum ambient lead concentration by calendar quarters. Modeling for 1972 automobile emissions only. 1-winter, 1.0 $\mu g/m^3$ isopleth; 2-spring, 1.0 $\mu g/m^3$ isopleth; 3-summer, 1.2 $\mu g/m^3$ isopleth; 4-autumn, 1.3 $\mu g/m^3$ isopleth. S = industrial source, M = LACC monitor.

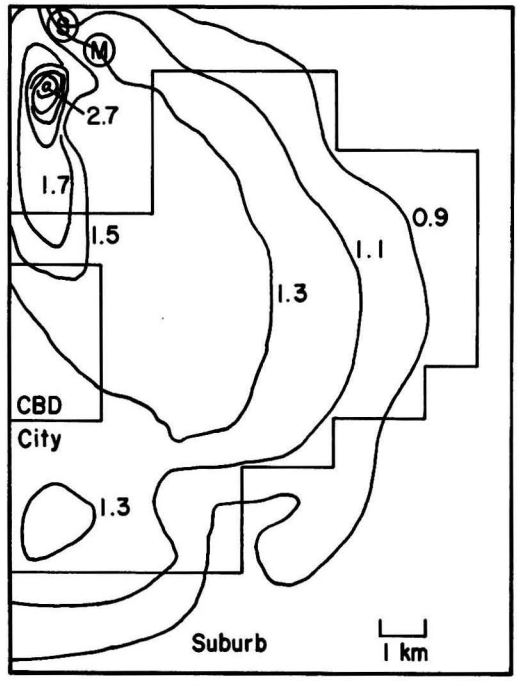

Figure 3. Isopleths of ambient lead concentrations ($\mu g/m^3$). Modeling for autumn, 1972 automobile and industrial emissions. S = industrial source, M = LACC monitor.

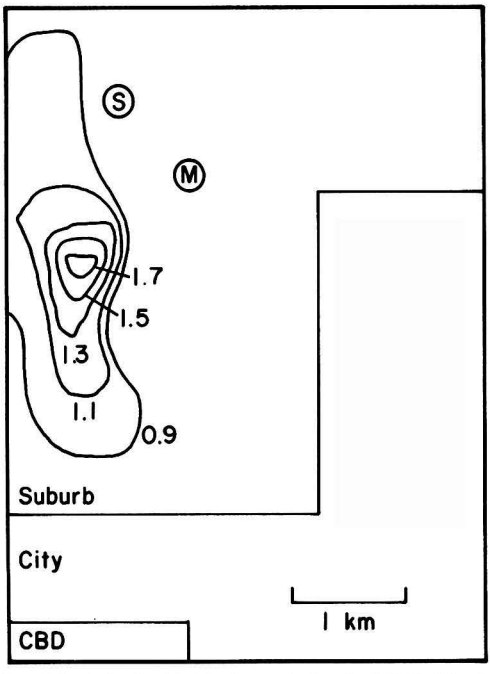

Figure 4. Isopleths of ambient lead concentrations (mg/m³). Modeling for autumn, 1978 automobile and industrial emissions. S = industrial source, M = LACC monitor.

3. Federal Register, **43** (194), 46246 (October 5, 1978).
4. "Louisiana State Implementation Plan for Lead," Department of Natural Resources, Baton Rouge, Louisiana.
5. Busse, A. D., and J. R. Zimmerman, "User's Guide for the Climatological Dispersion Model," EPA-R4-73-024, Research Triangle Park, North Carolina (1973).
6. Prahm, L. P., and M. Christensen, "Validation of a Multiple Source Gaussian Air Quality Model," *Atmospheric Environment*, **11**, 791 (1977).
7. Turner, D. B., J. R. Zimmerman, and A. D. Busse, "An Evaluation of Some Climatological Dispersion Models," in "User's Guide for the Climatological Dispersion Model" (A. D. Busse and J. R. Zimmerman, ed.), p. 107, EPA-R4-73-024, Research Triangle Park, North Carolina (1973).
8. Calder, K. L., "A Climatological Model for Multiple Source Urban Air Pollution," in "User's Guide for the Climatological Dispersion Model" (A. D. Busse and J. R. Zimmerman, ed.), p. 73, EPA-R4-73-024, Research Triangle Park, North Carolina (1973).
9. "Guidelines for Lead Implementation Plans," EPA-450/2-78-038, Research Triangle Park, North Carolina (1978).

Carolyn S. Monteith is supervisor of the environmental chemistry laboratory at Gulf South Research Institute in New Orleans, La. She received an M.S. in environmental engineering sciences from the University of Florida and is a member of the ACS and APCA.

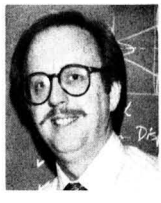

Jim Henry is on the chemical engineering faculty at the University of Tennessee at Chattanooga. He has taught previously at Tulane University and has worked for the Department of Energy. His education was at Rice and Princeton universities. He is a registered professional engineer and is a member of AIChE, APCA, and Sigma Xi.

Mitigation of Acid Rain—Policy Alternatives

The question of "acid rain" is fast becoming a political football as well as an environmental phenomenon. Here are the facts.

Duane A. Knudson and David G. Streets, Argonne National Laboratory, Argonne, Ill. 60439

This paper addresses what may well prove to be one of the most sensitive environmental issues of the 1980s: mitigation of acid-rain impacts. The emphasis here is not on the need for such measures nor the benefits that might be gained, but rather on the relative effects of a number of different policy options that could be invoked. The relative advantages and disadvantages of alternative strategies for the reduction of sulfur-dioxide emissions from coal-fired electric generating stations are described.

In the mid-1950s an ambient monitoring program was established in northern and western Europe in response to allegations that atmospheric acidic deposition was harming fishery resources in Scandinavia. This monitoring program, termed the European Air Chemistry Network, was designed to quantify international air pollution fluxes. The general conclusion based on data from this network was straightforward: the decreased fish populations and reduced forest productivity in Scandinavia was a direct consequence of the long-range transport of sulfur emissions originating in the United Kingdom and industrialized western Europe.

This initial concern led to the establishment of a comprehensive five-year research program that had the goal of determining the relative importance of local and distant sources of sulfur compounds for the European countries. The results of that major field study have recently been summarized by Barnes [*1*]. In general, the study concluded that sulfur compounds may travel long distances and may measurably affect air quality in neighboring countries.

In the early 1970s a regional sulfur transport phenomenon similar to that affecting the northern European countries was postulated to exist in the northeastern U.S. Declining fish populations in the Adirondacks were linked

ISSN 0278-4491-82-5864-0146-$2.00.

to increased acidic deposition in an analogous manner to that suggested for the Scandinavian countries. [2].

Since publication of this assessment, considerable effort has been expended to verify its validity. Various studies have been performed to elucidate every conceivable aspect of the deposition phenomenon. The results of these studies, however, have led to few conclusions that are totally nonrefutable. Dissenting viewpoints are still to be found on such crucial aspects as definition of long-term trends; the composition of deposited material; atmospheric transport, transformation, and removal processes; and source contributions.

This paper does not enter into the debate surrounding these various aspects of the phenomenon. The discussion is limited to an examination of various methods for reducing SO_2 emissions from the electric utility industry, the major contributor to sulfur emissions in the eastern U.S. However, no explicit assumption is made concerning the contribution of this source category to the total deposition. Also, conclusions are not drawn on the amount of ambient impact reduction that would accompany a given reduction in emissions. Instead, several scenarios are described which achieve various levels of emission reduction for the utility sector through the year 2000 in the eastern U.S. The scenarios were developed in a joint U.S. Department of Energy/Environmental Protection Agency cooperative effort and are designed to simulate a range of possible regulatory options.

Projecting such variables as future emission levels, generating capacity additions, and environmental control costs requires sophisticated modeling of the electric utility industry. The results presented in this paper were provided by Teknekron Research Inc., using the Utility Simulation Model (USM) [3].

METHODOLOGY

Utility decisions are formulated in response to a variety of external stimuli. The simulation of these factors within USM is accomplished by a number of elements, which include electricity demand levels, financial market conditions, fuel characteristics and availability, advanced technology development and utilization, and environmental regulations. The model computes emissions and cost projections based on unit-specific data at the county level. A least-cost dispatching algorithm is used for the various generating units and capacity classes owned by all of the utilities within each state. Eighty-six hypothetical utility systems provide the basis for state and regional projections, which are the aggregate of individual units in the simulated systems.

For each scenario, the model calculates the following, for each year through 2000:

- System characteristics
  - —Electricity generated by unit type
  - —Capital requirements by source
  - —Plant and equipment requirements
- Financial data for utility firms
- Average electricity prices

In the analysis, several parameters were defined to reflect expected operating conditions through the end of the century. These parameters are summarized in Table 1.

TABLE 1. DEFINITION OF MAJOR MODEL PARAMETERS

Expected Plant Life
Nuclear and Oil—35 years Coal and Gas—45 years
Capacity Factor
Dispatches 17 classes of units to meet utility firm-specific 24-hour seasonal load curves each year. Nuclear units operate at 65 percent annual capacity.
Heat Rate
Oil = 10,900 Btu/kWh Gas = 10,200 Coal on line prior to 1966 = 13,000 Coal on line 1966-1977 = 11,024 Coal on line during or after 1978 = 9,600 New oil and gas = 9,600
Electricity Demand—National Average
1979-1985 3.4%/year 1985-1990 3.4 1991-1995 2.5 1996-2000 2.0 State-specific growth rates were derived.
Oil and Gas Retirement Rates

	Oil	Gas	
1985	3.4	2.8	Quads
1990	2.6	3.1	
1995	2.1	2.6	
2000	1.7	2.1	

Nuclear Capacity	
1980	53.3 GW
1985	80.3
1990	114.5
1995	137.2
2000	146.0

Compliance Options

Compliance options available to fossil-fuel generating units are chosen on a least-cost basis to meet a specified emission limit. The available options include use of current coals, wet and dry flue gas desulfurization (FGD), coal cleaning, low-sulfur coal, coal blending, and various combinations of these. Selection of the unit-specific, least-cost option considers the remaining lifetime of the unit. For example, a low-sulfur or cleaned-coal strategy is costed by taking the incremental cost above the present fuel cost and then levelizing over the period. In contrast, a wet or dry scrubbing strategy is costed by taking the annual capital cost incurred, using a fixed charge rate, and adding to that the levelized cost of scrubber-system operation and maintenance.

The electric generating units subject to this compliance strategy selection are the coal-fired units which began construction prior to August, 1971. These units are subject to State Implementation Plan (SIP) emission limits, which are generally less stringent than New Source Performance Standards. The regulatory strategies examined in this analysis for reducing SO_2 emissions from those SIP-regulated units are defined in Table 2.

The BAS scenario serves as the base case and is useful for comparative purposes; it is not an emission reduction scenario. The scenarios listed in the table are not the complete list of options evaluated in the study. However, they do represent a broad range of variable possibilities and consequences.

TABLE 2. SCENARIO DESCRIPTIONS*

Abbreviation	Regulatory Strategy	Description
BAS	SIP Compliance	All SIP units are required to meet promulgated regulations by 1985. Compliance is determined by comparing annual average emissions with specified SIP regulations.
CP4	4 lb $SO_2/10^6$ Btu ceiling	All SIP units are required to meet promulgated regulations by 1985. No SIP SO_2 limit is allowed to exceed 4 lb/10^6 Btu.
CP2	2 lb $SO_2/10^6$ Btu ceiling	All SIP units are required to meet promulgated regulations by 1985. No SIP SO_2 limit is allowed to exceed 2 lb/10^6 Btu.
CL4	4 lb $SO_2/10^6$ Btu ceiling with local coals	Same as scenario CP4, requiring a maximum SIP limit of 4 lb $SO_2/10^6$ Btu. However, coal-switching options are limited to locally produced coals for those states that are major coal producers. Affected units are permitted only to switch to local coals from within state or to install FGD. Unaffected units can continue current purchase patterns.
CL2	2 lb $SO_2/10^6$ Btu ceiling with local coals	Same as scenario CP2, requiring a maximum SIP limit of 2 lb $SO_2/10^6$ Btu. However, coal-switching options are limited to locally produced coals for those states that are major coal producers, as in scenario CL4.
F30	30% SO_2 reduction by FGD retrofit	A 30% SO_2 reduction beyond SIP compliance levels is achieved by retrofitting scrubbers on units where retrofitting is most cost-effective. Cost-effectiveness is determined by ranking units on the basis of dollars per ton of SO_2 reduced over current practice.
F50	50% SO_2 reduction by FGD retrofit	A 50% SO_2 reduction beyond SIP compliance levels is achieved by retrofitting scrubbers where retrofitting is most cost-effective.

* All scenarios assume that units will at least meet the base-case SIP limits. Units of less than 100 MW or on line prior to 1950, however, are not required to meet the more stringent SIPS.

The analysis of utility emissions reductions and cost requirements is limited to an area consisting of the states east of the Mississippi River plus Iowa, Missouri, Arkansas, and Louisiana. These 31 states are termed the Acid Rain Mitigation (ARM) region, in this analysis.

ANALYSIS

Projections of emission rates, annual revenue requirements and cost effectiveness, under the subject emission reduction strategies are summarized in Table 3. The summary presents incremental changes relative to the base case (BAS) projections, which assume SIP compliance by 1985. Control costs are given in terms of annual utility revenue requirements and the cost per additional (beyond BAS) ton of SO_2 removed. Cost per ton removed includes capital costs and fixed and variable operation and maintenance (O&M) costs. Utility annual revenue requirements are based on expenses which include capital, O&M, and fuel costs.

Immediately apparent are the three general levels of emission reduction achieved by the scenarios. The lowest level of reduction of about 1.5 million tons SO_2 per year is accomplished through the 4 lb $SO_2/10^6$ Btu SIP limit (4 lb limit). Reductions of about 5.0 to 5.5 million tons SO_2 per year are projected for the 2 lb $SO_2/10^6$ Btu SIP limit (2 lb limit) and the 30% regional SO_2 reduction by FGD retrofit. The highest level of emissions reduction is obtained with the regional 50% SO_2 reduction through FGD retrofit.

An accompanying observation is the increased revenue requirements for the larger SO_2 reductions. Annual revenue requirements for reducing SO_2 emissions to achieve compliance with current SIP limits range from $100.7 billion in 1985 to $151.4 billion in 2000. Revenue requirements range from less than $0.5 billion for an additional reduction of about 1.5 million tons per year to about $4.0 billion in 1995 necessary to achieve an additional reduction of about 8 million tons beyond SIP levels.

Emission-reduction strategies which allow the utility to choose among the broadest range of compliance methods for reducing emissions tend to be the most cost effective. This is illustrated through comparison of the 4 lb and 2 lb SIP emission ceilings allowing for unrestrained and local coal use. These scenarios are represented by the abbreviations CP4 and CL4 and CP2 and CL2, respectively. Annual emission reductions under CP4 and CL4 average about 1.4 million tons through the simulation period. Cost effectiveness and revenue requirements are quite dissimilar, however, for the two scenarios. In 1995, CP4 projections show a cost effectiveness of $296/ton SO_2 removed with total additional annual revenue requirements of $460 million. Projections for the same year under the same emission ceiling with the local coal constraint (CL4) yield values of $473/ton SO_2 removed with total annual revenue requirements of about $710 million. Comparison of the 2 lb emission ceiling scenarios show additional reductions of about 5.4 million tons of SO_2 with smaller differences between unrestrained and local coal market scenarios for cost effectiveness and annual revenue requirements. The cost effectiveness changes from $406/ton SO_2 to $470/ton SO_2 removed with annual revenue requirements of an additional $2.24 billion and $2.56 billion, respectively, for the two scenarios.

An important feature of imposing an emissions ceiling on the SIP is that emissions reductions are applied only to those units with emissions in excess of that value. These scenarios therefore localize emission reductions and incurred costs to those utilities with units presently operating beyond the specified values and to states with lenient SIP requirements. This may not be the case, however, under those regulatory scenarios which are designed to provide a given percentage reduction in SO_2 emissions throughout the region by retrofitting FGD systems on a cost-effectiveness basis. Following this methodology, the largest sources, in terms of tons per year, may be overlooked.

Because each state contains a different composition of generating capacity, the effectiveness of these scenarios varies substantially among the affected states. As previously discussed, the model forms 86 hypothetical utilities for which unit-specific projections are computed. These projections are then aggregated to state totals. In the analysis that follows, three states—Ohio, West Virginia, and Illinois—are examined in detail to illustrate the state-specific impacts of the various policy alternatives.

The summary for Ohio, presented in Figure 1, compares total annual emissions and concomitant average electricity prices under several regulatory scenarios in the top part of the figure for the years 1985 and 2000. The lower segment of the figure shows the cost effectiveness of the subject

TABLE 3. UTILITY SO_2 EMISSIONS AND CONTROL COST PROJECTIONS—TOTAL FOR THE ACID RAIN MITIGATION REGION*

	BAS	ΔCP4	ΔCL4	ΔCP2	ΔCL2	ΔF30	ΔF50
1985							
SO_2 Emissions (10^6 tons/year)	16.0	−1.5	−1.5	−5.5	−5.4	−5.0	−8.4
Annual Revenue Requirement (10^9 1980$)	100.7	0.37	0.70	2.27	2.61	1.70	3.52
Cost/Additional Ton SO_2 Removed (1980$)	—	227	462	411	479	340	419
1995							
SO_2 Emissions (10^6 tons/year)	16.0	−1.5	−1.5	−5.5	−5.4	−5.0	−8.2
Annual Revenue Requirement (10^9 1980$)	119.6	0.46	0.71	2.24	2.56	1.77	3.86
Cost/Additional Ton SO_2 Removed (1980$)	—	296	473	406	470	357	471
2000							
SO_2 Emissions (10^6 tons/year)	14.8	−1.3	−1.3	−5.1	−5.0	−4.4	−7.4
Annual Revenue Requirement (10^9 1980$)	151.4	0.24	0.38	1.01	1.01	1.22	1.65
Cost/Additional Ton SO_2 Removed (1980$)	—	181	289	198	204	279	223

* All states east of the Mississippi River plus Iowa, Missouri, Arkansas, and Louisiana.

scenarios. A large portion of Ohio's utility-related SO_2 emissions currently originates from units that are operating beyond the 4.0 lb and 2.0 lb emission limits. Because these units have access to coal which meets these limits, the CP4 and CP2 scenarios yield up to a 50-percent reduction in statewide emissions (CP2) with a consistently better cost effectiveness than the other senarios.

Addition of the constraint that these emission ceilings (4.0 and 2.0 lb) must be met with locally available coal, if possible, increases the cost per ton removed while achieving about the same level of emission reduction. The result of this is a substantial difference in electricity prices in 1985 between the nonconstrained and constrained coal-

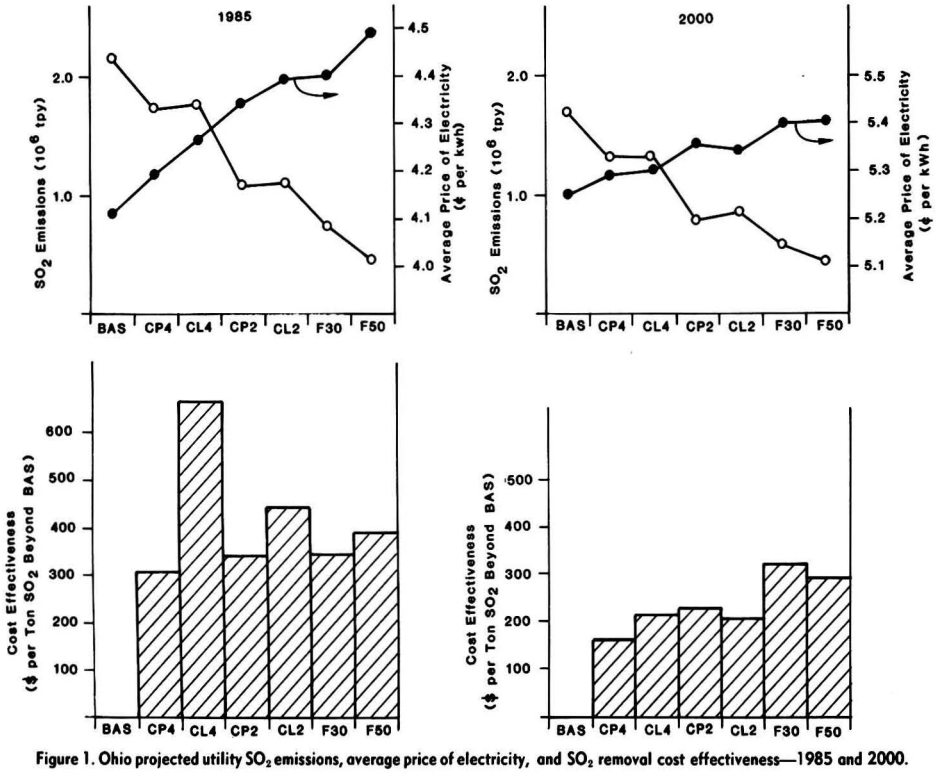

Figure 1. Ohio projected utility SO_2 emissions, average price of electricity, and SO_2 removal cost effectiveness—1985 and 2000.

access scenarios. However, in 2000 this difference virtually disappears.

The retrofitting of scrubbers on Ohio generating stations, on a least-cost basis, to achieve a region-wide emissions reduction of 30 to 50% beyond SIP compliance results in state-wide reductions of about 67 and 76%, respectively. Average electricity prices for these scenarios, while the highest of any of the scenarios presented, represent increases of less than 10% above those for SIP compliance (BAS).

The impact of the subject scenarios on utilities in West Virginia is summarized in Figure 2. The format for the presentation is identical to that used for Ohio. West Virginia has only a few power plants operating in excess of 4.0 lb $SO_2/10^6$ Btu, and has access to local coal that complies with this limit. Because of this, the CP4 and CL4 scenarios achieve only modest reductions in total state-wide emissions at virtually no extra cost. Under the 2 lb SIP ceiling, emission reductions in the range of 30 percent beyond that for compliance with the present SIP (BAS) are projected throughout the period. The effect of the local coal restriction on compliance costs for meeting the 2 lb cap (CL2) is minimal. The implication here is that compliance methodology and costs are insensitive to the local coal restriction at the 2 lb level. Retrofitting FGD systems to achieve 30 and 50% reductions throughout the region (F30 and F50), yields additional emission reductions on the order of 40 and 60% in West Virginia. Although these emission reductions are achieved with the largest additional cost to the consumer, the cost per additional ton of SO_2 removed does not exceed $90.

Information for Illinois presented in Figure 3 is analogous to that presented for Ohio and West Virginia in Figures 1 and 2. In a similar fashion to that observed for Ohio, reasonable (up to about 50 percent) emission reductions beyond the projections under BAS assumptions are possible by imposition of the 4 lb and 2 lb emission limits. Emission reductions under these scenarios are achieved in a relatively cost-effective manner, with costs of additional SO_2 removed ranging from about $350/ton (CP2 in 1985) to $160/ton (CP2 in 2000). The cost per ton removed increases substantially (especially in 1985) when the constraint for local coal use is applied. In terms of average electricity prices, however, this increase essentially disappears by 2000.

The regulatory scenarios designed to reduce region-wide emissions by 30 and 50% (F30 and F50) are also quite effective in Illinois. State-wide emissions are reduced by about 50 and 60% beyond BAS projections. The emission reduction under the F30 scenario is comparable to those projected under the 2 lb cap (CP2 and CL2). However, the F30 scenario is marginally less cost effective than the 2 lb cap, which leads to 0.06 ¢/kWh difference (5.55-5.49) in average electricity prices between the two scenarios by the year 2000.

Although similarities exist among these states in the impact and effectiveness of the subject scenarios, application of a uniform emission-reduction methodology for all of the states does not appear to be warranted. As an example, consider the effectiveness of the 4 lb SIP emission ceiling. In both Illinois and Ohio this strategy provides about a 20% reduction beyond that associated with the present SIP, compared to about 10% additional reduction in West Virginia. This additional 10% reduction in West Virginia can be accomplished at virtually no additional cost to the utility or the consumer. On the other hand, the additional 20% emission reduction could cost as much as $830/additional ton in Ohio and $530/additional ton in Illinois, under the constraint that locally available coal must be used. Without this constraint, the cost effectiveness improves considerably to just less than $200/additional ton for both states by 2000.

Coal Consumption

Although a cost analysis of the impact of the various emission-reduction scenarios on the coal industry was not

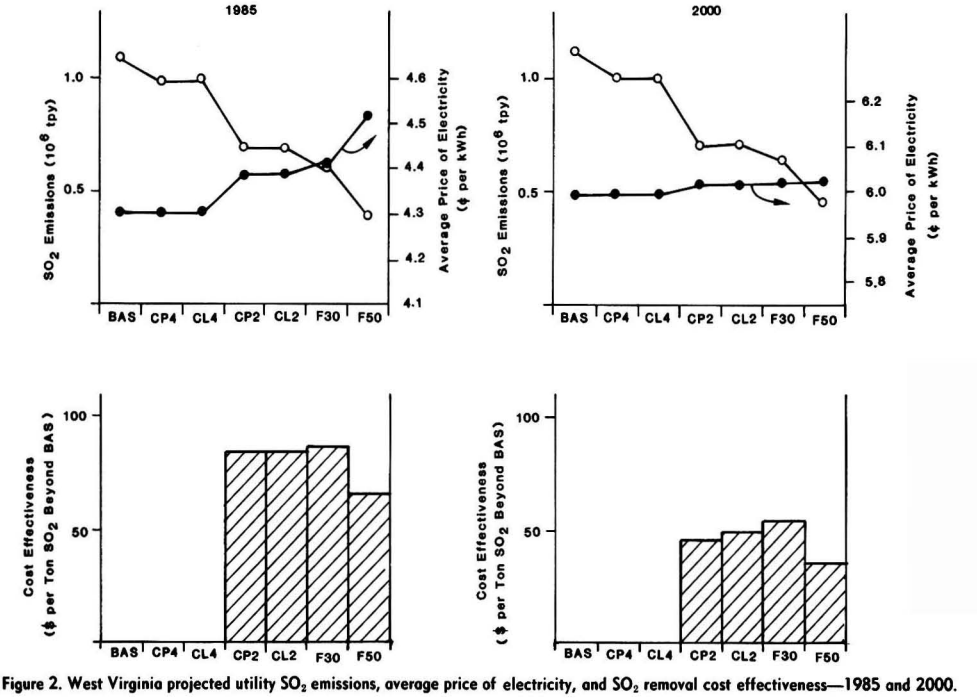

Figure 2. West Virginia projected utility SO_2 emissions, average price of electricity, and SO_2 removal cost effectiveness—1985 and 2000.

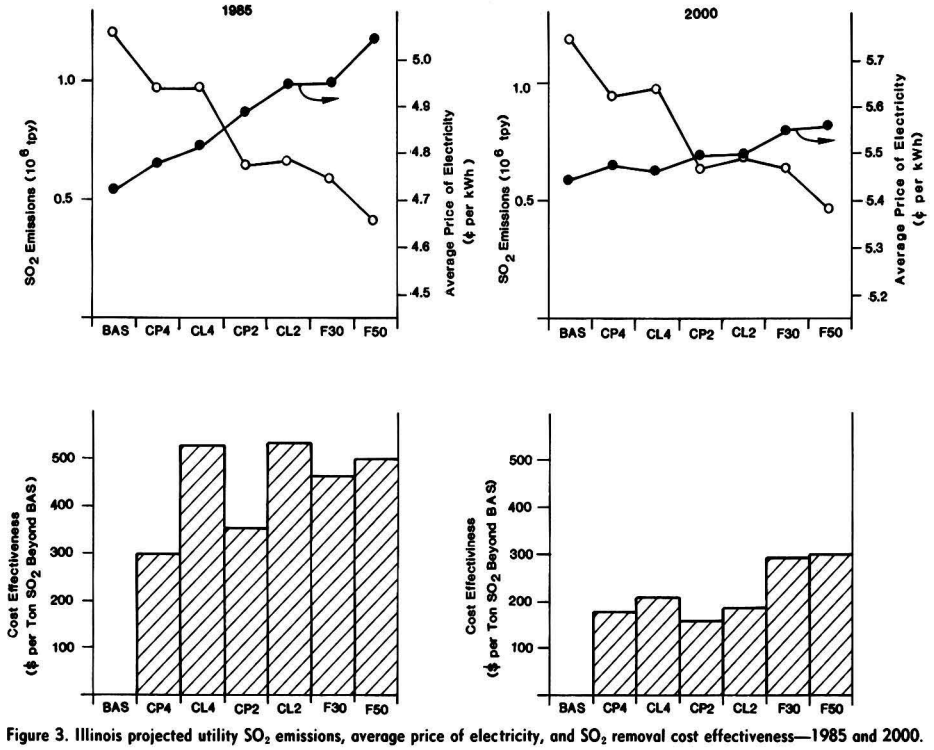

Figure 3. Illinois projected utility SO_2 emissions, average price of electricity, and SO_2 removal cost effectiveness—1985 and 2000.

performed, utility coal consumption for major supply regions was computed. Projected coal consumption for 1985 and 2000 for the three-states discussed previously is presented in Figures 4 and 5. The coal consumption values provide an indication of potential major coal market shifts which detract from a scenario that has other desirable features. Such coal market shifts are characterized by the projections for coal use in Ohio. The accessibility of the

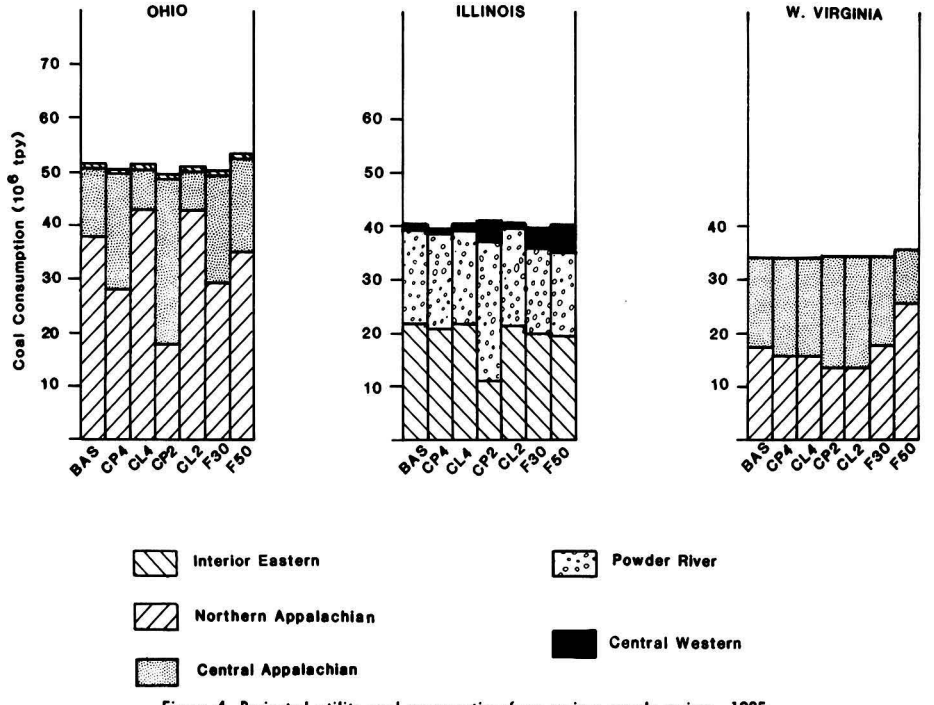

Figure 4. Projected utility coal consumption from various supply regions—1985.

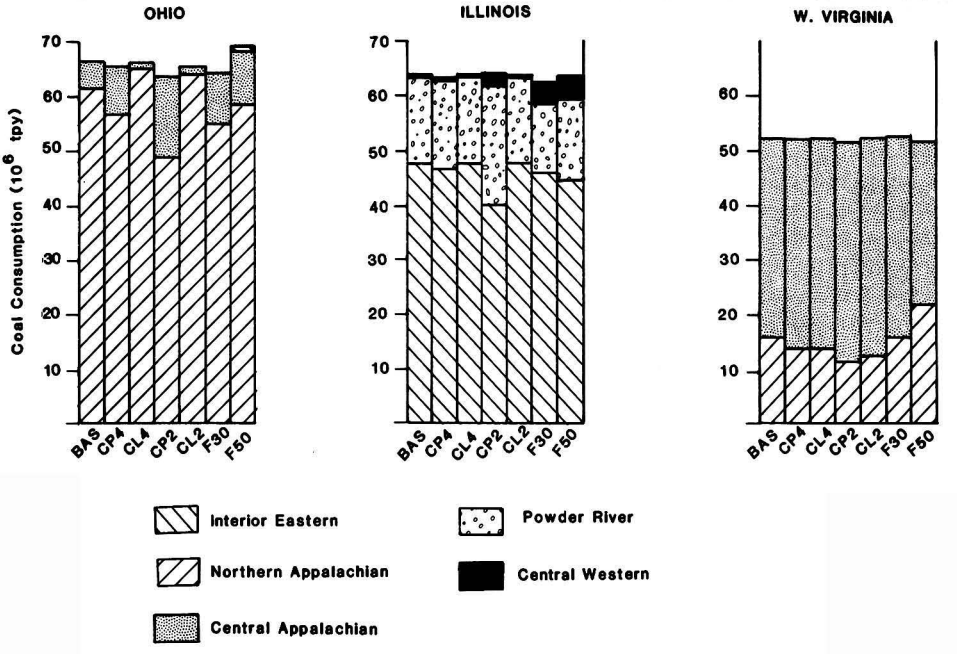

Figure 5. Projected utility coal consumption from various supply regions—2000.

lower-sulfur Central Appalachian coals results in substantial shifts to use of those coals to meet the SIP emission ceiling requirements of 4 lb and 2 lb $SO_2/10^6$ Btu. The 30 and 50% retrofit scenarios (F30 and F50) also show reductions in local coal use. These shifts probably reflect the cost advantage of designing and operating FGD systems for regionally available lower-sulfur coal, rather than very efficient systems using local high-sulfur coal.

The market for high-sulfur Interior Eastern coal to Illinois utilities is less vulnerable to the emission reduction scenarios than that for Northern Appalachian coals to Ohio utilities. The market for Interior Eastern coal is not sensitive to local coal constraints under the 4 lb emission ceiling. The 2 lb ceiling results in reductions of Eastern Interior coal consumption by Illinois utilities of approximately 10 million tons and 8 million tons per year in 1985 and 2000, respectively. This reduction is compensated for by increased use of low-sulfur western coals. The requirement for retrofitting FGD systems on Illinois generating units has no discernible effect on local coal use, but is responsible for a slight shift in western coal selection.

The impact of the emission reduction strategies on coal production areas serving utilities in West Virginia is minimal. This is largely a result of portions of both the Central and Northern Appalachian coal-producing regions being within West Virginia. Coal use under the F50 scenario is the only exception to this coal market insensitivity.

SUMMARY

The results of several strategies for reducing SO_2 emissions from existing utility coal-fired generating units have been presented. Projections are based on the TRI Utility Simulation Model, which anticipates future utility decisions given a number of financial and regulatory parameters. Model projections of total annual emissions, cost effectiveness, consumer cost, and coal market trends have been examined for scenarios which include compliance with the existing SIP by 1985, 4 lb and 2 lb $SO_2/10^6$ Btu SIP ceilings with and without local coal use constraints and FGD retrofit to achieve a 30% and 50% reduction in regional utility SO_2 emissions.

Utility SO_2 emissions for the ARM region are projected at about 16 million tons annually by 1985, given that all existing units comply with SIPs by that time. The assumption of static regulatory conditions through the end of the century results in decreasing annual utility SO_2 emissions to about 14.8 million tons in 2000. The emission reduction scenarios examined can generally be categorized into three groups: CP4 and CL4 give about 1.5 million tons/year reduction; CP2, CL2, and F30 achieve 5.0 to 5.5 million tons/year; and F50 gives about 8 million tons/year. The total reductions from each of these strategies remain about the same throughout the period. The relative cost effectiveness and annual revenue requirements also remain largely unchanged.

However, selection of a preferable regional emission-reduction option from these national data alone neglects the characteristics of each state and the potential ramifications of a proposed solution. Such state-specific features as generating capacity mix, sub-regional coal availabilities, retrofit FGD effectiveness, electricity demand projections, and a specific state's contribution to total regional emissions determine the effectiveness of the strategy within the state.

Three states with somewhat disparate projections were examined. Analysis of emission-reduction strategies for Ohio, Illinois and West Virginia indicates that those states with SIPs which allow emissions greater than 4 lb $SO_2/10^6$ Btu could realize moderate emission reductions in a cost-effective manner by imposing a 4 lb limit on SIP emissions. However, this action could substantially reduce the market for locally produced coal. This effect is magnified for the 2 lb ceiling, reducing the consumption of Interior Eastern coal in Illinois and Northern Appalachian coal in Ohio by 50% in 1985. Constraining the flux of out-of-state low-sulfur coal to meet these limits eliminates the cost-effectiveness advantage of these scenarios.

Retrofitting FGD systems on existing units on a cost-effectiveness basis in order to achieve 30% and 50% re-

gional emission reductions (beyond SIP levels) results in the largest environmental benefit for the three states examined. However, because these options result in large capital expenditures, their impact on the average price of electricity is greatest.

ACKNOWLEDGMENTS

The modeling of alternative control strategies was performed by Teknekron Research, Inc. (TRI). Andrew Van Horn of TRI provided clarification of some of the details of the model output. The modeling effort was jointly funded by the U.S. Department of Energy and the U.S. Environmental Protection Agency, and managed by Argonne National Laboratory. This particular analysis of the results was funded by the Regulatory Analysis Division, Office of Environmental Assessments, Assistant Secretary for Environment, U.S. Department of Energy. The DOE project officer was Doug Carter. The opinions expressed in this paper are those of the authors alone; they should not be construed as representing the policy of Argonne National Laboratory, the Department of Energy, or the Environmental Protection Agency.

LITERATURE CITED

1. Barnes, R. A., "The Long-Range Transport of Air Pollution—A review of European Experience," JAPCA 29(12):1219-1235 (1979).
2. Harr, T. E., and P. E. Coffey, "Acid Precipitation in New York State," New York State Department of Environmental Conservation, Technical Paper No. 43 (1975).
3. Van Horn, A., *et al.*, Teknekron Research Inc., "Electric Utility Emissions Control Strategies and Costs," Draft Report (April, 1981).

Duane A. Knudson is an environmental policy analyst in the Energy and Environmental Systems Division at Argonne National Laboratory. He graduated from Northern Illinois University in 1974 with a B.S. degree in meteorology. Graduate training at the University of Missouri—Columbia led to a M.S. degree in atmospheric science in 1974. He worked for three years in the Air Quality Branch of the Tennessee Valley Authority. He is involved in a variety of air quality policy assessment activities.

David G. Streets is manager of the Policy Sciences section of the Energy and Environmental Systems Division at Argonne National Laboratory. He received B.Sc. and Ph.D. degrees in physics from the University of London, England. He has been a Postdoctoral Fellow under the sponsorship of the National Science Foundation in 1971-1972 and Imperial Chemical Industries in 1972-1974. He joined Argonne in 1975 and is presently responsible for management of an interdisciplinary group analyzing energy and environmental issues for the U.S. Department of Energy.

Three Mile Island Cleanup

Experiences, Waste Disposal, And Environmental Impact

Lester J. King and James H. Opelka, Editors

"The papers included in this book deal with the experiences and problems in cleaning up Three Mile Island Unit-2 (TMI-2) following the accident . . . and the waste disposal and environmental impacts of the cleanup.

The material damages and losses resulting from the accident are very high. Cleanup will take many years and . . . costs will certainly be somewhere near $1 billion" (from the foreword).

Contents:

- Three Mile Island Unit 2 (TMI-2) Reactor Building Venting Experience.
- TMI Containment Entry Program.
- Water Decontamination Process Improvement Tests and Considerations.
- Processing TMI Accident Waste Water.
- TMI-2 Technical Information and Examination Program.
- Generation, Classification, Treatment and Disposal of Solid Waste Forms Resulting from Cleanup of TMI-2.
- Three Mile Island Waste Management: A DOE Perspective.
- Radiation Effects on Ion Exchange Materials Used in Waste Management.
- Three Mile Island Zeolite Vitrification Demonstration Program.

Material presented was selected from papers presented at AIChE's National Meeting in Detroit, Michigan, August 16-19, 1981.

Pub. #S-213

AIChE Members $17.50; Others $35.00

Send orders to:

Publications Sales, Dept. P
American Institute of Chemical Engineers
345 East 47 Street
New York, NY 10017

Pub. #S-213. THREE MILE ISLAND CLEANUP.

No. of copies_____ $_____

No. of copies_____ Free

Membership No._____

Amount enclosed $_____

Name _____

Address _____

City _____ State_____ ZIP_____

Please be sure to include check or money order in U.S. dollars. U.S. postage is prepaid. Please add $2.00 per book to cover postage on foreign orders. Members must include Membership No. in order to qualify for member price, and may order only one copy of each title at the member price.

TECHNICAL SECTION CHAIRMAN

AIR SECTION ..... **Richard D. Siegel**
Stone & Webster Engineering Corp.
P.O. Box 2325
Boston, MA 02107 617-973-7620

WATER SECTION ..... **Robert L. Irvine**
Department of Civil Engineering
University of Notre Dame
Notre Dame, IN 46556 219-283-6173

SOLIDS SECTION ..... **Michael R. Overcash**
North Carolina State University
P.O. Box 5906
Raleigh, NC 27650 919-737-3121

COMMITTEE CHAIRMEN

PROGRAMMING BOARD ..... **Leonard K. Peters**
Dept. of Chemical Engineering **D. Bhattacharyya**
University of Kentucky
Lexington, KY 40506 606-258-4958

AID/LIFE ..... **Michael R. Overcash**
North Carolina State University
P.O. Box 5906
Raleigh, NC 27650 919-737-3121

AMERICAN ACADEMY OF ENVIRONMENTAL ENGINEERS ..... **Robert T. Jaske**
7980 Chelton
Bethesda, MD 20014 301-427-8171

AWARDS ..... **Les Lash**
2827 Kentucky Avenue 801-277-8319
Salt Lake City, UT 801-266-4103

CONTINUING EDUCATION ..... **Michael R. Overcash**
North Carolina State University
P.O Box 5906
Raleigh, NC 27650 919-737-3121

PUBLIC RELATIONS & MEMBERSHIP ..... **Marx Isaacs**
1513 Barbee Avenue
Houston, TX 77004 713-523-6049

NOMINATING ..... **Jacoby A. Scher**
5519 Yarwell
Houston, TX 77096
(Fluor Engineers & Constructors) 713-662-4062

PEER REVIEW
(to come)

WATER TASK FORCE ..... **David B. Nelson**
Monsanto Research Corp.
Station B, Box 8
Dayton, OH 45407 513-268-3411

SOLIDS & HAZARDOUS WASTE TASK FORCE ..... **David P. Schoen**
Coulton Chemical Corp.
6600 Sylvania Avenue
Sylvania, OH 43560 419-885-4661

AIR TASK FORCE ..... **Jack F. Erdmann**
Union Carbide Corp.
P.O. Box 471
Texas City, TX 77590 713-948-5126

INTERSOCIETY LIAISON ..... **Robert A. Baker**
U.S. Geological Survey
Gulf Coast Hydroscience Center
NSTL Station, MS 39529 601-688-3130

EDITOR-ENVIRONMENTAL PROGRESS ..... **Gary F. Bennett**
Department of Chemical Engineering
University of Toledo
Toledo, OH 43606 419-537-2520

AIChE CONTINUING EDUCATION COURSES ON THE ENVIRONMENT DURING 1982

Advanced Waste Water Treatment
Cleveland, August 28-29
Los Angeles, November 13-14

Air Pollution Control
Cleveland, August 27-29
Los Angeles, November 12-14

Hazard Control in the Chemical and Allied Industries
Anaheim, June 9-10
Cleveland, August 30-31
Los Angeles, November 15-16

Hazardous Waste Management
Los Angeles, November 17-18

Industrial Water Conditioning
Cleveland, August 30-31
Los Angeles, November 15-16

Integrated Hazardous Waste Management
Los Angeles, November 17-18

Land Treatment of Hazardous and Non-Hazardous Industrial Wastes
Los Angeles, November 17-18

Water Quality Engineering for Industry
Cleveland, August 26-27
Los Angeles, November 11-12

AIChE Booklet Examines Factors Affecting Revision Of Clean Air Act

The AIChE task force, as part of a continuing program of educating the public on a host of technical topics, has just published "Air Quality Laws and Regulations," which deals with the thornier problems of legislating air pollution control.

The 15-page booklet identifies several technical factors that the nation's legislators must consider when amending the Clean Air Act, now before the Congress. The goals of these revisions, as well as the suggestions put forth in the booklet, are to maintain, or in some cases, re-establish, the delicate balance between the precarious state of both the environment and the economy.

"As a technical organization, the American Institute of Chemical Engineers is in a unique position to assist members of Congress, the news media, and the public at large in understanding these complex issues," states the booklet in its introduction. "With the broad spectrum of knowledge and opinion of our membership as a foundation, we have prepared this brochure to identify some of the major considerations in the revision of the Clean Air Act."

Limiting its discussion to control of stationery source emissions, the booklet focuses on Parts C & D of the Clean Air Act, which covers permitting procedures from the Prevention of Significant Deterioration (PSD) and Non-attainment areas. The booklet lists the following as some principal concerns.

- The Prevention of Significant Deterioration application procedure could be streamlined. One way to do this is to reduce the preliminary data collection or leave the establishment of background levels to the government rather than industry.
- Decisions on Prevention of Significant Deterioration applications could be made within six months, rather than a year, as is a current practice.
- The requirement for use of the air dispersion models specified by the Environmental Protection Agency could use modification. Current models are neither flexible enough to cover all situations, nor particularly reliable.
- The Lowest Achieveable Emission Rate (LAER) requirement often forces companies to use untested equipment which jeopardizes its ability to meet production schedules and cuts efficiency.
- The emission offset program, whereby a company can store "credits" of emissions to offset a new emission source, often creates more problems than it solves. This "banking" procedure can, under certain circumstances, tend to encourage the status quo rather than the improvement of air quality.
- The problem of acid precipitation (for example, acid rain) presents a unique environmental quandry. The exact cause of this phenomena is not known at this time. Since the source of acid precipitation and the place where the effects are noticed are often separated by large distances, acid precipitation becomes a problem of interstate and international relations as well. Legislators in revising the Clean Air Act have to face two questions: do you take strong precursor action against large potential emission sources right away and face the potential economic consequences of drastic overregulation? Or, do you wait until the cause is known and then impose restrictions when it may possibly be too late?

The booklet also raises issues such as to what degree should National Ambient Air Quality standard siting procedures consider factors like risk to public health, margins of safety, or cost/benefit analyses, and what are the difficulties of predicting long-range impact of new emission sources on air quality.

"Air Quality Laws and Regulations" is the latest in a series of AIChE booklets to grapple with technical issues of vital concern to America today. Past booklets have dealt with the potential use of ethyl alcohol as a motor fuel, with the handling and treatment of radioactive wastes, and the development and utilization of synthetic fuels.

For additional information, contact AIChE, Public Communications Department, 345 E. 47th Street, New York, NY 10017. Telephone: 212-705-7660-1.

Water Section Report

The Environmental Division is presently divided into three sections: Air, Water and Solid Wastes. During the past Annual Meeting in New Orleans several discussions were held regarding the appropriateness of these classical sections to the needs and capabilities of Chemical Engineers. As a result four new sections were proposed to replace the existing three. These are: Source Control (i.e. Process Modification); Reuse, Recycle and Recovery; Fundamentals (including Treatment); and Effects. In order to carry out such a restructuring of the Environmental Division successfully, active support will have to come from our present division membership and members from other AIChE divisions. As a result, we decided in New Orleans to open discussion of the proposed reorganization at "model" sessions at the upcoming meetings in Cleveland and Houston.

In Cleveland the Water Section has a symposium entitled "Wastewater Management from Source Control to Effects." The format of the session follows exactly the proposed modification. Four half-hour papers deal, in order, with source control in chrome finishing, resource recovery in a chloro-alkali facility, treatment by photo-oxidation, and effects assessment of environmental hazards. A one hour discussion period follows the presentations. Hooker Chemical Company has kindly agreed to supply all four speakers. We hope that other industries will support our efforts at reorganization by involving its representatives at this symposium in Cleveland and by making contributions, similar to that of Hooker, at future meetings. Please contact Bob Irvine at the University of Notre Dame for contributions and recommendations for the Houston and future meetings. He can be reached at (219) 239-6306.

Seminar Announcement

A rather unusual seminar on the Impact of Applied Genetics in Pollution Control will be held at the University of Notre Dame on May 24, 25 and 26, 1982. During the first day microbiologists, biochemists, chemical engineers and bioengineers will present basic concepts of genetic engineering and examples of its use in the fermentation industry. During the second and third days, the possible application of genetic engineering to pollution control will be discussed. A registration fee of $55 will be used to cover costs of four planned meals, a plant tour and coffee breaks. Because of enrollment limitations and the late publication date of this issue, please contact Professor Robert L. Irvine by telephone (219-239-6306) if you are interested.

1982 Cleveland AIChE Meeting

ENVIRONMENTAL PROGRAM

August 29-September 1, 1982

Program Coordinators: D. Bhattacharyya and L. K. Peters University of Kentucky, Lexington, Ky. 606-258-4956

WATER Sessions

James E. Alleman
Dept. of Civil Engineering
Univ. of Maryland
College Park, MD 20742
(301) 454-3108
Program Co-Chairman
(Bob Irvine) (219-239-6306)

THEME

Future Directions in Industrial Water & Wastewater Treatment

1. **Water and Wastewater Treatment for the Synfuels Program**
   Sheila S. Farthing (and D. Bhattacharyya)
   Bureau of Energy Research
   Kentucky Department of Energy
   Iron Works Pike
   Lexington, KY 40578
   Phone: (606) 252-5535 (Farthing); (606) 258-2794 (Bhattacharyya)

2. **Environmental Control for Oil Shale Utilization**
   Richard I. Kermode
   Department of Chemical Engineering
   University of Kentucky
   Lexington, KY 40506
   Phone: (606) 258-2823

3. **Physical-Chemical Treatment of Industrial Water & Wastewater Streams—Part I**
   Robert W. Peters
   Department of Civil Engineering
   Purdue University
   West Lafayette, IN 47907
   Phone: (317) 494-2191

4. **Physical-Chemical Treatment of Industrial Water & Wastewater Streams—Part II**
   Robert Gesumaria
   Roy F. Weston Inc.
   Western Way
   Westchester, PA 19380
   Phone: (215) 692-3030

5. **Activated-Carbon Systems for Industrial Waste Treatment**
   William Brian Arbuckle
   Department of Environmental Engineering Science
   University of Florida
   Gainesville, FL 32611
   Phone: (904) 392-0847

6. **Hazardous Wastes—Part I. Minimization, Treatment and Process Alternatives**
   Alfred Craig
   Industrial Environmental Research Lab
   U.S. Environmental Protection Agency
   Cincinnati, OH 45268
   Phone: (513) 684-4491

7. **Hazardous Wastes—Part II. Innovative Treatment Options**
   Michael D. LaGrega
   Department of Civil Engineering
   Bucknell University
   Lewisburg, PA 17837
   Phone: (315) 423-2311

8. **Industrial Waste Stream Pretreatment**
   Lawrence Ramsey
   O'Brien & Gere, Inc.
   1200 15th Street, N.W.
   Washington, DC
   Phone: (202) 861-0026

9. **Industrial Water & Wastewater Treatment—Case Histories**
   James S. Whang

AEPCO, Inc.
2301 Research Boulevard
Rockville, MD 20850
Phone: (301) 840-0293

10. **Biological Treatment of Industrial Wastewaters**
    Robert W. Dennis
    Exxon Research & Development
    Florham Park, NJ 07932
    Phone: (201) 765-1480

11. **Developments in Applied Biotechnology for Treatment of Industrial Process Waters and Hazardous Wastes**
    Mark Krupka
    Poly bac Corp.
    1251 Cedar Crest Boulevard
    Allentown, PA 18103
    Phone: (215) 433-1711

12. **International Activities in Water Pollution Control**
    Dr. James E. Alleman
    Univ. of Maryland
    College Park, Maryland 20742
    Phone: (301) 454-3108

13. **Potpurri: Industrial & Toxic Waste**
    Dr. Charles N. Haas
    Illinois Institute of Technology
    Chicago, Illinois 60616
    Phone: (312) 567-3537

14. **Membrane Processes for Industrial Wastewater Treatment**
    Dr. B. M. Kim (and D. Bhattacharyya)
    Corporate Res. & Dev.
    General Electric Co.
    Schenectady, N.Y.
    Phone: (518) 385-8824

Solid and Hazardous Waste Sessions

Program Chairman: Dr. M. R. Overcash
Department of Chemical Engineering
P.O. Box 5035
North Carolina State University
Raleigh, NC 27650
Phone: (919) 737-2325

1. **Hazardous Waste Disposal Options**
   Chairman: Tod Delaney
   Fred C. Hart Assoc.
   New York, N.Y. 10036

2. **Waste Incineration and Environmental Impacts**
   Chairman: Gene Krumpler
   Office of Solid Waste
   U.S. EPA
   Washington, D.C. 20460

3. **The Recovery Phase of RCRA**
   Chairman: Richard L. Elton, III
   Engineering-Science
   3109 North Interregional
   Austin, TX 78722

4. **The Secure Landfill: Design, Use and Long-term Stability**
   Chairman: William Tambo
   SCA Services
   60 State Street
   Boston, MA 02109

5. **New Technologies in Hazardous Waste Disposal**
   Chairman: Tod Delaney
   Fred C. Hart Assoc.
   530 Fifth Avenue
   New York, NY 10036

6. **Case Studies of Hazardous Waste Listing and Delisting**
   Chairman: Stacey L. Daniels
   DOW Chemical Company
   1702 Building
   Midland, MI 48640

7. **Economics of Hazardous Waste Management**
   Chairman: Thomas L. Ferguson
   Midwest Research Institute
   425 Volker Boulevard
   Kansas City, MO 64110

AIR Sessions

Program Chairman: Dr. Leo Weitzman
Acurex Corp.
8078 Beechmont
Cincinnati, OH 45230
(513) 474-4420
(Coordinators, D. Bhattacharyya & L. K. Peters, University of Kentucky)

1. **Fine Particulate Matter Emissions and Control**
   Tom Hughes
   Monsanto Research
   Station B, Box 8
   Dayton, OH 45407
   Phone: (513) 268-3411

2. **Iron and Steel Making Emission Control**
   Franklin A. Ayer
   Research Triangle Institute
   P.O. Box 12194
   Research Triangle Park, NC 27711
   Phone: (919) 541-6260

3. **Fugitive Emissions and Ambient Air Impacts**
   Dennis Martin—TRC Environmental Consultants
   800 Connecticut Boulevard
   E. Hartford, CT 06108
   Phone: (203) 289-8631

4. **NO_x and Simultaneous SO_x-NO_x Removal**
   K. Lim and C. Castaldini
   Acurex Corp.
   485 Clyde Ave.
   Mountain View, Calif. 94042
   Phone: (415) 964-3200

5. **Acid Rain**
   Dr. A. Johannes
   Rensselaer
   Polytechnique Inst.
   Troy, N.Y. 12181
   Phone: (518) 270-6381

6. **Transport and Chemistry of Air Pollutants**
   John W. Wilson
   Stone and Webster Engineering
   245 Summer Street
   Boston, MA 02107
   Phone: (617) 973-2898

7. **Industrial Process Sulfur Control**
   Dr. Leo Weitzman
   Acurex Corporation
   8078 Beechmont
   Cincinnati, Ohio 45230
   Phone: (513) 474-4420

8. **Integrated Control of Industrial Pollution Problems: Air, Water, and Solid**
   Dave Becker
   NUS Corporation
   4 Research Place
   Rockville, MD 20850
   Phone: (301) 948-5216

9. **The "Bubble" Concept: It's Effect on Industry Emission Control Planning**
   John F. Erdman
   Union Carbide Corporation
   P.O. Box 471
   Texas City, Texas 77590
   Phone: (713) 948-5126

10. **Industrial Boiler SO_x Control**
    Jim Dickerman
    Radian Corporation
    8501 Mopac Boulevard
    Austin, TX 78766
    Phone: (512) 454-4797

General Sessions (Environmental Div.)

Program Chairman: D. Bhattacharyya
University of Kentucky
Dept. of Chemical Engineering
Lexington, KY. 40506
Phone: 606-258-4956

1. **Wastewater Management at a Chemical Company from Source Control to Effects**
   Robert L. Irvine
   Dept. of Civil Eng.
   Univ. of Notre Dame
   Notre Dame, Indiana 46556
   (219) 239-6306
   Joseph F. Colarwotolo
   Hooker Research Center
   Long Road
   Grand Island, N.Y.
   (716) 773-8525

2. **Engineering Solutions to the PCB Problem**
   Bryce I. MacDonald
   General Electric Co.
   3135 Easton Turnpike
   Fairfield, CT 06431
   (203) 373-3317
   John H. Craddock
   Monsanto Industrial
   Chemicals Co.
   800 N. Lindberg Blvd.
   St. Louis, MO 63166
   (314) 694-1000

3. **New Wastewater Treatment Technologies for Industrial Application**
   Steven C. Chiesa
   Dept. of Civil Engineering
   Univ. of Notre Dame
   Notre Dame, Indiana 46556
   (219) 239-5380
   Robert P. G. Bowker
   USEPA
   MERL
   Cincinnati, Ohio 45268
   (513) 684-7620

ENVIRONMENTAL®
PROGRESS

May, 1982
Vol. 1, No. 2